# Orchestrating the Ubiquitin Solos in the Hematopoietic Symphony

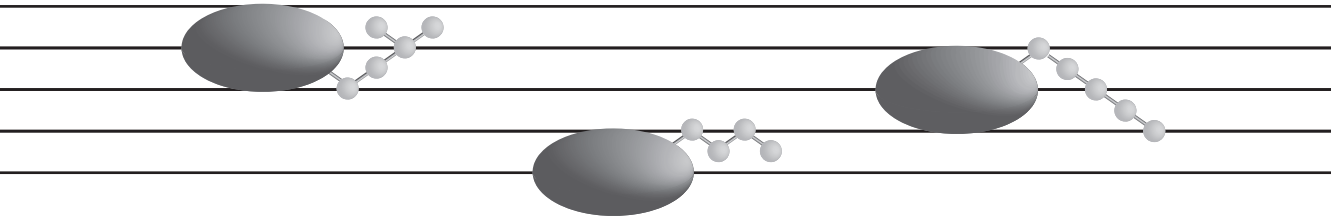

## Genomic & Proteomic studies on ubiquitination in normal and malignant blood cell development

Sylvie M. Noordermeer

ISBN/EAN: 978-94-6182-117-1

Orchestrating the Ubiquitin Solos in the Hematopoietic Symphony
S.M. Noordermeer

Layout and cover design: S.M. Noordermeer
*The musical excerpt on the cover is adapted from Nicolai Rimsky-Korsakov's symphonic suite Antar.*

Printed by: Off Page, Amsterdam

The studies described in this thesis were performed from November 2007 until March 2012 at the Laboratory of Hematology, Department of Laboratory Medicine, at the Radboud University Nijmegen Medical Centre, Nijmegen Centre for Molecular Life Sciences, Nijmegen, The Netherlands. The research was financially supported by the Vanderes foundation.

# Orchestrating the Ubiquitin Solos in the Hematopoietic Symphony

Genomic & Proteomic studies on ubiquitination
in normal and malignant blood cell development

**Proefschrift**

ter verkrijging van de graad van doctor
aan de Radboud Universiteit Nijmegen
op gezag van de rector magnificus prof. mr. S.C.J.J. Kortmann
volgens besluit van het college van decanen
in het openbaar te verdedigen op vrijdag 22 juni 2012
om 12.30 uur precies

door

**Sylvie Madeleen Noordermeer**

geboren op 22 mei 1984
te Sittard

**Promotor:**

Prof. dr. T.J.M. de Witte

**Copromotoren:**

Dr. B.A. van der Reijden
Dr. J.H. Jansen

**Manuscriptcommissie:**

Prof. dr. A.H.M. Geurts-van Kessel (voorzitter)
Prof. dr. B. Wieringa
Prof. dr. J.J. Schuringa (*Universitair Medisch Centrum Groningen*)

*Voor mijn ouders*

# Table of Contents

# Introduction

1

## 1.1 Thesis objective

In the late 1970s, a ubiquitously present protein was discovered to mediate protein turnover: '*Most cellular proteins are in a dynamic state of constant turnover. The mechanism of protein breakdown* […] *is composed of several essential components. One of these, a small heat-stable polypeptide, was subsequently identified as ubiquitin, a universally occurring polypeptide of previously unknown function. Ubiquitin is covalently linked to protein substrates in an ATP-requiring reaction.* […] *This may be the initial signal event in protein degradation, since the ubiquitin-protein conjugates are degraded rapidly*' (quote from Hershko and Ciechanover, 1982[1]).

Since the discovery of the ubiquitin proteasome system in the late 1970s – which was awarded with the 2004 Nobel Prize in Chemistry - it has become clear that the post-translational modification of proteins with ubiquitin has many more sophisticated functions than solely acting as a degradation signal to eliminate proteins from the cell. Therefore, ubiquitin is nowadays regarded as an important signaling molecule.

Leukemia's are cancer types that occur in both children and adults, and are still poorly curable in most adult cases. These cancer types are caused by malignant transformation of cells in the hematopoietic system, our blood cell development system. Hematopoiesis is a tightly regulated process which balances apoptosis, cell proliferation and differentiation. Imbalances in these processes are the cause of malignant transformation, which can occur *de novo*, or by external factors such as toxic chemicals, infections or auto-immune diseases. The importance of ubiquitination has been shown in all three processes, which makes ubiquitination an interesting target to study during malignant transformation. The objective of this thesis is to study the signaling role of ubiquitination in normal and malignant hematopoiesis by using genome- and proteome-wide top down and dedicated bottom up approaches.

## 1.2 Hematopoiesis

In daily life, we are constantly exposed to harmful pathogens. Our defense to infections of these pathogens relies on the highly efficient immune system: particular cells in the blood that move through our body on constant guard. Next to pathogen defense, the blood system is needed for transport of necessary nutrients and oxygen to all organs, and for transport of waste to the waste organs, the liver and kidneys. Furthermore, our blood system is involved in blood vessel repair after mechanical damage[2].



All these different roles of the blood are performed by many different, highly specific blood cells. Most of these cells are only short-lived and therefore need to be replenished constantly. At the apex of the hematopoietic system are the hematopoietic stem cells which give rise to all mature blood cells via a tightly regulated process, as explained below (paragraph 1.2.1)[3]. The mature blood cells can be subdivided in myeloid and lymphoid types. The myeloid lineage consists of cells involved in the innate immune system (*e.g.* monocytes, macrophages, granulocytes), the erythroblasts giving rise to the red blood cells and megakaryocytes that produce platelets needed for hemostasis. The lymphoid lineage contains the B- and T-cells, important in the adaptive immune system, and the NK cells, part of the innate immune system (figure 1.1).

### *1.2.1 Regulation of Hematopoiesis*

During fetal development, hematopoiesis initially occurs in the yolk sac. Later during embryonic development, blood cell formation is regulated in the spleen, liver and lymph nodes. When bone marrow starts to be formed, it slowly takes over the process, resulting in a complete takeover after birth. However, maturation and activation of some lymphoid cells will remain a function of the secondary lymphoid organs (spleen, thymus and lymph nodes)[2].

The hematopoietic stem cells (HSCs) reside in the bone marrow. In order to constitute the complete array of blood cells, they contain some important stem cell characteristics. This cell type is long-lived and quiescent, with both self-renewal capacities to retain a constant pool of these cells and pluripotent capacities to differentiate towards all different types of mature blood cells[4]. The balance between self-renewal and differentiation is a tightly regulated process. Deregulation of this process may have severe consequences as will be discussed below (paragraph 1.3). HSCs give rise to multipotent progenitors (MPPs): a group of proliferating cells which lose lineage potential by passing lineage restriction points as they progress during differentiation. Originally, it was suggested that MPPs make strict lineage decisions towards the common myeloid-erythroid progenitor (CMP) or the common lymphoid progenitor (CLP) (figure 1.1a). However, recent data suggest that such an absolute subdivision is not occurring. In contrast, it seems that HSCs can give rise to several MPPs with varying lineage restriction, such as EPLMs (early progenitors with lymphoid and myeloid potential)[5] and LMPPs

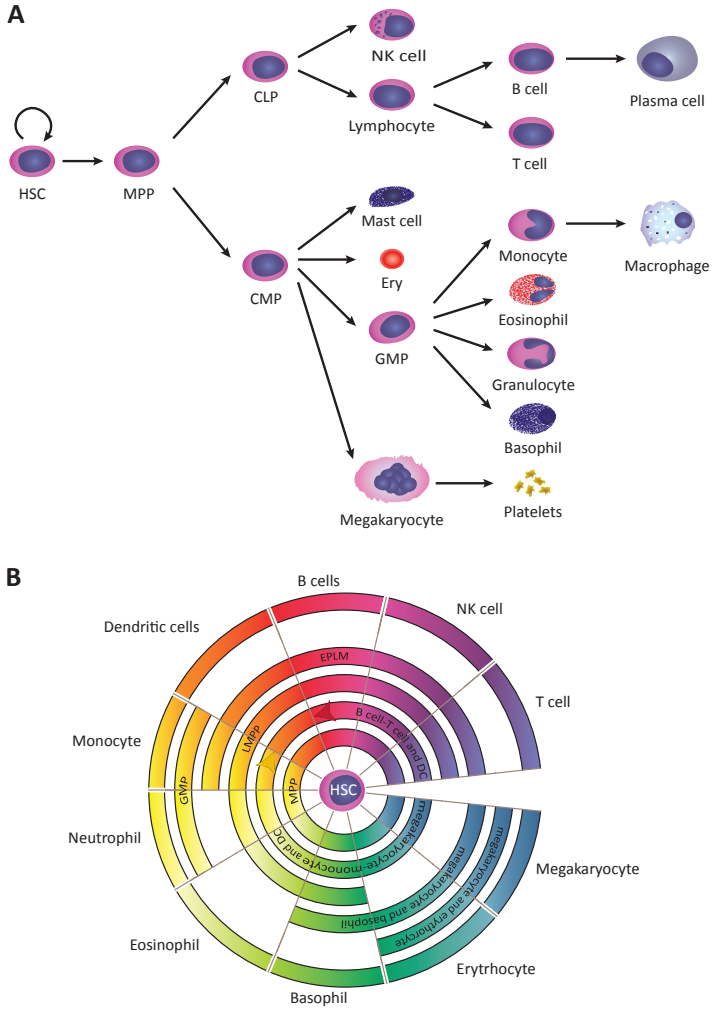


**Figure 1.1: Hematopoiesis**

**A.** In the established model of hematopoiesis, the hematopoietic stem cell gives rise to myeloid and lymphoid progenitors, which further mature towards all mature blood cells. **B.** In recent models of hematopoiesis, there is no absolute separation of the myeloid and lymphoid lineage. In contrast, there are several progenitors, each with distinct differentiation capacities. In this model, most mature blood cells can originate from more than one progenitor. Abbreviations used: HSC, hematopoietic stem cell; MPP, multipotent progenitor; CLP, common lymphoid progenitor; CMP, common myeloid progenitor; NK, natural killer; ery, erythrocyte; GMP, granulocyte-monocyte progenitor; DC, dendritic cell; LMPP, lymphoid-primed multi-potent progenitors; EPLM, early progenitor with lymphoid and myeloid potential. Figure 1.1b is adapted from Brown *et al.*[3].

(lymphoid-primed multi-potent progenitors)[6,7] (figure 1.1b).

The differentiation of HSCs into MPPs and further on towards mature blood cells is regulated by the action of cytokines, including growth factors and chemokines. These extracellular proteins induce intracellular signaling pathways upon binding to their cognate receptors. This leads to altered transcription factor activity and thereby altered expression profiles. The altered expression programs will direct a cell to proliferate, apoptose, or differentiate. For example, the transcription factor CEBPα limits HSC self-renewal and commits progenitor cells towards a monocytic fate[8].



## 1.3 Malignant hematopoiesis

The complexity of hematopoiesis is reflected by the multitude of hematopoietic malignancies. Broadly, hematological malignancies can be divided into two categories: myeloid and lymphoid neoplasms. Acute myeloid leukemia (AML) is the main subject of this thesis, which belongs to the class of myeloid neoplasms. A myeloid neoplasm is considered AML when the percentage of neoplastic cells in the peripheral blood or bone marrow exceeds 20%[9].

### *1.3.1 Acute Myeloid Leukemia*

AML is diagnosed in about 600 new patients each year in The Netherlands, and consequently is among the 10 most occurring types of cancer in the adult population (data from the Dutch integrated cancer centers, www.iknl.nl). AML also occurs in children, albeit less frequently. Despite major research efforts in this disease, molecular knowledge has not been able to raise the overall five year survival rate above 40% for adults younger than 60 years[10,11] (for children this is 65%[12]). In the elderly population (above 60 years), which represents the majority of the patients, outcome is very poor with less than 15% survival after five years[13].

In AML, the myeloid lineage is affected. The uncontrolled proliferation of the immature leukemic cells will outcompete the healthy bone marrow cells. Therefore, patients often suffer from fatigue and anemia, caused by lack of erythrocytes, bruising because of thrombocyte insufficiency, and high susceptibility to infections due to the lack of healthy white blood cells.

A multitude of underlying genetic defects has been identified in AML. At diagnosis, patients are subdivided in different classes of AML, depending on the genetic defects present and the cellular morphology of the leukemic cells. This latter gives information about the differentiation state of the malignant clone. Depending on the genetic background, the five year overall survival prediction can vary from up to 80% to less than 10%. Together with the morphological data, a suitable treatment regimen will be determined, which may include chemotherapy, bone marrow transplantations, and targeted therapies for specific genetic defects.

*1.3.2 The hierarchical organization of AML*

AML is characterized by the clonal expansion of progenitor cells, which lack the intrinsic capacity to differentiate into more mature cells. There is much debate on the origin of leukemia and whether this disease is caused by malignant transformation of stem cells or progenitors. The fact that human AML cells can be subdivided into fractions that can or cannot induce leukemia in NOD/SCID mouse recipients shows that AML is hierarchically organized with self-renewing cells (which are often referred to as leukemia stem cells (LSCs)) at the apex of the organization[14]. At first, it was suggested that LSCs belong to a specific cellular fraction of the AML cells, the immature $CD34^+CD38^-$ cells. However, recent data have shown that in several cases LSCs can also be found in more mature fractions, such as $CD34^+CD38^+$ cells[15,16]. These data pose a controversy to the definition leukemic *stem* cell, as these cells appear not to be equivalent to the normal $CD34^+CD38^-$ hematopoietic *stem* cell. Although more mature fractions can show LSC activity, the leukemic organization remains hierarchical, as these more mature cells give rise to the same mature phenotype in secondary recipients but will never revert back to an immature phenotype. On the contrary, the more immature LSCs give rise to both immature and mature phenotypes in secondary recipients[7]. The fact that LSCs show different degrees of differentiation suggests that the 'cell of origin' (*e.g.* the normal hematopoietic cell that transforms into a malignant cell with stem cell characteristics) might be different between patients[16,17].

Identifying the true LSC is of great importance for the treatment of leukemia. Nowadays, treatments are directed to the bulk of leukemia cells. However, as the LSC is in a quiescent state, this cell might not be targeted by the current treatment strategies such as chemotherapy, explaining the high incidence of relapse. Ultimately, eradication of the LSC cell would lead to a cure. Therefore, effort has been made to understand the genetic background and function of these cells. For this, expression profiles of several AML LSC fractions have been compared to their normal counterparts. These studies showed that leukemic cells most closely resemble their normal progenitor counterparts, and not the HSCs. However, the LSCs show a self-renewal-associated expression program not observed in normal progenitors[18]. This self-renewal expression program represents the stemness of the LSCs and appears to influence clinical outcome in AML: patients that highly express stem-cell related genes show a worse prognosis compared to patients with lower expression of stemness genes[15].

Until now, a combined genetic, flow cytometric and functional characterization of the LSC at single cell level has been unrealizable. Therefore, the true LSC has not been identified yet. With the advancing technologies, I have confidence that it will be possible to fully characterize this cell type within the next ten years. Only then we will be able to determine which processes cause normal cells to transform into malignant clones, which likely will result in better understanding of the clinical diversity of the disease.

*1.3.3 Acquired genetic abnormalities in AML*

Although the issue of identifying the LSC in AML is not completely solved, much is known about genetic aberrations present in AML cells, making them distinct from normal hematopoietic cells. These aberrations include chromosomal translocations, inversions, duplications or deletions of complete or partial chromosomes, subtle point mutations and altered expression of particular genes. Based on diagnostic testing of recurrent chromosomal aberrations, specific point mutations and gene expression alterations, patients are currently classified into three prognostic groups with good, intermediate and poor prognosis[10] (see table 1.1a and 1.1b). Despite improved prognostications for genetic subgroups of AML, predicting the correct outcome of individual patients remains an elusive goal. In the last decade, global gene expression arrays have been conducted on large AML cohorts to gain better insight into the correlation of gene expression in AML blasts with disease outcome[19,20]. Indeed, specific gene expression profiles that correlate with survival have been identified via this approach. Profiling is still a promising technique to identify novel prognostic markers, as will be shown in chapter 3 of this thesis which describes the prognostic impact of *BRE* expression in AML. Deregulated expression of this gene was identified via global gene expression analysis.

*1.3.4 Deregulated pathways involved in AML development*

The genetic aberrations occurring in AML have a direct influence on important cellular pathways. The aberrations affect transcription factors, nuclear pore complexes, epigenetic regulators, signaling molecules, and more[21-23]. The altered activity of transcription factors caused by some of these aberrations (expression of *AML-ETO*, *PML-RAR*, and *CBFb-MYH11* fusion genes due to chromosomal translocations, and *CEBPA* double mutations) leads to a global change in expression profile[19,20]. However, other mutations or translocations do not trigger common global expression alterations. In those cases, the affected pathways seem to have more subtle effects. Recently, several research lines have linked aberrant ubiquitination to the pathogenesis of AML, as several mutations and expression alterations in the ubiquitination machinery have been identified in AML[24,25] (see table 1.2).

**Table 1.1A: Prognostic classification of aberrant karyotypes in AML**

| Favorable prognosis | Intermediate prognosis | Unfavorable prognosis |
|---|---|---|
| • inv(16) | • All entities not classified as favorable or unfavorable prognosis | • abn(3q) excluding t(3;5) |
| • t(15;17) | | • inv(3)/t(3;3) |
| • t(8;21) | | • add(5q), del(5q), -5 |
| | | • -7, add(7q)/del(7q) (except cases with favorable karyotype) |
| | | • t(6;11) |
| | | • t(10;11) |
| | | • 11q23 aberrations (excluding t(9;11), t(11;19)) |
| | | • t(9;22) |
| | | • -17/abn(17p) |
| | | • Complex (≥4 unrelated abnormalities) |
| | | • Monosomal karyotype[189] (at least two chromosomal monosomies or one single monosomy in combination with at least one other structural abnormality) |

(adapted from Grimwade *et al.*[10])

**Table 1.1B: Recurrent gene mutations and altered expression levels in AML**

| Aberration | Prognostic impact |
|---|---|
| *ASXL1* mutation | Poor prognosis[190,191] |
| *BAALC* high expression | Poor prognosis[192,193] |
| *cCBL* mutation | None[194] |
| *CEBPA* mutation | Biallelic mutation: favorable prognosis[195] |
| *cKIT* mutation | Poor prognosis among core binding leukemia's[196-198] |
| *DNMT3A* mutation | Poor prognosis[199-201] |
| *EVI1* epxression | Poor prognosis[202] |
| *FLT3* Internal Tandem Duplication | Poor prognosis[203,204] |
| *FLT3* Tyrosine Kinase Domain mutation | Controversial[194] |
| *JAK2* mutation | None[194] |
| *KRAS* mutation | None[23] |
| *MN1* high expression | Poor prognosis[205,206] |
| *NRAS* mutation | None[23] |
| *NPM1* mutation | In *FLT3*-ITD negative group: favorable prognosis[207] |
| *RUNX1* mutation | Poor prognosis[208] |
| *TET2* mutation | Poor prognosis in intermediate risk subgroup[209] and cytogenetically normal AML[210] |
| *TP53* mutation | Poor prognosis[211] |
| *WT1* mutation | Uncertain[23] |

## 1.4 Ubiquitination acts as a post-translational signaling role for cellular proteins

Protein activity is regulated at many levels. First of all, proteins are produced in a time-dependent fashion by transcriptional and translational regulation. After translation, their activity and abundance can be regulated via several post-translational modifications, like phosphorylation and glycosylation. Another important post-translational modification is ubiquitination. In this process, one or more ubiquitin moieties are covalently attached to a cellular protein, the substrate (see paragraph 1.4.1). Initially, ubiquitination was regarded as a degradation mark for the substrate[26]. However, over the last decades, many more functions have been assigned to this modification, like protein trafficking and complex formation[27] and ubiquitination is thereby more and more regarded as a modification with general signaling function (see paragraph 1.4.2).



### *1.4.1 The ubiquitination cascade*

Ubiquitin is a small polypeptide of 76 amino acids. Four genes in the human genome encode a total of 14 ubiquitin mRNA copies, of which the majority is translated as ubiquitin polymers[28]. These polymers are processed into single ubiquitin peptides by the action of deubiquitinases (DUBs). Ubiquitin can then be attached to a cellular substrate protein in a three step cascade. First, ubiquitin is activated by an E1 activating enzyme in an ATP-dependent process. Next, the activated ubiquitin is transferred to an E2 conjugating enzyme, by forming a thio-ester bond between the C-terminal glycine of ubiquitin and the catalytic site cysteine of the E2. In the final step, the E2 binds to an E3 ligase, which recruits the substrate, thereby linking E2 and substrate. In the E2-E3-substrate complex, the ubiquitin molecule is transferred from the E2 to an internal lysine (K) of the substrate, forming an isopeptide bond via the C-terminal glycine backbone of ubiquitin[29] (figure 1.2a). Many E3 ligases contain a specific structural domain involved in E2 binding, like RING and HECT domains. Ubiquitin can be directly transferred from the E2 to the substrate as is the case for RING E3 ligase complexes. HECT E3 ligases, on the other hand, form an intermediate thio-ester with ubiquitin before transferring ubiquitin to the substrate. This latter property has recently been shown for members of the TRIAD class[30] of RING ligases as well, which are characterized by two RING fingers interspersed by a RING-like domain (DRIL, double RING finger linked) (J. Smit *et al.*, manuscript submitted and Wenzel *et al.* 2011[31]). DUBs are not only involved in processing newly translated ubiquitin polymers, but are also able to reverse ubiquitination by hydrolyzing the covalent interaction of ubiquitin with its substrate. This enables a time dependent regulation of ubiquitination.

Within the ubiquitin cascade, the E2 determines which type of ubiquitin chain is formed (see paragraph 1.4.2) and the E3 is responsible for the substrate specificity of the modification. The human genome encodes only a few E1 enzymes. Over 40 E2

enzymes have been identified, all containing the specific catalytic core UBC (UBiquitin Conjugating) domain. In contrast to this few E1s and E2s, hundreds of E3 ligases are encoded by the human genome[32]. It is currently assumed that a large proportion of the cellular proteome is subject to ubiquitination. This explains the presence of the hundreds of E3s, acting as the factors that introduce substrate specificity to this process. Still, the human proteome is much larger than the number of E3s, implying that a single E3 must be able to ubiquitinate more than one substrate, which is indeed known for many studied E3s[33,34].



*1.4.2 Structurally different ubiquitin chains regulate different substrate outcomes*

The ubiquitin peptide is attached to an internal lysine of the substrate. As ubiquitin itself contains seven lysines (K6, 11, 27, 29, 33, 48, and 63), it can be a substrate of its own modification: consecutive ubiquitin molecules can bind with their C-termini to lysines of their preceding counterparts, hence forming chains (figure 1.2a). Another type of chain is the head-to-tail chain (also known as linear chain), in which the C-terminus of one ubiquitin forms a covalent bond with the N-terminus of a preceding ubiquitin, resembling the ubiquitin polymers formed during translation. These options for chain formation induce much versatility. Some cellular proteins are marked with a single ubiquitin on a single lysine (mono-ubiquitination) or on multiple lysines (multiple mono-ubiquitination). Poly-ubiquitination involves the formation of chains. When a chain is formed via identical ubiquitin lysines or linear linkages, homotypic chains are formed. Mixed chains occur when multiple ubiquitin lysines are used within one chain[35,36] (figure 1.2b).

In theory, two other possibilities in substrate ubiquitination are conceivable: N-terminal substrate ubiquitination, using the $\alpha NH_2$-group of the substrate as ubiquitin acceptor site, or ubiquitination of cysteine, serine or threonine side chains, forming a thio- or oxy-ester linked modification. Although indirect data suggest that both modification types exist, direct evidence and information on the physiological relevance is still limited[37-40].

The internal ubiquitin lysine used for chain formation determines the structure of the chain. Currently, crystal structures of K11-, K48-, K63-linked and linear ubiquitin chains are available. Linear and K63-linked chains closely resemble each other being the most extended chains with open conformations, in contrast to the more compact K48- and K11-linked chains[41-45]. Depending on the chain structure, different effectors can bind and will determine the consequence of the modification for the substrate. K48-chains lead to the degradation of the substrate by the 26S proteasome. The 26S proteasome is composed of a regulatory multi-protein 19S subunit and a catalytic 20S subunit. Ubiquitinated proteins associate with proteasome subunits containing ubiquitin binding domains (UBDs) specific for K48-linked chains. During proteasome association, the substrate is unfolded and degraded in the catalytic core, while ubiquitin

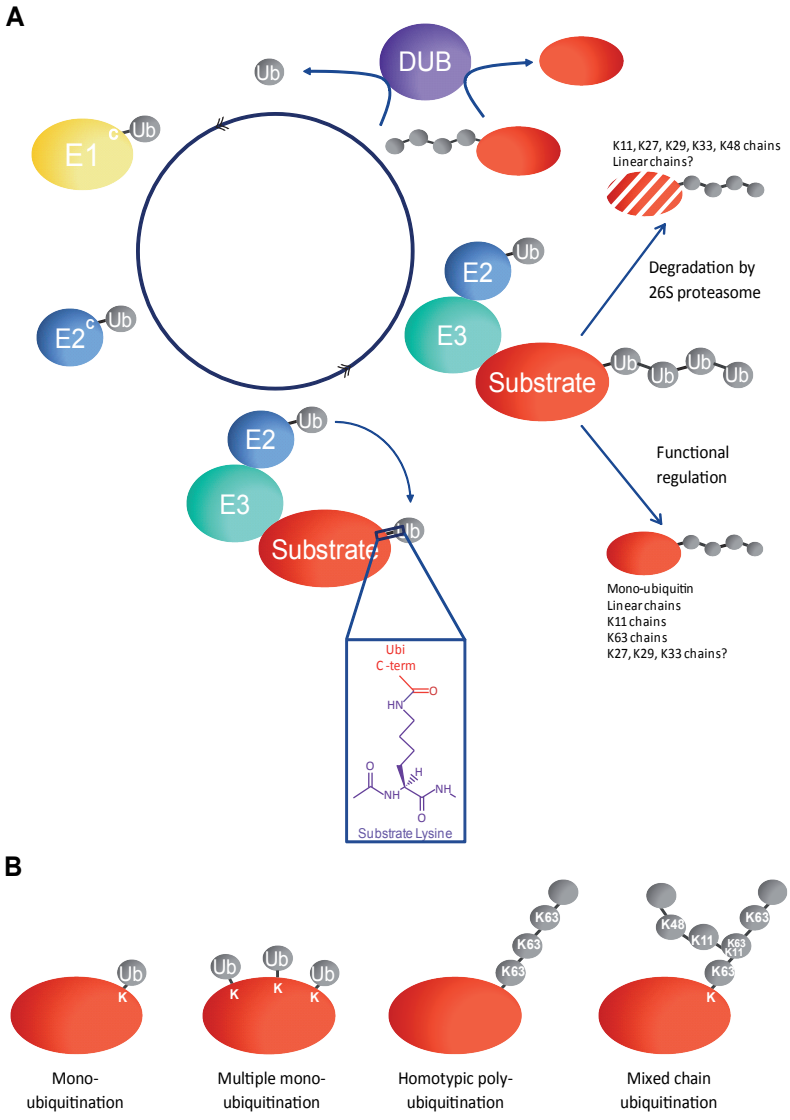


**Figure 1.2: The ubiquitination cascade**

**A.** The covalent attachment of ubiquitin to a cellular protein is achieved in a three step cascade, involving E1, E2 and E3 enzymes. Deubiquitinases (DUBs) are involved in the removal of ubiquitin from a substrate, making this modification reversible. Different types of chains can be formed, and will determine the outcome for the substrate. **B.** Ubiquitin can be attached to a substrate as monomer or as chains which are formed by internal lysine linkages. Chains can be formed via identical lysine linkages which are called homotypic chains or via usage of multiple lysines, which are called mixed chains. Abbreviations used in figure: K=lysine, C=cysteine.

is recycled by DUBs that disassemble the ubiquitin chains[46].

K63-linked chains do not lead to proteasomal degradation, but serve a signaling role in cellular processes. This holds true for mono-ubiquitination as well. These processes involve, among others, receptor internalization, protein complex formation, and cellular translocation of substrates. K63-linked ubiquitination will be discussed in more detail in the following paragraphs. The role of the other ub-linkages is still under debate. Proteomic studies have shown that the abundance of all linkages, except K63-linked chains, increase after chemical inhibition of the 26S proteasome[47-49], suggesting that all chains except K63-linked chains target substrates for degradation. K11-linked chains indeed seem to be *bona fide* degradation signals and are involved in protein degradation during cell cycle and endoplasmic-reticulum-associated degradation (ERAD)[47,50,51]. The physiological relevance of the other chains, however, remains unclear[36].

*1.4.2.1 K63-linked ubiquitin chains fulfill signaling functions for their substrates*

K63-linked chains do not target substrates for proteasomal degradation, but alter the activity of the substrate protein. So far, the only E2 known catalyzing these chains is UBC13[52,53]. To function as E2, UBC13 needs a cofactor. Two cofactors have been identified so far, UEV1a and MMS2. These UEVs (Ubiquitin E2 variant) closely resemble E2 enzymes, though they are not catalytically active as they lack the active site cysteine. By elucidating the structure of the UBC13-MMS2-donor ubiquitin intermediate, the specificity of this E2 complex towards K63-linked chain catalysis could be explained[54-56]. The UEV binds the acceptor ubiquitin in such a conformation that lysine 63 is placed in close proximity to the E2 active site which is bound to the donor ubiquitin via a thio-ester bond. In this conformation, K63 of the acceptor ubiquitin can attack the thio-ester bond and forms an isopeptide bond with the donor ubiquitin. The process is then repeated as the donor ubiquitin will move across the E2 complex and will become the acceptor ubiquitin in the next round while a new donor ubiquitin will be attracted by UBC13.

The E2 variant cooperating with UBC13 depends on the biological context. Two important pathways that depend on K63-ubiquitination are DNA damage repair (see paragraph 1.5.2.1) and NF-κB signaling (see paragraph 1.5.2.2). The combination UBC13 and UEV1a is involved in NF-κB activation, as shown below[52,57,58]. In contrast, in the process of DNA damage repair, UBC13 uses MMS2 as cofactor[52]. However, it has been suggested that MMS2 and UEV1a are both dispensable for the DNA damage response, as depletion of both enzymes did not inhibit downstream signaling[59].

Another important role of K63-linked chains is cell-surface receptor internalization. These endocytic processes rely on the recognition of mono- or K63-ubiquitinated receptors by the ESCRT machinery[60-63]. Proteins can then be recycled back to the membrane or translocated to the lysosomes, where degradation will take place (see paragraph 1.5.2.3).

### *1.4.3 Ubiquitin binding domains mediate ubiquitination function*

The general principle for downstream effects of ubiquitination, either degradative or non-degradative, relies on ubiquitin recognition and binding by other proteins. Proteins that interact with ubiquitin are characterized by small ubiquitin binding domains (UBDs). There is much variety in UBDs with already more than twenty different structural UBD families identified to date. Among the major UBD families are the UIMs (ubiquitin interacting motifs) and UBA-domains (ubiquitin associated). Many of the domains display chain specificity[43,64,65]. Hence, UBDs mediate the functional outcome of ubiquitination. One of these domains, the UBD of TAB2, is subject of a methodological study to isolate K63-ubiquitinated proteins, described in chapter 7.

### *1.4.4 The application of mass spectrometry in studying ubiquitination*

A major challenge in the field of ubiquitination is determining the ubiquitin chain architecture on a protein. Currently, most information available on chain linkages comes from studies using chain-specific antibodies (available for mono- and poly-ubiquitin and K11-, K48-, and K63-specific poly-ubiquitin chains[66-68]) or studies using ubiquitin mutants lacking one or more lysines. Using these methods, specific chains have been identified on several substrates.

The nature of the covalent interaction of ubiquitin with its substrate makes it suitable to study this modification by tandem mass spectrometry (tandem-MS). Trypsin digestion of an ubiquitinated lysine leads to a double glycine (diG) remnant of the C-terminus of ubiquitin, observed as a 114D mass shift in MS analysis of the parent-peptide. In this way, the abundance of ubiquitin linkages has been quantified in cells[47,69]. The percentage of mono-ubiquitination varies from 30% to 80% of the total ubiquitin pool depending on organism and cell type[70-72]. This percentage includes -apart from true substrate mono-ubiquitination- free ubiquitin and end-capped ubiquitin, representing the last ubiquitin molecule in a chain. The current view is that K48-linked chains account for approximately 40% of the total poly-ubiquitin chain population, followed by K63- and K11-linked chains, which both account for 10-20% of the total chains. The other types of chains (linked via K6, K27, K29, and K33) are detectable, though much less abundant[47,69,70]. The drawback of MS-analysis of ubiquitination is that the protein configuration is disrupted by the trypsin digestion before measurement. Therefore, it is challenging to prove the existence of mixed chains. Researchers have claimed the presence of these chains by showing MS spectra of more than one ub-linkage per purified protein[73,74]. However, this does not provide proof for mixed chains, as there might be multiple populations of the protein containing different homotypic chains. The only real proof of the existence of mixed chains has been reported by Kim *et al.* They show diG-remnants on two neighboring ubiquitin-lysines within the same peptide. However, this has only been shown in extracellular *in vitro* ubiquitination assays[75].

The diG-remnant of ubiquitin on a modified lysine after trypsin digestion is used to identify the modified substrate lysines by MS analysis. As only one or few lysines of a particular substrate are ubiquitinated, the abundance of these modified peptides is only low in the total trypsin digested sample. Recently, a novel method was introduced to preselect peptides with diG-remnants using an antibody recognizing diG-remnants in immunoprecipitation experiments. This greatly enhanced the subsequent MS-mediated identification rate of modified lysines, with over 5,000 peptide identifications in single experiments[49,76-78].



*1.4.5 Ubiquitin is part of a larger family of posttranslational modifiers*

Ubiquitin adopts a three-dimensional structure that is found in several other proteins as well, which are called ubiquitin-like proteins (UBLs). Some of these proteins can also be used for post-translational modification, like SUMO, NEDD8 and ISG15[79]. In other cases, the UBL domain is part of a larger protein in which it serves as a binding site for other proteins. The role of the various UBLs is outside the scope of this thesis.

## 1.5 The diverse role of ubiquitination in hematopoiesis

A wide cross-section of the cellular proteome is ubiquitinated at some point. This already suggests that virtually all cellular processes are somehow dependent on ubiquitination. Indeed, ubiquitination has been shown to be involved in cell cycle regulation, receptor signaling, autophagy, DNA damage repair, apoptosis and many more processes[80]. Aberrancies in protein ubiquitination can have serious consequences that can contribute to the pathogenesis of various diseases, including cancer.

The tight regulation of cell cycle progression, apoptosis and differentiation during hematopoiesis is on many levels dependent on ubiquitination. Several important hematopoietic regulators are well known subjects for ubiquitin mediated degradation, for example GFI1[81], GATA2[82], AML1[83], CEBPα[84], and MLL[85]. Another important function of ubiquitination in hematopoiesis is cell surface receptor internalization. For example, two important receptors regulating cell expansion, the FLT3-receptor and c-KIT, are ubiquitinated by the E3 cCBL and consequently internalized[86].

*1.5.1 Aberrant ubiquitination in malignant hematopoiesis*

In hematopoiesis, cell cycle regulation needs to be properly controlled to balance differentiation and self-renewal. Cell cycle regulation is highly dependent on ubiquitin, with an important role for the E3 ligase component FBW7, mutated in several hematological malignancies[87-89] (see table 1.2). The importance of ubiquitination in growth factor receptor signaling is exemplified by mutations in the E3 ligase cCBL[90,91] (table 1.2).

A well studied protein in cancer development is p53, an important cell cycle

**Table 1.2: Ubiquitin-modifiers involved in malignant hematopoiesis**

| Aberrations | Protein function | Disease | Ref. |
|---|---|---|---|
| *A20* inactivation | DUB; regulation of NF-κB signaling (see par.1.5.2.2) | Various hematological malignancies | 212 |
| *BRE* over-expression | Member of BRCA1 E3 ligase complex involved in DNA damage repair | AML, breast cancer | this thesis; 32, 213 |
| *cCBL* mutations | E3 ligase; negative regulation of receptor tyrosine kinase activity | Myeloid neoplasms | 91, 194 |
| *CYLD* hemizygous deletions and mutations | DUB; regulation of NF-κB signaling (see par.1.5.2.2) | Multiple Myeloma | 214, 215 |
| Mutations in Fanconi Anemia genes | E3 ligase complex in DNA damage repair | Aplastic anemia<br>Myeloid leukemia<br>Squamous cell carcinomas<br>Gynecological cancers | 216 |
| *FBW7* mutations | E3 ligase; regulation of cell cycle, mTOR, cMyc, Jun | Various malignancies, incl. T-ALL (no other hematological malignancies) | 87-89 |
| *MDM2* over-expression | E3 ligase for p53 | Various hematological malignancies | 93, 94 |
| *TRIB1* gain of function mutations | Enhanced ERK phosphorylation and CEBPα degradation | Case study of Down syndrome-related acute megakaryocytic leukemia | 217, 218 |
| *TRIB2* over-expression | Enhanced CEBPα degradation | AML | 84, 219 |
| *USP9X* over-expression | DUB; stabilization of pro-survival protein MCL1 | Multiple Myeloma, diffuse large B-cell lymphoma | 220 |

and apoptosis regulator. This protein is mutated in more than 50% of solid tumors. This is in strong contrast to hematopoietic malignancies that show p53 mutations in less than 10% of the patients[92]. This 'gatekeeper of our genome' is likely inactivated by other ways in leukemia's in order to promote malignant transformation. Indeed, it has been suggested that p53 is inactivated in AML by increased proteasomal degradation mediated by the E3 ligase Mdm2[93,94], although a one to one correlation of p53 and Mdm2 levels could not be confirmed[92]. A specific inhibitor of the Mdm2-p53 complex restores normal p53 levels in AML and thereby opposes the malignancy, which makes this a promising therapeutic agent in AML[95,96].

The involvement of the ubiquitin system and it's drugability in malignant hematopoiesis might be best exemplified in multiple myeloma (MM). This disease is

characterized by neoplastic proliferation of plasma cells. Therapies using the proteasome inhibitor bortezomib greatly improved patient outcome, resulting in complete clinical responses for patients with otherwise refractory and rapidly advancing disease[97]. Considering the countless pathways which depend on ubiquitination, it is not surprising that more aberrations in ubiquitination have consequences for malignant transformation. In table 1.2, a short overview can be found of ubiquitin related processes involved in malignant hematopoiesis.



*1.5.2 K63-linked ubiquitination in hematopoiesis*

Different types of ubiquitination (*e.g.* mono, K48-, K63-linked ubiquitination) all have important roles in hematopoiesis. This thesis focuses on K63-non-proteolytic ubiquitination. Signaling dependent on K63-linked ubiquitination is involved in four pathways: DNA damage repair, NF-κB and MAP kinase signaling, and receptor turnover. Deregulated DNA damage repair is inextricably linked to virtually all malignancies: underlying genetic defects, such as chromosomal translocations originate from misrepaired double strand DNA breaks (DSBs) or other types of DNA damage. The role of K63-linked ubiquitination in DNA damage repair will be explained in detail in paragraph 1.5.2.1. NF-κB signaling is shown to be hyperactive in leukemia stem cells[98,99] and survival of these cells might depend on this type of signaling[100]. The role of K63-linked ubiquitination in this pathway is explained in more detail in paragraph 1.5.2.2. Finally, deregulated receptor turnover, which is dependent on K63-linked ubiquitination, is involved in leukemia pathogenesis, as mutations in E3 ligases in this pathway occur in various hematologic malignancies (see paragraph 1.5.2.3).

Based on the relationships between K63-linked ubiquitination and malignant hematopoiesis, research has been aimed at elucidating the role of UBC13 in normal hematopoiesis, using various mouse models. *Ubc13*$^{-/-}$ mice are embryonically lethal, emphasizing the importance of this gene[101,102]. To study the role of UBC13 in hematopoiesis and NF-κB signaling, inducible gene ablation techniques were used in mouse models. *Ubc13* haploinsufficient mice, born at Mendelian frequencies, displayed resistance to LPS challenges, accompanied by reduced cytokine secretion[101]. In contrast to these data, another group found no impact of homozygous *Ubc13* deletion on TNF- or LPS-induced IκB degradation in mouse embryonic fibroblasts (MEFs)[102]. Interestingly, they only showed modest effects on NF-κB signaling, and more profound effects on MAP kinase signaling[103]. Although the downstream signaling effects seem different for the two systems, the overall effect is the same as also *Ubc13*$^{-/-}$ conditional knockout mouse macrophages show impaired TLR-induced cytokine production[102].

Recently, a hematopoiesis-restricted inducible *Ubc13* knockout mouse has been generated, displaying death within a two week period after *Ubc13* depletion[104]. A severe reduction of white blood cells (of both myeloid and lymphoid origin) and platelets in the peripheral blood was observed. Erythrocyte numbers were also decreased, although

to a lesser extent. The loss of mature blood cells was explained by a reduced frequency of hematopoietic progenitors in the bone marrow of *Ubc13*$^{-/-}$ mice, which was partially caused by increased apoptosis of these cells. In adoptive bone marrow transplantations in which *Ubc13*$^{+/+}$ and *Ubc13*$^{-/-}$ cells were mixed 1:1, it was shown that wildtype *Ubc13* cells completely outcompeted the knockout cells in all tested compartments of hematopoiesis (LSK, LK cells, B cells and myeloid cells), indicating a severe proliferation and differentiation disadvantage of *UBC13*$^{-/-}$ cells[104].

An additional role for UBC13 might lie in myeloid differentiation as *UBC13* was among the most down-regulated genes during gefitinib-induced granulocytic differentiation of HL60 cells[105]. This promyelocytic cell line model can be differentiated towards granulocytes by several external stimuli[106]. The mechanism by which gefitinib induces differentiation in these cells is not understood. Originally, gefitinib was designed as a tyrosine kinase inhibitor of the epidermal growth factor receptor (EGFR)[107]. As HL60 cells do not express EGFR, other, off-target mechanisms of action must apply in these cells. Chapter 6 will describe data on the role of UBC13 in myeloid differentiation.

All studies discussed above show an importance of UBC13 function in hematopoiesis. However, the molecular pathways and targets have not been identified, which might very well depend on cell type and stimulation. To better understand the multiple roles of K63-linked ubiquitination, the next paragraphs will review the four major pathways that depend on this type of ubiquitination.

*1.5.2.1 K63-linked ubiquitination in DNA double strand break repair*

Among a multitude of different DNA lesions, DNA double strand breaks (DSBs) are one of the most harmful ones as unrepaired DSBs can lead to chromosomal rearrangements and consequently to tumorigenesis[108]. Fortunately, cells are equipped with highly specialized repair mechanisms to quickly and reliably repair the induced DNA damage to maintain chromosomal integrity. The first steps in the repair mechanism of DSBs are highly reliant on phosphorylation, which activates a second signaling pathway mediated via K63-linked ubiquitination.

Double strand breaks are sensed by the MRE11/RAD50/NBS1 (MRN) complex via interaction of NBS1 with single stranded DNA[109]. This complex recruits the ATM kinase[110,111], which phosphorylates surrounding histone H2AX at Ser139[112,113]. Phosphorylated H2AX (γH2AX) forms the binding platform for MDC1[114,115], which is then also phosphorylated by ATM. This enforces a positive feedback loop[115-119] and catalyzes downstream signaling initiated by binding of the RING finger E3 ligase RNF8[120-122].

Downstream of RNF8 are the activation of the 53BP1 and BRCA1 signaling E3 ligase complexes that regulate the actual repair mechanisms. Recruitment of both complexes is dependent on a catalytically active RNF8 protein, as deletion of its RING domain abolishes 53BP1 or BRCA1 recruitment to the damaged DNA. Although several E2s can bind to RNF8[123], UBC13 seems to be the important E2 for DNA damage repair.

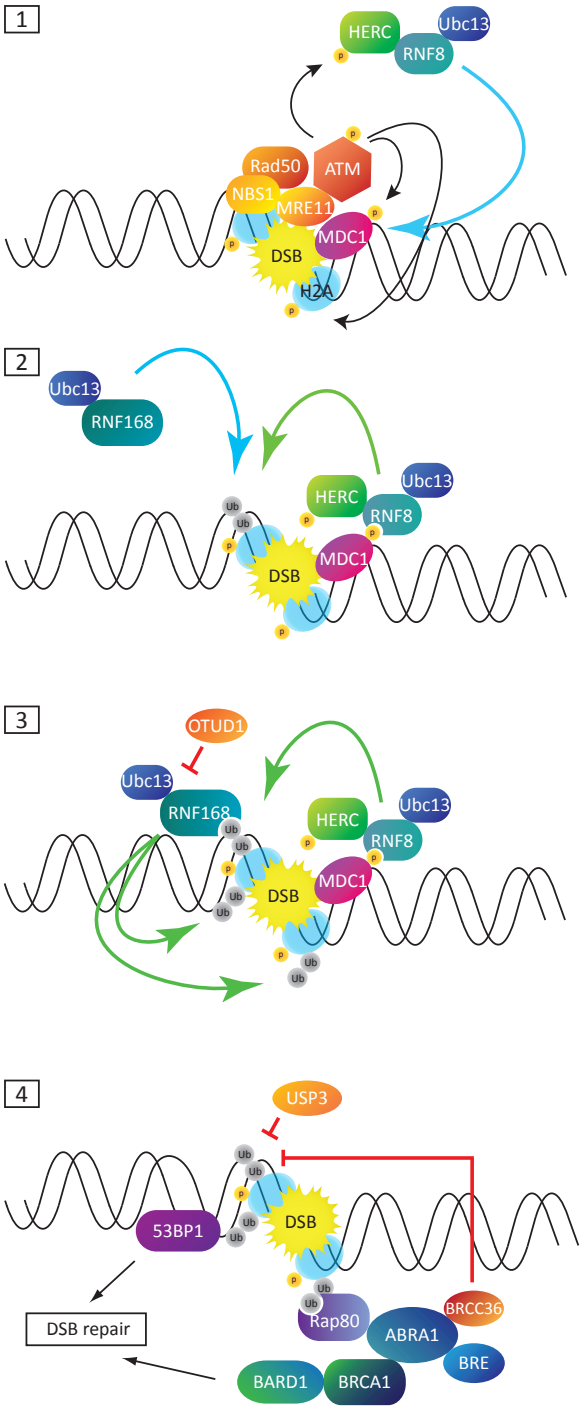


**Figure 1.3: Ubiquitination regulates DSB repair**
DNA double strand break (DSB) repair occurs in four steps. **1.** The break is sensed by the MRN-complex, which recruits MDC1 and ATM. ATM phosphorylates MDC1, H2A, H2AX and itself. MDC1 phosphorylation leads to RNF8 binding. HERC2, a binding partner of RNF8 is also phosphorylated. This E3 complex catalyzes ubiquitination on H2A and H2AX in concert with UBC13. **2.** RNF168 is recruited to the ubiquitin chains on H2A(X) **3.** RNF168 amplifies the ubiquitination. **4.** The ubiquitin chains form a binding platform for the BRCA1 E3 ligase complex and might lead to structural chromosomal reorganization and hence 53BP1 recruitment. These two complexes will activate downstream repair pathways. Throughout the pathway, several DUBs can inhibit ubiquitination by actively removing ubiquitin from the histones (USP3, BRCC36) or inhibiting the UBC13-RNF168 complex (OTUD1). Black arrows indicate phosphorylation, blue arrows indicate recruitment, green arrows indicate ubiquitination and red lines indicate deubiquitination.

Indeed, either UBC13 or RNF8 depletion completely abolishes downstream signaling. As UBC13 is currently the only E2 known to catalyze regulatory K63-linked ubiquitin chains[52], this indicates that DSB repair relies on this type of chain. RNF8 and UBC13, in combination with the cofactor MMS2 catalyze ubiquitination on surrounding H2A and H2AX, presumably in the form of di-ubiquitin chains[120,122]. An overview of the pathway is illustrated in figure 1.3.

In the last few years, two other E3 ligases have been identified in DSB repair. A second RING finger protein, RNF168, is recruited to the damaged region by binding ubiquitinated H2A via its UIM, thereby responding to RNF8 activity[124,125]. This gene is mutated in patients suffering from the immunodeficiency RIDDLE syndrome[124], a disease associated with defective DSB repair[126]. RNF168 depletion almost completely phenocopies the depletion of RNF8[124,125]. Resembling RNF8, RNF168 functions as an E3 ligase in conjunction with UBC13 and amplifies the RNF8-induced ubiquitination of H2A. Ubiquitination assays indicate that also RNF168 catalyzes ubiquitin K63-linked chain formation[124,125]. Recent data suggest that RNF168 is actually the main E3 ligase catalyzing K63-linked chains in this process, and RNF8 in addition is involved in K48-chain formation[127,128]. By marking substrates for degradation by K48-linked chains, RNF8 seems to regulate the activity of KU80, an effector protein in non homologous end joining (NHEJ) DNA repair and the checkpoint kinase 2 (CHK2), an important cell cycle regulator[127]. These recent data suggest that these first steps of DNA damage sensing are not only dependent on K63-linked ubiquitination, but also on K48-linked ubiquitination. However, exact regulation and effects of RNF8 activity are currently unknown.

In contrast to RNF168, that does not bind RNF8, the second newly identified E3 ligase, HERC2, forms a complex with RNF8 and facilitates UBC13-mediated K63-linked ubiquitin chain formation[129]. Cells depleted of HERC2 show impaired interaction of UBC13 and RNF8. This indicates that HERC2 is needed for RNF8 and UBC13 complex formation. Whether HERC2 itself is acting as E3 ligase in this pathway is however still an unanswered question[129].

A proper orchestration of the ubiquitination events in DSB repair is important. In addition, the removal of ubiquitin is equally important to prevent uncontrolled accumulation of the repair machinery in undamaged cells and to restore normal DNA replication and transcription once the DNA has been repaired. Several DUBs opposing the activity of RNF8 and RNF168 have been described, for example USP3, USP11, OTUB1 and BRCC36[130-133].

The RNF8-RNF168-HERC2 machinery forms a link between the upstream MRN, γH2AX and MDC1 early DSB sensors and the more downstream effector complexes of 53BP1 and BRCA1. Although 53BP1 recruitment is dependent on the ubiquitin signaling of RNF8/RNF168, it is currently unclear how 53BP1 senses these signals[134-136]. The recruitment of BRCA1 to the upstream RNF8-mediated ubiquitination

is much better understood, and depends on the formed K63-linked chains. BRCA1 is part of the so-called BRCA1 A complex. Next to BRCA1, this complex involves RAP80, BRCC36, BRE, ABRAXAS and MERIT40[137,138]. Rap80 contains two UIMs that directly interact with ubiquitinated histones at DNA damage sites[139-143]. Rap80 shows specificity to K6- and K63-linkages[139,142], consistent with the chains formed by the RNF8/RNF168 machinery and the BRCA1 complex. BRCA1 itself represents an E3 ligase. Together with BARD1 it catalyzes formation of the unconventional ubiquitin K6-chains[144,145]. However, *bona fide* substrates are not identified yet.

Another subunit of the BRCA1 complex is BRE, which is subject of chapter 3, 4 and 5 of this thesis. This 45kD protein binds the BRCA1 complex by direct interaction with ABRAXAS[137,138,146]. It contains two putative UEV domains and is able to interact with ubiquitin chains[138]. However, it is not yet known whether the UEV domains are needed for ubiquitin binding. Knockdown of *BRE* induced increased sensitivity to ionizing radiation and diminished BRCA1 and MERIT40 foci formation, indicating a functional role for BRE in the DNA damage response[137,138,146-148]. Next to a role in DNA damage, it has been proposed that BRE functions in the TNF-receptor pathway as *BRE* overexpression suppressed TNFα and cycloheximide induced apoptosis[149].

Although it is clear that ubiquitination is important in regulating the repair process of double strand breaks, some important issues remain unsolved, especially regarding the divergent substrates of RNF8 and RNF168, the recruitment of 53BP1 and downstream substrates of BRCA1, and the role of K48-linked chains in this process.

### *1.5.2.2 The role of linear and K63-linked ubiquitin chains in the regulation of NF-κB and MAP kinase pathways*

The MAP kinase and NF-κB pathways are important mediators in cellular responses to danger signals. The two pathways share the first steps in their activation following cellular binding of pathogens or other danger signals. As will be described below, this activation is highly dependent on the signaling function of ubiquitination[150].

NF-κB proteins are a class of transcription factors regulating immune responses and other cytokine related processes. The NF-κB signaling pathway can be stimulated by various agents, for example the pro-inflammatory cytokines TNFα and IL-1β or bacterial danger signals such as LPS (lipopolysaccharide). These extracellular molecules bind to their cognate receptors on the cell membrane. Upon ligand binding, RIP1, TRAF2, TRAF5, TRAF6 and cIAP1/2 are recruited to the receptor[151-154]. These E3 ligases catalyze the formation of K63-linked ubiquitin chains in combination with the E2 complex UBC13-UEV1a[67,155-157]. Substrates of this modification are RIP1, TRAF2 and TRAF6 itself and NEMO. Upon ubiquitination, a complex of TAK1, TAB2 and TAB3 is recruited via an interaction of the TAB-UBDs with the K63-linked chains on the ligases[43,158]. The recruitment and activation of this complex is essential for the activation of the Inhibitor of κB Kinase (IKK) complex. This complex, comprising two

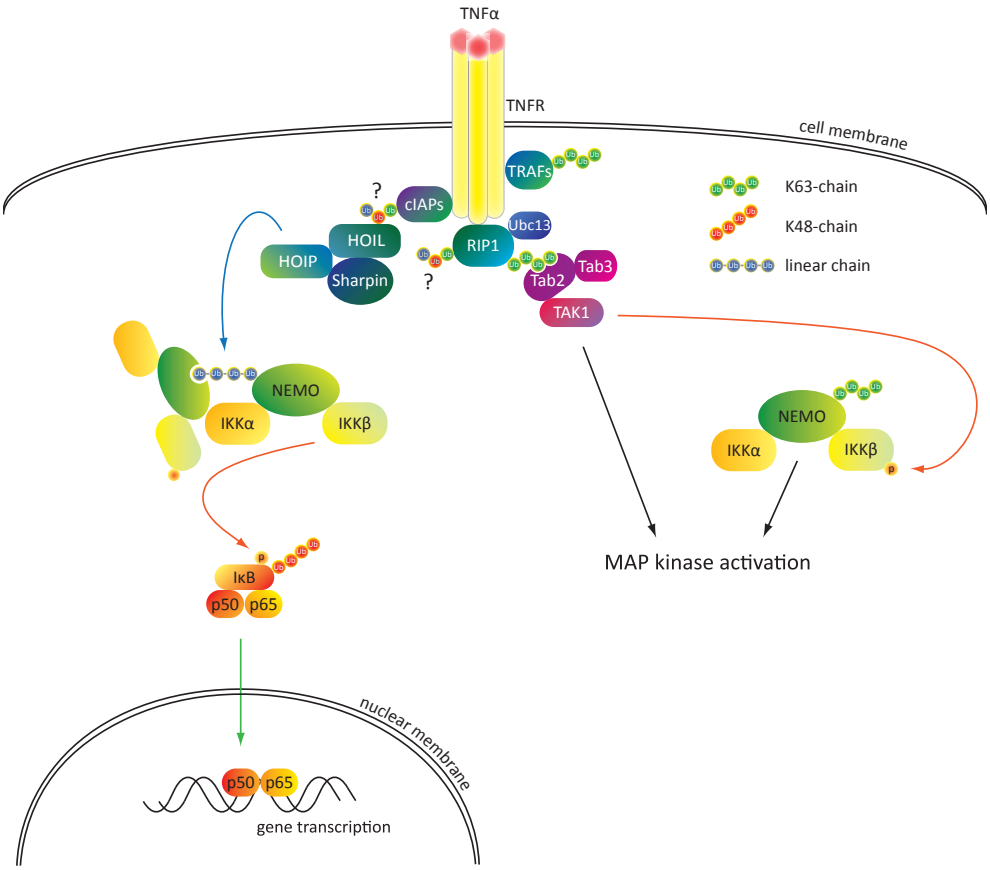


**Figure 1.4: Unconventional ubiquitination in the NF-κB pathway**
NF-κB transcription factor activation is highly dependent on ubiquitination. Upon ligand binding to the cell surface receptor, several E3 ligases are recruited to the receptor (TRAFs, cIAPs, RIP1, LUBAC complex (HOIL, HOIP, Sharpin)). These E3 ligases auto-ubiquitinate or ubiquitinate other substrates (e.g. NEMO) with K63- or linear chains. The IKK complex (NEMO-IKKα-IKKβ) is activated by linear chains on NEMO, which might lead to multimerization. Activated IKKβ phosphorylates IκB, which is then targeted for proteasomal degradation by K48-ubiquitin chains. The released NF-κB subunits translocate to the nucleus where they will induce transcription of immune regulatory genes.

catalytic domains, IKKα and IKKβ, and the regulatory subunit NEMO is recruited to the K63-linked chains present on RIP1[159] and IKKβ is subsequently phosphorylated[160,161]. In an unstimulated setting, NF-κB dimers are bound to their inhibitor IκB and are thereby kept in the cytoplasm. Upon activation of the IKK complex, IκB is phosphorylated by IKKβ, followed by poly-ubiquitination with K48-linked ubiquitin chains and

subsequent degradation[162]. The NF-κB subunits then are released and translocate to the nucleus to activate gene transcription.

The above described data suggest that this process is highly dependent on UBC13-mediated K63-linked ubiquitination. It was therefore unexpected that conditional knockout of UBC13 or ubiquitin replacement studies using K63R mutants had only little effect on NF-κB activation, although the MAP kinase pathway was severely impaired[102,163]. These data indicate that other E2s might be involved in the K63-linked chain formation or that other types of ubiquitination are important. Indeed, the latter has been shown in the past years.

In 2006, Kirisako *et al*. described the formation of linear ubiquitin chains by LUBAC (linear chain assembly complex), a complex consisting of two TRIAD domain E3 ligases, HOIP and HOIL[164]. Overexpression of LUBAC, but not expression of either ligase alone, induces NF-κB activation in several cell line models[165]. SHARPIN was recently described as a third member of the linear ubiquitin ligase complex[166-168]. LUBAC interacts with and catalyzes linear chains on NEMO[165]. Importantly, NEMO contains a ubiquitin binding domain (UBAN domain) specific for K63- and linear chains, although this domain shows lower affinity for K63-linked chains[169,170]. The binding to linear chains on a neighboring NEMO-molecule might therefore be implicated in multimerization of several NEMO-subunits, promoting the activation of IKK kinases[169].

In the early models of NF-κB activation, recruitment of NEMO was supposed to be dependent on K63-linked chains attached to RIP1. However, with the novel knowledge that K63-linked chains are dispensable for activation, it was unclear how NEMO is recruited and ubiquitinated upon ligand binding. Data from Haas *et al*. suggest simultaneous recruitment of the TAK1 complex, the IKK complex and LUBAC[171]. Once recruited, LUBAC ubiquitinates NEMO, leading to downstream signaling. An overview of the pathway can be found in figure 1.4.

All these data together propose a model in which the type of ubiquitin chain dictates the downstream signaling. Linear chains formed by LUBAC activate NF-κB signaling, whereas UBC13 mediated K63-linked chains activate the MAPK pathway[102,165]. However, the discrimination between these two pathways is not black and white, as crosstalk appears to happen[172].

To prevent improper activation of the NF-κB pathway, the pathway is negatively regulated by several DUBs. The two most studied DUBs in this pathway are A20 and CYLD. However, others have been described as well, for example USP21[173] and Cezanne[174]. Cezanne is a specific DUB for K11-chains, introducing another chain complexity contributing to NF-κB signaling[41]. The A20 DUB is rapidly upregulated upon NF-κB activation[175] and might therefore be important for terminating NF-κB activation[176]. In contrast, CYLD is active in non-stimulated cells and thereby prevents spontaneous activation of the pathway[177-179]. However, after activation of NF-κB, this protein is inactivated by phosphorylation[180,181], enabling full-blown NF-κB activation.

*1.5.2.3 Membrane receptor turnover is regulated by K63-linked ubiquitination*

Cells use a multitude of membrane associated proteins for environmental sensing. Strength and duration of downstream cellular signaling is in many cases regulated by membrane turnover of these proteins via endocytosis. Following activation, membrane proteins are often internalized in endosomes and consequently recycled back to the membrane in case of re-activation or further directed to the multivesicular bodies (MVB) and degraded in downstream lysosomes, which are, next to the proteasome, the most important protein degradation sites in the cell[182].

This sorting process is regulated by so-called 'endosomal sorting complex required for transport' (ESCRT) complexes 0 to III. Mono-ubiquitination of a cargo protein is sufficient for direct lysosomal sorting[183], however, many examples show the involvement of K63-linked chains in this process, like for the turnover of EGFR, TrkA and MHC class 1 molecules[61-63]. The current view is that K63-linked chains greatly enhance the association of ubiquitinated proteins to the MVB compared to mono-ubiquitination[184]. Following ubiquitination of the membrane receptor, the modification is recognized by the UIM and VHS domains of Hrs and STAM[185], which are part of the ESCRT-0 complex. This is followed by recruitment of ESCRT-I, -II and –III that recognize the ubiquitinated protein via several ubiquitin binding domains in each complex, leading to translocation of the modified protein to the MVB[186]. Before lysosomal degradation of the proteins, ubiquitin is recycled via the action of the K63- and mono-ubiquitin specific DUBs AMSH[187] and USP8[188].

## 1.6 Outline of this Thesis

The work described in this thesis was aimed at studying the role of ubiquitination during normal and malignant hematopoiesis, emphasizing on K63-linked ubiquitination. For this, different approaches were undertaken. A genome-wide approach was used to study correlations between clinical outcome and altered expression of ubiquitin related genes in AML. Dedicated studies on the K63-specific E2 conjugating enzyme UBC13 were performed to study its role in myeloid differentiation and proteome-wide studies were applied for the identification of substrates modified with K63-linked ubiquitin chains.

When studying correlations between gene expression and disease outcome in large patient cohorts, as described in chapter 3 and 5, it is important to obtain as much information as possible on the clinico-pathological data of the cohort, such as genetic abnormalities. Therefore, novel methods are being designed to screen for genomic aberrations in large cohorts with higher sensitivity, better reliability and reduced analysis time. **Chapter 2** describes the application of High Resolution Melting (HRM) analysis as a fast and reliable technique for screening of the recently identified mutations in *IDH1* and *IDH2* in AML.

In **Chapter 3**, differences in expression levels of genes encoding the ubiquitination machinery are correlated to disease outcome in AML. Using expression data of more than 1,600 ubiquitin related genes, high expression of the BRCA1-complex member *BRE* was identified as a favorable prognostic marker in AML, especially in patients with the recurrent chromosomal *MLL-AF9* translocation. **Chapter 4** describes the mutually exclusive expression of *BRE* with the poor prognostic factor *EVI1* in AML. The data of these two chapters improve patient classification in AML.



The BRCA1-complex is well-known for its involvement in breast cancer, as mutations in *BRCA1* occur in many familial breast cancer patients. We therefore studied whether *BRE* expression correlated with prognosis in breast cancer as well. Indeed, in **chapter 5** we show that *BRE* expression predicted disease outcome in breast cancer. Depending on whether patients received radiotherapy or not as part of their primary treatment, high *BRE* expression at diagnosis predicted a favorable or an adverse outcome, respectively.

In **chapter 6**, the role of UBC13 is studied during myelopoiesis. UBC13 levels were downregulated during granulocytic and monocytic differentiation of different cell line models. Knockdown of UBC13 in the U937 cell line hampered monocytic differentiation, indicating that the high expression in progenitor cells might be needed for subsequent differentiation.

**Chapter 7** describes a novel method to isolate endogenous substrates of K63-linked ubiquitination. Until now, research has relied on overexpression of tagged ubiquitin mutants to study specific chain formation. However, overexpression and the use of tags introduce negative side effects. The novel method described in chapter 7 is based on the isolation of proteins with K63-linked ubiquitin chains from cellular extracts using K63-specific ubiquitin binding domains. After isolation, protein identification was achieved by mass spectrometry.

## Reference List


1. Hershko,A. & Ciechanover,A. Mechanisms of intracellular protein break down. *Annu. Rev. Biochem.* **51**, 335-364 (1982).
2. Hoffbrand,A.V., Moss,P.A.H., & Pettit,J.E. *Essential Hematology* (2006).
3. Brown,G., Hughes,P.J., Michell,R.H., & Ceredig,R. The versatility of haematopoietic stem cells: implications for leukaemia. *Crit Rev. Clin. Lab Sci.* **47**, 171-180 (2010).
4. Dick,J.E. Stem cell concepts renew cancer research. *Blood* **112**, 4793-4807 (2008).
5. Balciunaite,G., Ceredig,R., Massa,S., & Rolink,A.G. A B220+ CD117+ CD19- hematopoietic progenitor with potent lymphoid and myeloid developmental potential. *Eur. J. Immunol.* **35**, 2019-2030 (2005).
6. Adolfsson,J. *et al.* Identification of Flt3+ lympho-myeloid stem cells lacking erythro-megakaryocytic potential a revised road map for adult blood lineage commitment. *Cell* **121**, 295-306 (2005).
7. Goardon,N. *et al.* Coexistence of LMPP-like and GMP-like leukemia stem cells in acute myeloid leukemia. *Cancer Cell* **19**, 138-152 (2011).
8. Zhang,P. *et al.* Enhancement of hematopoietic stem cell repopulating capacity and self-renewal in the absence of the transcription factor C/EBP alpha. *Immunity.* **21**, 853-863 (2004).
9. Vardiman,J.W. *et al.* The 2008 revision of the World Health Organization (WHO) classification of myeloid neoplasms and acute leukemia: rationale and important changes. *Blood* **114**, 937-951 (2009).
10. Grimwade,D. *et al.* Refinement of cytogenetic classification in acute myeloid leukemia: determination of prognostic significance of rare recurring chromosomal abnormalities among 5876 younger adult patients treated in the United Kingdom Medical Research Council trials. *Blood* **116**, 354-365 (2010).
11. Mandelli,F. *et al.* Daunorubicin versus mitoxantrone versus idarubicin as induction and consolidation chemotherapy for adults with acute myeloid leukemia: the EORTC and GIMEMA Groups Study AML-10. *J. Clin. Oncol.* **27**, 5397-5403 (2009).
12. Manola,K.N. Cytogenetics of pediatric acute myeloid leukemia. *Eur. J. Haematol.* **83**, 391-405 (2009).
13. Burnett,A.K. *et al.* The impact of dose escalation and resistance modulation in older patients with acute myeloid leukaemia and high risk myelodysplastic syndrome: the results of the LRF AML14 trial. *Br. J. Haematol.* **145**, 318-332 (2009).
14. Bonnet,D. & Dick,J.E. Human acute myeloid leukemia is organized as a hierarchy that originates from a primitive hematopoietic cell. *Nat. Med.* **3**, 730-737 (1997).
15. Eppert,K. *et al.* Stem cell gene expression programs influence clinical outcome in human leukemia. *Nat. Med.* **17**, 1086-1093 (2011).
16. Taussig,D.C. *et al.* Anti-CD38 antibody-mediated clearance of human repopulating cells masks the heterogeneity of leukemia-initiating cells. *Blood* **112**, 568-575 (2008).
17. Wang,J.C. & Dick,J.E. Cancer stem cells: lessons from leukemia. *Trends Cell Biol.* **15**, 494-501 (2005).
18. Krivtsov,A.V. *et al.* Transformation from committed progenitor to leukaemia stem cell initiated by MLL-AF9. *Nature* **442**, 818-822 (2006).
19. Valk,P.J. *et al.* Prognostically useful gene-expression profiles in acute myeloid leukemia. *N. Engl. J. Med.* **350**, 1617-1628 (2004).
20. Bullinger,L. et al. Use of gene-expression profiling to identify prognostic subclasses in adult acute myeloid leukemia. N. Engl. J. Med. 350, 1605-1616 (2004).
21. Mardis,E.R. *et al.* Recurring mutations found by sequencing an acute myeloid leukemia genome. *N. Engl. J. Med.* **361**, 1058-1066 (2009).

22. Dash,A. & Gilliland,D.G. Molecular genetics of acute myeloid leukaemia. *Best. Pract. Res. Clin. Haematol.* **14**, 49-64 (2001).
23. Renneville,A. *et al.* Cooperating gene mutations in acute myeloid leukemia: a review of the literature. *Leukemia* **22**, 915-931 (2008).
24. Marteijn,J.A., Jansen,J.H., & van der Reijden,B.A. Ubiquitylation in normal and malignant hematopoiesis: novel therapeutic targets. *Leukemia* **20**, 1511-1518 (2006).
25. Heuze,M.L., Lamsoul,I., Moog-Lutz,C., & Lutz,P.G. Ubiquitin-mediated proteasomal degradation in normal and malignant hematopoiesis. *Blood Cells Mol. Dis.* **40**, 200-210 (2008).
26. Hershko,A., Ciechanover,A., Heller,H., Haas,A.L., & Rose,I.A. Proposed role of ATP in protein breakdown: conjugation of protein with multiple chains of the polypeptide of ATP-dependent proteolysis. *Proc. Natl. Acad. Sci. U. S. A* **77**, 1783-1786 (1980).
27. Hoeller,D. & Dikic,I. Targeting the ubiquitin system in cancer therapy. *Nature* **458**, 438-444 (2009).
28. Komander,D., Clague,M.J., & Urbe,S. Breaking the chains: structure and function of the deubiquitinases. *Nat. Rev. Mol. Cell Biol.* **10**, 550-563 (2009).
29. Schwartz,A.L. & Ciechanover,A. The ubiquitin-proteasome pathway and pathogenesis of human diseases. *Annu. Rev. Med.* **50**, 57-74 (1999).
30. van der Reijden,B.A., Erpelinck-Verschueren,C.A., Lowenberg,B., & Jansen,J.H. TRIADs: a new class of proteins with a novel cysteine-rich signature. *Protein Sci.* **8**, 1557-1561 (1999).
31. Wenzel,D.M., Lissounov,A., Brzovic,P.S., & Klevit,R.E. UBCH7 reactivity profile reveals parkin and HHARI to be RING/HECT hybrids. *Nature* **474**, 105-108 (2011).
32. Noordermeer,S.M. *et al.* High BRE expression predicts favorable outcome in adult acute myeloid leukemia, in particular among MLL-AF9-positive patients. *Blood* **118**, 5613-5621 (2011).
33. van Wijk,S.J. *et al.* A comprehensive framework of E2-RING E3 interactions of the human ubiquitin-proteasome system. *Mol. Syst. Biol.* **5**, 295 (2009).
34. Deshaies,R.J. & Joazeiro,C.A. RING domain E3 ubiquitin ligases. *Annu. Rev. Biochem.* **78**, 399-434 (2009).
35. Ikeda,F. & Dikic,I. Atypical ubiquitin chains: new molecular signals. 'Protein Modifications: Beyond the Usual Suspects' review series. *EMBO Rep.* **9**, 536-542 (2008).
36. Komander,D. The emerging complexity of protein ubiquitination. *Biochem. Soc. Trans.* **37**, 937-953 (2009).
37. Ciechanover,A. & Ben-Saadon,R. N-terminal ubiquitination: more protein substrates join in. *Trends Cell Biol.* **14**, 103-106 (2004).
38. Cadwell,K. & Coscoy,L. Ubiquitination on nonlysine residues by a viral E3 ubiquitin ligase. *Science* **309**, 127-130 (2005).
39. Wang,X., Herr,R.A., & Hansen,T.H. Ubiquitination of substrates by esterification. *Traffic.* **13**, 19-24 (2012).
40. Breitschopf,K., Bengal,E., Ziv,T., Admon,A., & Ciechanover,A. A novel site for ubiquitination: the N-terminal residue, and not internal lysines of MyoD, is essential for conjugation and degradation of the protein. *EMBO J.* **17**, 5964-5973 (1998).
41. Bremm,A., Freund,S.M., & Komander,D. Lys11-linked ubiquitin chains adopt compact conformations and are preferentially hydrolyzed by the deubiquitinase Cezanne. *Nat. Struct. Mol. Biol.* **17**, 939-947 (2010).
42. Eddins,M.J., Varadan,R., Fushman,D., Pickart,C.M., & Wolberger,C. Crystal structure and solution NMR studies of Lys48-linked tetraubiquitin at neutral pH. *J. Mol. Biol.* **367**, 204-211 (2007).
43. Komander,D. *et al.* Molecular discrimination of structurally equivalent Lys 63-linked and linear polyubiquitin chains. *EMBO Rep.* **10**, 466-473 (2009).
44. Varadan,R., Walker,O., Pickart,C., & Fushman,D. Structural properties of polyubiquitin chains in

solution. *J. Mol. Biol.* **324**, 637-647 (2002).
45. Varadan,R. *et al.* Solution conformation of Lys63-linked di-ubiquitin chain provides clues to functional diversity of polyubiquitin signaling. *J. Biol. Chem.* **279**, 7055-7063 (2004).
46. Navon,A. & Ciechanover,A. The 26 S proteasome: from basic mechanisms to drug targeting. *J. Biol. Chem.* **284**, 33713-33718 (2009).
47. Xu,P. *et al.* Quantitative proteomics reveals the function of unconventional ubiquitin chains in proteasomal degradation. *Cell* **137**, 133-145 (2009).
48. Meierhofer,D., Wang,X., Huang,L., & Kaiser,P. Quantitative analysis of global ubiquitination in HeLa cells by mass spectrometry. *J. Proteome. Res.* **7**, 4566-4576 (2008).
49. Wagner,S.A. *et al.* A proteome-wide, quantitative survey of in vivo ubiquitylation sites reveals widespread regulatory roles. *Mol. Cell Proteomics.* **10**, M111 (2011).
50. Baboshina,O.V. & Haas,A.L. Novel multiubiquitin chain linkages catalyzed by the conjugating enzymes E2EPF and RAD6 are recognized by 26 S proteasome subunit 5. *J. Biol. Chem.* **271**, 2823-2831 (1996).
51. Jin,L., Williamson,A., Banerjee,S., Philipp,I., & Rape,M. Mechanism of ubiquitin-chain formation by the human anaphase-promoting complex. *Cell* **133**, 653-665 (2008).
52. Andersen,P.L. *et al.* Distinct regulation of Ubc13 functions by the two ubiquitin-conjugating enzyme variants Mms2 and Uev1A. *J. Cell Biol.* **170**, 745-755 (2005).
53. Hofmann,R.M. & Pickart,C.M. Noncanonical MMS2-encoded ubiquitin-conjugating enzyme functions in assembly of novel polyubiquitin chains for DNA repair. *Cell* **96**, 645-653 (1999).
54. VanDemark,A.P., Hofmann,R.M., Tsui,C., Pickart,C.M., & Wolberger,C. Molecular insights into polyubiquitin chain assembly: crystal structure of the Mms2/Ubc13 heterodimer. *Cell* **105**, 711-720 (2001).
55. Eddins,M.J., Carlile,C.M., Gomez,K.M., Pickart,C.M., & Wolberger,C. Mms2-Ubc13 covalently bound to ubiquitin reveals the structural basis of linkage-specific polyubiquitin chain formation. *Nat. Struct. Mol. Biol.* **13**, 915-920 (2006).
56. Moraes,T.F. *et al.* Crystal structure of the human ubiquitin conjugating enzyme complex, hMms2-hUbc13. *Nat. Struct. Biol.* **8**, 669-673 (2001).
57. Deng,L. *et al.* Activation of the IkappaB kinase complex by TRAF6 requires a dimeric ubiquitin-conjugating enzyme complex and a unique polyubiquitin chain. *Cell* **103**, 351-361 (2000).
58. Syed,N.A., Andersen,P.L., Warrington,R.C., & Xiao,W. Uev1A, a ubiquitin conjugating enzyme variant, inhibits stress-induced apoptosis through NF-kappaB activation. *Apoptosis.* **11**, 2147-2157 (2006).
59. Huen,M.S. *et al.* Noncanonical E2 variant-independent function of UBC13 in promoting checkpoint protein assembly. *Mol. Cell Biol.* **28**, 6104-6112 (2008).
60. Kamsteeg,E.J. *et al.* Short-chain ubiquitination mediates the regulated endocytosis of the aquaporin-2 water channel. *Proc. Natl. Acad. Sci. U. S. A* **103**, 18344-18349 (2006).
61. Geetha,T., Jiang,J., & Wooten,M.W. Lysine 63 polyubiquitination of the nerve growth factor receptor TrkA directs internalization and signaling. *Mol. Cell* **20**, 301-312 (2005).
62. Duncan,L.M. *et al.* Lysine-63-linked ubiquitination is required for endolysosomal degradation of class I molecules. *EMBO J.* **25**, 1635-1645 (2006).
63. Huang,F., Kirkpatrick,D., Jiang,X., Gygi,S., & Sorkin,A. Differential regulation of EGF receptor internalization and degradation by multiubiquitination within the kinase domain. *Mol. Cell* **21**, 737-748 (2006).
64. Buchberger,A. From UBA to UBX: new words in the ubiquitin vocabulary. *Trends Cell Biol.* **12**, 216-221 (2002).
65. Dikic,I., Wakatsuki,S., & Walters,K.J. Ubiquitin-binding domains - from structures to functions. *Nat. Rev. Mol. Cell Biol.* **10**, 659-671 (2009).

66. Matsumoto,M.L. *et al.* K11-linked polyubiquitination in cell cycle control revealed by a K11 linkage-specific antibody. *Mol. Cell* **39**, 477-484 (2010).
67. Newton,K. *et al.* Ubiquitin chain editing revealed by polyubiquitin linkage-specific antibodies. *Cell* **134**, 668-678 (2008).
68. Wang,H. *et al.* Analysis of nondegradative protein ubiquitylation with a monoclonal antibody specific for lysine-63-linked polyubiquitin. *Proc. Natl. Acad. Sci. U. S. A* **105**, 20197-20202 (2008).
69. Danielsen,J.M. *et al.* Mass spectrometric analysis of lysine ubiquitylation reveals promiscuity at site level. *Mol. Cell Proteomics.* **10**, M110 (2011).
70. Kaiser,S.E. *et al.* Protein standard absolute quantification (PSAQ) method for the measurement of cellular ubiquitin pools. *Nat. Methods* **8**, 691-696 (2011).
71. Phu,L. *et al.* Improved quantitative mass spectrometry methods for characterizing complex ubiquitin signals. *Mol. Cell Proteomics.* **10**, M110 (2011).
72. Ziv,I. *et al.* A perturbed ubiquitin landscape distinguishes between ubiquitin in trafficking and in proteolysis. *Mol. Cell Proteomics.* **10**, M111 (2011).
73. Phu,L. *et al.* Improved quantitative mass spectrometry methods for characterizing complex ubiquitin signals. *Mol. Cell Proteomics.* **10**, M110 (2011).
74. Boname,J.M. *et al.* Efficient internalization of MHC I requires lysine-11 and lysine-63 mixed linkage polyubiquitin chains. *Traffic.* **11**, 210-220 (2010).
75. Kim,H.T. *et al.* Certain pairs of ubiquitin-conjugating enzymes (E2s) and ubiquitin-protein ligases (E3s) synthesize nondegradable forked ubiquitin chains containing all possible isopeptide linkages. *J. Biol. Chem.* **282**, 17375-17386 (2007).
76. Kim,W. *et al.* Systematic and quantitative assessment of the ubiquitin-modified proteome. *Mol. Cell* **44**, 325-340 (2011).
77. Emanuele,M.J. *et al.* Global identification of modular cullin-RING ligase substrates. *Cell* **147**, 459-474 (2011).
78. Xu,G., Paige,J.S., & Jaffrey,S.R. Global analysis of lysine ubiquitination by ubiquitin remnant immunoaffinity profiling. *Nat. Biotechnol.* **28**, 868-873 (2010).
79. Hochstrasser,M. Origin and function of ubiquitin-like proteins. *Nature* **458**, 422-429 (2009).
80. Hoeller,D., Hecker,C.M., & Dikic,I. Ubiquitin and ubiquitin-like proteins in cancer pathogenesis. *Nat. Rev. Cancer* **6**, 776-788 (2006).
81. Marteijn,J.A. *et al.* Diminished proteasomal degradation results in accumulation of Gfi1 protein in monocytes. *Blood* **109**, 100-108 (2007).
82. Minegishi,N., Suzuki,N., Kawatani,Y., Shimizu,R., & Yamamoto,M. Rapid turnover of GATA-2 via ubiquitin-proteasome protein degradation pathway. *Genes Cells* **10**, 693-704 (2005).
83. Huang,G. *et al.* Dimerization with PEBP2beta protects RUNX1/AML1 from ubiquitin-proteasome-mediated degradation. *EMBO J.* **20**, 723-733 (2001).
84. Dedhia,P.H. *et al.* Differential ability of Tribbles family members to promote degradation of C/EBPalpha and induce acute myelogenous leukemia. *Blood* **116**, 1321-1328 (2010).
85. Liu,H., Cheng,E.H., & Hsieh,J.J. Bimodal degradation of MLL by SCFSkp2 and APCCdc20 assures cell cycle execution: a critical regulatory circuit lost in leukemogenic MLL fusions. *Genes Dev.* **21**, 2385-2398 (2007).
86. Toffalini,F. & Demoulin,J.B. New insights into the mechanisms of hematopoietic cell transformation by activated receptor tyrosine kinases. *Blood* **116**, 2429-2437 (2010).
87. Welcker,M. & Clurman,B.E. FBW7 ubiquitin ligase: a tumour suppressor at the crossroads of cell division, growth and differentiation. *Nat. Rev. Cancer* **8**, 83-93 (2008).
88. Reavie,L. *et al.* Regulation of hematopoietic stem cell differentiation by a single ubiquitin ligase-substrate complex. *Nat. Immunol.* **11**, 207-215 (2010).
89. Thompson,B.J. *et al.* Control of hematopoietic stem cell quiescence by the E3 ubiquitin ligase

Fbw7. *J. Exp. Med.* **205**, 1395-1408 (2008).
90. Toffalini,F. & Demoulin,J.B. New insights into the mechanisms of hematopoietic cell transformation by activated receptor tyrosine kinases. *Blood* **116**, 2429-2437 (2010).
91. Ogawa,S. *et al.* Deregulated intracellular signaling by mutated c-CBL in myeloid neoplasms. *Clin. Cancer Res.* **16**, 3825-3831 (2010).
92. Long,J. *et al.* Multiple distinct molecular mechanisms influence sensitivity and resistance to MDM2 inhibitors in adult acute myelogenous leukemia. *Blood* **116**, 71-80 (2010).
93. Bueso-Ramos,C.E. *et al.* The human MDM-2 oncogene is overexpressed in leukemias. *Blood* **82**, 2617-2623 (1993).
94. Watanabe,T., Ichikawa,A., Saito,H., & Hotta,T. Overexpression of the MDM2 oncogene in leukemia and lymphoma. *Leuk. Lymphoma* **21**, 391-7, color (1996).
95. Carter,B.Z. *et al.* Simultaneous activation of p53 and inhibition of XIAP enhance the activation of apoptosis signaling pathways in AML. *Blood* **115**, 306-314 (2010).
96. Kojima,K. *et al.* MDM2 antagonists induce p53-dependent apoptosis in AML: implications for leukemia therapy. *Blood* **106**, 3150-3159 (2005).
97. Shah,J.J. & Orlowski,R.Z. Proteasome inhibitors in the treatment of multiple myeloma. *Leukemia* **23**, 1964-1979 (2009).
98. Guzman,M.L. *et al.* Nuclear factor-kappaB is constitutively activated in primitive human acute myelogenous leukemia cells. *Blood* **98**, 2301-2307 (2001).
99. Konopleva,M.Y. & Jordan,C.T. Leukemia stem cells and microenvironment: biology and therapeutic targeting. *J. Clin. Oncol.* **29**, 591-599 (2011).
100. Guzman,M.L. *et al.* Preferential induction of apoptosis for primary human leukemic stem cells. *Proc. Natl. Acad. Sci. U. S. A* **99**, 16220-16225 (2002).
101. Fukushima,T. *et al.* Ubiquitin-conjugating enzyme Ubc13 is a critical component of TNF receptor-associated factor (TRAF)-mediated inflammatory responses. *Proc. Natl. Acad. Sci. U. S. A* **104**, 6371-6376 (2007).
102. Yamamoto,M. *et al.* Key function for the Ubc13 E2 ubiquitin-conjugating enzyme in immune receptor signaling. *Nat. Immunol.* **7**, 962-970 (2006).
103. Yamamoto,M. *et al.* Cutting Edge: Pivotal function of Ubc13 in thymocyte TCR signaling. *J. Immunol.* **177**, 7520-7524 (2006).
104. Wu,X., Yamamoto,M., Akira,S., & Sun,S.C. Regulation of hematopoiesis by the K63-specific ubiquitin-conjugating enzyme Ubc13. *Proc. Natl. Acad. Sci. U. S. A* **106**, 20836-20841 (2009).
105. Stegmaier,K. *et al.* Gefitinib induces myeloid differentiation of acute myeloid leukemia. *Blood* **106**, 2841-2848 (2005).
106. Gallagher,R. *et al.* Characterization of the continuous, differentiating myeloid cell line (HL-60) from a patient with acute promyelocytic leukemia. *Blood* **54**, 713-733 (1979).
107. Wakeling,A.E. *et al.* ZD1839 (Iressa): an orally active inhibitor of epidermal growth factor signaling with potential for cancer therapy. *Cancer Res.* **62**, 5749-5754 (2002).
108. Jeggo,P.A. & Lobrich,M. DNA double-strand breaks: their cellular and clinical impact? *Oncogene* **26**, 7717-7719 (2007).
109. Bekker-Jensen,S. *et al.* Spatial organization of the mammalian genome surveillance machinery in response to DNA strand breaks. *J. Cell Biol.* **173**, 195-206 (2006).
110. Lee,J.H. & Paull,T.T. ATM activation by DNA double-strand breaks through the Mre11-Rad50-Nbs1 complex. *Science* **308**, 551-554 (2005).
111. Uziel,T. *et al.* Requirement of the MRN complex for ATM activation by DNA damage. *EMBO J.* **22**, 5612-5621 (2003).
112. Rogakou,E.P., Pilch,D.R., Orr,A.H., Ivanova,V.S., & Bonner,W.M. DNA double-stranded breaks induce histone H2AX phosphorylation on serine 139. *J. Biol. Chem.* **273**, 5858-5868 (1998).

113. Burma,S., Chen,B.P., Murphy,M., Kurimasa,A., & Chen,D.J. ATM phosphorylates histone H2AX in response to DNA double-strand breaks. *J. Biol. Chem.* **276**, 42462-42467 (2001).
114. Stewart,G.S., Wang,B., Bignell,C.R., Taylor,A.M., & Elledge,S.J. MDC1 is a mediator of the mammalian DNA damage checkpoint. *Nature* **421**, 961-966 (2003).
115. Stucki,M. *et al.* MDC1 directly binds phosphorylated histone H2AX to regulate cellular responses to DNA double-strand breaks. *Cell* **123**, 1213-1226 (2005).
116. Chapman,J.R. & Jackson,S.P. Phospho-dependent interactions between NBS1 and MDC1 mediate chromatin retention of the MRN complex at sites of DNA damage. *EMBO Rep.* **9**, 795-801 (2008).
117. Lou,Z. *et al.* MDC1 maintains genomic stability by participating in the amplification of ATM-dependent DNA damage signals. *Mol. Cell* **21**, 187-200 (2006).
118. Melander,F. *et al.* Phosphorylation of SDT repeats in the MDC1 N terminus triggers retention of NBS1 at the DNA damage-modified chromatin. *J. Cell Biol.* **181**, 213-226 (2008).
119. Spycher,C. *et al.* Constitutive phosphorylation of MDC1 physically links the MRE11-RAD50-NBS1 complex to damaged chromatin. *J. Cell Biol.* **181**, 227-240 (2008).
120. Huen,M.S. *et al.* RNF8 transduces the DNA-damage signal via histone ubiquitylation and checkpoint protein assembly. *Cell* **131**, 901-914 (2007).
121. Kolas,N.K. *et al.* Orchestration of the DNA-damage response by the RNF8 ubiquitin ligase. *Science* **318**, 1637-1640 (2007).
122. Mailand,N. *et al.* RNF8 ubiquitylates histones at DNA double-strand breaks and promotes assembly of repair proteins. *Cell* **131**, 887-900 (2007).
123. Ito,K. *et al.* N-Terminally extended human ubiquitin-conjugating enzymes (E2s) mediate the ubiquitination of RING-finger proteins, ARA54 and RNF8. *Eur. J. Biochem.* **268**, 2725-2732 (2001).
124. Stewart,G.S. *et al.* The RIDDLE syndrome protein mediates a ubiquitin-dependent signaling cascade at sites of DNA damage. *Cell* **136**, 420-434 (2009).
125. Doil,C. *et al.* RNF168 binds and amplifies ubiquitin conjugates on damaged chromosomes to allow accumulation of repair proteins. *Cell* **136**, 435-446 (2009).
126. Stewart,G.S. *et al.* RIDDLE immunodeficiency syndrome is linked to defects in 53BP1-mediated DNA damage signaling. *Proc. Natl. Acad. Sci. U. S. A* **104**, 16910-16915 (2007).
127. Feng,L. & Chen,J. The E3 ligase RNF8 regulates KU80 removal and NHEJ repair. *Nat. Struct. Mol. Biol.*(2012).
128. Lok,G.T. *et al.* Differential regulation of RNF8-mediated Lys48- and Lys63-based poly-ubiquitylation. *Nucleic Acids Res.* **40**, 196-205 (2012).
129. Bekker-Jensen,S. *et al.* HERC2 coordinates ubiquitin-dependent assembly of DNA repair factors on damaged chromosomes. *Nat. Cell Biol.* **12**, 80-86 (2010).
130. Nicassio,F. *et al.* Human USP3 is a chromatin modifier required for S phase progression and genome stability. *Curr. Biol.* **17**, 1972-1977 (2007).
131. Shao,G. *et al.* The Rap80-BRCC36 de-ubiquitinating enzyme complex antagonizes RNF8-Ubc13-dependent ubiquitination events at DNA double strand breaks. *Proc. Natl. Acad. Sci. U. S. A* **106**, 3166-3171 (2009).
132. Wiltshire,T.D. *et al.* Sensitivity to poly(ADP-ribose) polymerase (PARP) inhibition identifies ubiquitin-specific peptidase 11 (USP11) as a regulator of DNA double-strand break repair. *J. Biol. Chem.* **285**, 14565-14571 (2010).
133. Nakada,S. *et al.* Non-canonical inhibition of DNA damage-dependent ubiquitination by OTUB1. *Nature* **466**, 941-946 (2010).
134. Huyen,Y. *et al.* Methylated lysine 79 of histone H3 targets 53BP1 to DNA double-strand breaks. *Nature* **432**, 406-411 (2004).
135. Botuyan,M.V. *et al.* Structural basis for the methylation state-specific recognition of histone

H4-K20 by 53BP1 and Crb2 in DNA repair. *Cell* **127**, 1361-1373 (2006).
136. Yang,H. & Mizzen,C.A. The multiple facets of histone H4-lysine 20 methylation. *Biochem. Cell Biol.* **87**, 151-161 (2009).
137. Dong,Y. *et al.* Regulation of BRCC, a holoenzyme complex containing BRCA1 and BRCA2, by a signalosome-like subunit and its role in DNA repair. *Mol. Cell* **12**, 1087-1099 (2003).
138. Wang,B., Hurov,K., Hofmann,K., & Elledge,S.J. NBA1, a new player in the Brca1 A complex, is required for DNA damage resistance and checkpoint control. *Genes Dev.* **23**, 729-739 (2009).
139. Sobhian,B. *et al.* RAP80 targets BRCA1 to specific ubiquitin structures at DNA damage sites. *Science* **316**, 1198-1202 (2007).
140. Wang,B. *et al.* Abraxas and RAP80 form a BRCA1 protein complex required for the DNA damage response. *Science* **316**, 1194-1198 (2007).
141. Wang,B. & Elledge,S.J. Ubc13/Rnf8 ubiquitin ligases control foci formation of the Rap80/Abraxas/Brca1/Brcc36 complex in response to DNA damage. *Proc. Natl. Acad. Sci. U. S. A* **104**, 20759-20763 (2007).
142. Kim,H., Chen,J., & Yu,X. Ubiquitin-binding protein RAP80 mediates BRCA1-dependent DNA damage response. *Science* **316**, 1202-1205 (2007).
143. Yan,J. *et al.* The ubiquitin-interacting motif containing protein RAP80 interacts with BRCA1 and functions in DNA damage repair response. *Cancer Res.* **67**, 6647-6656 (2007).
144. Nishikawa,H. *et al.* Mass spectrometric and mutational analyses reveal Lys-6-linked polyubiquitin chains catalyzed by BRCA1-BARD1 ubiquitin ligase. *J. Biol. Chem.* **279**, 3916-3924 (2004).
145. Wu-Baer,F., Lagrazon,K., Yuan,W., & Baer,R. The BRCA1/BARD1 heterodimer assembles polyubiquitin chains through an unconventional linkage involving lysine residue K6 of ubiquitin. *J. Biol. Chem.* **278**, 34743-34746 (2003).
146. Feng,L., Huang,J., & Chen,J. MERIT40 facilitates BRCA1 localization and DNA damage repair. *Genes Dev.* **23**, 719-728 (2009).
147. Hu,X. *et al.* NBA1/MERIT40 and BRE interaction is required for the integrity of two distinct deubiquitinating enzyme BRCC36-containing complexes. *J. Biol. Chem.* **286**, 11734-11745 (2011).
148. Shao,G. *et al.* MERIT40 controls BRCA1-Rap80 complex integrity and recruitment to DNA double-strand breaks. *Genes Dev.* **23**, 740-754 (2009).
149. Li,Q. *et al.* A death receptor-associated anti-apoptotic protein, BRE, inhibits mitochondrial apoptotic pathway. *J. Biol. Chem.* **279**, 52106-52116 (2004).
150. Karin,M. & Gallagher,E. TNFR signaling: ubiquitin-conjugated TRAFfic signals control stop-and-go for MAPK signaling complexes. *Immunol. Rev.* **228**, 225-240 (2009).
151. Micheau,O. & Tschopp,J. Induction of TNF receptor I-mediated apoptosis via two sequential signaling complexes. *Cell* **114**, 181-190 (2003).
152. Hsu,H., Huang,J., Shu,H.B., Baichwal,V., & Goeddel,D.V. TNF-dependent recruitment of the protein kinase RIP to the TNF receptor-1 signaling complex. *Immunity.* **4**, 387-396 (1996).
153. Shu,H.B., Takeuchi,M., & Goeddel,D.V. The tumor necrosis factor receptor 2 signal transducers TRAF2 and c-IAP1 are components of the tumor necrosis factor receptor 1 signaling complex. *Proc. Natl. Acad. Sci. U. S. A* **93**, 13973-13978 (1996).
154. Cao,Z., Xiong,J., Takeuchi,M., Kurama,T., & Goeddel,D.V. TRAF6 is a signal transducer for interleukin-1. *Nature* **383**, 443-446 (1996).
155. Wertz,I.E. *et al.* De-ubiquitination and ubiquitin ligase domains of A20 downregulate NF-kappaB signalling. *Nature* **430**, 694-699 (2004).
156. Ea,C.K., Deng,L., Xia,Z.P., Pineda,G., & Chen,Z.J. Activation of IKK by TNFalpha requires site-specific ubiquitination of RIP1 and polyubiquitin binding by NEMO. *Mol. Cell* **22**, 245-257 (2006).
157. Li,H., Kobayashi,M., Blonska,M., You,Y., & Lin,X. Ubiquitination of RIP is required for tumor

necrosis factor alpha-induced NF-kappaB activation. *J. Biol. Chem.* **281**, 13636-13643 (2006).
158. Kanayama,A. *et al.* TAB2 and TAB3 activate the NF-kappaB pathway through binding to polyubiquitin chains. *Mol. Cell* **15**, 535-548 (2004).
159. Wu,C.J., Conze,D.B., Li,T., Srinivasula,S.M., & Ashwell,J.D. Sensing of Lys 63-linked polyubiquitination by NEMO is a key event in NF-kappaB activation [corrected]. *Nat. Cell Biol.* **8**, 398-406 (2006).
160. Schomer-Miller,B., Higashimoto,T., Lee,Y.K., & Zandi,E. Regulation of IkappaB kinase (IKK) complex by IKKgamma-dependent phosphorylation of the T-loop and C terminus of IKKbeta. *J. Biol. Chem.* **281**, 15268-15276 (2006).
161. Wang,C. *et al.* TAK1 is a ubiquitin-dependent kinase of MKK and IKK. *Nature* **412**, 346-351 (2001).
162. Chen,Z. *et al.* Signal-induced site-specific phosphorylation targets I kappa B alpha to the ubiquitin-proteasome pathway. *Genes Dev.* **9**, 1586-1597 (1995).
163. Xu,M., Skaug,B., Zeng,W., & Chen,Z.J. A ubiquitin replacement strategy in human cells reveals distinct mechanisms of IKK activation by TNFalpha and IL-1beta. *Mol. Cell* **36**, 302-314 (2009).
164. Kirisako,T. *et al.* A ubiquitin ligase complex assembles linear polyubiquitin chains. *EMBO J.* **25**, 4877-4887 (2006).
165. Tokunaga,F. *et al.* Involvement of linear polyubiquitylation of NEMO in NF-kappaB activation. *Nat. Cell Biol.* **11**, 123-132 (2009).
166. Tokunaga,F. *et al.* SHARPIN is a component of the NF-kappaB-activating linear ubiquitin chain assembly complex. *Nature* **471**, 633-636 (2011).
167. Ikeda,F. *et al.* SHARPIN forms a linear ubiquitin ligase complex regulating NF-kappaB activity and apoptosis. *Nature* **471**, 637-641 (2011).
168. Gerlach,B. *et al.* Linear ubiquitination prevents inflammation and regulates immune signalling. *Nature* **471**, 591-596 (2011).
169. Rahighi,S. *et al.* Specific recognition of linear ubiquitin chains by NEMO is important for NF-kappaB activation. *Cell* **136**, 1098-1109 (2009).
170. Lo,Y.C. *et al.* Structural basis for recognition of diubiquitins by NEMO. *Mol. Cell* **33**, 602-615 (2009).
171. Haas,T.L. *et al.* Recruitment of the linear ubiquitin chain assembly complex stabilizes the TNF-R1 signaling complex and is required for TNF-mediated gene induction. *Mol. Cell* **36**, 831-844 (2009).
172. Shim,J.H. *et al.* TAK1, but not TAB1 or TAB2, plays an essential role in multiple signaling pathways in vivo. *Genes Dev.* **19**, 2668-2681 (2005).
173. Xu,G. *et al.* Ubiquitin-specific peptidase 21 inhibits tumor necrosis factor alpha-induced nuclear factor kappaB activation via binding to and deubiquitinating receptor-interacting protein 1. *J. Biol. Chem.* **285**, 969-978 (2010).
174. Enesa,K. *et al.* NF-kappaB suppression by the deubiquitinating enzyme Cezanne: a novel negative feedback loop in pro-inflammatory signaling. *J. Biol. Chem.* **283**, 7036-7045 (2008).
175. Opipari,A.W., Jr., Boguski,M.S., & Dixit,V.M. The A20 cDNA induced by tumor necrosis factor alpha encodes a novel type of zinc finger protein. *J. Biol. Chem.* **265**, 14705-14708 (1990).
176. Sun,S.C. Deubiquitylation and regulation of the immune response. *Nat. Rev. Immunol.* **8**, 501-511 (2008).
177. Kovalenko,A. *et al.* The tumour suppressor CYLD negatively regulates NF-kappaB signalling by deubiquitination. *Nature* **424**, 801-805 (2003).
178. Trompouki,E. *et al.* CYLD is a deubiquitinating enzyme that negatively regulates NF-kappaB activation by TNFR family members. *Nature* **424**, 793-796 (2003).
179. Brummelkamp,T.R., Nijman,S.M., Dirac,A.M., & Bernards,R. Loss of the cylindromatosis

tumour suppressor inhibits apoptosis by activating NF-kappaB. *Nature* **424**, 797-801 (2003).
180. Reiley,W., Zhang,M., Wu,X., Granger,E., & Sun,S.C. Regulation of the deubiquitinating enzyme CYLD by IkappaB kinase gamma-dependent phosphorylation. *Mol. Cell Biol.* **25**, 3886-3895 (2005).
181. Hutti,J.E. *et al.* Phosphorylation of the tumor suppressor CYLD by the breast cancer oncogene IKKepsilon promotes cell transformation. *Mol. Cell* **34**, 461-472 (2009).
182. Clague,M.J. & Urbe,S. Ubiquitin: same molecule, different degradation pathways. *Cell* **143**, 682-685 (2010).
183. Reggiori,F. & Pelham,H.R. Sorting of proteins into multivesicular bodies: ubiquitin-dependent and -independent targeting. *EMBO J.* **20**, 5176-5186 (2001).
184. Lauwers,E., Jacob,C., & Andre,B. K63-linked ubiquitin chains as a specific signal for protein sorting into the multivesicular body pathway. *J. Cell Biol.* **185**, 493-502 (2009).
185. Bache,K.G., Raiborg,C., Mehlum,A., & Stenmark,H. STAM and Hrs are subunits of a multivalent ubiquitin-binding complex on early endosomes. *J. Biol. Chem.* **278**, 12513-12521 (2003).
186. Welchman,R.L., Gordon,C., & Mayer,R.J. Ubiquitin and ubiquitin-like proteins as multifunctional signals. *Nat. Rev. Mol. Cell Biol.* **6**, 599-609 (2005).
187. McCullough,J., Clague,M.J., & Urbe,S. AMSH is an endosome-associated ubiquitin isopeptidase. *J. Cell Biol.* **166**, 487-492 (2004).
188. Mizuno,E. *et al.* Regulation of epidermal growth factor receptor down-regulation by UBPY-mediated deubiquitination at endosomes. *Mol. Biol. Cell* **16**, 5163-5174 (2005).
189. Breems,D.A. *et al.* Monosomal karyotype in acute myeloid leukemia: a better indicator of poor prognosis than a complex karyotype. *J. Clin. Oncol.* **26**, 4791-4797 (2008).
190. Metzeler,K.H. *et al.* ASXL1 mutations identify a high-risk subgroup of older patients with primary cytogenetically normal AML within the ELN "favorable" genetic category. *Blood*(2011).
191. Chou,W.C. *et al.* Distinct clinical and biological features of de novo acute myeloid leukemia with additional sex comb-like 1 (ASXL1) mutations. *Blood* **116**, 4086-4094 (2010).
192. Langer,C. *et al.* High BAALC expression associates with other molecular prognostic markers, poor outcome, and a distinct gene-expression signature in cytogenetically normal patients younger than 60 years with acute myeloid leukemia: a Cancer and Leukemia Group B (CALGB) study. *Blood* **111**, 5371-5379 (2008).
193. Metzeler,K.H. *et al.* ERG expression is an independent prognostic factor and allows refined risk stratification in cytogenetically normal acute myeloid leukemia: a comprehensive analysis of ERG, MN1, and BAALC transcript levels using oligonucleotide microarrays. *J. Clin. Oncol.* **27**, 5031-5038 (2009).
194. Marcucci,G., Haferlach,T., & Dohner,H. Molecular genetics of adult acute myeloid leukemia: prognostic and therapeutic implications. *J. Clin. Oncol.* **29**, 475-486 (2011).
195. Dufour,A. *et al.* Acute myeloid leukemia with biallelic CEBPA gene mutations and normal karyotype represents a distinct genetic entity associated with a favorable clinical outcome. *J. Clin. Oncol.* **28**, 570-577 (2010).
196. Schnittger,S. *et al.* KIT-D816 mutations in AML1-ETO-positive AML are associated with impaired event-free and overall survival. *Blood* **107**, 1791-1799 (2006).
197. Boissel,N. *et al.* Incidence and prognostic impact of c-Kit, FLT3, and Ras gene mutations in core binding factor acute myeloid leukemia (CBF-AML). *Leukemia* **20**, 965-970 (2006).
198. Cairoli,R. *et al.* Prognostic impact of c-KIT mutations in core binding factor leukemias: an Italian retrospective study. *Blood* **107**, 3463-3468 (2006).
199. Shen,Y. *et al.* Gene mutation patterns and their prognostic impact in a cohort of 1,185 patients with acute myeloid leukemia. *Blood*(2011).
200. Thol,F. *et al.* Incidence and prognostic influence of DNMT3A mutations in acute myeloid

leukemia. *J. Clin. Oncol.* **29**, 2889-2896 (2011).
201. Ley,T.J. *et al.* DNMT3A mutations in acute myeloid leukemia. *N. Engl. J. Med.* **363**, 2424-2433 (2010).
202. Lugthart,S. *et al.* High EVI1 levels predict adverse outcome in acute myeloid leukemia: prevalence of EVI1 overexpression and chromosome 3q26 abnormalities underestimated. *Blood* **111**, 4329-4337 (2008).
203. Frohling,S. *et al.* Prognostic significance of activating FLT3 mutations in younger adults (16 to 60 years) with acute myeloid leukemia and normal cytogenetics: a study of the AML Study Group Ulm. *Blood* **100**, 4372-4380 (2002).
204. Yanada,M., Matsuo,K., Suzuki,T., Kiyoi,H., & Naoe,T. Prognostic significance of FLT3 internal tandem duplication and tyrosine kinase domain mutations for acute myeloid leukemia: a meta-analysis. *Leukemia* **19**, 1345-1349 (2005).
205. Heuser,M. *et al.* MN1 overexpression induces acute myeloid leukemia in mice and predicts ATRA resistance in patients with AML. *Blood* **110**, 1639-1647 (2007).
206. Langer,C. *et al.* Prognostic importance of MN1 transcript levels, and biologic insights from MN1-associated gene and microRNA expression signatures in cytogenetically normal acute myeloid leukemia: a cancer and leukemia group B study. *J. Clin. Oncol.* **27**, 3198-3204 (2009).
207. Verhaak,R.G. *et al.* Mutations in nucleophosmin (NPM1) in acute myeloid leukemia (AML): association with other gene abnormalities and previously established gene expression signatures and their favorable prognostic significance. *Blood* **106**, 3747-3754 (2005).
208. Tang,J.L. *et al.* AML1/RUNX1 mutations in 470 adult patients with de novo acute myeloid leukemia: prognostic implication and interaction with other gene alterations. *Blood* **114**, 5352-5361 (2009).
209. Chou,W.C. *et al.* TET2 mutation is an unfavorable prognostic factor in acute myeloid leukemia patients with intermediate-risk cytogenetics. *Blood* **118**, 3803-3810 (2011).
210. Metzeler,K.H. *et al.* TET2 mutations improve the new European LeukemiaNet risk classification of acute myeloid leukemia: a Cancer and Leukemia Group B study. *J. Clin. Oncol.* **29**, 1373-1381 (2011).
211. Wattel,E. *et al.* p53 mutations are associated with resistance to chemotherapy and short survival in hematologic malignancies. *Blood* **84**, 3148-3157 (1994).
212. Hymowitz,S.G. & Wertz,I.E. A20: from ubiquitin editing to tumour suppression. *Nat. Rev. Cancer* **10**, 332-341 (2010).
213. Balgobind,B.V. *et al.* High BRE expression in pediatric MLL-rearranged AML is associated with favorable outcome. *Leukemia* **24**, 2048-2055 (2010).
214. Keats,J.J. *et al.* Promiscuous mutations activate the noncanonical NF-kappaB pathway in multiple myeloma. *Cancer Cell* **12**, 131-144 (2007).
215. Kim,M.S., Chung,N.G., Yoo,N.J., & Lee,S.H. Somatic mutation of CYLD gene is rare in hematologic and solid malignancies. *Leuk. Res.* **35**, e136-e137 (2011).
216. D'Andrea,A.D. Targeting DNA repair pathways in AML. *Best. Pract. Res. Clin. Haematol.* **23**, 469-473 (2010).
217. Yokoyama,T. *et al.* Trib1 links the MEK1/ERK pathway in myeloid leukemogenesis. *Blood* **116**, 2768-2775 (2010).
218. Yokoyama,T. *et al.* Identification of TRIB1 R107L gain-of-function mutation in human acute megakaryocytic leukemia. *Blood* **119**, 2608-2611(2012).
219. Keeshan,K. *et al.* Tribbles homolog 2 inactivates C/EBPalpha and causes acute myelogenous leukemia. *Cancer Cell* **10**, 401-411 (2006).
220. Schwickart,M. *et al.* Deubiquitinase USP9X stabilizes MCL1 and promotes tumour cell survival. *Nature* **463**, 103-107 (2010).

# Rapid identification of *IDH1* and *IDH2* mutations in acute myeloid leukemia using high resolution melting curve analysis

**Sylvie M. Noordermeer, Evelyn Tönnissen, Inge Vissers, Adrian van der Heijden, Louis T. van de Locht, Piëtte P. Deutz-Terlouw, Erik W.A. Marijt, Joop H. Jansen, and Bert A. van der Reijden**

**This chapter was adapted from:**
***British Journal of Haematology*, 2011 Feb; 152(4):493-496.**

**Abstract**

**High resolution melting (HRM) analysis is a useful technique for rapid pre-screening of recurrent mutations. Here we compared the performance of HRM analysis with direct sequencing for *IDH1/2* mutation detection in acute myeloid leukemia. Direct sequencing detected *IDH1/2* mutations in 32/168 (19%) cases. HRM analysis detected all mutations while the false positive discovery rate was only 4% (7/168). By determining *IDH1* R132H allele frequencies, we observed that there were no samples with low frequencies that would be missed by HRM analysis. In conclusion, mutational pre-screening by HRM analysis, followed by sequencing of positive samples identified by HRM analysis, significantly increases the speed to detect recurrent mutations.**

## Introduction

Screening for recurrent mutations in leukemia is becoming increasingly important because many of them have an impact on disease outcome. Nowadays, mutational detection is mostly based on DNA sequencing of PCR products or QPCR using allele specific probes. With the increasing number of recurrent mutations identified in cancer, the development of fast and efficient approaches for mutational screening is needed. An alternative technique for mutation detection is high resolution melting (HRM) analysis[1]. HRM analysis is a fast 'single-well-technique' which combines PCR using a fluorescent saturating dye that is intercalated in the DNA and melt curve analysis afterwards. As mutations cause changes in the melting property of the PCR product, they are identified when compared to non-mutated samples. Positive samples in HRM analysis can be sequenced subsequently to determine exact nucleotide changes.

Recently, mutations in the $NADP^+$-dependent isocitrate dehydrogenase genes *IDH1* and *IDH2* were identified in acute myeloid leukemia (AML), myeloid dysplastic syndromes and myeloproliferative diseases[2-8]. We study the application of HRM analysis and direct sequencing to screen for these mutations in a cohort of 168 AML patients using the real-time PCR platform of Applied Biosystems (Carlsbad, CA, USA).

## Materials and Methods

*Patient material*

168 adult AML patients treated in the department of Hematology of the Radboud University Nijmegen Medical Centre in Nijmegen and the Leiden University Medical Centre in Leiden, the Netherlands were included in this study. Paired bone marrow and peripheral blood samples were available from two patients. Samples were collected with informed consent of all patients and healthy individuals. The study was conducted according to the Declaration of Helsinki. Genomic DNA was isolated from bone marrow or peripheral blood, according to the manufacturers' protocol (Qiagen, Hilden, Germany or Machery-Nagel, Düren, Germany). Molecular screening of 11q23 translocations, *FLT3*, *TET2* and *NPM1* mutations and *EVI1* overexpression was carried out using standard procedures.

*HRM analysis of IDH1 and IDH2 mutations*

*IDH1* R132 and *IDH2* R140 and R172 mutations were detected by HRM analysis using the 7500 fast-real time-PCR platform of Applied Biosystems (Carlsbad, CA, USA). PCR was performed using 20 ng of genomic DNA, 6 pmol of forward and reverse primers (Supplemental table 2.3) and 10 μL MeltDoctor HRM Master Mix containing basic PCR ingredients (Applied Biosystems). PCR was followed by melting curve

measurements and data were analyzed using HRM software v1.0 (Applied Biosystems).

*Sequence analysis of IDH1 and IDH2 mutations*

Sequence analysis of *IDH1* R132 mutations was carried out on purified PCR products generated during HRM analysis using M13 forward or reverse primers. For *IDH2* mutation detection by sequence analysis, a separate PCR was used. PCR was carried out with 50 ng genomic DNA, 7.5 pmol forward and reverse primers including M13-sequences (Supplemental table 2.3), 5 mM $MgCl_2$ and 0.25 mM dNTPs using Taqman Gold polymerase (Applied Biosystems). After purification, sequence analysis was carried out with forward or reverse M13 primers. All identified mutations were confirmed by independent analyses.



*SNP array*

Genomic DNA of the patient with a homozygous R140W *IDH2* mutation was analyzed using a 250k SNP array (Affymetrix, Santa Clara, CA, USA) as described[9].

*Allele frequency analysis of IDH1 and IDH2 mutations*

Allele frequencies of *IDH1* R132C and *IDH2* R140Q mutations in the patient harboring both mutations were determined by pyrosequencing as described[9] using primers indicated in supplemental table 2.4. Relative allele frequencies of *IDH1* R132H mutations were measured on genomic DNA using an allele specific primer in QPCR (Supplemental table 2.3). Allele frequencies were normalized using an albumin QPCR[10] and the ΔCt method. QPCR was performed with Taqman Gold polymerase using an ABI Prism 7700 (Applied Biosystems).

## Results and Discussion

Sequence analysis detected *IDH1* or *IDH2* mutations in 32 out of 168 patients (19%) (supplemental tables 2.1&2.2). Using the methods as described, mutations could also be detected by HRM analysis (used primer combinations are indicated in supplemental table 2.3). Different primers with and without M13-sequences were tested, showing differential results for *IDH1* or *IDH2* mutations (figure 2.1). No mutations were missed by HRM analysis. For *IDH1* R132, 12 mutated samples (7.1%) were found both by HRM and sequence analysis while an additional 3 positive samples (1.8%) were found only by HRM analysis. To elucidate whether the extra mutations found by HRM analysis were false positives, we compared the sensitivity of both techniques. For this, a dilution series of genomic DNA from a mutated sample was measured by HRM analysis and followed by direct sequencing. Positivity in HRM analysis was lost at an allele frequency of approximately 9%, whereas the mutation could still be detected at a frequency of 4% by sequencing (supplemental figure 2.1). As sequencing was more

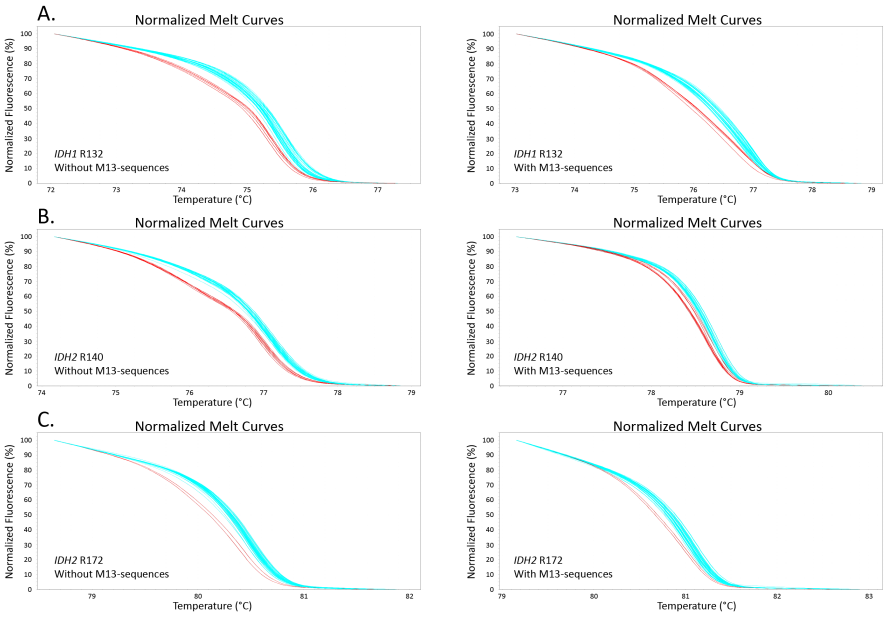


**Figure 2.1: Effect of addition of M13-sequence to primers used in HRM analysis**
Representative HRM analysis of 30 samples using primer combinations for *IDH1* R132 (**A**), *IDH2* R140 (**B**) and R172 (**C**) with (right panel) or without the addition of M13-sequences to the primers (left panel). Samples with a mutation are shown in red, wild type samples in turquoise, as assigned by the HRM software. Addition of M13-sequences to the primers only minimally affected the discrimination between mutant and wild type *IDH1*, but negatively influenced the discrimination of *IDH2* R140 and R172 mutations.

sensitive, this suggested that the extra positive samples found by HRM analysis (which did not contain any SNPs), represented false positive results. 19 samples were positive for the *IDH2* R140 mutation (11.3%) by sequence analysis. Initial HRM analysis for this mutation identified many false positive results. However, exclusion of samples with low PCR yields (Ct>26.8, 8 samples) significantly improved the discrimination between mutated and wild type samples. After exclusion, all positive samples found by sequencing were confirmed by HRM analysis while an additional two false positive cases were identified by HRM. R172 *IDH2* mutations were found in two patients (1.2%) both by HRM and sequence analysis and two false positive samples were found by HRM (1.2%) (supplemental table 2.1&2.2).

One patient showed both an *IDH1* R132C and an *IDH2* R140Q mutation. Allele frequencies of the mutations were measured by pyrosequencing to test whether the two mutations co-occur in the same leukemic clone (primer combinations are specified in supplemental table 2.4). The allele frequency of the *IDH1* R132C

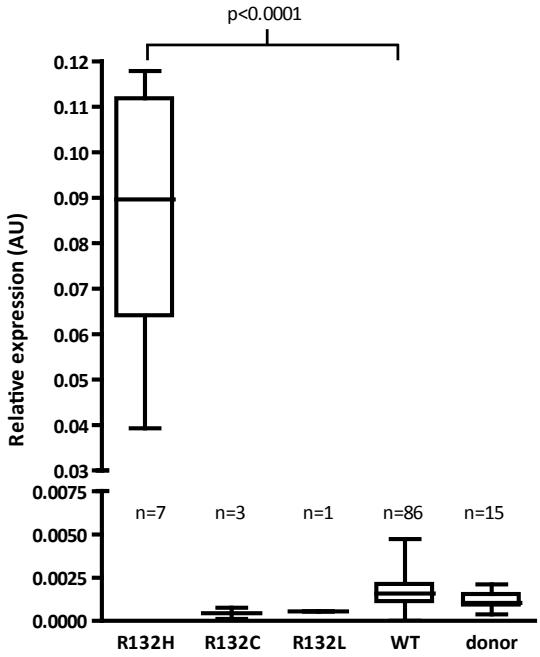


**Figure 2.2: Relative allele frequencies of *IDH1* R132H mutations**
DNA samples of AML patients with or without (WT) *IDH1* R132 mutations and donor samples were measured using an R132H specific QPCR. A more than 8-fold difference was observed between the sample with the lowest allele frequency among the R132H mutants compared to the sample with the highest allele frequency among the WT samples. Data are represented as relative quantity adjusted to albumin using the ΔCt method (arbitrary units (AU)), plotted in a box and whiskers plot (box: extends from the 25% to the 75% percentiles, with a line at the median; whiskers: minimal and maximal value). The p-value was calculated using an unpaired student's t-test.

mutation was 15.5%, while the *IDH2* R140Q frequency was even lower (data not shown). Because *IDH1* and *IDH2* mutations are typically heterozygous and the total allele frequencies of both mutations was below 50%, we cannot conclude whether the mutations represent one and the same, or independent clones. One patient exhibited a homozygous *IDH2* R140W mutation, identified by both sequence and HRM analysis (supplemental figure 2.2). SNP array analysis showed that the homozygous mutation was caused by uniparental disomy (UPD) on a large part of chromosome 15, including the *IDH2* locus (supplemental figure 2.3). Of the 32 patients with *IDH* mutations, we found co-occurrences with other chromosomal aberrations confirming data of previous studies[3,4,7,8,11]. Furthermore, none of the *IDH1* or *IDH2* mutated patients showed over-expression of *EVI1* (supplemental table 2.1).

Low frequencies of mutated alleles may be missed using sequencing or HRM analysis. To test whether *IDH1* mutations occur at frequencies below the detection limit of HRM analysis, we designed an allele specific QPCR for the most frequently occurring *IDH1* R132H mutation (for primer combinations, see supplemental table 2.3). We tested genomic DNA of mutation positive samples and compared these to healthy control samples and AML samples negative for the *IDH1* R132H mutation (figure 2.2). Using healthy control samples, low allele frequencies were observed as represented by large ΔCt values between the housekeeping gene albumin and the allele specific *IDH1* QPCR. These low allele frequencies are likely caused by aspecific

annealing of the mutant specific primer to wild type sequences. Importantly, the allele frequencies of healthy controls and AML patients lacking the *IDH1* R132H mutation were comparable. In contrast, the mutated R132H samples showed low ΔCt values representing high allele frequencies. The minimal difference between the lowest value of the *IDH1* R132H mutated samples and the highest value of the wild type AML samples was 8.3 fold. Allele frequencies within the group of patients with the *IDH1* R132H mutation showed a minimal difference of only three-fold. As the mutation positive samples were all detected by HRM analysis, and there were no samples with intermediate allele frequencies, *i.e.* between the *IDH1* R132H positive and negative groups, we conclude that HRM analysis is sensitive enough to detect all positive samples for this mutation, without false negative results. During the preparation of this manuscript, HRM analysis of *IDH1* and *IDH2* mutations in brain tumors was described using the less frequently used Roche platform (Lightcycler, Roche Applied Science, Basel, Switzerland)[12]. As the Applied Biosystems QPCR platform used by us is among the most frequently used platforms in diagnostic laboratories, HRM analysis would be widely applicable.

We conclude that HRM analysis is a fast and efficient way to screen patients for *IDH1* and *IDH2* mutations. After DNA isolation, HRM analysis is fast, using a closed, single well system, without any post-PCR processing. Afterwards, only samples positive in HRM analysis need to be sequenced to identify the base pair changes using the same PCR product, thereby significantly reducing time consuming sequencing work especially when large cohorts need to be addressed. HRM analysis might be a useful alternative for the detection of other recurrent mutations (*e.g.* in *NPM1*, *FLT3* and *CEBPA*) as well.

## Acknowledgements

This work was supported by the Vanderes foundation.

## Reference List


1. Wittwer,C.T. High-resolution DNA melting analysis: advancements and limitations. *Hum. Mutat.* **30**, 857-859 (2009).
2. Abbas,S. *et al.* Acquired mutations in the genes encoding IDH1 and IDH2 both are recurrent aberrations in acute myeloid leukemia: prevalence and prognostic value. *Blood* **116**, *2122-2126 (2010).*
3. Kosmider,O. *et al.* Mutations of IDH1 and IDH2 genes in early and accelerated phases of myelodysplastic syndromes and MDS/myeloproliferative neoplasms. *Leukemia* **24**, 1094-1096 (2010).
4. Wagner,K. *et al.* Impact of IDH1 R132 mutations and an IDH1 single nucleotide polymorphism in cytogenetically normal acute myeloid leukemia: SNP rs11554137 is an adverse prognostic factor. *J. Clin. Oncol.* **28**, 2356-2364 (2010).
5. Mardis,E.R. *et al.* Recurring mutations found by sequencing an acute myeloid leukemia genome. *N. Engl. J. Med.* **361**, 1058-1066 (2009).
6. Green,A. & Beer,P. Somatic mutations of IDH1 and IDH2 in the leukemic transformation of myeloproliferative neoplasms. *N. Engl. J. Med.* **362**, 369-370 (2010).
7. Chou,W.C. *et al.* Distinct clinical and biologic characteristics in adult acute myeloid leukemia bearing the isocitrate dehydrogenase 1 mutation. *Blood* **115**, 2749-2754 (2010).
8. Marcucci,G. *et al.* IDH1 and IDH2 gene mutations identify novel molecular subsets within de novo cytogenetically normal acute myeloid leukemia: a Cancer and Leukemia Group B study. *J. Clin. Oncol.* **28**, 2348-2355 (2010).
9. Langemeijer,S.M. *et al.* Acquired mutations in TET2 are common in myelodysplastic syndromes. *Nat. Genet.* **41**, 838-842 (2009).
10. van Oers,M.H. *et al.* BCL-2/IgH polymerase chain reaction status at the end of induction treatment is not predictive for progression-free survival in relapsed/resistant follicular lymphoma: results of a prospective randomized EORTC 20981 phase III intergroup study. *J. Clin. Oncol.* **28**, 2246-2252 (2010).
11. Paschka,P. *et al.* IDH1 and IDH2 mutations are frequent genetic alterations in acute myeloid leukemia and confer adverse prognosis in cytogenetically normal acute myeloid leukemia with NPM1 mutation without FLT3 internal tandem duplication. *J. Clin. Oncol.* **28**, 3636-3643 (2010).
12. Horbinski,C., Kelly,L., Nikiforov,Y.E., Durso,M.B., & Nikiforova,M.N. Detection of IDH1 and IDH2 mutations by fluorescence melting curve analysis as a diagnostic tool for brain biopsies. *J. Mol. Diagn.* **12**, 487-492 (2010).

**Supplemental table 2.1: Characteristics of patients with *IDH1/IDH2* mutations**

| | Karyotype | 11q23[a] | *FLT3* ITD | *FLT3* TKD | *TET2* | *NPM1* | *EVI1* O.E.[b] | *IDH1* R132 | *IDH2* R140 | *IDH2* R172 |
|---|---|---|---|---|---|---|---|---|---|---|
| **1** | normal | POS | wt | wt | wt | wt | neg | R132C[d] | R140Q[d] | wt |
| **2** | normal | neg | wt | MUT | wt | MUT | neg | R132C | wt | wt |
| **3** | 47, XXY | neg | wt | wt | wt | MUT | neg | R132C | wt | wt |
| **4** | normal | neg | MUT | wt | wt | wt | neg | R132H | wt | wt |
| **5** | normal | neg | wt | wt | wt | MUT | neg | R132H | wt | wt |
| **6** | normal | neg | MUT | wt | wt | wt | neg | R132H | wt | wt |
| **7** | ND[c] | ND[c] | MUT | wt | wt | MUT | neg | R132H | wt | wt |
| **8** | ND[c] | ND[c] | wt | wt | wt | MUT | neg | R132H | wt | wt |
| **9** | normal | neg | wt | wt | wt | MUT | neg | R132H | wt | wt |
| **10** | normal | neg | MUT | wt | wt | MUT | neg | R132H | wt | wt |
| **11** | normal | neg | MUT | wt | wt | ND[c] | neg | R132H | wt | wt |
| **12** | 9q- | neg | wt | wt | wt | wt | neg | R132L | wt | wt |
| **13** | normal | neg | MUT | wt | wt | MUT | neg | wt | R140Q | wt |
| **14** | normal | neg | wt | wt | SNP[g] | MUT | neg | wt | R140Q | wt |
| **15** | normal | neg | MUT | wt | wt | MUT | neg | wt | R140Q | wt |
| **16** | normal | neg | wt | MUT | wt | MUT | neg | wt | R140Q[c] | wt |
| **17** | der(7;12(q10;q10) 7p(der(7;12)) | neg | wt | wt | wt | wt | neg | wt | R140Q | wt |
| **18** | normal | neg | MUT | ND[c] | wt | MUT | neg | wt | R140Q | wt |
| **19** | 47XX,der(7;10), +10,+11 | neg | wt | wt | wt | ND[c] | neg | wt | R140Q | wt |
| **20** | normal | neg | MUT | wt | wt | wt | neg | wt | R140Q | wt |
| **21** | ND[c] | ND[c] | wt | wt | wt | wt | neg | wt | R140Q | wt |
| **22** | normal | neg | wt | wt | wt | ND[c] | neg | wt | R140Q | wt |
| **23** | normal | neg | wt | wt | wt | wt | neg | wt | R140Q | wt |
| **24** | normal | neg | wt | wt | wt | MUT | neg | wt | R140Q | wt |
| **25** | 46, XY[10] | ND[c] | wt | wt | wt | MUT | neg | wt | R140Q | wt |
| **26** | ND[c] | neg | wt | wt | wt | MUT | neg | wt | R140Q | wt |
| **27** | normal | neg | wt | wt | ND[c] | ND[c] | ND[c] | wt | R140Q | wt |
| **28** | ND[c] | ND[c] | MUT | wt | ND[c] | MUT | ND[c] | wt | R140Q | wt |
| **29** | ND[c] | ND[c] | wt | wt | wt | MUT | neg | wt | R140Q | wt |
| **30** | ND[c] | ND[c] | MUT | wt | wt | MUT | neg | wt | R140W[f] | wt |
| **31** | ND[c] | ND[c] | wt | wt | MUT | wt | neg | wt | wt | R172K |
| **32** | ND[c] | ND[c] | wt | wt | wt | wt | neg | wt | wt | R172K |

[a]11q23 translocations;
[b]*EVI1* overexpression;
[c]No data available;
[d]Patient 1 harbors a mutation at *IDH1* R132 as well as at *IDH2* R140;
[c]Mutation found in bone marrow and peripheral blood sample;
[f]Patient 28 harbors a homozygous mutation at *IDH2* R140;
[g]Mutation found in AML blasts, but also in T-cells: mutation is probably a single nucleotide polymorphysm (SNP).

**Supplemental table 2.2: HRM data of *IDH1* and *IDH2* mutations in 168 AML patients**

| | Samples screened | Wild type | Mutated | False positive | Omitted[a] |
|---|---|---|---|---|---|
| ***IDH1* R132** | 170[b] | 155 | 12 | 3 | 0 |
| ***IDH2* R140** | 170[b] | 139 | 20[c] | 2 | 8 |
| ***IDH2* R172** | 168[b] | 164 | 2 | 2 | 0 |

[a]Samples omitted based on high Ct values, reflecting inefficient PCR product amplification;
[b]Samples of 168 or 166 patients including two patients with bone marrow and peripheral blood samples;
[c]20 samples of 19 patients including one patient with a paired bone marrow and blood sample.

2

**Supplemental table 2.3: Primer combinations for mutation detection of *IDH1* R132, *IDH2* R140 and R172**

**A.** optimal primer combinations for HRM analysis

| | |
|---|---|
| **M13-*IDH1* forward** | 5'-*tgtaaaacgacggccagt*GGCACGGTCTTCAGAGAAGC-3' |
| **M13-*IDH1* reverse** | 5'-*caggaaacagctatgacc*CAACATGACTTACTTGATCCCCATAA-3' |
| ***IDH2*-R140 forward** | 5'-AGTTCAAGCTGAAGAAGATGTGGAA-3' |
| ***IDH2*-R140 reverse** | 5'-CGTGGGATGTTTTTGCAGATG-3' |
| ***IDH2*-R172 forward** | 5'-GCCCATCATCTGCAAAAACATC-3' |
| ***IDH2*-R172 reverse** | 5'-AGGATGGCTAGGCGAGGAG-3' |

**B.** primers for Sanger sequencing

| | |
|---|---|
| **M13-forward** | 5'-*tgtaaaacgacggccagt*-3' |
| **M13-reverse** | 5'-*caggaaacagctatgacc*-3' |
| **M13-*IDH2*-R140 forward** | 5'-*tgtaaaacgacggccagt*CGTCTGGCTGTGTTGTTGCTT-3' |
| **M13-*IDH2* reverse** | 5'-*caggaaacagctatgacc*AGGATGGCTAGGCGAGGAG-3' |

**C.** primers and probe for *IDH1* R132H allele specific QPCR

| | |
|---|---|
| ***IDH1*-Cons-F** | 5'-GGGTGGCACGGTCTTCAG-3' |
| ***IDH1*-R132H-R2** | 5'-ACTTACTTGATCCCCATAAGCATCAT-3' |
| ***IDH1*-FAM-MGB probe** | 5'-TTATCTGCAAAAATATCC-3' |

Bases in Italics: M13 forward or reverse sequence;
Bases underlined: 2 mismatches compared to wild type *IDH1*, 1 mismatch compared to R132H mutation. The extra mutation was incorporated in the reverse primer to enhance discrimination between wild type and mutated samples.

**Supplemental table 2.4: Primer combinations used for pyrosequencing**

| | | | |
|---|---|---|---|
| ***IDH1* R132** | PCR | *IDH1*-R132-forward-primer | 5'-GTGGCACGGTCTTCAGAGAAG-3' |
| | | *IDH1*-R132-reverse-primer-Univ1 | 5'-*AGCGCTGCTCCGGTTCATAGATT*-TGCCAACATGACTTACTTGATCC-3' |
| | | Univ1-Biotin | 5'-Biotin-*GCTGCTCCGGTTCATAGATT*-3' |
| | Pyro-sequencing | *IDH1*-R132-forward-seq primer | 5'-GGGTAAAACCTATCATCATA-3' |
| ***IDH2* R140** | PCR | *IDH2*-R140-forward-primer | 5'-CGTCTGGCTGTGTTGTTGC-3' |
| | | *IDH1*-R140-reverse-primer-Univ1 | 5'-*AGCGCTGCTCCGGTTCATAGATT*-AGACAGTCCCCCCCAGGAT-3' |
| | | Univ1-Biotin | 5'-Biotin-*GCTGCTCCGGTTCATAGATT*-3' |
| | Pyro-sequencing | *IDH1*-R140-forward-seq primer | 5'-AAGTCCCAATGGAACTATC-3' |

Bases in Italics: universal sequence in reverse primer and in biotin-primer to add biotin label to PCR product using three primers in the PCR.

A

| Concentration positive sample (%) | Allele frequency (%) | Results HRM | | Results Sequencing | |
|---|---|---|---|---|---|
| | | Duplo 1 | Duplo 2 | Duplo 1 | Duplo 2 |
| 100 | 15.5 | Variant 1 | Variant 1 | mutant | mutant |
| 66.7 | 10.3 | Variant 1 | Variant 1 | mutant | mutant |
| 53.3 | 8.3 | Variant 1 | Variant 2 | mutant | mutant |
| 40 | 6.2 | Variant 2 | Variant 2 | mutant | mutant |
| 26.7 | 4.1 | Variant 2 | Variant 2 | mutant | mutant |
| 13.3 | 2.1 | Variant 2 | Variant 2 | mutant | mutant |
| 6.7 | 1.0 | Variant 2 | Variant 2 | WT | WT |
| 1.3 | 0.2 | Variant 2 | Variant 2 | WT | WT |
| 0 | 0 | Variant 2 | Variant 2 | WT | Not measured |

B

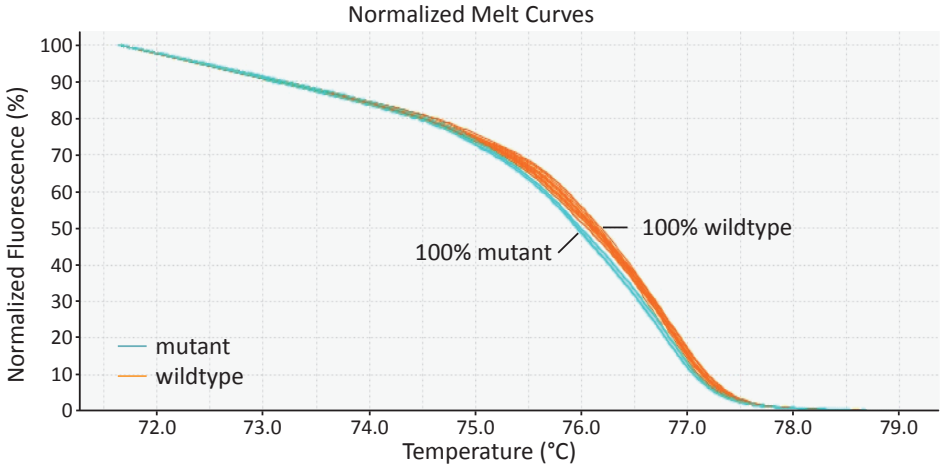


C

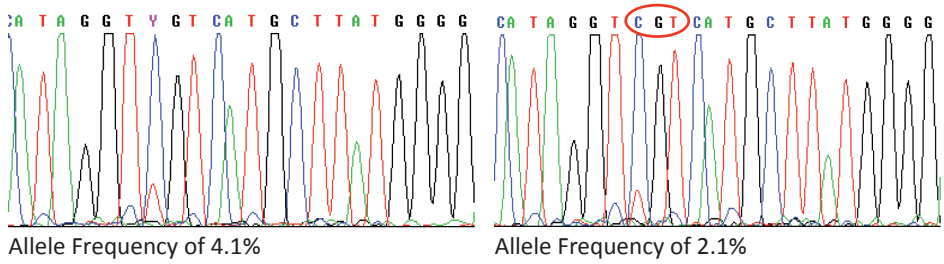


**Supplemental figure 2.1: Comparing sensitivity of HRM analysis and sequencing**
Genomic DNA from an *IDH1* R132C positive sample (allele frequency of 15.5%, as measured by pyrosequencing) was diluted in genomic DNA of an EBV-immortalized cell line with wild type *IDH1* in a concentration range as indicated in (**A**). Samples were measured in duplo with HRM analysis (**B**) or sequencing analysis (**C**). The HRM software autocalling showed discordant calling between duplicates at a dilution of 53.3% (allele frequency of 8.3%). Direct sequencing discriminated the mutated allele at a dilution of 26.7% (allele frequency of 4.1%) and was lost at a dilution of 13.3% (allele frequency of 2.1%).

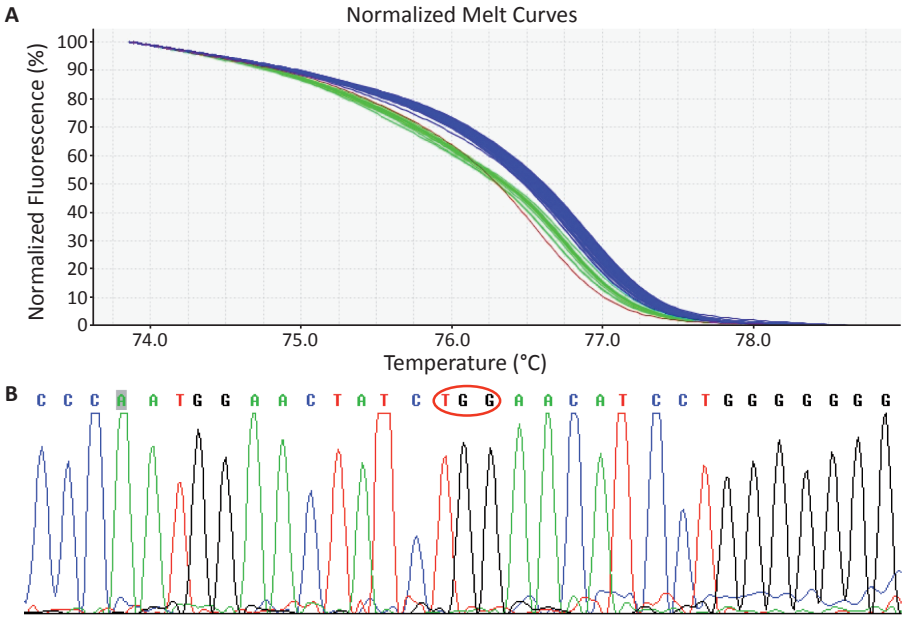


**Supplemental figure 2.2: HRM and sequence analysis of a patient harboring a homozygous R140W *IDH2* mutation**

**A.** HRM analysis showed a clear difference in the melting temperature of wild type samples (blue lines) and the homozygous mutation (red line). The heterozygous mutations (green lines) showed a double melt temperature as expected for heterozygous samples. **B.** Sequence analysis revealed a single homozygous T peak in the TGG codon (red marking), causing an Arg (CGG) to Trp substitution at codon 140 in the PCR product of *IDH2*.

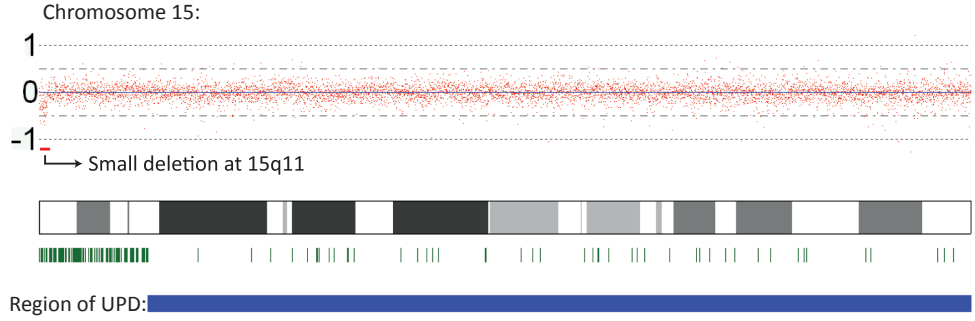


**Supplemental figure 2.3: The homozygous *IDH2* R140W mutation is caused by UPD**

The patient with the homozygous *IDH2* R140W mutation was screened for loss of heterozygosity using a 250k SNP array, showing UPD of a large part of chromosome 15 and a small deletion at 15q11. Red dots represent loss (signal<0) or gain (signal>0) of individual SNPs. Green lines represent heterozygous SNPs found. UPD is indicated with a blue bar.

# High *BRE* expression predicts favorable outcome in adult acute myeloid leukemia, in particular among *MLL-AF9* positive patients

**Sylvie M. Noordermeer, Mathijs A. Sanders, Christian Gilissen, Evelyn Tönnissen, Adrian van der Heijden, Konstanze Döhner, Lars Bullinger, Joop H. Jansen, Peter J.M. Valk, and Bert A. van der Reijden**

**This chapter was adapted from:**
***Blood*, 2011 Nov; 118(20):5613-5621.**

3


## Abstract

**Aberrations in protein ubiquitination have recently been identified in the pathogenesis of acute myeloid leukemia (AML). We studied whether expression changes of over 1600 ubiquitination related genes correlated with clinical outcome in 525 adult AML patients. High expression of one of these genes, *BRE*, was observed in 3% of the cases and predicted favorable prognosis independently of known prognostic factors (5-year overall survival: 57%). Remarkably, unsupervised expression profiling showed that 86% of high *BRE* expressing patients were confined to a previously unrecognized cluster. High *BRE* expression was mutually exclusive with *FLT3* ITD, *CEBPA*, *IDH1* and *IDH2* mutations, *EVI1* overexpression, and favorable karyotypes. In contrast, high *BRE* expression co-occurred strongly with FAB M5 morphology and *MLL-AF9* fusions. Within the group of *MLL-AF9* positive patients, high *BRE* expression predicted superior survival, while normal *BRE* expression predicted extremely poor survival (5-year overall survival of 80% versus 0%, respectively, p=0.0002). Both the co-occurrence of high *BRE* expression with *MLL-AF9* and its prognostic impact were confirmed in an independent cohort of 436 AML patients. Thus, high *BRE* expression defines a novel subtype of adult AML characterized by a favorable prognosis. This work contributes to improved risk stratification in AML, especially among *MLL-AF9* positive patients.**

## Introduction

Acute myeloid leukemia (AML) is a heterogeneous disease characterized by recurrent genetic lesions that have different prognostic impact. These lesions affect various biological processes like gene transcription, nuclear transport, epigenetics, and signal transduction[1-3]. Recently, mutations in genes that are involved in ubiquitination have been identified in AML pathogenesis as well[4]. Ubiquitination is a post-translational modification of cellular proteins. In this process, the small ubiquitin protein is conjugated to substrate proteins as a single moiety or as ubiquitin chains. This may mark substrates for degradation by the 26S proteasome or may alter the substrate's functional activity, depending on the type of ubiquitin chain that is attached[4]. Substrate ubiquitination is catalyzed via a three step cascade involving E1 activating enzymes, E2 conjugating enzymes, and E3 ligases. Like other post-translational modifications, ubiquitination is a reversible process, as deubiquitinases (DUBs) remove ubiquitin chains from substrates.

Because of its versatile role in many biological pathways, it is not surprising that changes in protein ubiquitination contribute to cancer development including malignant hematopoiesis[4,5]. For example, mutations in the E3 ligase c-CBL have been described in AML and other myeloid neoplasms[6,7]. Mutations in this important negative regulator of receptor tyrosine kinases lead to prolonged receptor signaling and hence enhanced proliferation. Apart from gene mutations, altered expression of proteins that regulate ubiquitination can also contribute to leukemogenesis. An example is TRIB2 overexpression which triggers proteasomal degradation of CEBPα. This results in impaired myeloid differentiation and the onset of leukemia in mouse models[8]. Independent research lines have shown the potential of interfering with the ubiquitination process as anti-cancer therapy. Several of these therapies are currently tested in clinical trials for hematological malignancies[9-12].

Recurrent mutations in AML have an impact on disease outcome. Treatment decisions are therefore dependent on the presence or absence of these mutations. Since expression levels of certain genes, like *EVI1*[13], are significantly associated with disease outcome, the type of treatment is also guided by expression levels of individual genes. In the last decade, gene expression profiles of large AML cohorts have been generated. By combining these expression data with clinical data, new prognostic AML subgroups have been identified[14-16]. Despite improved molecular based risk stratification, the survival within prognostic subgroups still shows large variation. The identification of novel recurrent mutations or expression markers with prognostic value may therefore improve individualized treatment strategies.

Here we studied whether changes in expression of genes involved in ubiquitination (hereafter referred to as Ub-genes) correlated with disease outcome using outlier gene expression analysis. With this type of analysis, genes that are differentially expressed in a subset of patients are identified. By comparing the expression data of these genes

with clinical parameters of the patients, correlations with survival can be studied. Since gene expression data of large AML cohorts are available nowadays, outlier analysis has great potential in the identification of novel prognostic factors. Indeed, by applying this approach for Ub-genes, we identified a novel prognostic factor in AML. This work may add to the risk stratification of AML patients.

## Materials and Methods

*Selection of Ub-genes*

The interpro database (www.ebi.ac.uk/interpro/) was used to generate a list of structural protein domains involved in ubiquitination, using several enzyme classes as search terms (e.g. E2 conjugating enzyme, E3 ligase, deubiquitinating enzyme, proteasome), as well as the overall term 'ubiquitin'. The list of interpro codes was subsequently filtered manually for domains with a clear link to ubiquitination, including UBA (ubiquitin associated) and UBL (ubiquitin like) domains, resulting in a total of 121 individual codes, (supplemental table 3.1A). Using the gene ontology database, GO-terms involving ubiquitination were collected as well (75 GO-terms, supplemental table 3.1B).

By use of the biomart database (www.biomart.org/biomart/martview/) genes containing the relevant interpro domains and GO-terms were identified. To ensure maximal completeness, this list of unique refseq entries was merged with a list of Ub-genes previously published by W. Harper and colleagues[17] and an overview of human deubiquitinases (DUBs) generated by S. Urbé and S. Hayes (personal communication).

*Gene expression profiling of AML samples*

For the present study, our previously published cohort of 525 AML patient samples, 11 $CD34^+$ donor samples, and 5 normal bone marrow (NBM) control samples was used[18]. Details on clinical data and experimental procedures of the micro-array profiling on the Affymetrix HG-U133 plus 2.0 arrays (Santa Clara, CA, USA) can be found elsewhere[18]. The array data are accessible online at the Gene Expression Omnibus (GSE14468).

To validate observed findings in an independent cohort, 40k cDNA array data (arrays manufactured by the Stanford Functional Genomics Facility) of a second previously published cohort of 436 AML patients were analyzed, including 11 *MLL-AF9* positive patients (GSE16432)[19]. In addition, Affymetrix HG-U133 2.0 plus array data of 14 adult *MLL-AF9* positive AML patients were used for data validation. These samples were provided by the German-Austrian AML Study Group (AMLSG) with patient informed consent obtained in accordance with the Declaration of Helsinki and institutional review board approval from all participating centers. Patients were entered into AML HD93, AML HD98A, AMLSG 06-04 and AMLSG 07-04 treatment protocols.

For the validation *MLL-AF9* data set (n=25), *BRE* expression data of the

HG-U133 plus 2.0 arrays (11 *MLL-AF9* samples) and the 40k cDNA arrays (14 *MLL-AF9* samples) were combined. Data normalization and filtering for well expressed genes was performed separately for the cDNA and Affymetrix data sets as previously described[20,21]. Subsequently, data sets were combined following (i) the averaging of the expression of multiple clones/probe sets measuring the same gene (based on the gene symbols), and (ii) the mean-centering of the cDNA and Affymetrix data in order to reduce platform specific effects. Normalized *BRE* expression data of these 25 patients are available in supplemental table 3.2.

*Cell isolation*

For the isolation of primary donor blood cells, mononuclear cells were first isolated from buffy coats using ficoll 1077 gradients (GE Healthcare, Chalfont St. Giles, UK). Subsequently, T cells were isolated by magnetic cell sorting (MACS) using anti-CD3 micro beads (Miltenyi Biotec, Bergisch Gladbach, Germany). From the remaining fraction, monocytes, NK cells and B cells were isolated by fluorescence activated cell sorting (FACS) using CD14 (Becton Dickinson, Franklin Lakes, NJ, USA), CD19 (DAKO, Glostrup, Denmark) and CD56 (Becton Dickinson) antibodies, respectively. Granulocytes were isolated from total blood samples by MACS using anti-CD14 micro beads (Miltenyi Biotec). Cell purity of the hematopoietic fractions was confirmed to be 90% or higher by flow cytometric analyses. In addition to primary cells, the t(9;11) positive cell lines Molm13, Monomac-6 and THP1 were used. Isolation of AML cells, RNA purification, and cDNA preparation have been described before[18,20].

*BRE QPCR and MLL-AF9 fusion gene detection*

*BRE* expression was measured by QPCR on cDNA samples using a commercially available primer/probe set (Applied Biosystems, Carlsbad, CA, USA, Hs01046283_m1), and data were normalized by *PBGD* or *beta-ACTIN* QPCR[22]. *MLL-AF9* breakpoint PCR on the cohort of 525 patients was performed as described before[23,24]. For the validation cohort, conventional chromosome banding and fluorescence-in-situ-hybriization (FISH) for *MLL-AF9* translocations was performed as previously described[25].

*Statistical analyses*

Genes with outlier expression were defined as probe sets that showed expression values of more than four times the standard deviation above or below the mean expression of all AML samples for at least one sample. As this analysis does not involve a discernible null-hypothesis, a p-value is not obtained. It is therefore unattainable to perform corrections for multiple testing. For survival analyses we selected probe sets detecting outlier expression in at least ten patients since this accounts for at least 2% of the patients, a percentage that we consider biologically and clinically relevant. In addition, the likelihood that correlations are found by chance would increase in smaller groups.

The Cox proportional hazard model was used for multivariate analyses to identify whether genes were independent prognostic factors for overall survival (OS) and event free survival (EFS) (with events defined as: relapse, death by any cause, and no complete remission), including known prognostic factors in the model (that is, age (continuous variable), white blood cell count (WBC, continuous variable), FAB M5 morphology (positive versus negative), stem cell transplantation status, favorable karyotypes (t(8;21), t(15;17), inv(16)), *CEBPA* double mutations, *FLT3* ITD, and *NPM1* mutations). Before performing multivariate analyses, the proportional hazard assumption was tested for high *BRE* expression and no indication of non-proportionality was found.

Differences between variables of patient subgroups were statistically tested by performing $\chi^2$ tests, Fisher exact tests, or Mann-Whitney U-tests. Survival differences were visualized using Kaplan-Meier plots. Significance of survival differences between patient groups was calculated using the log rank method. All analyses were performed two-tailed. Because we anticipated that only small numbers of patients were identified with outlier expression per probe set, we considered $p<0.05$ as statistically significant.



## Results

*Identification of genes with prognostic impact in AML using outlier analysis*

To study the expression of genes encoding proteins involved in ubiquitination, we selected these proteins based on the presence of catalytic domains used in the ubiquitin pathway and relevant GO-terms. In total, 1,618 proteins (based on HGNC nomenclature) were selected, which are encoded by 2,608 refseq entries (table 3.1). The Ub-genes are represented by 2,890 probe sets on the used Affymetrix HG-U133 plus 2.0 micro-array.

Since the introduction of micro-arrays to study gene expression in AML, novel prognostic subclasses have been identified based on similarities in expression profiles. Here, we conducted outlier expression analysis on a cohort of 525 AML patients as an alternative approach to study whether distinct expression of individual Ub-genes in subsets of patients correlated with survival. Outlier expression was defined as an expression level of more than four times the standard deviation above or below the mean expression of all AML samples (see Materials and Methods). In total, fifteen probe sets were identified that showed outlier expression in at least ten patients (supplemental table 3.3). Subsequently, overall survival of patient groups exhibiting outlier expression was compared to the remaining AML patients. Of these fifteen probe sets, three showed a significant correlation with OS (supplemental figure 3.1). One of these probe sets represented *EVI1*, which is a known prognostic factor in AML[13]. The other two represented *BRE* (Brain and Reproductive organ-Expressed), a member of the BRCA1 E3 ubiquitin ligase complex.

**Table 3.1: Representation of important ubiquitination core enzyme families in the human genome**

| Protein Family | Structural domains | # Refseq IDs | # HGNC proteins[a] |
|---|---|---|---|
| **E1 activating enzymes** | Ubiquitin activating domain[40] | 9 | 4 |
| **E2 conjugating enzymes** | UBC core domain[41] | 78 | 43 |
| **E3 ligases** | RING[42] | 562 | 334 |
| | TRIAD[43] | 33 | 22 |
| | HECT[44] | 45 | 28 |
| | PHD[45] | 290 | 173 |
| | U box[46] | 42 | 31 |
| **E3 complex formation** | SOCS box[47] | 54 | 39 |
| **Substrate recruitment** | F-box[48] | 115 | 72 |
| | BTB[49] | 273 | 188 |
| **Proteasome complex** | | 85 | 68 |
| **DUB** | UCH, USP, OUT, Josephin, JAMM[50] | 98 | 86 |

DUB indicates deubiquitinating enzyme.
[a]Number of proteins based on protein nomenclature by the HGNC: HUGO Gene Nomenclature Committee.



*High BRE expression correlates with FAB M5 morphology and the MLL-AF9 fusion*

By outlier analysis, twelve high *BRE* expressing samples were identified based on the cut-off used for outlier expression. Figure 3.1 shows that these twelve samples actually belong to a distinct group of fourteen patients with high *BRE* expression (which all showed *BRE* expression higher than 3 x the standard deviation above the mean), representing 3% of the total AML cohort of 525 samples (figure 3.1A). Two samples showed intermediate expression and the remaining patients showed limited variation in *BRE* expression. To validate the *BRE* array expression data, a *BRE* specific QPCR was performed. The QPCR confirmed the array data as a good correlation between the two types of data was observed (linear regression $r^2>0.8$, $p<0.001$, supplemental figure 3.2). We also studied whether *BRE* was differentially expressed during normal hematopoiesis. Its expression was measured in $CD34^+$ cells, total bone marrow, and several mature blood cell fractions from healthy donors (T-, B-, NK- cells, granulocytes, and monocytes). All fractions showed *BRE* expression comparable to levels observed in the majority of the AML samples, and no high *BRE* expression was observed (Supplemental figure 3.3).

Evaluating the co-occurrence of high *BRE* expression with known parameters in AML revealed high co-occurrence with FAB M5 morphology ($p<0.001$, figure 3.1B, table 3.2). Furthermore, co-occurrence was found with the t(9;11) translocation ($p<0.001$), and a relatively young age ($p=0.006$). In contrast to these positive correlations, high *BRE* expression was mutually exclusive with *FLT3* ITD mutations ($p=0.027$). High *BRE* expression was also mutually exclusive with favorable karyotypes, *CEBPA* mutations,

**Table 3.2: Characteristics of patients with high *BRE* expression (#14 patients)**

| | normal *BRE* expressing patients | | high *BRE* expressing patients[a] | | *P* |
|---|---|---|---|---|---|
| **Sex** (N=518), no. (%) | | | | | 0.788[b] |
| Male | 252 | (50) | 6 | (42.9) | |
| Female | 252 | (50) | 8 | (57.1) | |
| **Age** (N=518), years | | | | | 0.006[c] |
| median (range) | 47 | (14-77) | 37.5 | (17-49) | |
| **WBC** (N=518), x $10^9$/L | | | | | 0.500[c] |
| median (range) | 28.6 | (0.3-510) | 68 | (1-240) | |
| **Transplantation status** (N=525), no. (%) | | | | | 0.130[b] |
| No transplantation | 302 | (59.1) | 5 | (35.7) | |
| Autologous transplantation | 68 | (13.3) | 2 | (14.3) | |
| Allogeneic transplantation | 141 | (27.6) | 7 | (50) | |
| **FAB classification** (N=509), no. (%) | | | | | <0.001[d] |
| M0 | 17 | (3.4) | 1 | (7.1) | 0.400[b] |
| M1 | 100 | (20.2) | 0 | (0) | 0.083[b] |
| M2 | 130 | (26.3) | 1 | (7.1) | 0.130[b] |
| M3 | 23 | (4.6) | 0 | (0) | 1.000[b] |
| M4 | 93 | (18.8) | 0 | (0) | 0.084[b] |
| M5 | 104 | (21.0) | 12 | (85.7) | <0.001[b] |
| M6 | 7 | (1.4) | 0 | (0) | 1.000[b] |
| Other/unknown | 21 | (4.2) | 0 | (0) | 1.000[b] |

*EVI1* overexpression, and *IDH1* and *IDH2* mutations. The corresponding p-values were not significant in this cohort, likely due to low sample numbers (table 3.2).

High *BRE* expression was strongly associated with t(9;11) translocations as shown above. This translocation, leading to the *MLL-AF9* fusion gene, can be missed by routine cytogenetic analysis. Therefore, we re-analyzed the complete cohort for the presence of the *MLL-AF9* fusion by RT-PCR. All samples that were t(9;11) positive based on cytogenetic findings were also positive for the *MLL-AF9* fusion in the PCR reaction. However, eight additional *MLL-AF9* positive samples were identified by PCR (supplemental figure 3.4). This yielded a total incidence of 3.5% of AML cases with *MLL-AF9* fusions (table 3.2). Five of the newly identified *MLL-AF9* positive samples showed high *BRE* expression. In total, ten out of fourteen samples with high *BRE* expression contained the *MLL-AF9* fusion, one had an *MLL-ENL* translocation, one had an *MLL-AF10* translocation and the other two were 11q23 negative (table 3.2, figure 3.1C).

**Table 3.2 (continued)**

| | normal *BRE* expressing patients | | high *BRE* expressing patients[a] | | *P* |
|---|---|---|---|---|---|
| **Cytogenetics**, no. (%) | | | | | |
| t(15;17) (N=522) | 25 | (4.9) | 0 | (0) | 1.000[b] |
| t(8;21) (N=522) | 38 | (7.5) | 0 | (0) | 0.613[b] |
| inv(16) (N=522) | 42 | (8.3) | 0 | (0) | 0.617[b] |
| 11q23 (N=522) | 21 | (4.1) | 12 | (85.7) | <0.001[b] |
| *MLL-AF9* (N=522) | 8 | (1.6) | 10 | (71.4) | <0.001[b] |
| *MLL-AF10* (N=522) | 2 | (0.4) | 1 | (7.1) | 0.080[b] |
| *MLL-ENL* (N=522) | 0 | (0) | 1 | (7.1) | 0.027[b] |
| **Other genetic aberrations**, no. (%) | | | | | |
| *FLT3* ITD mutations (N=525) | 143 | (28.0) | 0 | (0) | 0.015[b] |
| *FLT3* TKD mutations (N=523) | 51 | (10.0) | 2 | (14.3) | 0.643[b] |
| *NPM1* mutations (N=525) | 157 | (30.7) | 1 | (7.1) | 0.075[b] |
| *CEBPA* single mutations (N=525) | 12 | (2.3) | 0 | (0) | 1.000[b] |
| *CEBPA* double mutations (N=525) | 26 | (5.1) | 0 | (0) | 1.000[b] |
| *EVI1* overexpression (N=518) | 52 | (10.3) | 0 | (0) | 0.380[b] |
| *IDH1* mutations (N=522) | 38 | (7.5) | 0 | (0) | 0.613[b] |
| *IDH2* mutations (N=522) | 49 | (9.6) | 0 | (0) | 0.382[b] |

WBC indicates white blood cell count; FAB, French-American-British.
[a]Cut-off used for high BRE expression was mean of all AML + 3 x standard deviation;
[b]p-values are based on Fisher exact tests;
[c]p-values are based on Mann-Whitney U-tests;
[d]p-values are based on $\chi^2$ tests.

*High BRE expression but not MLL-AF9 is an independent factor for favorable OS and EFS*

To determine whether high *BRE* expression was an independent predictor for favorable OS, a multivariate analysis with the Cox proportional hazard model was performed, including known prognostic factors (see Materials and Methods section). First, analyses were performed comparing the survival of the twelve patients with outlier-high *BRE* expression to the survival of the remaining cohort. Using this cut-off, high *BRE* expression was an independent factor for both OS and EFS (hazard ratio's: 0.15 and 0.13, p-value's=0.003 and 0.002 for OS and EFS, respectively) (table 3.3A). Afterwards, the analysis was repeated, but now by comparing the fourteen patients with the highest *BRE* expression (which showed distinct *BRE* expression) to the rest of the cohort. Also in this analysis high *BRE* expression was an independent factor for OS and EFS (hazard ratio's: 0.3 and 0.26, p-value's=0.047 and 0.023 for OS and EFS, respectively). In contrast, the presence of the *MLL-AF9* fusion did not correlate significantly with OS or

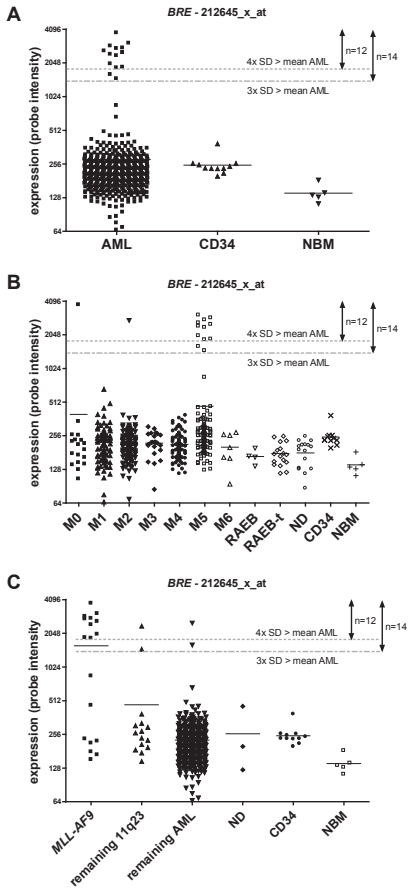


**Figure 3.1: High *BRE* expression correlated strongly with FAB M5 morphology and *MLL-AF9* rearrangements**

**A.** Gene expression profiling showed that high *BRE* expression, as represented by the probe set intensity of 212645_x_at, occurred in 14 out of 525 AML patients, accounting for 3% of the cohort. Donor CD34+ and normal bone marrow cells did not show high *BRE* expression. **B.** High *BRE* expression correlated with FAB M5. *BRE* expression is visualized per FAB morphology class. **C.** High *BRE* expression co-occurred with the presence of the *MLL-AF9* fusion. *BRE* expression is represented by the fluorescent intensity of probe set 212645_x_at. Other probe sets representing *BRE* (205550_s_at and 211566_x_at) showed comparable results (data not shown). The mean per subclass is represented by a horizontal line. Dotted lines represent the mean of all AML samples plus 3 or 4 x the standard deviation of *BRE* expression, used as values for outlier analysis and cut-off for high *BRE* expression, assigning 14 or 12 samples with high expression, respectively.

EFS in the complete AML cohort (table 3.3A-B).

Among intermediate and high risk AML groups, patients with *MLL-AF9* translocations have been reported to show a relatively good prognosis[26,27], although others have not been able to confirm this[28]. To address this issue in the cohort studied here, we determined the effect of the presence of an *MLL-AF9* fusion on OS and EFS in intermediate and high risk patients (excluding patients with favorable karyotypes and *CEBPA* double mutations). This showed that *MLL-AF9* positivity did not correlate significantly with favorable OS or EFS (figure 3.2A). As all fourteen patients with high *BRE* expression also belonged to the intermediate and high risk prognostic groups, we visualized the predictive value of high *BRE* expression on survival among these patients as well. In contrast to *MLL-AF9* positivity, both OS and EFS of the fourteen patients with high *BRE* expression were significantly better compared to the remaining patients (5-year OS of 27.5±2.3 vs. 57.1±13.2%, p-value=0.04 and 5-year EFS of 20.0±2.1

**Table 3.3: High *BRE* expression is an independent prognostic factor for OS and EFS, based on the multivariate Cox regression hazard model**

**A.** High *BRE* expression based on mean of all AML + 4x standard deviation (12 patient samples)

| | OS | | | EFS | | |
|---|---|---|---|---|---|---|
| | *HR* | *95% CI* | *P* | *HR* | *95% CI* | *P* |
| **High *BRE*** | 0.15 | 0.042-0.52 | 0.003 | 0.13 | 0.038-0.47 | 0.002 |
| ***MLL-AF9*** | 1.82 | 0.81-4.1 | 0.15[d] | 1.52 | 0.68-3.4 | 0.31[d] |
| **Favorable karyotype[a]** | 0.30 | 0.21-0.43 | <0.001 | 0.32 | 0.23-0.44 | <0.001 |
| ***CEBPA* double mutation** | 0.26 | 0.14-0.50 | <0.001 | 0.28 | 0.16-0.50 | <0.001 |
| ***NPM1* mutation** | 0.45 | 0.34-0.59 | <0.001 | 0.41 | 0.31-0.53 | <0.001 |
| ***FLT3* ITD** | 1.60 | 1.2-2.1 | <0.001 | 1.55 | 1.2-2.0 | 0.001 |
| **Transplantation status[b]** | 0.68 | 0.60-0.78 | <0.001 | 0.75 | 0.66-0.85 | <0.001 |
| **FAB M5** | 1.05 | 0.80-1.4 | 0.73 | 1.00 | 0.77-1.3 | 0.98 |
| **Age[c]** | 1.01 | 1.0-1.0 | 0.080 | 1.00 | 1.0-1.0 | 0.52 |
| **WBC[c]** | 1.00 | 1.0-1.0 | 0.097 | 1.00 | 1.0-1.0 | 0.027 |

**B.** High *BRE* expression based on mean of all AML + 3x standard deviation (14 patient samples)

| | OS | | | EFS | | |
|---|---|---|---|---|---|---|
| | *HR* | *95% CI* | *P* | *HR* | *95% CI* | *P* |
| **High *BRE*** | 0.30 | 0.094-0.98 | 0.047 | 0.26 | 0.08-0.83 | 0.023 |
| ***MLL-AF9*** | 1.29 | 0.52-3.22 | 0.58[d] | 1.11 | 0.46-2.7 | 0.82[d] |
| **Favorable karyotype[a]** | 0.31 | 0.22-0.45 | <0.001 | 0.33 | 0.24-0.46 | <0.001 |
| ***CEBPA* double mut** | 0.28 | 0.15-0.52 | <0.001 | 0.30 | 0.17-0.52 | <0.001 |
| ***NPM1* mut** | 0.47 | 0.36-0.62 | <0.001 | 0.43 | 0.33-0.56 | <0.001 |
| ***FLT3* ITD** | 1.54 | 1.2-2.0 | 0.001 | 1.48 | 1.1-1.9 | 0.003 |
| **Transplantation status[b]** | 0.70 | 0.61-0.80 | <0.001 | 0.76 | 0.67-0.87 | <0.001 |
| **FAB M5** | 1.09 | 0.83-1.4 | 0.54 | 1.05 | 0.81-1.4 | 0.72 |
| **Age[c]** | 1.01 | 1.0-1.0 | 0.059 | 1.00 | 1.0-1.0 | 0.43 |
| **WBC[c]** | 1.00 | 1.0-1.0 | 0.32 | 1.00 | 1.0-1.0 | 0.13 |

Mut indicates mutation; FAB, French-American-British; WBC, White Blood Cell count; OS, Overall Survival; EFS, Event Free Survival; HR, Hazard Ratio; CI, confidence interval.

[a]Favorable karyotype: t(8;21), t(15;17), and inv(16);

[b]Transplantation status: either no transplantation, autologous transplantation or allogeneic transplantation;

[c]Continuous variables;

[d]The p-value of *MLL-AF9* is mainly affected by co-occurrence with high *BRE* expression (based on correlation of regression coefficients, data not shown).

vs. 57.1±13.2%, p-value=0.01 for patients with normal and high *BRE* expression, respectively) (figure 3.2B). In conclusion, high *BRE* expression correlated with favorable outcome in poor and intermediate risk prognostic groups and was an independent factor for clinical outcome in AML.

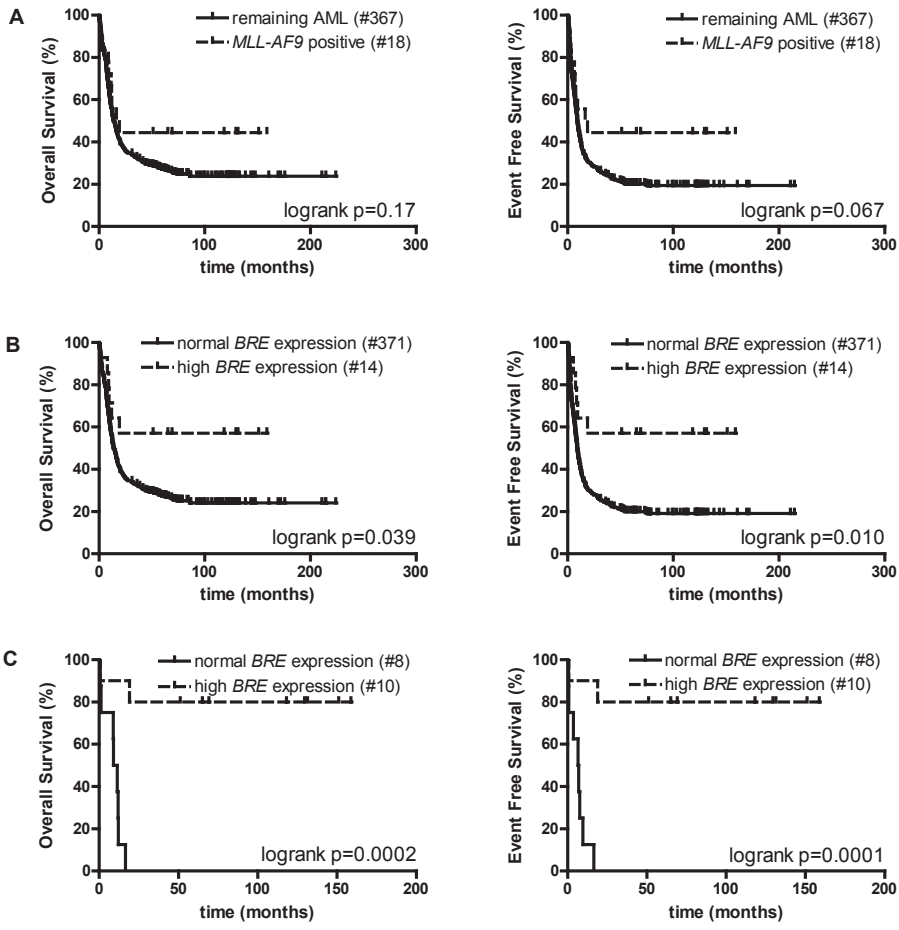


**Figure 3.2: High *BRE* expression correlated with superior OS in intermediate and poor risk patients**

**A.** Kaplan-Meier plots for OS (left panels) and EFS (right panel) showed that *MLL-AF9* positivity did not correlate significantly with a good OS or EFS among the intermediate and poor risk AML patients (i.e. excluding patients with t(15;17), t(8;21), inv(16) and *CEBPA* double mutations) (5-year OS of 27.2±2.4 vs. 44.4±11.7%, p-value=0.17 and 5-year EFS of 20.2±2.1 vs. 44.4±11.7%, p-value=0.067 for *MLL-AF9* negative and positive patients, respectively). **B.** In the group of intermediate and poor risk AML patients, patients with high *BRE* expression exhibited a significantly better OS and EFS (5-year OS of 27.5±2.3 vs. 57.1±13.2%, p-value=0.04 and 5-year EFS of 20.0±2.1 vs. 57.1±13.2%, p-value=0.01 for patients with normal and high *BRE* expression, respectively). **C.** Within the group of *MLL-AF9* positive patients, high *BRE* expression correlated with a significantly better OS and EFS (5-year OS of 0% vs. 80%, p-value=0.0002 and 5-year EFS of 0% vs. 80%, p-value=0.0001 for patients with normal and high *BRE* expression, respectively). P-values were determined with the logrank test. The number of patients included in the analyses is shown in brackets.

*High BRE expression correlates with superior survival within MLL-AF9 positive AML patients*

Of the eighteen *MLL-AF9* positive AML samples, ten cases showed high *BRE* expression (table 3.2, figure 3.1C). We therefore questioned whether *BRE* expression predicted disease outcome within the group of *MLL-AF9* positive patients. This analysis showed that *MLL-AF9* positive patients with high *BRE* expression exhibited a superior survival while the remaining *MLL-AF9* positive patients did very poor (figure 3.2C), both with respect to OS and EFS (5-year OS and EFS of 0% vs. 80% for patients with normal and high *BRE* expression, respectively, p=0.0002 (OS) and p=0.0001 (EFS)).

*Validation of the prognostic value of BRE expression in an independent AML cohort*

When studying the statistical impact of large numbers of genes, correlations can be found by chance. Therefore, we studied an independent cohort of 436 AML patients[19]. All non-predictive outliers identified in the first cohort did not predict outcome in the second cohort either (data not shown). With regard to *BRE*, outlier expression was



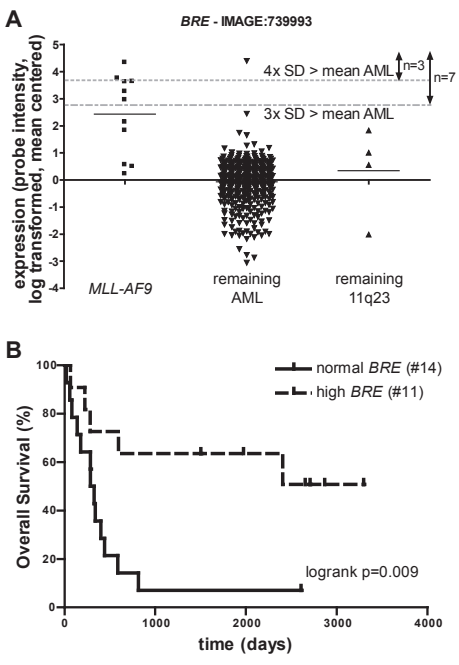


**Figure 3.3: An independent AML cohort confirmed the positive effect of high *BRE* expression on prognosis**

**A.** *BRE* expression was high in a subset of a second cohort of 436 AML patients and co-occurred strongly with *MLL-AF9* translocations (p<0.001 based on Fisher Exact tests). 40k cDNA expression array data of *BRE* (clone: IMAGE:739993) were log transformed and mean centered. Patients were subdivided into three groups based on *MLL-AF9* and 11q23 positivity. Dotted lines represent the mean of all AML samples plus 3 or 4 x the standard deviation of *BRE* expression, used as values for outlier analysis and cut-off for high *BRE* expression. **B.** High *BRE* expression accounts for good OS within an independent *MLL-AF9* cohort (5-year OS of 7.1±6.9 vs. 63.6±14.5%, p=0.0089 for patients with normal and high *BRE* expression, respectively). *BRE* array expression data of two cohorts of *MLL-AF9* positive patients were combined by log transformation and mean centering of the data. Based on the cut-off used for high *BRE* expression in figure 3.3A (mean of 436 AML samples + 3 x standard deviation), *MLL-AF9* patients were subdivided into two groups: high and normal *BRE* expression (see supplemental table 3.2). P-values were determined with the logrank test. The number of patients included in the analyses is shown in brackets.

also observed in a subset of this second cohort (figure 3.3A). Patients with high *BRE* expression (3 times the standard deviation above the mean of the complete cohort) had a favorable outcome compared to the remaining intermediate and high risk patients in this cohort as well (5-year OS of 25.6±2.6 vs. 71.4±17.1%, p=0.039 for patients with normal and high *BRE* expression, respectively) (supplemental figure 3.5). Despite the clear prognostic effect, we were unable to confirm the independent prognostic value of high *BRE* expression in this cohort. This could be explained by the low number of

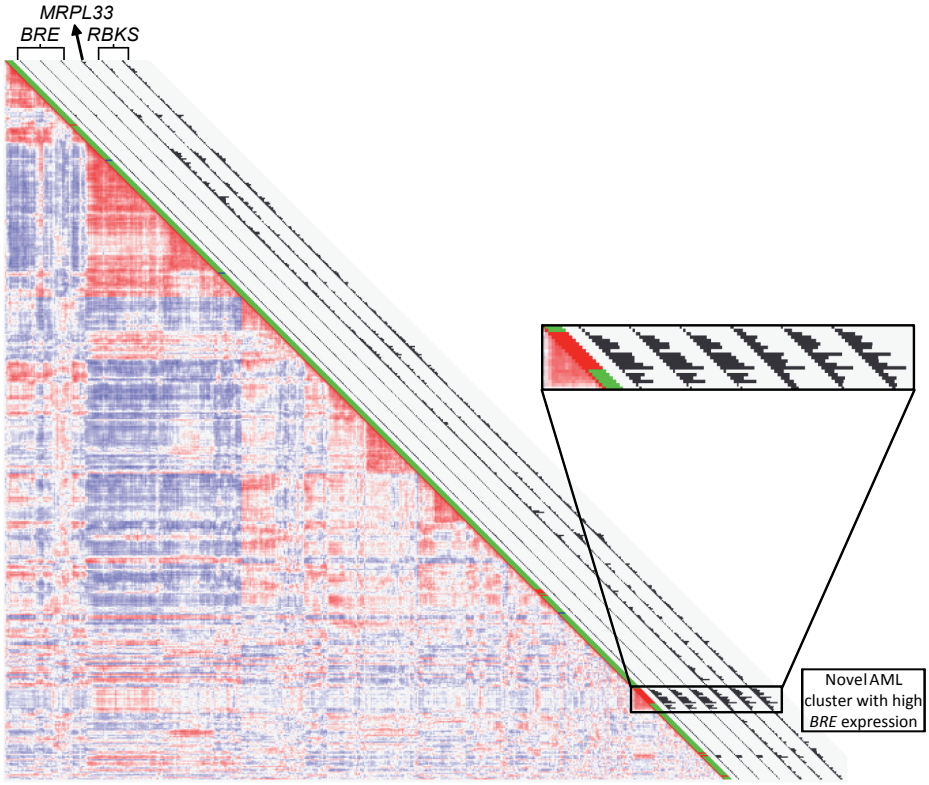


**Figure 3.4: Patients with high *BRE* expression were confined to a novel AML subclass**
Pairwise correlations of 525 AML patients based on optimal clustering as described before[16] identified several clusters of patients with similar expression profiles which can be recognized by the red blocks showing high correlation along the diagonal. One of these clusters was represented by a high incidence (86%) of patients with high *BRE* expression (left three black bars show the relative intensity of the three probe sets representing *BRE* expression on the array). The other three black bars show the relative expression intensity of the probe set for *MRPL33* and two probe sets for *RBKS* as indicated in the figure, revealing co-expression of these chromosomal neighbors with *BRE*. The *MLL-AF9* status of the samples is represented in the green bar (green: negative, red: positive, blue: ND).

high *BRE* expressing patients and lack of sufficient molecular data of more than 50% of the patients. Furthermore, the co-occurrence with *MLL-AF9* in this cohort was even stronger than in the primary cohort (6 out of 7 high *BRE* patients were *MLL-AF9* positive, p<0.001, figure 3.4A).

To validate the effect of *BRE* expression on survival within *MLL-AF9* patients, we combined the *BRE* expression data of the eleven *MLL-AF9* positive patients in this cohort with an additional group of fourteen *MLL-AF9* positive patients. These 25 patients were subdivided according to normal and high *BRE* expression based on the cut-off used in the second AML cohort of 436 samples. Also in this *MLL-AF9* cohort, the OS of the patients with high *BRE* expression was significantly better than the OS of the remaining *MLL-AF9* positive patients (5-year OS of 7.1±6.9 vs. 63.6±14.5%, p=0.0089 for patients with normal and high *BRE* expression, respectively) (figure 3.3B). We conclude that high *BRE* expression is a good prognostic factor, especially among *MLL-AF9* positive cases, based on data from two large independent AML cohorts.



*Patients with high BRE expression are confined to a new subclass in AML*

Unsupervised cluster analysis of gene expression profiles in the first AML cohort revealed that patients with high *BRE* expression were confined almost completely to a previously uncharacterized cluster (twelve of the fourteen patients with high *BRE* expression) (figure 3.4). Two additional samples without high *BRE* expression belonged to this cluster as well. *MLL-AF9* positivity was overrepresented in this cluster (ten of the eighteen *MLL-AF9* positive patients) as was expected because of its co-occurrence with high *BRE* expression. However, the correlation of the cluster with *MLL-AF9* positivity was less than the correlation with high *BRE* expression. The OS of the patients within this cluster was significantly better than the remaining cohort, as could be anticipated based on the overrepresentation of patients with high *BRE* expression (data not shown).

## Discussion

Several mutations and changes in expression of Ub-genes are implicated in the pathogenesis of AML[4,6-8]. By correlating outlier expression of Ub-genes with clinical outcome in 525 AML patients, we identified differentially high expression of *EVI1* and *BRE* as prognostic factors. Previous research has already shown that high *EVI1* expression is an independent poor prognostic factor[13], providing proof-of-principle that outlier analysis is a powerful approach to identify prognostic factors.

BRE is a subunit of the BRCA1-BARD1 DNA damage repair ubiquitin E3 ligase complex and enhances its activity[29,30]. BRE also downregulates TNFα signaling by binding death receptors[31] and overexpression of BRE inhibits apoptosis[31-33]. Differentially high *BRE* expression occurred in 3% of the AML patients, while the remaining patients showed only small differences in *BRE* expression. No high *BRE* expression was

found in donor CD34+ cells, total bone marrow or several mature blood cells, nor in several t(9;11) cell lines tested by us (supplemental figure 3.3) or others[23]. Importantly, the differential expression found in AML was an independent factor for both favorable OS and EFS (table 3.3). High *BRE* expression co-occurred with FAB M5 morphology, a relatively young age and *MLL-AF9* fusions. In contrast, high expression was mutually exclusive with favorable karyotypes, *CEBPA* mutations, *FLT3* ITD, *EVI1* overexpression, and *IDH1* and *IDH2* mutations in the studied cohort (table 3.2). The co-occurrence of high *BRE* expression with *MLL-AF9* fusions and its favorable prognostic value in AML was validated in an independent cohort of 436 patients.

T(9;11) translocations can be missed by routine cytogenetic analysis. Indeed, re-analysis of the 525 AML samples by *MLL-AF9* RT-PCR identified eight additional *MLL-AF9* positive samples (total=18 samples), indicating that 44% of the cases were missed by cytogenetic analysis. Previous research in various cohorts showed that the prognostic value of *MLL-AF9* positivity in AML is controversial[26-28]. In the cohort studied here, the total group of *MLL-AF9* positive patients showed an intermediate survival, which was not significantly different compared to the remaining intermediate and high risk patients. Importantly, our data suggest that the *MLL-AF9* positive group actually consists of two prognostic groups that are characterized by the level of *BRE* expression: *MLL-AF9* positive patients with high *BRE* expression showed a superior survival while patients without high *BRE* expression showed a very poor outcome (figure 3.2C). The prognostic impact of high *BRE* expression was reinforced by showing the favorable effect of high *BRE* expression on overall survival in an independent cohort of *MLL-AF9* positive patients. Thus, patients with high *BRE* expression constitute a novel favorable prognostic group in AML.

During the preparation of this manuscript, Balgobind *et al.* showed correlations of high *BRE* expression with favorable relapse free survival (RFS) in pediatric AML[23]. They did not observe correlations with OS and EFS, as described here for adult AML. In their study, high *BRE* expression was associated with FAB M5 morphology and 11q23 translocations (primarily t(9;11)) as well. They showed a favorable RFS of *MLL* rearranged pediatric patients with high *BRE* expression, compared to the remaining *MLL* rearranged patients without high *BRE* expression. However, they did not address survival among *MLL-AF9* patients, as was done in this study. Nevertheless, high *BRE* expression is a prognostic factor both in pediatric and adult AML, although the effect of high *BRE* expression on clinical outcome is different for adults and children. Additional studies are required to determine whether this is caused by differences in treatment regimens.

Genome wide expression profiling supported the fact that patients with high *BRE* expression constitute a new subtype in AML, since unsupervised cluster analysis showed that most patients with high *BRE* expression were confined to a distinct cluster (figure 3.4). This indicates that these patients shared global expression profiles. In this

cluster no recurrent genetic aberrations were identified other than the expected partial co-occurrence with the *MLL-AF9* fusion. Within this cluster, high *BRE* expression was more frequently observed than *MLL-AF9* positivity, proposing a better correlation of high *BRE* expression than *MLL-AF9* positivity with this cluster. In addition, *BRE* appeared to be among the most discriminatively expressed genes when comparing this cluster to the other AML samples (data not shown).

The frequent co-occurrence of high *BRE* expression and *MLL-AF9* fusions could suggest that *BRE* is a direct target of the oncogenic fusion protein. However, independent mouse studies did not identify *BRE* as *MLL-AF9* target in untransformed or transformed cells[34,35]. We observed that about half of the *MLL-AF9* positive patients did not show high *BRE* expression, strongly suggesting that it is not a direct target in all cases. Furthermore, the unique expression profile characteristic for patients with high *BRE* expression co-occurred only partially with *MLL-AF9* positivity (figure 3.4). This could suggest that other factors than *MLL-AF9* determine this profile. Although we observed no correlations between *BRE* expression and known *MLL-AF9* target genes such as *HoxA7*, *HoxA9* and *MLL* (data not shown), we did observe an inverse correlation with the *MLL-AF9* target *MEIS1* (supplemental figure 3.6). This could suggest that *MLL-AF9* uses separate tumor dependent co-factors to activate different gene programs, one including *BRE*, the other including *MEIS1*. Whether *MLL-AF9* binds different regulatory DNA sequences depending on the availability of co-factors needs to be addressed in future research.

By studying genes that showed co-expression with high *BRE* expression, we found that two co-expressed genes, *RBKS* and *MRPL33*, are located directly upstream of *BRE* on chromosome 2 (2p23.2) (figure 3.4). High *BRE* expression was inextricably linked with high *RBKS* and *MRPL33* expression. Reversely, high *RBKS* or *MRPL33* expression did not necessarily co-occur with high *BRE* expression. Genes more up- or downstream of *BRE* did not show this co-expression (data not shown). These data might indicate that a larger chromosomal locus is deregulated in patients with high *BRE* expression. To our knowledge, no small aberrations in the chromosomal region comprising the *BRE* locus have been identified in AML patients so far[36-39]. Therefore, it will be important to determine in more detail whether the high expression of the three consecutive genes on this locus is due to local changes in transcriptional regulation or whether this is caused by chromosomal aberrations.

We conclude that unbiased statistical outlier analyses of Ub-gene expression distributions in AML allowed us to identify high *BRE* expression as a novel prognostic factor. Furthermore, we identified a previously unrecognized subtype in AML with favorable outcome, represented by the differentially high *BRE* expression. These findings provide new insights into the risk stratification of AML, especially within the group of *MLL-AF9* positive patients.

**Acknowledgements**

This work was supported by the Vanderes foundation. We thank S. Urbé and S. Hayes for sharing their overview of human DUBs with us.

## Reference List


1. Mardis,E.R. *et al.* Recurring mutations found by sequencing an acute myeloid leukemia genome. *N. Engl. J. Med.* **361**, 1058-1066 (2009).
2. Dash,A. & Gilliland,D.G. Molecular genetics of acute myeloid leukaemia. *Best. Pract. Res. Clin. Haematol.* **14**, 49-64 (2001).
3. Renneville,A. *et al.* Cooperating gene mutations in acute myeloid leukemia: a review of the literature. *Leukemia* **22**, 915-931 (2008).
4. Marteijn,J.A., Jansen,J.H., & van der Reijden,B.A. Ubiquitylation in normal and malignant hematopoiesis: novel therapeutic targets. *Leukemia* **20**, 1511-1518 (2006).
5. Hoeller,D. & Dikic,I. Targeting the ubiquitin system in cancer therapy. *Nature* **458**, 438-444 (2009).
6. Sargin,B. *et al.* Flt3-dependent transformation by inactivating c-Cbl mutations in AML. *Blood* **110**, 1004-1012 (2007).
7. Abbas,S., Rotmans,G., Lowenberg,B., & Valk,P.J. Exon 8 splice site mutations in the gene encoding the E3-ligase CBL are associated with core binding factor acute myeloid leukemias. *Haematologica* **93**, 1595-1597 (2008).
8. Keeshan,K. *et al.* Tribbles homolog 2 inactivates C/EBPalpha and causes acute myelogenous leukemia. *Cancer Cell* **10**, 401-411 (2006).
9. Shah,J.J. & Orlowski,R.Z. Proteasome inhibitors in the treatment of multiple myeloma. *Leukemia* **23**, 1964-1979 (2009).
10. Xu,G.W. *et al.* The ubiquitin-activating enzyme E1 as a therapeutic target for the treatment of leukemia and multiple myeloma. *Blood* **115**, 2251-2259 (2010).
11. Kojima,K. *et al.* MDM2 antagonists induce p53-dependent apoptosis in AML: implications for leukemia therapy. *Blood* **106**, 3150-3159 (2005).
12. Andreeff,M. *et al.* A Multi-Center, Open-Label, Phase I Study of Single Agent RG7112, A First In Class p53-MDM2 Antagonist, In Patients with Relapsed/Refractory Acute Myeloid and Lymphoid Leukemias (AML/ALL) and Refractory Chronic Lymphocytic Leukemia/Small Cell Lymphocytic Lymphomas (CLL/SCLL). *ASH Annual Meeting Abstracts* **116**, 657 (2010).
13. Groschel,S. *et al.* High EVI1 expression predicts outcome in younger adult patients with acute myeloid leukemia and is associated with distinct cytogenetic abnormalities. *J. Clin. Oncol.* **28**, 2101-2107 (2010).
14. Wouters,B.J., Lowenberg,B., & Delwel,R. A decade of genome-wide gene expression profiling in acute myeloid leukemia: flashback and prospects. *Blood* **113**, 291-298 (2009).
15. Bullinger,L. *et al.* Use of gene-expression profiling to identify prognostic subclasses in adult acute myeloid leukemia. *N. Engl. J. Med.* **350**, 1605-1616 (2004).
16. Valk,P.J. *et al.* Prognostically useful gene-expression profiles in acute myeloid leukemia. *N. Engl. J. Med.* **350**, 1617-1628 (2004).
17. Stegmeier,F. *et al.* Anaphase initiation is regulated by antagonistic ubiquitination and deubiquitination activities. *Nature* **446**, 876-881 (2007).
18. Wouters,B.J. *et al.* Double CEBPA mutations, but not single CEBPA mutations, define a subgroup of acute myeloid leukemia with a distinctive gene expression profile that is uniquely associated with a favorable outcome. *Blood* **113**, 3088-3091 (2009).
19. Kharas,M.G. *et al.* Musashi-2 regulates normal hematopoiesis and promotes aggressive myeloid leukemia. *Nat. Med.* **16**, 903-908 (2010).
20. Bullinger,L. *et al.* An FLT3 gene-expression signature predicts clinical outcome in normal karyotype AML. *Blood* **111**, 4490-4495 (2008).
21. Sander,S. *et al.* MYC stimulates EZH2 expression by repression of its negative regulator miR-26a.

*Blood* **112**, 4202-4212 (2008).
22. Marteijn,J.A. *et al.* The E3 ubiquitin-protein ligase Triad1 inhibits clonogenic growth of primary myeloid progenitor cells. *Blood* **106**, 4114-4123 (2005).
23. Balgobind,B.V. *et al.* High BRE expression in pediatric MLL-rearranged AML is associated with favorable outcome. *Leukemia* **24**, 2048-2055 (2010).
24. Jansen,M.W., Van der Velden,V., & Van Dongen,J.J. Efficient and easy detection of MLL-AF4, MLL-AF9 and MLL-ENL fusion gene transcripts by multiplex real-time quantitative RT-PCR in TaqMan and LightCycler. *Leukemia* **19**, 2016-2018 (2005).
25. Schlenk,R.F. *et al.* Mutations and treatment outcome in cytogenetically normal acute myeloid leukemia. *N. Engl. J. Med.* **358**, 1909-1918 (2008).
26. Grimwade,D. *et al.* Refinement of cytogenetic classification in acute myeloid leukemia: determination of prognostic significance of rare recurring chromosomal abnormalities among 5876 younger adult patients treated in the United Kingdom Medical Research Council trials. *Blood* **116**, 354-365 (2010).
27. Krauter,J. *et al.* Prognostic factors in adult patients up to 60 years old with acute myeloid leukemia and translocations of chromosome band 11q23: individual patient data-based meta-analysis of the German Acute Myeloid Leukemia Intergroup. *J. Clin. Oncol.* **27**, 3000-3006 (2009).
28. Schoch,C. *et al.* AML with 11q23/MLL abnormalities as defined by the WHO classification: incidence, partner chromosomes, FAB subtype, age distribution, and prognostic impact in an unselected series of 1897 cytogenetically analyzed AML cases. *Blood* **102**, 2395-2402 (2003).
29. Dong,Y. *et al.* Regulation of BRCC, a holoenzyme complex containing BRCA1 and BRCA2, by a signalosome-like subunit and its role in DNA repair. *Mol. Cell* **12**, 1087-1099 (2003).
30. Wang,B., Hurov,K., Hofmann,K., & Elledge,S.J. NBA1, a new player in the Brca1 A complex, is required for DNA damage resistance and checkpoint control. *Genes Dev.* **23**, 729-739 (2009).
31. Li,Q. *et al.* A death receptor-associated anti-apoptotic protein, BRE, inhibits mitochondrial apoptotic pathway. *J. Biol. Chem.* **279**, 52106-52116 (2004).
32. Tang,M.K. *et al.* Comparative proteomic analysis reveals a function of the novel death receptor-associated protein BRE in the regulation of prohibitin and p53 expression and proliferation. *Proteomics.* **6**, 2376-2385 (2006).
33. Chen,H.B. *et al.* Comparative proteomic analysis reveals differentially expressed proteins regulated by a potential tumor promoter, BRE, in human esophageal carcinoma cells. Biochem. *Cell Biol.* **86**, 302-311 (2008).
34. Chen,W. *et al.* Malignant transformation initiated by Mll-AF9: gene dosage and critical target cells. *Cancer Cell* **13**, 432-440 (2008).
35. Krivtsov,A.V. *et al.* Transformation from committed progenitor to leukaemia stem cell initiated by MLL-AF9. *Nature* **442**, 818-822 (2006).
36. Parkin,B. *et al.* Acquired genomic copy number aberrations and survival in adult acute myelogenous leukemia. *Blood* **116**, 4958-4967 (2010).
37. Tiu,R.V. *et al.* New lesions detected by single nucleotide polymorphism array-based chromosomal analysis have important clinical impact in acute myeloid leukemia. *J. Clin. Oncol.* **27**, 5219-5226 (2009).
38. Walter,M.J. *et al.* Acquired copy number alterations in adult acute myeloid leukemia genomes. *Proc. Natl. Acad. Sci. U.S.A* **106**, 12950-12955 (2009).
39. Bullinger,L. *et al.* Identification of acquired copy number alterations and uniparental disomies in cytogenetically normal acute myeloid leukemia using high-resolution single-nucleotide polymorphism analysis. *Leukemia* **24**, 438-449 (2010).
40. Groettrup,M., Pelzer,C., Schmidtke,G., & Hofmann,K. Activating the ubiquitin family: UBA6 challenges the field. *Trends Biochem. Sci.* **33**, 230-237 (2008).

41. Christensen,D.E. & Klevit,R.E. Dynamic interactions of proteins in complex networks: identifying the complete set of interacting E2s for functional investigation of E3-dependent protein ubiquitination. *FEBS J.* **276**, 5381-5389 (2009).
42. Deshaies,R.J. & Joazeiro,C.A. RING domain E3 ubiquitin ligases. *Annu. Rev. Biochem.* **78**, 399-434 (2009).
43. van der Reijden,B.A., Erpelinck-Verschueren,C.A., Lowenberg,B., & Jansen,J.H. TRIADs: a new class of proteins with a novel cysteine-rich signature. *Protein Sci.* **8**, 1557-1561 (1999).
44. Rotin,D. & Kumar,S. Physiological functions of the HECT family of ubiquitin ligases. *Nat. Rev. Mol. Cell Biol.* **10**, 398-409 (2009).
45. Coscoy,L. & Ganem,D. PHD domains and E3 ubiquitin ligases: viruses make the connection. *Trends Cell Biol.* **13**, 7-12 (2003).
46. Hatakeyama,S. & Nakayama,K.I. U-box proteins as a new family of ubiquitin ligases. *Biochem. Biophys. Res. Commun.* **302**, 635-645 (2003).
47. Piessevaux,J., Lavens,D., Peelman,F., & Tavernier,J. The many faces of the SOCS box. *Cytokine Growth Factor Rev.* **19**, 371-381 (2008).
48. Ho,M.S., Ou,C., Chan,Y.R., Chien,C.T., & Pi,H. The utility F-box for protein destruction. *Cell Mol. Life Sci.* **65**, 1977-2000 (2008).
49. Perez-Torrado,R., Yamada,D., & Defossez,P.A. Born to bind: the BTB protein-protein interaction domain. *Bioessays* **28**, 1194-1202 (2006).
50. Komander,D., Clague,M.J., & Urbe,S. Breaking the chains: structure and function of the deubiquitinases. *Nat. Rev. Mol. Cell Biol.* **10**, 550-563 (2009).

**Supplemental table 3.1A: Interpro codes of ubiquitination related domains**

| Interpro code | Interpro short description |
|---|---|
| IPR000011 | Ubiquitin-activating enzyme, E1 |
| IPR000127 | Ubiquitin-activating enzyme repeat |
| IPR000306 | Zinc finger, FYVE-type |
| IPR000315 | Zinc finger, B-box |
| IPR000426 | Proteasome alpha-subunit, conserved site |
| IPR000449 | Ubiquitin-associated/translation elongation factor EF1B, N-terminal |
| IPR000569 | HECT |
| IPR000594 | UBA/THIF-type NAD/FAD binding fold |
| IPR000608 | Ubiquitin-conjugating enzyme, E2 |
| IPR000626 | Ubiquitin |
| IPR001232 | SKP1 component |
| IPR001334 | E6 early regulatory protein |
| IPR001353 | 20S proteasome, A and B subunits |
| IPR001370 | Proteinase inhibitor I32, inhibitor of apoptosis |
| IPR001373 | Cullin, N-terminal region |
| IPR001394 | Peptidase C19, ubiquitin carboxyl-terminal hydrolase 2 |
| IPR001496 | SOCS protein, C-terminal |
| IPR001578 | Peptidase C12, ubiquitin carboxyl-terminal hydrolase 1 |
| IPR001607 | Zinc finger, UBP-type |
| IPR001680 | WD40 repeat |
| IPR001810 | Cyclin-like F-box |
| IPR001841 | Zinc finger, RING type |
| IPR001965 | Zinc finger, PHD-type |
| IPR001975 | Ribosomal protein L40e |
| IPR002004 | Polyadenylate-binding protein/Hyperplastic disc protein |
| IPR002083 | MATH |
| IPR002714 | Tumour suppressor protein, von Hippel-Lindau disease |
| IPR002867 | Zinc finger, C6HC-type |
| IPR002906 | Ribosomal protein S27a |
| IPR003105 | SRA-YDG |
| IPR003126 | Zinc finger, N-recognin |
| IPR003153 | Adaptor protein Cbl, N-terminal helical |
| IPR003185 | Proteasome activator pa28, REG alpha subunit |
| IPR003323 | Ovarian tumour, otubain |
| IPR003613 | U box |
| IPR003649 | B-box, C-terminal |
| IPR003653 | Peptidase C48, SUMO/Sentrin/Ubl1 |

| | |
|---|---|
| IPR003892 | Ubiquitin system component Cue |
| IPR003903 | Ubiquitin interacting motif |
| IPR003977 | Parkin |
| IPR004162 | Seven in absentia protein |
| IPR004170 | WWE |
| IPR004806 | UV excision repair protein Rad23 |
| IPR004854 | Ubiquitin fusion degradation protein UFD1 |
| IPR004939 | Anaphase-promoting complex, subunit 10 |
| IPR005062 | SAC3/GANP/Nin1/mts3/eIF-3 p25 |
| IPR005176 | Protein of unknown function DUF298 |
| IPR005375 | Ubiquitin-like, Ufm1 |
| IPR005607 | BSD |
| IPR006285 | E1-like protein-activating enzyme Gsa7p/Apg7p |
| IPR006575 | RWD |
| IPR006615 | Ubiquitin carboxyl-terminal hydrolase, N-terminal region 1 |
| IPR006746 | 26S proteasome non-ATPase regulatory subunit Rpn12 |
| IPR006928 | Peptidase C76, herpesvirus UL36 UL36 deubiquitinylating peptidase |
| IPR007192 | Cdc23 |
| IPR007397 | F-box associated region |
| IPR007527 | Zinc finger, SWIM-type |
| IPR007901 | MoeZ/MoeB |
| IPR008401 | Apc13p |
| IPR008402 | Anaphase-promoting complex, Apc15p-like |
| IPR008974 | TRAF-like |
| IPR009060 | UBA-like |
| IPR009109 | Ran-GTPase activating protein 1, C-terminal |
| IPR010309 | E3 ubiquitin ligase, region of unknown function DUF908 |
| IPR010314 | E3 ubiquitin ligase, region of unknown function DUF913 |
| IPR010460 | Ubiquitin carboxyl-terminal hydrolase, N-terminal region 2 |
| IPR010606 | Mib-herc2 |
| IPR011011 | Zinc finger, FYVE/PHD-type |
| IPR011016 | Zinc finger, variant RING-type |
| IPR011333 | BTB/POZ fold |
| IPR012462 | Peptidase C78, ubiquitin fold modifier-specific peptidase 1 and 2 |
| IPR013010 | Zinc finger, SIAH-type |
| IPR013069 | BTB/POZ |
| IPR013083 | Zinc finger, RING/FYVE/PHD-type |
| IPR013246 | Sgf11, transcriptional regulation |
| IPR013322 | TRAF-type |

| | |
|---|---|
| IPR013323 | SIAH-type |
| IPR013896 | Ubiquitin-associated region 2 |
| IPR013956 | E3 ubiquitin ligase, BRE1 |
| IPR014645 | Target of Myb protein 1 |
| IPR014741 | Adaptor protein Cbl, EF hand-like |
| IPR014742 | Adaptor protein Cbl, SH2-like |
| IPR014761 | UV excision repair protein Rad23, C-terminal |
| IPR014764 | Defective in cullin neddylation |
| IPR014786 | Anaphase promoting complex subunit 2 |
| IPR014857 | Zinc finger, RING-like |
| IPR014891 | DWNN domain |
| IPR014929 | E2 binding |
| IPR015036 | USP8 interacting |
| IPR015063 | Region of unknown function DUF1873 |
| IPR015133 | E3 ubiquitin ligase, AvrPtoB |
| IPR015155 | PFU (PLAA family ubiquitin binding) |
| IPR015221 | Ubiquitin related modifier 1 |
| IPR015228 | Ubiquitin-associated |
| IPR015342 | Peroxisome biogenesis factor 1, N-terminal |
| IPR015343 | Peroxisome biogenesis factor 1, alpha/beta |
| IPR015458 | MDM4/MDMX protein |
| IPR015459 | Ubiquitin-protein ligase E3 MDM2 |
| IPR015496 | Ubiquilin |
| IPR015580 | RUB1 conjugating enzyme Ubc12 |
| IPR015581 | Ubiquitin-conjugating enzyme |
| IPR015582 | Ubiquitin-conjugating enzyme E2 H10 |
| IPR015940 | Ubiquitin-associated/translation elongation factor EF1B, N-terminal, eukaryote |
| IPR015943 | WD40/YVTN repeat-like |
| IPR016010 | Parkin, C-terminal |
| IPR016072 | SKP1 component, dimerisation |
| IPR016073 | SKP1 component, POZ |
| IPR016135 | Ubiquitin-conjugating enzyme/RWD-like |
| IPR016157 | Cullin, conserved site |
| IPR016158 | Cullin homology |
| IPR016159 | Cullin repeat-like |
| IPR016398 | E3 ubiquitin-protein ligase p28 |
| IPR016615 | Ubiquitin thioesterase Otubain |
| IPR016652 | Ubiquitinyl hydrolase |
| IPR016806 | COP9 signalosome complex, subunit 9 |

| | |
|---|---|
| IPR016897 | E3 ubiquitin ligase, SCF complex, Skp subunit |
| IPR017073 | Ubiquitin binding protein, Hrs/VPS27 |
| IPR017134 | Ubiquitin-protein ligase E6-AP |
| IPR017335 | E3 ubiquitin ligase, RNF8 |
| IPR017390 | Ubiquitinyl hydrolase, UCH37 type |

**Supplemental table 3.1B: GO terms of ubiquitin related processes**

| GO term code | GO term name |
|---|---|
| GO:0000151 | ubiquitin ligase complex |
| GO:0000152 | nuclear ubiquitin ligase complex |
| GO:0000153 | cytoplasmic ubiquitin ligase complex |
| GO:0000209 | protein polyubiquitination |
| GO:0000502 | proteasome complex |
| GO:0000835 | ER ubiquitin ligase complex |
| GO:0000836 | Hrd1p ubiquitin ligase complex |
| GO:0004221 | ubiquitin thiolesterase activity |
| GO:0004839 | ubiquitin activating enzyme activity |
| GO:0004842 | ubiquitin-protein ligase activity |
| GO:0004843 | ubiquitin-specific protease activity |
| GO:0005838 | proteasome regulatory particle |
| GO:0005839 | proteasome core complex |
| GO:0006511 | ubiquitin-dependent protein catabolic process |
| GO:0006513 | protein monoubiquitination |
| GO:0008537 | proteasome activator complex |
| GO:0008538 | proteasome activator activity |
| GO:0008539 | proteasome inhibitor activity |
| GO:0008641 | small protein activating enzyme activity |
| GO:0010390 | histone monoubiquitination |
| GO:0010498 | proteasomal protein catabolic process |
| GO:0010860 | proteasome regulator activity |
| GO:0016567 | protein ubiquitination |
| GO:0016574 | histone ubiquitination |
| GO:0016578 | histone deubiquitination |
| GO:0016579 | protein deubiquitination |
| GO:0016925 | protein sumoylation |
| GO:0019005 | SCF ubiquitin ligase complex |
| GO:0019773 | proteasome core complex, alpha-subunit complex |
| GO:0019783 | small conjugating protein-specific protease activity |
| GO:0019787 | small conjugating protein ligase activity |
| GO:0022624 | proteasome accessory complex |

| | |
|---|---|
| GO:0031145 | anaphase-promoting complex-dependent proteasomal ubiquitin-dependent protein catabolic process |
| GO:0031146 | SCF-dependent proteasomal ubiquitin-dependent protein catabolic process |
| GO:0031371 | ubiquitin conjugating enzyme complex |
| GO:0031386 | protein tag |
| GO:0031396 | regulation of protein ubiquitination |
| GO:0031397 | negative regulation of protein ubiquitination |
| GO:0031398 | positive regulation of protein ubiquitination |
| GO:0031461 | cullin-RING ubiquitin ligase complex |
| GO:0031462 | Cul2-RING ubiquitin ligase complex |
| GO:0031593 | polyubiquitin binding |
| GO:0031597 | cytosolic proteasome complex |
| GO:0031624 | ubiquitin conjugating enzyme binding |
| GO:0031625 | ubiquitin protein ligase binding |
| GO:0032434 | regulation of proteasomal ubiquitin-dependent protein catabolic process |
| GO:0032435 | negative regulation of proteasomal ubiquitin-dependent protein catabolic process |
| GO:0032436 | positive regulation of proteasomal ubiquitin-dependent protein catabolic process |
| GO:0033182 | regulation of histone ubiquitination |
| GO:0033522 | histone H2A ubiquitination |
| GO:0033523 | histone H2B ubiquitination |
| GO:0034450 | ubiquitin-ubiquitin ligase activity |
| GO:0042787 | protein ubiquitination during ubiquitin-dependent protein catabolic process |
| GO:0043130 | ubiquitin binding |
| GO:0043161 | proteasomal ubiquitin-dependent protein catabolic process |
| GO:0043161 | proteasomal ubiquitin-dependent protein catabolic process |
| GO:0043162 | ubiquitin-dependent protein catabolic process via the multivesicular body sorting pathway |
| GO:0043248 | proteasome assembly |
| GO:0051436 | negative regulation of ubiquitin-protein ligase activity during mitotic cell cycle |
| GO:0051437 | positive regulation of ubiquitin-protein ligase activity during mitotic cell cycle |
| GO:0051438 | regulation of ubiquitin-protein ligase activity |
| GO:0051439 | regulation of ubiquitin-protein ligase activity during mitotic cell cycle |
| GO:0051443 | positive regulation of ubiquitin-protein ligase activity |
| GO:0051444 | negative regulation of ubiquitin-protein ligase activity |
| GO:0051865 | protein autoubiquitination |
| GO:0055105 | ubiquitin-protein ligase inhibitor activity |
| GO:0055106 | ubiquitin-protein ligase regulator activity |
| GO:0070086 | ubiquitin-dependent endocytosis |
| GO:0070530 | K63-linked polyubiquitin binding |

| | |
|---|---|
| GO:0070534 | protein K63-linked ubiquitination |
| GO:0070535 | histone H2A K63-linked ubiquitination |
| GO:0070536 | protein K63-linked deubiquitination |
| GO:0070537 | histone H2A K63-linked deubiquitination |
| GO:0070844 | polyubiquitinated protein transport |
| GO:0070845 | polyubiquitinated misfolded protein transport |

**Supplemental table 3.2: Normalized *BRE* expression data of the validation cohort of 25 *MLL-AF9* positive patients**

| sample | array type | *BRE* expression[a] |
|---|---|---|
| 1 | cDNA | -2.22 |
| 2 | U133plus2.0 | -2.04 |
| 3 | cDNA | -1.94 |
| 4 | cDNA | -1.88 |
| 5 | U133plus2.0 | -0.99 |
| 6 | U133plus2.0 | -0.94 |
| 7 | U133plus2.0 | -0.88 |
| 8 | U133plus2.0 | -0.73 |
| 9 | cDNA | -0.61 |
| 10 | U133plus2.0 | -0.56 |
| 11 | U133plus2.0 | -0.50 |
| 12 | cDNA | -0.30 |
| 13 | U133plus2.0 | -0.29 |
| 14 | U133plus2.0 | -0.05 |
| 15 | cDNA | 0.52 |
| 16 | cDNA | 0.83 |
| 17 | cDNA | 1.18 |
| 18 | cDNA | 1.20 |
| 19 | cDNA | 1.31 |
| 20 | U133plus2.0 | 1.32 |
| 21 | U133plus2.0 | 1.52 |
| 22 | U133plus2.0 | 1.53 |
| 23 | U133plus2.0 | 1.84 |
| 24 | cDNA | 1.90 |
| 25 | U133plus2.0 | 1.93 |

[a]Log transformed *BRE* expression data of the Affymetrix HG U133 plus2.0 array were mean centered and averaged from three independent probe sets (212645_x_at, 211566_x_at, and 205550_s_at). For the cDNA array samples, the data of clone IMAGE:739993 were log transformed and mean centered. Afterwards, the data of the two arrays were combined. The cutoff for high *BRE* expression (grey shaded samples) was obtained from analyses in the second cohort of 436 AML patients profiled on the cDNA array.

**Supplemental table 3.3: Ubiquitin related probe sets with 10 or more outlier samples**

| Probe set (gene name) | Number of outlier samples[a,b] | Mean expression of outliers ± SD[c] | Mean expression of remaining AML samples ± SD[c] |
|---|---|---|---|
| 202318_s_at (*SENP6*) | 10 | 1306 ± 85 | 503 ± 123 |
| 205550_s_at (*BRE*) | 10 | 3253 ± 672 | 347 ± 152 |
| 205856_at (*SLC14A1*) | 10 | 457 ± 90 | 41 ± 57 |
| 207600_at (*KCNC3*) | 10 | 27 ± 5 | 5.3 ± 3.0 |
| 209962_at (*EPOR*) | 10 | 889 ± 206 | 54 ± 76 |
| 209963_s_at (*EPOR*) | 10 | 322 ± 64 | 31 ± 31 |
| 210638_s_at (*FBXO9*) | 10 | 3448 ± 655 | 588 ± 299 |
| 210885_s_at (*TRIM15*) | 10 | 53 ± 12 | 4 ± 5 |
| 243526_at (*WDR86*) | 10 | 239 ± 53 | 13 ± 24 |
| 36564_at (*RNF19B*) | 10 | 1794 ± 324 | 247 ± 182 |
| 37986_at (*EPOR*) | 10 | 606 ± 108 | 68 ± 71 |
| 211566_x_at (*BRE*) | 11 | 2489 ± 538 | 226 ± 121 |
| 221884_at (*EVI1*) | 11 | 648 ± 145 | 16 ± 51 |
| 212645_x_at (*BRE*) | 12 | 2581 ± 551 | 228 ±111 |
| 213038_at (*RNF19B*) | 12 | 1392 ± 259 | 213± 137 |

[a]Outlier expression is defined as an expression value more than four times the standard deviation above or under the mean expression of all AML samples;
[b]When performing the outlier analysis on the complete array dataset, 302 probe sets containing 10 or more outlier samples were identified;
[c]SD: standard deviation.

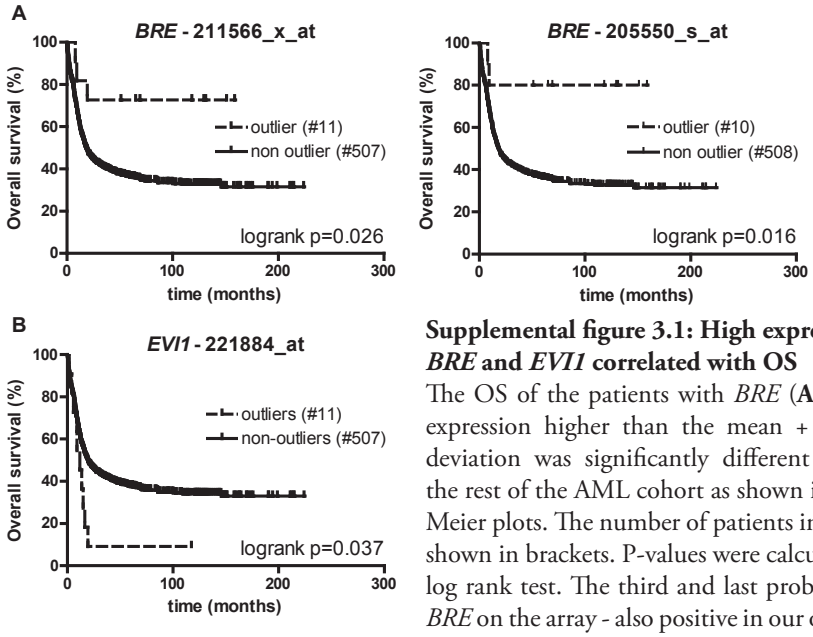


**Supplemental figure 3.1: High expression of *BRE* and *EVI1* correlated with OS**

The OS of the patients with *BRE* (**A**) or *EVI1* (**B**) expression higher than the mean + 4 x standard deviation was significantly different compared to the rest of the AML cohort as shown in the Kaplan-Meier plots. The number of patients in each group is shown in brackets. P-values were calculated with the log rank test. The third and last probe representing *BRE* on the array - also positive in our outlier analysis (212645_x_at) - showed a nearly significant p-value when analyzing OS of outliers compared to all other AML samples (p=0.055, data not shown). The survival curve differences for the different *BRE* probes were caused by the number of patients that were regarded as outlier (expression>4 x standard deviation above the mean), as this varied from 10 to 12 patients, depending on the probe set (see supplemental table 3.3).

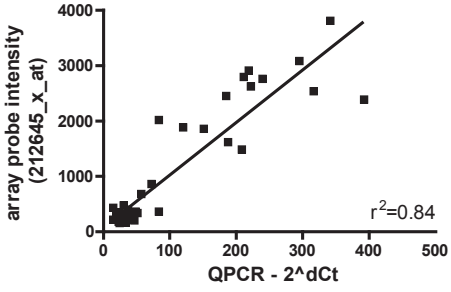


**Supplemental figure 3.2: Correlation of *BRE* array and QPCR expression data**

*BRE* expression measured by probe 212645_x_at on the HGU133 plus2.0 array was compared with QPCR data of the same samples using *PBGD* as housekeeping gene. Samples included for analysis were all samples with high *BRE* expression, as well as the intermediate *BRE* expressing samples and a subset of samples with normal *BRE* expression according to the array data. A good correlation was found with an r2 of 0.84 and p<0.001 as calculated by the Spearmann's correlation coefficient. Comparable correlations were found for the other two *BRE* probe sets of the array versus the QPCR data (r2=0.84 for 211566_x_at vs. QPCR and r2=0.81 for 205550_s_at vs. QPCR, p<0.001, data not shown).

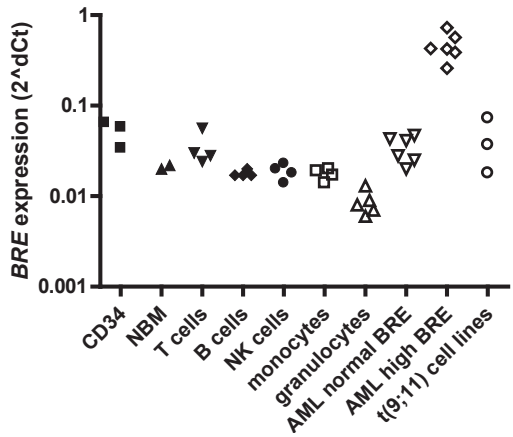


**Supplemental figure 3.3: *BRE* expression in hematopoietic sub fractions and t(9;11) cell lines**

*BRE* expression was measured by QPCR on cDNA of various hematopoietic sub fractions and three t(9;11) positive cell lines (Molm13, Monomac-6, THP1). As a comparison, representatives of normal and high *BRE* expressing AML samples were included in this graph. All data were normalized by β-*ACTIN* and represented as ΔCt ($2^{\Delta Ct}$).

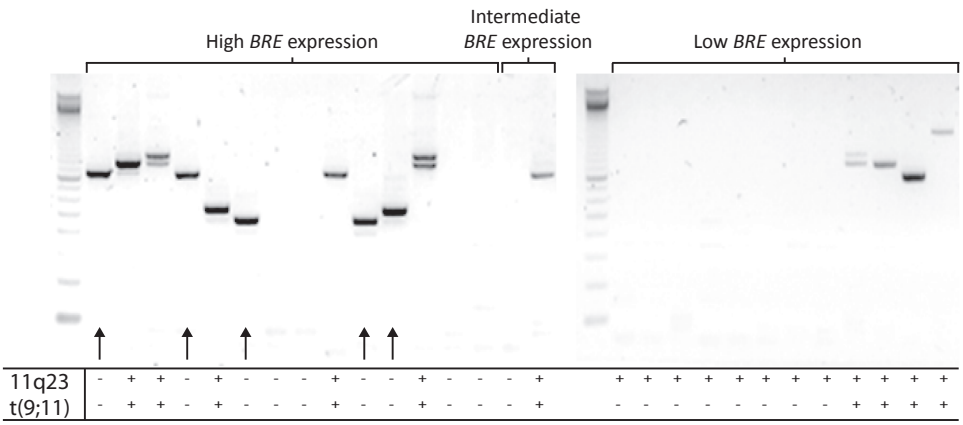


**Supplemental figure 3.4: *MLL-AF9* breakpoint PCR on high *BRE* expressing samples and 11q23 positive samples**

*MLL-AF9* breakpoint RT-PCR was performed on all samples. The gel image shows the resulting PCR products representing the samples with high *BRE* expression, intermediate *BRE* expression and samples with an 11q23 translocation. The table below the gel image shows the original karyotyping results. The arrows indicate the samples that were positive for the *MLL-AF9* breakpoint PCR but were t(9;11) negative based on routine cytogenetic analyses. In addition to the results shown here, three more *MLL-AF9* positive samples were identified after RT-PCR. These samples showed normal *BRE* expression levels.

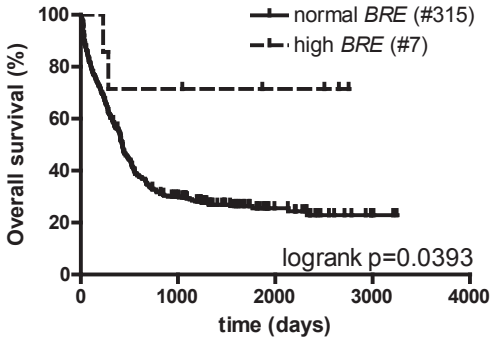


**Supplemental figure 3.5: High *BRE* expression predicts favorable OS in an independent cohort of intermediate and high risk AML patients**

The OS of intermediate and high risk patients (excluding t(8;21), inv(16), and t(15;17) patients) with normal or high *BRE* expression of a second, independent cohort was visualized by Kaplan Meier curves. The cut-off used for high *BRE* expression was based on the mean of all AML patients in this cohort plus 3 x the standard deviation. Patients with high *BRE* expression had a better prognosis than patients with normal *BRE* expression (5-year OS of 25.6±2.6 vs. 71.4±17.1%, p=0.039 for patients with normal *BRE* and high *BRE* expression, respectively). P-values were based on logrank tests. The number of patients included in the analysis is shown in brackets.

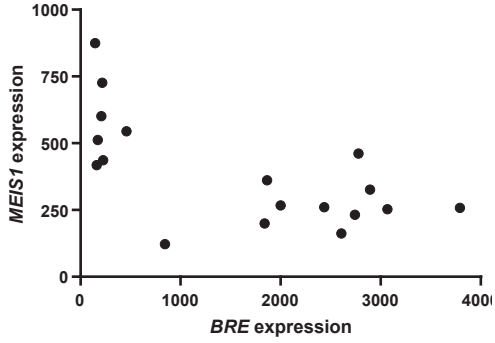


**Supplemental figure 3.6: *BRE* expression is inversely correlated to *MEIS1* expression in *MLL-AF9* positive patients**

Array expression data of *BRE* (probe set: 212645_x_at) and *MEIS1* (probe set 1559477_s_at) showed an inverse correlation within *MLL-AF9* positive patient samples. The calculated Spearmann correlation coefficient is -0.61 with a p-value of 0.007. Similar data were obtained when using other probe sets representing *MEIS1* on the Affymetrix micro-array.

# Improved classification of *MLL-AF9* positive acute myeloid leukemia patients based on *BRE* and *EVI1* expression

**Sylvie M. Noordermeer, Davide Monteferrario, Mathijs A. Sanders, Lars Bullinger, Joop H. Jansen, and Bert A. van der Reijden**

**Part of this chapter was adapted from:**
***Blood,* 2012 May; 119(18):4335-4337.**

## Abstract

**Acute myeloid leukemia (AML) is a heterogeneous disease with many different underlying genetic aberrations, which are often associated with disease development and clinical outcome. AML patients with *MLL-AF9* fusions are currently classified as intermediate risk. Recently, we showed that *MLL-AF9* positive patients can be subdivided into a favorable and a poor prognostic subgroup based on high or normal *BRE* expression, respectively. As *BRE* expression differences are relatively small between the two groups, testing *BRE* expression for diagnostic purpose is difficult using commonly available techniques such as QPCR. In this chapter we show mutually exclusive expression of *BRE* and *EVI1* within *MLL-AF9* positive patients. Only few patients were double negative for both genes. High *EVI1* expression is a poor prognostic marker in AML, and thereby explains the adverse prognosis of the majority of patients with normal *BRE* expression levels. Molecular screening for both high *EVI1* expression and *MLL-AF9* is therefore of importance for proper risk stratification. To study intrinsic differences between the two subtypes of *MLL-AF9* positive AML, global gene expression profiles of high *BRE* and high *EVI1* expressing *MLL-AF9* positive samples were compared. Patients with high *EVI1* expression did not share similar global expression profiles, in contrast to patients with high *BRE* expression. This indicates that *MLL-AF9* by itself does not provoke global expression differences. The *MLL-AF9* fusion encodes a mutated transcription regulator. *EVI1* is a direct target gene of the fusion protein but was not upregulated in all *MLL-AF9* patients. We show that this phenomenon also applied to two other direct targets of *MLL-AF9*, *HOXA9* and *MEIS1*. These data suggest that additional mechanisms and/or factors are involved in deregulating expression of *MLL-AF9* target genes.**

## Introduction

AML is a heterogeneous disease at the molecular level, with a variety of genetic aberrations. Many of these aberrancies influence disease development and consequently prognosis. However, disease outcome often differs substantially between patients within genetically defined subgroups. Therefore, knowledge on discriminating prognostic factors within those subgroups is needed for improved classification and risk dependent treatment.

Recently, we identified high *BRE* expression in 3% of AML patients, which associated with a favorable prognosis. The majority of the patients with high *BRE* expression was positive for the *MLL-AF9* translocation (±70%)[1]. The five-year overall survival (OS) rate of AML patients positive for the *MLL-AF9* fusion gene is approximately 40%[2,3]. Based on *BRE* expression, patients could be further subclassified into a favorable and an adverse prognostic subcategory: *MLL-AF9* positive patients with high *BRE* expression exhibited a superior outcome (five-year OS of 80% and 64% for two independent cohorts, respectively) while patients with normal *BRE* expression exhibited a very poor outcome (five-year OS of 0% and 7%)[1]. Genome-wide expression profiling identified a common global expression profile for more than 85% of the patients with high *BRE* expression[1].

Remarkably, 50% of the *MLL-AF9* patients showed high *BRE* expression. Therefore, there was only partial co-occurrence with the global expression profile characterized by high *BRE* expression[1]. These data suggest that the *MLL-AF9* translocation does not induce a common genome-wide expression program. In this chapter, we study whether *MLL-AF9* positive, *BRE* negative patients can be further characterized, and what the contribution of the *MLL*-translocation is on altered gene expression.

The Mixed Lineage Leukemia (*MLL*) gene encodes a methyltransferase, that is responsible for H3K4 (Histone 3 Lysine 4) methylation. This modification marks genes for active transcription[4,5]. In *MLL*-translocations, the methyltransferase activity is lost[6]. More than 50 fusion partners of *MLL* have been identified so far in acute leukemia's. *AF9*, *ELL* and *ENL* are the most frequently occurring partners in adult AML[6]. MLL-fusion proteins such as MLL-AF9 form a large complex including DOT1L and pTEFb[7]. DOT1L is a methyltransferase for histone 3 lysine 79 (H3K79), inducing an open chromatin formation for gene transcription. Recent data have shown that *MLL-AF9* positive cells show aberrant H3K79 methylation patterns[8]. However, deletion of DOT1L resulted in upregulation of only a small part of the genes showing the aberrant methylation, indicating no absolute correlation of the H3K79 activation mark and gene transcription. The deregulated genes identified were highly enriched for genes to which the MLL-fusion protein binds, often referred to as the direct targets, including *MEIS1* and *HOXA9*[7,8]. Both genes are highly expressed in *MLL-AF9* transformed mouse hematopoietic cells[9,10]. These data suggest a one to one correlation

of *MLL-AF9* transformation and expression of these targets.

Recently, also *EVI1* has been identified as a direct target of *MLL-AF9*[11]. High *EVI1* expression occurs in approximately 10% of AML cases and is associated with an inferior outcome[12,13]. High *EVI1* expression can be a direct consequence of 3q chromosomal aberrations, affecting the *EVI1* gene locus. However, *EVI1* overexpression also occurs in cells without 3q aberrations. For these cases, co-occurrence has been observed with *MLL* rearrangements including *MLL-AF9*[11-13]. However, not all *MLL-AF9* rearranged samples show high *EVI1* expression. This seems to impose a discrepancy with the data reporting *EVI1* as a direct target of *MLL-AF9*.

High *BRE* and *EVI1* expression both correlate partially with *MLL-AF9* translocations, but predict opposite disease outcome for patients. We therefore questioned whether high expression of these genes was mutually exclusive among *MLL-AF9* positive cases. We also studied the expression of the known *MLL*-fusion target genes *HOXA9* and *MEIS1* in individual *MLL*-rearranged AML cases to investigate whether these direct targets are highly expressed in all patients.



## Materials and Methods

*Patient samples and micro-array analyses*

For this study, three previously published and publically available micro-array studies were re-analyzed. AML cohort 1 consisted of 525 AML patients, including 18 *MLL-AF9* positive samples and 15 samples with other 11q23 aberrations (GSE14468)[14]. Gene expression was analyzed using the Affymetrix HG-U133 plus 2.0 array platform (Santa Clara, USA). Cohort 2 contained 436 AML patients, including 11 *MLL-AF9* samples and 4 other *MLL*-rearranged samples (GSE16432)[15]. For gene expression analyses, 40k cDNA arrays were used (manufactured by the Stanford Functional Genomics Facility). For both cohorts, 11q23 aberrations were analyzed by conventional chromosome banding and specific breakpoint PCR or FISH, as described elsewhere[1]. To validate *MEIS1* and *HOXA9* expression in *MLL*-rearranged cases, a third, publically available cohort of 542 AML patients was used, including 38 *MLL*-rearranged cases (GSE13159)[16]. Gene expression profiling of this cohort was performed using the Affymetrix HG-U133 plus 2.0 array platform. Array data normalization was performed separately for the three cohorts.

*Statistical analyses*

Positive or negative correlations between expression of two genes were statistically tested using Spearmann rank correlation tests. Unsupervised clustering analyses were performed as described before[17] and represented as a correlation view between the different samples included in the clustering.

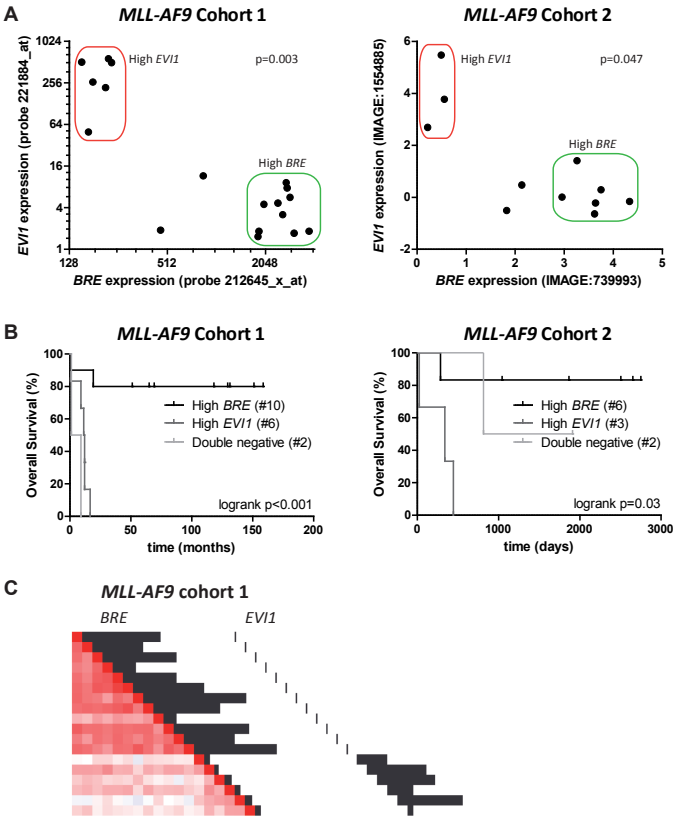


**Figure 4.1. Mutual exclusive expression of *BRE* and *EVI1* in *MLL-AF9* AML**

**A.** *BRE* expression was plotted against *EVI1* expression for *MLL-AF9* positive cases in two separate *MLL-AF9* cohorts[14, 15]. In cohort 1 (left plot), 33% (6/18) of the samples showed high *EVI1* expression, and 55.6% (10/18) showed high *BRE* expression. In cohort 2 (right plot), 27.3% of the samples showed high *EVI1* expression (3/11), and 54.5% showed high *BRE* expression (6/11). Both cohorts contained two patients with neither high *BRE* nor high *EVI1* expression. High *BRE* expression was defined as described before[1]. High *EVI1* was defined as the upper 10% of the total cohort. P-values for negative correlation were calculated using Spearmann correlation tests. **B.** Kaplan-Meier plots showed that patients characterized by high *BRE* expression had significantly better overall survival compared to patients with high *EVI1* expression among *MLL-AF9* positive cases. P-values were determined with the log-rank test. The number of patients included in the analyses is shown in brackets. **C.** Unsupervised genome-wide clustering of *MLL-AF9* patients from cohort 1 showed that *EVI1*-positive patients clustered apart from high *BRE* expressing patients. *EVI1*-positive patients showed less similar expression profiles compared to high *BRE* expressing patients. Unsupervised clustering was performed as described elsewhere[9] and clustering is represented as pairwise correlations between samples with red indicating a high correlation and blue a poor correlation. Black bars represent *BRE* (212645_x_at) and *EVI1* (221884_at) expression, as indicated.

## Results and Discussion

High *BRE* and *EVI1* expression co-occur with *MLL-AF9* translocations, yet both predict opposite disease outcome[1,11-13]. We therefore hypothesized that the expression of these two genes would be mutually exclusive in *MLL-AF9* rearranged AML cases. To determine the correlation between *BRE* and *EVI1* expression, we re-analyzed two *MLL-AF9* cohorts for which we previously reported high *BRE* expression[1,14,15]. This showed that high *BRE* and high *EVI1* expression are indeed mutually exclusive, with only a few cases that did not show high *BRE* or *EVI1* expression (figure 4.1A). As the number of these double negative patients was low, the poor prognosis of the majority of patients lacking high *BRE* expression was explained by high *EVI1* expression (figure 4.1B). Additional studies with larger patient numbers are required to determine the prognosis of the double negative patients.

In our previous study, 40% of *MLL-AF9* positive cases were missed by routine cytogenetics[1]. In addition, *MLL-AF9* positive cases with high *EVI1* expression lack chromosomal rearrangements encompassing the *EVI1* locus on chromosome 3[12,13]. Therefore, molecular screening for *MLL-AF9* and *EVI1* or *BRE* overexpression is strongly recommended to improve risk stratification in these patients. As the fold differences of *BRE* expression between patients with high and normal levels are relatively small[1], screening for *EVI1* overexpression is diagnostically more feasible, as diagnostic tests are already available.

To study whether the mutually exclusive *BRE* and *EVI1* expression represented global expression differences, we performed unsupervised genome-wide gene expression clustering analysis within *MLL-AF9* positive samples. Although the *EVI1*-positive patients were separated from the *BRE*-positive patients (figure 4.1C), they did not share highly similar expression profiles, while *BRE*-positive patients did[1]. Indeed, in an unsupervised clustering analysis of the total AML cohort, *MLL-AF9* positive patients with high *EVI1* expression clustered only partially, showing modest similarities in expression profiles (figure 4.2). Thus, *MLL-AF9* positive patients with high *BRE* expression seem to represent a specific molecular AML subclass with highly similar expression profiles, while the *MLL-AF9* positive patients with high *EVI1* expression do not.

As *EVI1* has been shown to be a direct target of *MLL-AF9*[11] but was only highly expressed in a subset of *MLL-AF9* rearranged patients, target gene transcription might not exclusively depend on the fusion protein. To study whether this phenomenon also applied to two other direct *MLL-AF9* target genes, *MEIS1* and *HOXA9*[8], we compared their expression as well as the expression of *BRE* and *EVI1* in individual *MLL-AF9* or other *MLL*-rearranged AML patients in cohort 1 (figure 4.3). In general, there was an overall higher expression of all four genes in both *MLL-AF9* and other *MLL*-rearranged samples compared to the remaining AML samples, validating data described before[1,10,11,18,19] (figure 4.3A). However, analysis of individual samples showed that none

of the four genes was consistently overexpressed in all *MLL*-rearranged patients. In fact, of the 33 patients with any type of *MLL*-rearrangement, a significant percentage of patients showed expression levels comparable to, or lower than the mean of non *MLL*-rearranged AML cases (18% for *MEIS1*, 12% for *HOXA9*, 58% for *EVI1* and 39% for *BRE*, figure 4.3). In addition, several patients showed high expression of *HOXA9*, but lacked high expression of *MEIS1* (for example, open yellow boxes within the *MLL-AF9* group, samples indicated by *, figure 4.3A) or vice versa (for example, open blue triangles within the 11q23 group, samples indicated by *, figure 4.3A). Indeed, there was no correlation of *MEIS1* and *HOXA9* expression within *MLL*-rearranged samples (p=0.2, figure 4.3B).

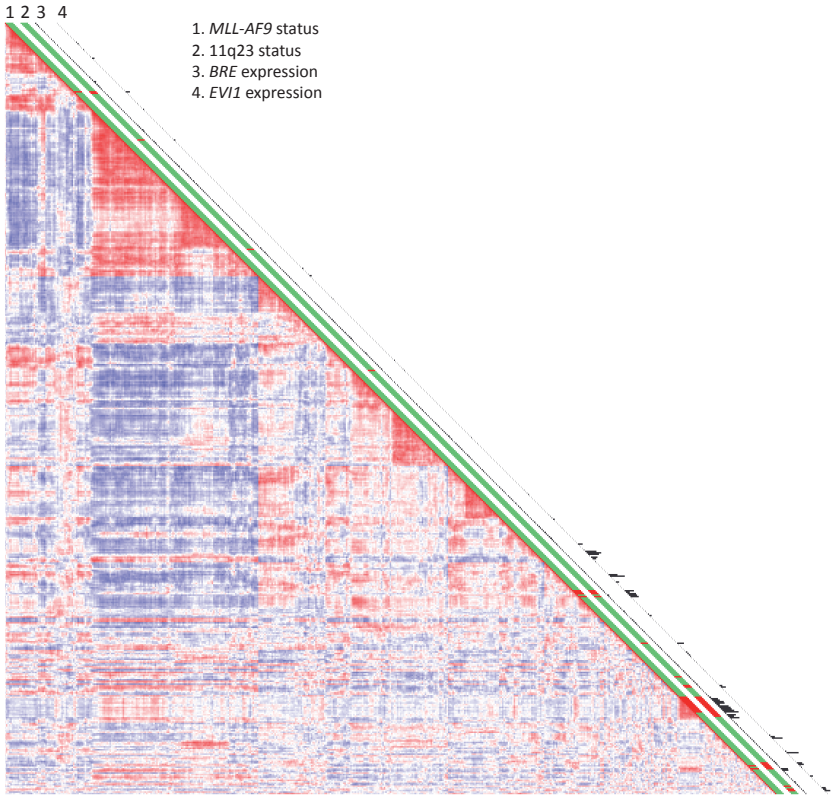


**Figure 4.2: Unsupervised clustering of 525 AML patients**
Unsupervised clustering of the total AML cohort 1 showed that *MLL-AF9* patients with high *BRE* expression clustered together almost completely, as described before1 (chapter 3 of this thesis). This was in contrast to *EVI1*-positive *MLL-AF9* patients, which showed partial clustering in the total cohort. This graph was adapted from a previously published figure[1], by including *EVI1* expression (221884_at). *MLL-AF9* status, 11q23 status and *BRE* and *EVI1* expression are indicated along the pairwise correlation graph by the numbers 1-4, respectively.

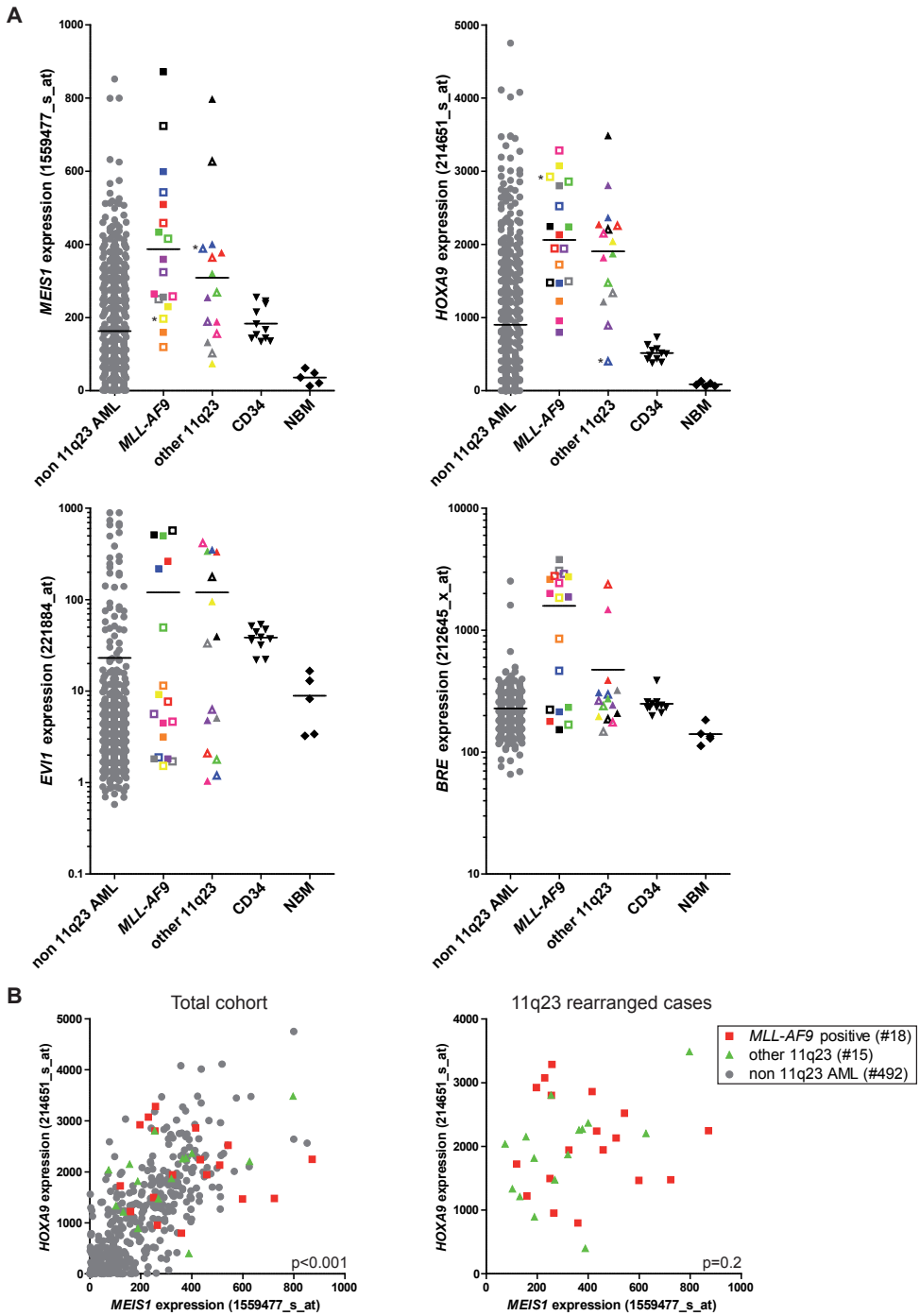
A
MEIS1 expression (1559477_s_at)
HOXA9 expression (214651_s_at)
EVI1 expression (221884_at)
BRE expression (212645_x_at)
non 11q23 AML
MLL-AF9
other 11q23
CD34
NBM
B
Total cohort
11q23 rearranged cases
MLL-AF9 positive (#18)
other 11q23 (#15)
non 11q23 AML (#492)
p<0.001
p=0.2

To confirm these data in another cohort, we studied the expression of *MEIS1*, *HOXA9*, *EVI1* and *BRE* in a third, large AML cohort, including 38 *MLL*-rearranged cases (figure 4.4)[16]. Also in this cohort, the overall expression of the four genes was higher in *MLL*-rearranged cases (figure 4.4A). Still, a number of individual cases showed expression levels of *MEIS1*, *EVI1* and *BRE* comparable to the mean of the non *MLL*-rearranged cases. In this cohort, *HOXA9* was almost exclusively high in *MLL*-rearranged cases (figure 4.4A). Remarkably, more than 60% of non *MLL*-rearranged cases showed high *MEIS1* (expression value >0.25) and *HOXA9* expression (expression value >0.4) (figure 4.4B). In cohort 1, this was the case for less than 35% of the samples (expression value of *MEIS1* >200, expression value *HOXA9* >600, figure 4.3). Despite the differences between the cohorts, the data imply that high expression of both targets is not a distinct phenomenon for *MLL*-rearrangements. Importantly, in pediatric AML, the correlation of high *MEIS1* and *HOXA9* expression to *MLL*-rearrangements seems stronger, as in a study on 23 *MLL*-rearranged versus 56 non-*MLL* pediatric AML cases, all rearranged cases showed high expression of both genes[20].

The above described data suggest that there are large differences in target gene expression between individual patients with *MLL-AF9* translocations or other 11q23 aberrations. In combination with the observation that *MLL-AF9* patients with high *BRE* expression share a similar expression profile, in contrast to the remaining *MLL-AF9* patients, this suggests that global gene expression regulation is not solely dependent on the *MLL-AF9* fusion gene. Although studying molecular mechanisms of *MLL*-transformation in mouse models, including epigenetic regulation and resultant gene expression profiling, has yielded much information on *MLL-AF9* mediated transformation, it seems unlikely that there will be only one molecular mechanism of malignant transformation applicable to all *MLL-AF9* positive or other *MLL*-rearranged patients. It is more likely that *MLL*-translocations can provoke various altered expression programs depending on, for example, different cofactors or the differentiation status of the transformed cells.



**Figure 4.3: Comparison of *MEIS1*, *HOXA9*, *EVI1*, and *BRE* expression among 11q23 AML patients (left page)**

**A.** Gene expression data of *MEIS1*, *HOXA9*, *EVI1* and *BRE* are represented for cohort 1 (525 AML samples and 16 control samples (CD34 or normal bone marrow (NBM)). Individual *MLL-AF9* and other 11q23 patients are indicated by different colors and open or closed symbols. Micro-array probesets used for analyses are indicated on the y-axis. The black line indicates the mean expression of the samples. * indicates samples mentioned in main text which show opposite expression levels of *MEIS1* and *HOXA9*. **B.** *HOXA9* expression was plotted against *MEIS1* expression in the total cohort (left panel) or within 11q23 rearranged samples only (right panel). *MLL-AF9* and remaining 11q23 patients are indicated in red and green, respectively. Although *MEIS1* and *HOXA9* expression showed a positive correlation in the total cohort ($p<0.001$), there is a poor correlation between *MEIS1* and *HOXA9* expression within 11q23 (including *MLL-AF9*) patients, based on Spearman rank correlation testing ($p=0.2$).

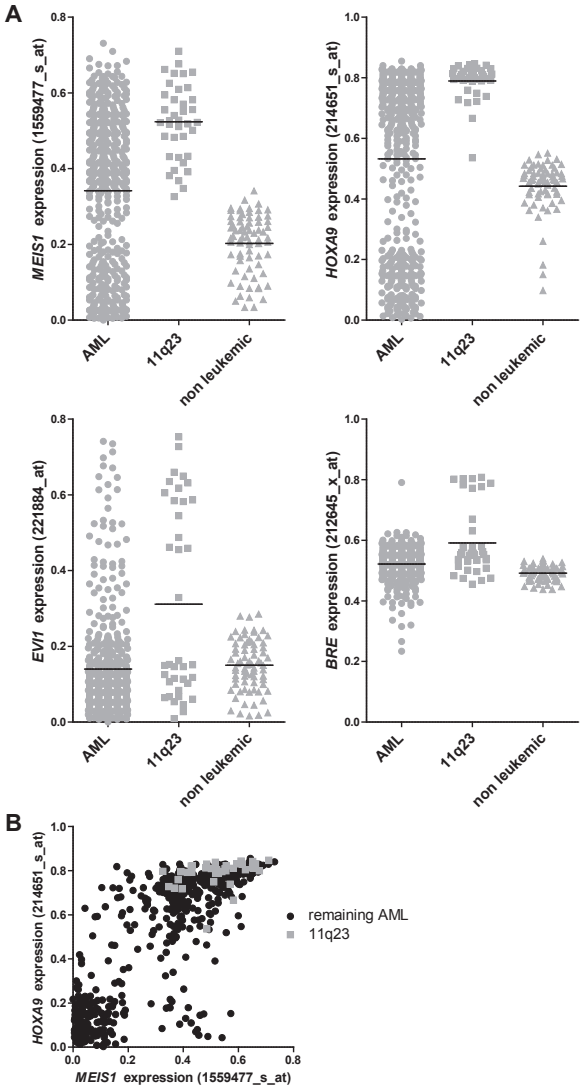


**Figure 4.4: Comparison of *MEIS1*, *HOXA9*, *EVI1*, and *BRE* expression among 11q23 AML patients in an independent cohort**

**A.** Gene expression data of *MEIS1*, *HOXA9*, *EVI1* and *BRE* are represented for cohort 3 comprising 542 AML patients, including 38 *MLL*-rearranged cases, and 73 control samples (healthy or non-leukemic bone marrow samples)[16]. Micro-array probesets used for analyses are indicated on the y-axis. The black line indicates the mean expression of the samples. **B.** *HOXA9* expression was plotted against *MEIS1* expression for the total cohort. *MLL*-rearranged cases are indicated in grey. Of the remaining AML cohort, 63% of the samples showed simultanleously high expression of *MEIS1* and *HOXA9* (expression level above 0.25 and 0.4 for *MEIS1* and *HOXA9*, respectively).

## Reference List


1. Noordermeer,S.M. *et al.* High BRE expression predicts favorable outcome in adult acute myeloid leukemia, in particular among MLL-AF9-positive patients. *Blood* **118**, 5613-5621 (2011).
2. Grimwade,D. *et al.* Refinement of cytogenetic classification in acute myeloid leukemia: determination of prognostic significance of rare recurring chromosomal abnormalities among 5876 younger adult patients treated in the United Kingdom Medical Research Council trials. *Blood* **116**, 354-365 (2010).
3. Rollig,C. *et al.* Long-term prognosis of acute myeloid leukemia according to the new genetic risk classification of the European LeukemiaNet recommendations: evaluation of the proposed reporting system. *J. Clin. Oncol.* **29**, 2758-2765 (2011).
4. Milne,T.A. *et al.* MLL targets SET domain methyltransferase activity to Hox gene promoters. *Mol. Cell* **10**, 1107-1117 (2002).
5. Nakamura,T. *et al.* ALL-1 is a histone methyltransferase that assembles a supercomplex of proteins involved in transcriptional regulation. *Mol. Cell* **10**, 1119-1128 (2002).
6. Krivtsov,A.V. & Armstrong,S.A. MLL translocations, histone modifications and leukaemia stem-cell development. *Nat. Rev. Cancer* **7**, 823-833 (2007).
7. Monroe,S.C. *et al.* MLL-AF9 and MLL-ENL alter the dynamic association of transcriptional regulators with genes critical for leukemia. *Exp. Hematol.* **39**, 77-86 (2011).
8. Bernt,K.M. *et al.* MLL-rearranged leukemia is dependent on aberrant H3K79 methylation by DOT1L. *Cancer Cell* **20**, 66-78 (2011).
9. Chen,W. *et al.* Malignant transformation initiated by Mll-AF9: gene dosage and critical target cells. *Cancer Cell* **13**, 432-440 (2008).
10. Krivtsov,A.V. *et al.* Transformation from committed progenitor to leukaemia stem cell initiated by MLL-AF9. *Nature* **442**, 818-822 (2006).
11. Arai,S. *et al.* Evi-1 is a transcriptional target of mixed-lineage leukemia oncoproteins in hematopoietic stem cells. *Blood* **117**, 6304-6314 (2011).
12. Groschel,S. *et al.* High EVI1 expression predicts outcome in younger adult patients with acute myeloid leukemia and is associated with distinct cytogenetic abnormalities. *J. Clin. Oncol.* **28**, 2101-2107 (2010).
13. Balgobind,B.V. *et al.* EVI1 overexpression in distinct subtypes of pediatric acute myeloid leukemia. *Leukemia* **24**, 942-949 (2010).
14. Wouters,B.J. *et al.* Double CEBPA mutations, but not single CEBPA mutations, define a subgroup of acute myeloid leukemia with a distinctive gene expression profile that is uniquely associated with a favorable outcome. *Blood* **113**, 3088-3091 (2009).
15. Kharas,M.G. *et al.* Musashi-2 regulates normal hematopoiesis and promotes aggressive myeloid leukemia. *Nat. Med.* **16**, 903-908 (2010).
16. Haferlach,T. *et al.* Clinical utility of microarray-based gene expression profiling in the diagnosis and subclassification of leukemia: report from the International Microarray Innovations in Leukemia Study Group. *J. Clin. Oncol.* **28**, 2529-2537 (2010).
17. Valk,P.J. *et al.* Prognostically useful gene-expression profiles in acute myeloid leukemia. *N. Engl. J. Med.* **350**, 1617-1628 (2004).
18. Balgobind,B.V. *et al.* High BRE expression in pediatric MLL-rearranged AML is associated with favorable outcome. *Leukemia* **24**, 2048-2055 (2010).
19. Somervaille,T.C. & Cleary,M.L. Identification and characterization of leukemia stem cells in murine MLL-AF9 acute myeloid leukemia. *Cancer Cell* **10**, 257-268 (2006).
20. Wang,Q.F. *et al.* MLL fusion proteins preferentially regulate a subset of wild-type MLL target genes in the leukemic genome. *Blood* **117**, 6895-6905 (2011).

# Expression of the BRCA1 complex member BRE predicts disease free survival in breast cancer

**Sylvie M. Noordermeer, Marloes Wennemers, Saskia M. Bergevoet, Adrian van der Heijden, Evelyn Tönnissen, Fred C.G.J. Sweep, Joop H. Jansen, Paul N. Span, and Bert A. van der Reijden**

**This work has been submitted for publication (february 2012)**

## Abstract

**Breast cancer is one of the leading causes of cancer mortality in women. Recent advances in gene expression profiling have indicated that breast cancer is a heterogeneous disease and that the current prognostication using clinico-pathological features is not sufficient to fully predict therapy response and disease outcome. In this retrospective study, we show that expression levels of *BRE*, which encodes a member of the BRCA1 DNA damage repair complex, predicted disease free survival in non-familial breast cancer patients. The predictive value of *BRE* expression depended on whether patients received radiotherapy as part of their primary treatment. In radiotherapy treated patients, high *BRE* expression predicted a favorable disease free survival (hazard ratio (HR)=0.47, 95% confidence interval (CI)=0.28-0.78, p=0.004), while in non-treated patients, high *BRE* expression predicted an adverse prognosis (HR=2.59, 95% CI=1.00-6.75, p=0.05). Among radiotherapy treated patients, the prognostic impact of *BRE* expression was confined to patients with smaller tumors (HR=0.23, 95% CI=0.068-0.75, p=0.015), and it remained an independent factor after correction for the other prognostic factors age, tumor size, lymph node involvement and histological grade (HR=0.50, CI=0.27-0.90, p=0.021). In addition, high *BRE* expression predicted a favorable relapse free survival in a publicly available dataset of 2,324 breast cancer patients (HR=0.59, CI=0.51-0.68, p<0.001). These data indicate that *BRE* is an interesting candidate for future functional studies aimed at developing targeted therapies.**

## Introduction

Despite great improvements in diagnostic imaging techniques and treatment, breast cancer remains one of the leading causes of cancer mortality in women. Prognostication of breast cancer patients nowadays relies highly on classical clinico-pathological features, such as tumor size, histological grade, age and lymph node metastases[1]. However, it remains a challenge to accurately predict disease outcome based on these parameters, which is necessary in order not to under- or over-treat patients.

Over the last twenty years, there has been great interest in developing prognostic patient classification methods based on molecular screenings. Genome-wide gene expression screens have identified expression profiles that predict disease outcome and therapy response. For example, in several large patient studies, a 70-gene signature called the 'MammaPrint' (Agendia, Amsterdam, The Netherlands) has been shown to outperform classical prognostication methods[2-4]. Together with other molecular classification methods[5,6], these data indicate that the identification of differential gene expression has great potential for improved prediction of disease outcome and subsequent treatment decisions.

DNA double strand breaks (DSBs) are one of the most cytotoxic types of DNA damage. The importance of proper repair of these breaks to maintain genomic integrity is exemplified by recurrent mutations of genes involved in DSB repair in various cancers, for example *BRCA1* mutations which occur in approximately 20% of the familial breast cancer cases[7-9]. The importance of the BRCA1 multi-protein complex has been illustrated by the identification of polymorphisms and haplotypes within other BRCA1 complex members, such as *RAP80* and *ABRAXAS*, both in *BRCA1/2* mutated and non-mutated familial breast cancer patients. However, the clinical impact of these polymorphisms remains to be confirmed[10-15]. Furthermore, *BRCA1* expression levels seem to predict breast cancer outcome in non familial cases[16-19], although data are not consistent[20].

Recently, it has been shown that high expression of *BRE* (Brain and Reproductive organ-Expressed), another member of the BRCA1 complex[21-24], denotes a favorable prognosis in acute myeloid leukemia (AML)[25,26]. In this study, we demonstrate that *BRE* expression levels in breast cancer tumor tissue contained prognostic information in a cohort of 229 non-familial breast cancer patients, establishing the relevance of this DNA damage repair factor in breast cancer.

## Materials and Methods

*Breast cancer samples*

Frozen breast cancer tissue sections were available of two independent cohorts of in total 229 patients who had undergone resection of their primary tumor, as described before[27-29]. Patients were treated by surgical resection of the tumor which was followed by adjuvant systemic treatment and/or radiotherapy for part of the cohort. Patient characteristics can be found in table 5.1. The median follow-up period of censored patients was 107.5 months. This study was performed according to REMARK guidelines[30].

*BRE QPCR*

Tissue collection, mRNA isolation and cDNA preparation have been described before[28]. *BRE* expression was measured in both cohorts by QPCR using a commercially available primer/probe set (Hs01046283_m1, Life Technologies, Carlsbad, CA, USA) and normalized to expression of the housekeeping gene *PBGD*, as described[26]. Normalized QPCR data were mean centered per analyzed cohort and afterwards the data of the cohorts were combined to increase patient numbers for further analyses.

*Statistical analyses*

To statistically test the correlation of *BRE* expression with clinical parameters, the complete cohort was subdivided into two equally sized groups based on *BRE* expression. Differences in patient characteristics were tested by $\chi^2$, Fisher exact, or Mann Whitney U tests, as indicated. Disease free survival (DFS; with an event defined as the diagnosis of recurrent or metastatic disease) was used as feature for disease outcome. The prognostic impact of *BRE* expression was visualized using Kaplan-Meier plots and statistically tested via the logrank method and univariate or multivariate Cox regression analyses. Statistical analyses were carried out using Graphpad (La Jolla, CA, USA) or SPSS (IBM Corporation, Armonk, NY, USA) software.

## Results

*BRE expression correlates with tumor size*

To study the prognostic effect of *BRE* expression in breast cancer, *BRE* mRNA levels were measured in tumor tissues collected at diagnosis of a cohort of 229 breast cancer patients by QPCR. Given the association of BRE with DNA damage repair, we subdivided the patient cohort *a priori* in two groups based on whether they had received radiotherapy as part of their primary treatment. *BRE* levels were gradually distributed and no difference was observed between radiotherapy treated or non-treated patients

(p=0.25). The dynamic range of expression was less than 50-fold (5.4Ct) and levels were normally distributed (based on a Kolmogorov-Smirnov test) (see figure 5.1a). This is in contrast to AML in which *BRE* is highly expressed in a distinctive subset of patients, while the remaining patients show little variation[26].

Comparisons of *BRE* expression with known clinico-pathological factors showed that *BRE* expression correlated with tumor size (p=0.014), but not with any of the other parameters (table 5.1). The correlation of *BRE* expression with tumor size was only observed in radiotherapy treated patients in which high *BRE* expression was more often found in smaller tumors (p=0.005, table 5.1).

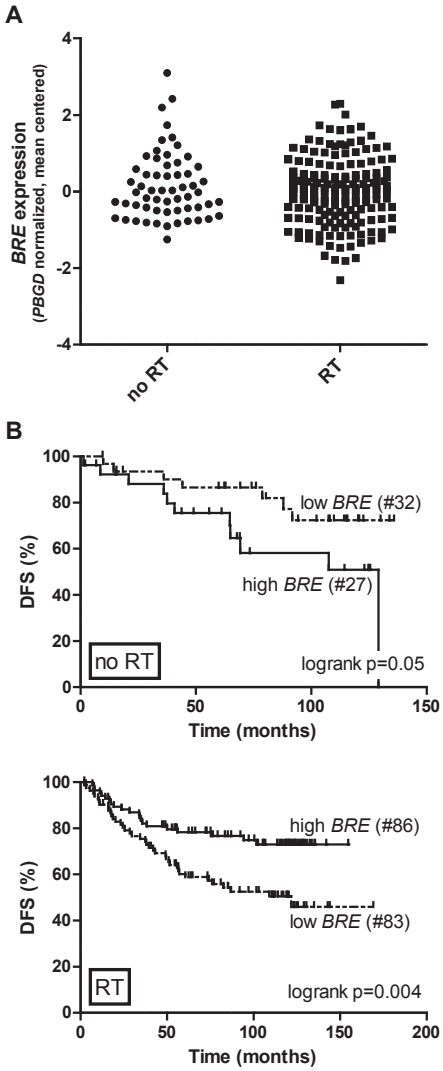


**Figure 5.1: *BRE* expression predicts disease free survival in breast cancer**

**A.** *BRE* expression was gradually distributed among 229 breast cancer patients. No significant differences were observed between radiotherapy (RT) and non-radiotherapy treated (no RT) patients. *BRE* expression was measured using QPCR and normalized to the housekeeping gene PBGD by the ΔCt method. Data shown are mean centered. Expression levels between radiotherapy treated and non-treated patients did not differ significantly (p=0.25 based on student's T-test). **B.** For Kaplan Meier analyses, the total cohort was divided into two equally sized groups based on *BRE* expression (high: solid line; low: dashed line, as indicated). *BRE* expression had opposing prognostic impact in non-radiotherapy treated (no RT: upper panel) and radiotherapy treated (RT: lower panel) patients. In non-radiotherapy treated patients, the 5-year DFS was 86.6 ± 6.2% and 75.5 ± 8.7% for low and high *BRE* expression, respectively (HR=2.59, CI=1.00-6.75, p=0.05). In radiotherapy treated patients, the 5-year DFS was 60.2 ± 5.5% and 78.3 ± 4.5% for low and high *BRE* expression, respectively (HR=0.47, CI=0.28-0.78, p=0.004). Patient numbers included in the analyses are indicated in brackets. P-values, HR's and CI's were calculated using the logrank method. Subdividing the cohort into three groups based on *BRE* expression obtained comparable results (data not shown).

**Table 5.1: Clinico-pathological characteristics of 229 non-familial breast cancer patients**

| | Total cohort | | | | | Non-radiotherapy treated | | | | | Radiotherapy treated | | | | |
|---|---|---|---|---|---|---|---|---|---|---|---|---|---|---|---|
| | Low *BRE*[a] (N=115) | | High *BRE*[a] (N=114[b]) | | *P* | Low *BRE*[a] (N=32) | | High *BRE*[a] (N=27[b]) | | *P* | Low *BRE*[a] (N=83) | | High *BRE*[a] (N=86[b]) | | *P* |
| **Age** (N=229), mean (range) | 59.9 | (31-88) | 59.2 | (32-86) | 0.775[d] | 63.0 | (33-88) | 61.5 | (35-86) | 0.784[d] | 58.7 | (31-85) | 58.3 | (32-83) | 0.816[d] |
| **Menopausal status** (N=229) | | | | | 1.000[e] | | | | | 1.000[e] | | | | | 1.000[e] |
| Premenopausal, no. (%) | 29 | (25.2) | 28 | (24.6) | | 6 | (18.8) | 5 | (18.5) | | 23 | (27.7) | 23 | (26.7) | |
| Postmenopausal, no. (%) | 86 | (74.8) | 86 | (75.4) | | 26 | (81.3) | 22 | (81.5) | | 60 | (72.3) | 63 | (73.3) | |
| **Nodal category** (N=208) | | | | | 0.923[e] | | | | | 0.310[e] | | | | | 0.806[e] |
| Negative, no. (%) | 61 | (58.1) | 59 | (57.3) | | 25 | (86.2) | 18 | (72.0) | | 36 | (47.4) | 41 | (52.6) | |
| 1-3 involved lymph nodes, no. (%) | 29 | (27.6) | 31 | (30.1) | | 4 | (13.8) | 7 | (28.0) | | 25 | (32.9) | 24 | (30.8) | |
| ≥4 involved lymph nodes, no. (%) | 15 | (14.3) | 13 | (12.6) | | 0 | (0) | 0 | (0) | | 15 | (19.7) | 13 | (16.7) | |
| **Radiotherapy** (N=228) | | | | | 0.547[e] | | | | | NA[g] | | | | | NA[g] |
| Treated, no. (%) | 83 | (72.2) | 86 | (76.1) | | 0 | (0) | 0 | (0) | | 83 | (100) | 86 | (100) | |
| Non-treated, no. (%) | 32 | (27.8) | 27 | (23.9) | | 32 | (100) | 27 | (100) | | 0 | (0) | 0 | (0) | |
| **Surgery** (N=229) | | | | | 0.282[e] | | | | | 0.495[f] | | | | | 0.219[f] |
| Mastectomy, no. (%) | 73 | (63.5) | 64 | (56.1) | | 30 | (93.8) | 27 | (100) | | 43 | (51.8) | 36 | (41.9) | |
| Lumpectomy, no. (%) | 42 | (36.5) | 50 | (43.9) | | 2 | (6.3) | 0 | (0) | | 40 | (48.2) | 50 | (58.1) | |
| **Adjuvant systemic therapy** (N=228) | | | | | 0.230[f] | | | | | 0.537[f] | | | | | 0.269[f] |
| None, no. (%) | 70 | (60.9) | 68 | (60.2) | | 26 | (81.3) | 18 | (66.7) | | 44 | (53.0) | 50 | (58.1) | |
| Endocrine therapy, no. (%) | 30 | (26.1) | 28 | (24.8) | | 3 | (9.4) | 4 | (14.8) | | 27 | (32.5) | 24 | (27.9) | |
| Chemotherapy, no. (%) | 13 | (11.3) | 9 | (8.0) | | 2 | (6.3) | 2 | (7.4) | | 11 | (13.3) | 7 | (8.1) | |
| Endocrine+Chemotherapy, no. (%) | 2 | (1.7) | 8 | (7.1) | | 1 | (3.1) | 3 | (11.1) | | 1 | (1.2) | 5 | (5.8) | |
| **Histology grade** (N=168) | | | | | 0.406[e] | | | | | 0.151[f] | | | | | 0.123[e] |
| I, no. (%) | 9 | (10.5) | 4 | (4.9) | | 1 | (4.3) | 1 | (5.3) | | 8 | (12.7) | 3 | (4.8) | |
| II, no. (%) | 36 | (41.9) | 35 | (42.7) | | 6 | (26.1) | 10 | (52.6) | | 30 | (47.6) | 25 | (39.7) | |
| III, no. (%) | 41 | (47.7) | 43 | (52.4) | | 16 | (69.6) | 8 | (42.1) | | 25 | (39.7) | 35 | (55.6) | |

| | | | | | | | | | | | | | | |
|---|---|---|---|---|---|---|---|---|---|---|---|---|---|---|
| **Tumor type** (N=193) | | | | | 0.744[e] | | | | | 0.721[f] | | | | 1.000[e] |
| Ductal, no. (%) | 73 | (73.0) | 70 | (75.3) | | 22 | (71.0) | 18 | (81.8) | | 51 | (73.9) | 52 | (73.2) | |
| Lubular, no. (%) | 15 | (15.0) | 15 | (16.1) | | 3 | (9.7) | 2 | (9.1) | | 12 | (17.4) | 13 | (18.3) | |
| Other (mixed/unknown), no. (%) | 12 | (12.0) | 8 | (8.6) | | 6 | (19.3) | 2 | (9.1) | | 6 | (8.7) | 6 | (8.5) | |
| **Tumor size** (N=227)[c] | | | | | 0.014[f] | | | | | 0.853[f] | | | | 0.005[e] |
| pT1, no. (%) | 33 | (28.7) | 50 | (44.6) | | 11 | (34.4) | 9 | (33.3) | | 22 | (26.5) | 41 | (48.2) | |
| pT2, no. (%) | 66 | (57.4) | 43 | (38.4) | | 19 | (59.4) | 15 | (55.6) | | 47 | (56.6) | 28 | (32.9) | |
| pT3/4, no. (%) | 16 | (13.9) | 19 | (17.0) | | 2 | (6.3) | 3 | (11.1) | | 14 | (16.9) | 16 | (18.8) | |
| **Estrogen receptor status** (N=196) | | | | | 0.769[e] | | | | | 0.265[e] | | | | 0.228[e] |
| Positive, no. (%) | 61 | (61.0) | 61 | (63.5) | | 18 | (66.7) | 12 | (50) | | 43 | (58.9) | 49 | (69.0) | |
| Negative, no. (%) | 39 | (39.0) | 35 | (36.5) | | 9 | (33.3) | 12 | (50) | | 30 | (41.1) | 22 | (31.0) | |
| **Progesterone receptor status** (N=197) | | | | | 0.776[e] | | | | | 0.579[e] | | | | 1.000[e] |
| Positive, no. (%) | 51 | (50.5) | 51 | (53.1) | | 12 | (44.4) | 13 | (54.2) | | 39 | (52.7) | 38 | (53.5) | |
| Negative, no. (%) | 50 | (49.5) | 45 | (46.9) | | 15 | (55.6) | 11 | (45.8) | | 35 | (47.3) | 33 | (46.5) | |

[a]High and low *BRE* expression is defined as expression above or below the median expression of the total cohort, respectively;
[b]As data on radiotherapy treatment was lacking for 1 patient (showing high *BRE* expression), the patient numbers in the radiotherapy treated and non-treated groups do not add up to the numbers of the total cohort;
[c]pT1: tumor size≤2cm, pT2: tumor size of 2-5cm, pT3/4 tumor size >5cm and/or direct extension to chest wall or skin.
[d]p-value is based on Mann-Whitney U test;
[e]p-value is based on $\chi 2$ test;
[f]p-value is based on Fisher Exact test;
[g]NA: not applicable.

*BRE expression predicts disease free survival in breast cancer*

Gradual differences in *BRE* expression (using continuous QPCR data) did not correlate with disease free survival (DFS) or overall survival (OS) in the total cohort, as tested by univariate Cox regression analysis (DFS: table 5.2, OS: data not shown). However, when the cohort was subdivided into radiotherapy treated and non-treated patients, *BRE* expression (tested as continuous variable) had prognostic impact on DFS within both groups (table 5.2). Remarkably, *BRE* expression showed opposite effects on prognosis. In the radiotherapy treated group (n=169), which accounted for the majority of the patients, high *BRE* expression correlated with a favorable DFS (Hazard ratio (HR)=0.72, 95% confidence interval (CI)=0.53-0.97, p=0.030), while in the non-radiotherapy treated group (n=59), high *BRE* expression correlated with a poor prognosis (HR= 1.79, CI=1.11-2.87, p=0.016, table 5.2). Similar results were obtained when subdividing patients into two or three groups based on *BRE* expression, instead of using gradual QPCR data (table 5.3, and data not shown).

**Table 5.2: Univariate analysis of the correlation of *BRE* expression with DFS**

| | **Total cohort** | | **Non-radiotherapy treated patients** | | **Radiotherapy treated patients** | |
|---|---|---|---|---|---|---|
| | ***P*** | **HR (95% CI)[a]** | ***P*** | **HR (95% CI)[a]** | ***P*** | **HR (95% CI)[a]** |
| ***BRE* expression (QPCR data)** | 0.342 | 0.877 (0.67-1.15) | 0.016 | 1.79 (1.11-2.87) | 0.030 | 0.72 (0.53-0.97) |

[a]HR: hazard ratio; CI: confidence interval.

The effect of *BRE* expression on DFS was visualized using Kaplan Meier plots by subdividing the total cohort into two groups using median *BRE* expression as cutoff. Among the patients that did not receive radiotherapy, high *BRE* expression predicted an adverse prognosis validating the Cox regression analysis (HR=2.59, CI=1.00-6.75, p=0.05). High *BRE* expression predicted a favorable prognosis among the patients that received radiotherapy (HR=0.47, CI=0.28-0.78, p=0.004) (figure 5.1b). Interestingly, within the radiotherapy treated patients, a significant correlation between *BRE* expression and disease free survival was only observed for the group of patients with smaller tumors (HR=0.23, CI=0.068-0.75, p=0. 015), which contained relatively more high *BRE* expressing patients (table 5.1, figure 5.2). No significant prognostic impact was observed in patients with larger tumors (figure 5.2).

*BRE expression is an independent prognostic factor in radiotherapy treated patients*

To determine whether *BRE* expression was an independent prognostic factor for DFS in breast cancer, multivariate Cox regression analyses were performed. These analyses showed that *BRE* expression was a prognostic factor within the group of radiotherapy treated patients, independent of the other prognostic factors age, tumor size, lymph

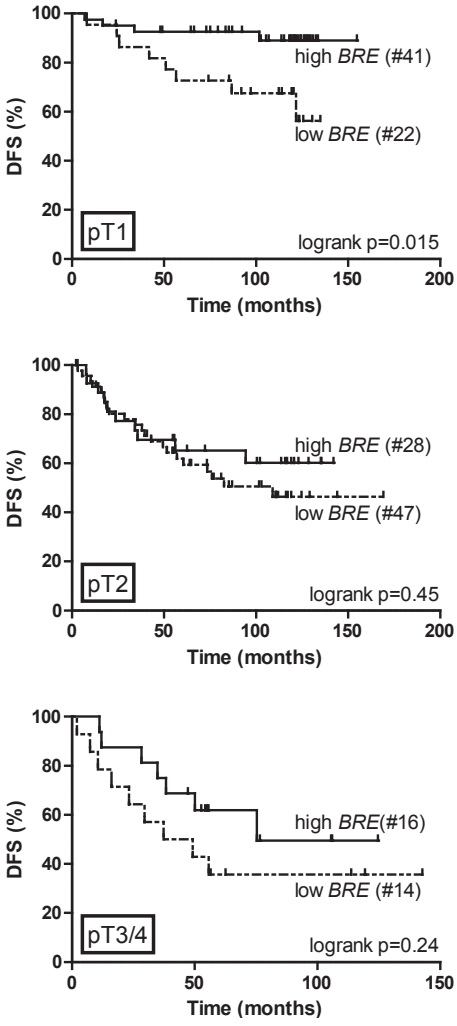


**Figure 5.2: *BRE* expression predicts favorable DFS in radiotherapy-treated patients with small tumors**

In radiotherapy-treated patients, *BRE* expression predicts DFS in patients with small tumors (pT1, upper panel). The 5-year DFS was 72.7 ± 9.5% and 92.6 ± 4.1% for the groups with low and high *BRE* expression respectively (HR=0.23, CI=0.068-0.75, p=0.015). For patients with larger tumors (pT2 and pT3/4), no statistically significant prognostic effect of *BRE* expression was observed. For this analysis, patients were subdivided into two groups based on *BRE* expression, as explained in figure 5.1. P-values, HR's and CI's were calculated using the logrank method.

node involvement and histological grade (HR=0.50, CI=0.27-0.90, p=0.021, table 5.3). Of note, also age, tumor size and the number of involved lymph nodes were independent prognostic factors in this group of patients. For non-radiotherapy treated patients, *BRE* expression did not significantly correlate with DFS in the multivariate analysis (table 5.3).

*BRE expression predicts outcome in a large independent breast cancer cohort*

We extended our studies to an independent cohort of breast cancer patients by evaluating the predictive value of *BRE* expression in a large publicly available micro-array dataset of 2,324 patients (see figure 5.3, Kaplan Meier Plotter[31] (www.kmplot.com)). This

**Table 5.3: Multivariate Cox regression analysis of *BRE* expression correlation with DFS**

| | Non-radiotherapy treated patients | | | | Radiotherapy treated patients | | | |
|---|---|---|---|---|---|---|---|---|
| | Univariate | | Multivariate[a] | | Univariate | | Multivariate[a] | |
| | ***P*** | **HR (95% CI)[b]** | ***P*** | **HR (95% CI)[b]** | ***P*** | **HR (95% CI)[b]** | ***P*** | **HR (95% CI)[b]** |
| ***BRE*** (2 groups[c]) | 0.059[f] | 2.51 (0.97-6.53) | 0.083[f] | 2.38 (0.89-6.35) | 0.004 | 0.46 (0.27-0.79) | 0.021 | 0.50 (0.27-0.90) |
| **Age** (continuous) | 0.349 | 0.98 (0.95-1.02) | 0.616 | 0.99 (0.95-1.03) | 0.112 | 0.98 (0.96-1.00) | 0.020 | 0.97 (0.95-1.00) |
| **Menopausal status** (post- vs. premenopausal) | 0.838 | 1.07 (0.57-1.99) | | | 0.140 | 0.81 (0.62-1.07) | | |
| **Tumor size[d]** (pT1 vs. pT2 vs. pT3/4) | 0.422 | 1.39 (0.62-3.09) | 0.465 | 1.56 (0.47-5.15) | <0.001 | 2.01 (1.42-2.84) | 0.014 | 1.70 (1.11-2.59) |
| **Histological grade** (I vs. II vs. III vs. ND[e]) | 0.941 | 0.97 (0.39-2.42) | 0.895 | 1.01 (0.86-1.19) | 0.032 | 1.70 (1.05-2.74) | 0.313 | 0.95 (0.86-1.05) |
| **Involved lymph nodes** (0 vs. 1-3 vs. ≥4) | 0.002 | 5.63 (1.84-17.3) | 0.034 | 3.92 (1.11-13.8) | 0.001 | 1.87 (1.30-2.68) | 0.013 | 1.66 (1.11-2.48) |
| **Estrogen receptor status** (positive vs. negative) | 0.680 | 0.82 (0.31-2.15) | | | 0.362 | 0. 78 (0.45-1.34) | | |
| **Progesterone receptor status** (positive vs. negative) | 0.866 | 0.92 (0.36-2.39) | | | 0.839 | 0.95 (0.55-1.62) | | |

[a]Factors included in multivariate analysis: *BRE* expression, age, tumor size, histological grade and involved lymph nodes;
[b]HR: hazard ratio; CI: confidence interval;
[c]The two groups are defined by *BRE* expression above or below the median expression of the total cohort, respectively;
[d]pT1: tumor size≤2cm, pT2: tumor size of 2-5cm, pT3/4: tumor size >5cm and/or direct extension to chest wall or skin;
[e]As data on histological grading were missing for a substantial number of patients, this group (ND: Not Done) was included in the multivariate analyses as separate group, next to histological grade I, II or III;
[f]In non-radiotherapy treated patients, *BRE* expression lost its significance when the median expression was used to divide patients based on *BRE* expression. When subdividing patients into three groups based on *BRE* expression, *BRE* was a significant predictor for DFS in both univariate and multivariate models.

cohort showed a favorable prognosis for patients with high *BRE* expression (upper 50% of the patients), and an adverse survival for patients with low *BRE* expression (lower 50%) (HR= 0.59, CI=0.51-0.68, p <0.001 after correction for multiple testing). As no data regarding radiotherapy treatment were available, the impact of *BRE* expression on disease outcome within these subgroups could not be determined.

**Figure 5.3: *BRE* expression predicts relapse free survival in a cohort of 2,324 breast cancer patients**
A publicly available database (Kaplan Meier Plotter[31]) was used to investigate the effect of *BRE* expression on relapse free survival (RFS) in a cohort of 2,324 breast cancer patients. Micro-array data (*BRE* probe set 211566_s_at) of these patients were used to divide patients into two equally sized groups. High *BRE* expression predicts a favorable prognosis (HR=0.51, CI=0.51-0.68, p<0.001). P-value, HR and CI were calculated using the logrank method. The p-value was corrected for multiple testing by Bonferroni correction.

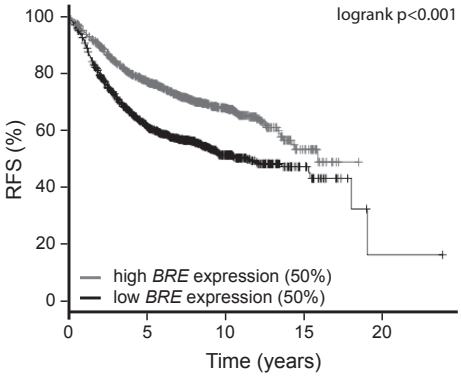


## Discussion

High expression of the BRCA1 complex member BRE has recently been identified in a subgroup of AML patients in whom it defines favorable prognosis[25,26]. Here, we show that the expression of this gene also predicted disease outcome in a cohort of 229 non-familial breast cancer patients. Interestingly, the predictive value of *BRE* expression at diagnosis on disease free survival depended on whether the patient received subsequent radiotherapy treatment. In radiotherapy treated patients, high *BRE* expression predicted a favorable disease outcome, whereas in non-radiotherapy treated patients it correlated with an adverse outcome (see figure 5.1, table 5.3). To extend our studies, *BRE* expression was evaluated in a publicly available dataset of 2,324 breast cancer patients[31]. In this large cohort, high *BRE* expression predicted a favorable relapse free survival. As this cohort represented a collection of previously published gene expression datasets, integral data on clinico-pathological factors were unavailable. Therefore, we were unable to determine the impact of *BRE* expression on disease outcome with regard to radiotherapy treatment. The identification of prognostic impact of *BRE* expression in two independent cohorts warrants further studies in large cohorts to validate the effects found in radiotherapy treated and non-treated patients.

The fact that *BRE* expression predicted opposing effects on disease outcome depending on radiotherapy treatment might imply that there are intrinsic differences in breast cancer patients who are treated or not treated with radiotherapy. Alternatively, there might be a direct effect of high *BRE* expression on radiotherapy response. The decision for radiotherapy treatment is closely related to the surgical treatment and depends on multiple factors, like tumor size and the involvement of axillary lymph nodes. As the patients were consequently not randomly assigned for treatment, it was not possible to

explain the opposing effect of *BRE* expression on the prognosis of radiotherapy treated versus non-treated patients in this cohort. Therefore, it would be of particular interest to test *BRE* expression in a cohort of patients that received radiotherapy in a randomized fashion, to evaluate a direct effect of *BRE* expression on therapy outcome.

BRE is a member of the BRCA1 complex, involved in DNA double strand break repair[21-24]. This complex is recruited to DNA damaged sites via binding of the complex member Rap80 to ubiquitin chains which are generated upon DNA damage[32-34]. Mutations in DNA repair factors are closely linked to familial breast cancer, as 25% of the cases is characterized by mutations in DNA damage repair factors, like BRCA1, BRCA2, PTEN, CHEK2, and ATM[7-9,35-38]. However, in non-familial breast cancer, these mutations are rare. In non-familial cases, associations between low BRCA1 expression with poor prognosis have been identified[16-19], resembling the observations we made for *BRE* expression in radiotherapy treated patients.

Depletion of BRE abrogates BRCA1 foci formation, indicating that BRE is needed for complex formation and downstream DNA repair[22-24,39]. Several studies have described an increased radio-sensitivity of cells upon *BRE* depletion[21,22]. Next to a role in the BRCA1 complex, BRE is also involved in death receptor mediated apoptosis, as it binds TNFα and FAS receptors and overexpression of *BRE* caused resistance to apoptosis induction by various stress-related stimuli[40]. This indicates that BRE serves an anti-apoptotic role following different types of stress. It was therefore unexpected to find a correlation between high *BRE* expression and a favorable breast cancer outcome in relation to radiotherapy. High expression would enhance DNA repair and hence would render cells resistant to radiotherapy. Indeed, this reasoning seems to be true for BRCA1, as radiotherapy has been shown to be especially beneficial for patients with low BRCA1 levels, whereas there was no benefit for patients with high BRCA1 levels[41]. On the other hand, high expression of the Mre11/Rad50/Nbs1 complex, also involved in DNA damage repair, predicts a good response to radiotherapy[42], indicating that DNA repair proteins can contribute differentially to radiotherapy response. In this case, high *BRE* expression might attenuate the DNA damage repair pathway following radiotherapy. The data described in this study indicate that BRE is an interesting candidate for functional studies in breast cancer to test its effect on radiotherapy responses.



## Acknowledgements

This study was financially supported by the Vanderes foundation.

## Reference List


1. Reis-Filho,J.S. & Pusztai,L. Gene expression profiling in breast cancer: classification, prognostication, and prediction. *Lancet* **378**, 1812-1823 (2011).
2. van 't Veer,L.J. *et al.* Gene expression profiling predicts clinical outcome of breast cancer. *Nature* **415**, 530-536 (2002).
3. Buyse,M. *et al.* Validation and clinical utility of a 70-gene prognostic signature for women with node-negative breast cancer. *J. Natl. Cancer Inst.* **98**, 1183-1192 (2006).
4. van de Vijver,M.J. *et al.* A gene-expression signature as a predictor of survival in breast cancer. *N. Engl. J. Med.* **347**, 1999-2009 (2002).
5 Paik,S. *et al.* A multigene assay to predict recurrence of tamoxifen-treated, node-negative breast cancer. *N. Engl. J. Med.* **351**, 2817-2826 (2004).
6. Perou,C.M. *et al.* Molecular portraits of human breast tumours. *Nature* **406**, 747-752 (2000).
7. Narod,S.A. & Foulkes,W.D. BRCA1 and BRCA2: 1994 and beyond. *Nat. Rev. Cancer* **4**, 665-676 (2004).
8. Miki,Y. *et al.* A strong candidate for the breast and ovarian cancer susceptibility gene BRCA1. *Science* **266**, 66-71 (1994).
9. Wooster,R. *et al.* Identification of the breast cancer susceptibility gene BRCA2. *Nature* **378**, 789-792 (1995).
10. Akbari,M.R. *et al.* Germline RAP80 mutations and susceptibility to breast cancer. *Breast Cancer Res. Treat.* **113**, 377-381 (2009).
11. Nikkila,J. *et al.* Familial breast cancer screening reveals an alteration in the RAP80 UIM domain that impairs DNA damage response function. *Oncogene* **28**, 1843-1852 (2009).
12. Novak,D.J. *et al.* Analysis of the genes coding for the BRCA1-interacting proteins, RAP80 and Abraxas (CCDC98), in high-risk, non-BRCA1/2, multiethnic breast cancer cases. *Breast Cancer Res. Treat.* **117**, 453-459 (2009).
13. Osorio,A. *et al.* Evaluation of the BRCA1 interacting genes RAP80 and CCDC98 in familial breast cancer susceptibility. *Breast Cancer Res. Treat.* **113**, 371-376 (2009).
14. Rebbeck,T.R. *et al.* Modification of BRCA1-Associated Breast and Ovarian Cancer Risk by BRCA1-Interacting Genes. *Cancer Res.* **71**, 5792-5805 (2011).
15. Solyom,S., Patterson-Fortin,J., Pylkas,K., Greenberg,R.A., & Winqvist,R. Mutation screening of the MERIT40 gene encoding a novel BRCA1 and RAP80 interacting protein in breast cancer families. *Breast Cancer Res. Treat.* **120**, 165-168 (2010).
16. Rakha,E.A. *et al.* Expression of BRCA1 protein in breast cancer and its prognostic significance. *Hum. Pathol.* **39**, 857-865 (2008).
17. Seery,L.T. *et al.* BRCA1 expression levels predict distant metastasis of sporadic breast cancers. *Int. J. Cancer* **84**, 258-262 (1999).
18. Taylor,J. *et al.* An important role for BRCA1 in breast cancer progression is indicated by its loss in a large proportion of non-familial breast cancers. *Int. J. Cancer* **79**, 334-342 (1998).
19. Yang,Q. *et al.* Prognostic significance of BRCA1 expression in Japanese sporadic breast carcinomas. *Cancer* **92**, 54-60 (2001).
20. Lambie,H. *et al.* Prognostic significance of BRCA1 expression in sporadic breast carcinomas. *J. Pathol.* **200**, 207-213 (2003).
21. Dong,Y. *et al.* Regulation of BRCC, a holoenzyme complex containing BRCA1 and BRCA2, by a signalosome-like subunit and its role in DNA repair. *Mol. Cell* **12**, 1087-1099 (2003).
22. Feng,L., Huang,J., & Chen,J. MERIT40 facilitates BRCA1 localization and DNA damage repair. *Genes Dev.* **23**, 719-728 (2009).
23. Shao,G. *et al.* MERIT40 controls BRCA1-Rap80 complex integrity and recruitment to DNA

double-strand breaks. *Genes Dev.* **23**, 740-754 (2009).
24. Wang,B., Hurov,K., Hofmann,K., & Elledge,S.J. NBA1, a new player in the Brca1 A complex, is required for DNA damage resistance and checkpoint control. *Genes Dev.* **23**, 729-739 (2009).
25. Balgobind,B.V. *et al.* High BRE expression in pediatric MLL-rearranged AML is associated with favorable outcome. *Leukemia* **24**, 2048-2055 (2010).
26. Noordermeer,S.M. *et al.* High BRE expression predicts favorable outcome in adult acute myeloid leukemia, in particular among MLL-AF9-positive patients. *Blood* **118**, 5613-5621 (2011).
27. Wennemers,M., Bussink,J., Grebenchtchikov,N., Sweep,F.C., & Span,P.N. TRIB3 protein denotes a good prognosis in breast cancer patients and is associated with hypoxia sensitivity. *Radiother. Oncol.* **101**, 198-202 (2011).
28. Wennemers,M. *et al.* Tribbles homolog 3 denotes a poor prognosis in breast cancer and is involved in hypoxia response. *Breast Cancer Res.* **13**, R82 (2011).
29. Span,P.N. *et al.* Mammaglobin is associated with low-grade, steroid receptor-positive breast tumors from postmenopausal patients, and has independent prognostic value for relapse-free survival time. *J. Clin. Oncol.* **22**, 691-698 (2004).
30. McShane,L.M. *et al.* REporting recommendations for tumor MARKer prognostic studies (REMARK). *Breast Cancer Res. Treat.* **100**, 229-235 (2006).
31. Gyorffy,B. *et al.* An online survival analysis tool to rapidly assess the effect of 22,277 genes on breast cancer prognosis using microarray data of 1,809 patients. *Breast Cancer Res. Treat.* **123**, 725-731 (2010).
32. Sobhian,B. *et al.* RAP80 targets BRCA1 to specific ubiquitin structures at DNA damage sites. *Science* **316**, 1198-1202 (2007).
33. Wang,B. & Elledge,S.J. Ubc13/Rnf8 ubiquitin ligases control foci formation of the Rap80/Abraxas/Brca1/Brcc36 complex in response to DNA damage. *Proc. Natl. Acad. Sci. U. S. A* **104**, 20759-20763 (2007).
34. Wang,B. *et al.* Abraxas and RAP80 form a BRCA1 protein complex required for the DNA damage response. *Science* **316**, 1194-1198 (2007).
35. FitzGerald,M.G. *et al.* Germline mutations in PTEN are an infrequent cause of genetic predisposition to breast cancer. *Oncogene* **17**, 727-731 (1998).
36. Meijers-Heijboer,H. *et al.* Low-penetrance susceptibility to breast cancer due to CHEK2(*)1100delC in noncarriers of BRCA1 or BRCA2 mutations. *Nat. Genet.* **31**, 55-59 (2002).
37. Sidransky,D. *et al.* Inherited p53 gene mutations in breast cancer. *Cancer Res.* **52**, 2984-2986 (1992).
38. Thompson,D. *et al.* Cancer risks and mortality in heterozygous ATM mutation carriers. *J. Natl. Cancer Inst.* **97**, 813-822 (2005).
39. Hu,X. *et al.* NBA1/MERIT40 and BRE interaction is required for the integrity of two distinct deubiquitinating enzyme BRCC36-containing complexes. *J. Biol. Chem.* **286**, 11734-11745 (2011).
40. Li,Q. *et al.* A death receptor-associated anti-apoptotic protein, BRE, inhibits mitochondrial apoptotic pathway. *J. Biol. Chem.* **279**, 52106-52116 (2004).
41. Soderlund,K., Skoog,L., Fornander,T., & Askmalm,M.S. The BRCA1/BRCA2/Rad51 complex is a prognostic and predictive factor in early breast cancer. *Radiother. Oncol.* **84**, 242-251 (2007).
42. Soderlund,K. *et al.* Intact Mre11/Rad50/Nbs1 complex predicts good response to radiotherapy in early breast cancer. *Int. J. Radiat. Oncol. Biol. Phys.* **68**, 50-58 (2007).

# Silencing of the E2 ubiquitin conjugating enzyme UBC13 decreases monocytic differentiation of U937 cells

**Sylvie M. Noordermeer, Saskia M. Bergevoet, Sanne M. Janssen, Tamara W. van Hal, Joop H. Jansen, and Bert A. van der Reijden**

**Manuscript in preparation**

6


## Abstract

**The E2 ubiquitin conjugating enzyme UBC13 catalyzes the formation of lysine 63 (K63) specific ubiquitin chains. Ubiquitin chains linked through K63 play an active role in various signaling routes. Conditional knockout of *Ubc13* in the hematopoietic system of mice impairs normal hematopoiesis affecting the survival of stem cells and early progenitors. In this study, we investigated the role of UBC13 in human myeloid differentiation models. We observed that UBC13 protein levels were downregulated during granulocytic as well as monocytic differentiation in several cell line models. The UBC13 cofactors MMS2 and UEV1a were also downregulated during differentiation. Silencing of *UBC13* in U937 cells decreased PMA-induced monocytic differentiation, based on lower CD11b expression as read-out. However, *UBC13* depletion did not affect apoptosis or cell cycle progression. These findings warrant further studies on the identification of proteins modified with K63-linked ubiquitin chains during myeloid differentiation.**

## Introduction

Ubiquitination is a post-translational modification that plays a pivotal role in many biological pathways. Within the process of modifying proteins with poly-ubiquitin chains, E2 conjugating enzymes dictate the type of ubiquitin chain formed. E3 ubiquitin ligases, which interact with E2s, determine which proteins are marked with ubiquitin. During ubiquitination, E2 enzymes first form a thio-ester bond with the C-terminus of ubiquitin via their catalytic site cysteine. Within the E2-E3-substrate complex, the E2-bound ubiquitin can attack lysine residue side chains, resulting in an isopeptide bond between ubiquitin and substrate protein. As ubiquitin itself contains seven lysine residues, ubiquitin chains can be formed via the covalent interaction of the C-terminus of a donor ubiquitin to an internal lysine of the acceptor ubiquitin. The E2 conjugating enzyme UBC13 is currently the only identified E2 that specifically catalyses the formation of K63-linked chains[1,2]. UBC13 activity depends on the cooperation of either one of its cofactors, MMS2 or UEV1a. These ubiquitin E2 variants (UEVs) lack the catalytic cysteine needed for thio-ester formation. However, they are able to bind ubiquitin non-covalently, thereby positioning the acceptor ubiquitin in such a way that the donor ubiquitin, bound to UBC13, can only attack the K63 side chain of the acceptor[3-5].

K63-linked ubiquitin chains play a role in several pathways including DNA damage responses, NF-κB and MAP kinase signaling and receptor trafficking[6]. All four pathways are involved in blood cell development, suggesting a role for UBC13 in hematopoiesis. The importance of UBC13-regulated signaling is illustrated by the early embryonic lethality of *Ubc13*$^{-/-}$ mice[7,8]. Recent studies using conditional tissue specific *Ubc13*$^{-/-}$ mouse models have shown an important role for this E2 in normal hematopoiesis[7-9]. Conditional knockout of the *Ubc13* gene in bone marrow cells and thymocytes of adult mice led to mortality within two weeks[9]. The lethality was accompanied by a strong reduction of platelets and white blood cells (of myeloid and lymphoid origin) in the peripheral blood. These cytopenias were caused by bone marrow hypoplasia with a severe reduction of stem cells and progenitor cells.

These data demonstrate an important role for UBC13 in early hematopoiesis. However, no studies have been performed on later stages of differentiation. Furthermore, all data currently available originated from mouse studies. In this study, we investigated the role of UBC13 in myeloid differentiation using the human U937 monocytic cell line model.

## Materials and Methods

*Cell Lines*

HEK293T and HEK 293FT cells were cultured in DMEM medium (Invitrogen, Carlsbad, USA), supplemented with 10% non heat-inactivated FCS (Invitrogen), 1% penicillin/streptomycin (MP biomedicals, Solon, USA), 0.1 mM Non-Essential Amino Acids (Invitrogen), 6 mM L-glutamine (Invitrogen) and 500 ng/mL geneticin (Invitrogen). NB4 and U937 cell lines were cultured in RPMI medium (Invitrogen) supplemented with 10% FCS and 1% penicillin/streptomycin. Cells were cultured at 37°C and 5% $CO_2$ in a humidified atmosphere. Granulocytic differentiation of NB4 cells and monocytic differentiation of U937 cells was induced by $10^{-6}$ M ATRA (all-trans retinoic acid) or 100 ng/mL PMA (phorbol-12-myristate-13-acetate), respectively.

*Cloning lentiviral inducible shRNA vectors*

Four independent short hairpin RNA (shRNA) sequences targeting *UBC13* were cloned into the puromycin-resistant, tetracycline inducible pLKO.1 (pLKO.1-Tet-on-puro) vector following the manufacturer's protocol (Addgene, Cambridge, USA). In short, double stranded shRNAs were designed with flanking single stranded sequences compatible with AgeI and EcoRI sticky ends and a loop containing the XhoI restriction site. The sequences were ligated into the pLKO.1 backbone which was digested with AgeI and EcoRI. The following sense sequences were used for *UBC13* shRNA construction: `AATCCAGATGATCCATTAGCA` (shRNA A; adapted from Matsuzawa *et al.*[10]), `GTTGGGAAGAATATGTTTAGA` (shRNA B; adapted from Xu *et al.*[11]), `GGGACTTTTAAACTTGAACTA` (shRNA C; adapted from Marteijn *et al.*[12]) and `GCCCGAGCAGGGACTACATTT` (shRNA D). A scrambled shRNA control was introduced in the pLKO.1-Tet-on-puro vector as negative control (`CCATGCCTGCATTCTTCAT`).

*Lentivirus production*

pLKO.1-Tet-on-puro vectors were co-transfected with the viral packaging vectors pLP1, pLP2 and pLP/VSVG (kindly provided by L. van Emst, Department of pediatric oncology, Radboud University Nijmegen Medical Centre, The Netherlands) in HEK293T or HEK 293FT cells using calcium phosphate. The medium was refreshed 16h after transfection. Virus-containing supernatant was harvested 72h following transfection.

*Viral transduction*

For lentiviral transduction, U937 cells were cultured on retronectin coated dishes in the presence of virus supernatant for 72h. Afterwards, transduced cells were selected with 1 μg/mL puromycin for 14 days. shRNA transcription was induced by the addition of 2

μg/mL doxycycline 72h before starting PMA-induced (100 ng/mL) myeloid differentiation. Differentiation was performed with continued doxycycline exposure.

*QPCR and Western blotting*

For quantification of *UBC13*, *MMS2* and *UEV1A* gene expression levels, total RNA was extracted using RNABee (AMS Biotechnology, Abingdon, UK). cDNA reactions were performed on 1 μg total RNA using M-MLV reverse transcriptase (Invitrogen). QPCR data were normalized to *beta-ACTIN* expression. Commercially available primer/probesets were used for QPCR of *MMS2*, *UEV1A* and *beta-ACTIN* (Applied Biosystems, Carlsbad, USA). For *UBC13* QPCR, the following primers and probe were designed:

forward primer: GAGCAGTGGAAGACCAACGAA;
reverse primer: AGTGATGCACACTTGATGATCGTAT;
FAM-MGB probe: ATAGAAACAGCTAGAGCATGGA.

To evaluate UBC13 protein expression, cells were lysed in RIPA lysis buffer (phosphate buffered saline with 1% Igepal CA-630, 0.5% Na-DOC, 0.1% SDS, 1 mM $MgCl_2$, and 10 μM $ZnCl_2$), supplemented with benzonase (Novagen, Merck, Darmstadt, Germany) and complete protease inhibitor cocktail (Roche, Basel, Switzerland). Proteins were separated on SDS-polyacrylamide gels and transferred to PVDF membranes. Immunostaining was performed with primary antibodies directed against UBC13 (Invitrogen) and GAPDH (Abcam, Cambridge, UK) or β-ACTIN (Sigma, St. Louis, USA) as loading control. Horseradish peroxidase-coupled secondary antibodies were used and staining was visualized with enhanced chemiluminescence using a Chemidoc XRS+ system (Biorad, Hercules, USA).

*Flow cytometric analysis*

To quantify myeloid differentiation, CD11b expression at the cell membrane was measured by flow cytometry using PE-coupled antibodies (Beckman Coulter, Brea, USA). Apoptosis was measured by Annexin-V (VPS Diagnostics, Hoeven, The Netherlands) and 7AAD (Sigma) staining. To study cell cycle distribution, cells were harvested and incubated for 16h at 4°C in PI-solution (0.3 mM Sodium citrate, 0.1 mg/mL RNAse A, 20 μg/mL Propidium Iodide (PI), 0.1% Triton X-100). DNA histograms were generated by measuring PI signals using flow cytometry.

*Statistical analyses*

Differences between conditions were statistically tested by two-sided student's t-tests. A p-value $<0.05$ was considered significant.

## Results

*UBC13 is downregulated during myeloid differentiation*

Previous results suggested that *UBC13* mRNA expression levels decreased during gefitinib induced granulocytic differentiation of promyelocytic HL60 cells[13]. To study whether this decrease was a general phenomenon of myeloid differentiation, other cell lines and differentiation inducing agents were tested. UBC13 protein levels were reduced after PMA-induced differentiation of myelomonocytic U937 cells (figure 6.1A, left panel). A similar decrease was observed in promyelocytic NB4 cells, which were differentiated using ATRA (figure 6.1A, right panel). In NB4 cells, *UBC13* mRNA levels were determined during differentiation. This showed a significant decrease in mRNA expression to approximately 20% after 96 hours of differentiation (figure 6.1B).

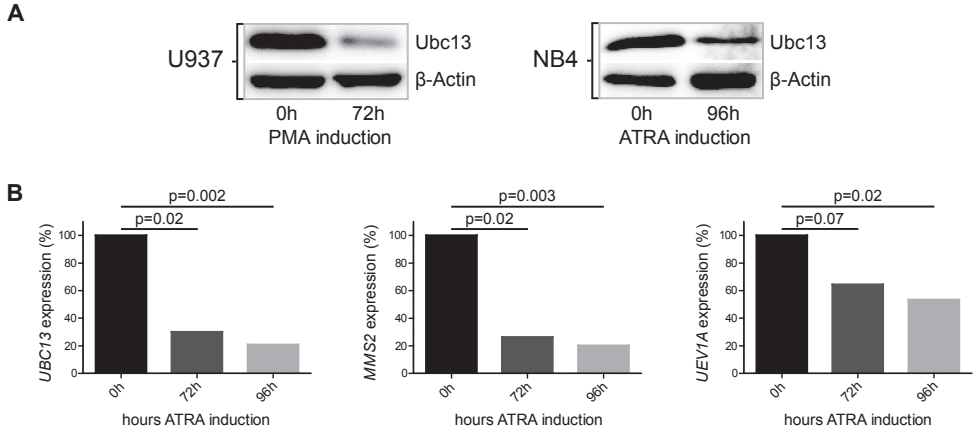


**Figure 6.1: UBC13 and its cofactors are downregulated during myeloid differentiation**
**A.** PMA-induced differentiation of U937 cells (left panel) and ATRA-induced differentiation of NB4 cells (right panel) led to decreased UBC13 protein expression. Cells were treated with 100 ng/mL PMA or $10^{-6}$ M ATRA for 72h or 96h before cell lysates were prepared as indicated. Equal loading of lysates was demonstrated by β-ACTIN staining. **B.** ATRA-induced differentiation of NB4 cells led to decreased mRNA expression of *UBC13* (left panel) and its cofactors *MMS2* (middle panel) and *UEV1A* (right panel). Cells were treated with $10^{-6}$ M ATRA for the indicated time, followed by RNA isolation and QPCR for the indicated genes. Gene expression was normalized to expression of the housekeeping gene *beta-ACTIN* (ΔCt). Data are represented as percentage $2^{-\Delta\Delta Ct}$ compared to time point 0. P-values were calculated via student's t-tests on ΔCt values (n=4).

As UBC13 needs one of its cofactors MMS2 or UEV1a for activity, gene expression of these two cofactors was quantified during ATRA induced differentiation of NB4 cells to determine whether these were differentially regulated as well. Both genes

were significantly downregulated during differentiation. The level of downregulation of *MMS2* was comparable to *UBC13*, while *UEV1A* displayed downregulation to a lesser extent (figure 6.1B). The two cofactors resemble each other for more than 90% at the protein level. As specific antibodies are currently unavailable, we were unable to test the individual downregulation at the protein level.

*Knockdown of UBC13 in U937 cells decreased monocytic differentiation*

To study the biological role of UBC13 during myeloid differentiation, lentiviral approaches for delivery and expression of *UBC13* targeting short hairpin RNA sequences (shRNAs) were established. Lentiviral vectors with four independent doxycycline-inducible shRNAs were tested for their ability to knockdown UBC13 protein levels in transduced U937 cells. As shown in figure 6.2, shRNA A, B and C efficiently knocked down endogenous UBC13 levels, while shRNA D showed no effect. Knockdown became evident after three days of doxycycline treatment and lasted for more than eight days (data not shown). As shRNA A, B and C expression resulted in UBC13 knockdown, subsequent studies were performed with these three shRNAs.

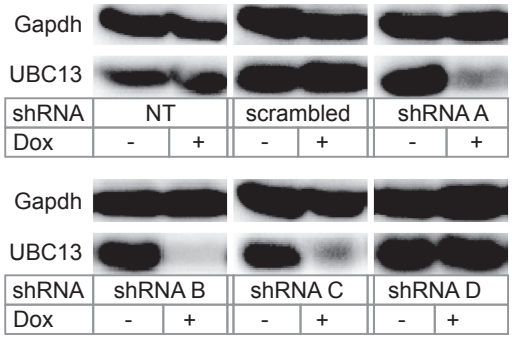


**Figure 6.2: Efficiency of UBC13 silencing by independent shRNA constructs**
Lentivirally transduced U937 cells with the indicated shRNAs or non-transduced cells (NT) were treated for 72h with 2 μg/mL doxycycline (Dox) to induce shRNA transcription. UBC13 expression was visualized by SDS-PAGE and Western blotting using a UBC13-specific antibody. Silencing of UBC13 was evident after induced expression of shRNA A, B and C but not D. GAPDH staining was included to assess equal protein loading.

To test the effect of *UBC13* silencing on monocytic differentiation, stably transduced U937 cells with inducible *UBC13* shRNAs were differentiated towards the monocytic lineage using PMA. To induce differentiation in a *UBC13* knockdown setting, U937 cells were first cultured for three days in the presence of doxycycline to induce knockdown, before starting differentiation by PMA addition. As read-out for differentiation, cell surface expression of the myeloid-specific marker CD11b was measured. *UBC13* silencing did not affect CD11b expression levels in undifferentiated cells (data not shown). However, *UBC13* silencing resulted in a significant decrease in CD11b expression four days after PMA-treatment compared to non-doxycycline treated controls and the scrambled control or non-transduced cells (figure 6.3).

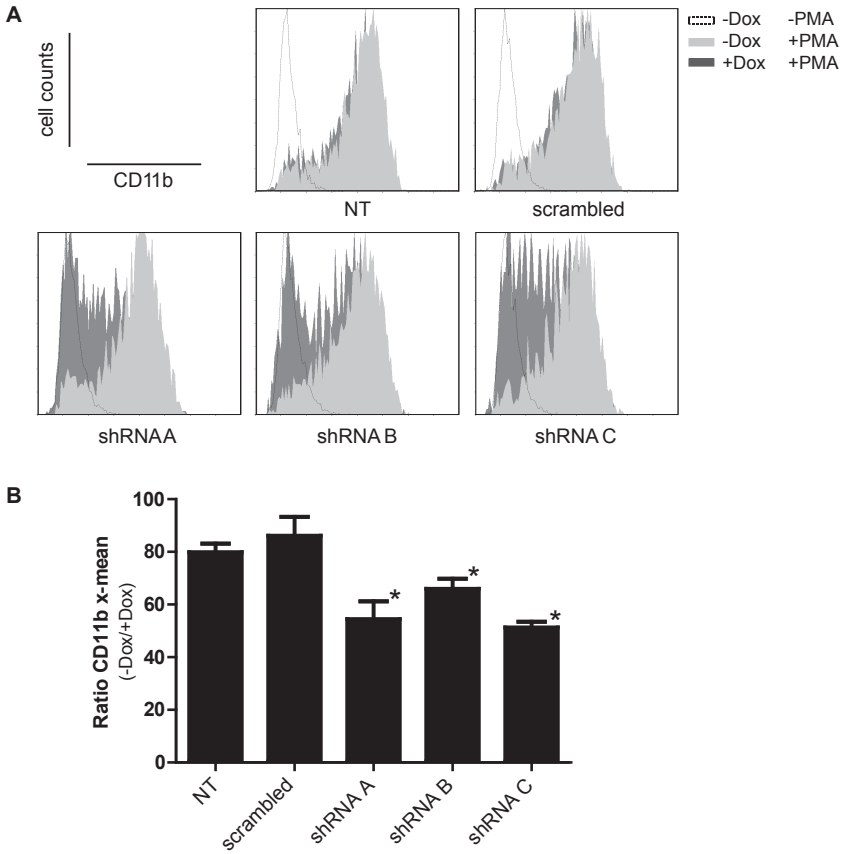


**Figure 6.3: UBC13 knockdown attenuates monocytic differentiation of U937 cells**
**A.** Non-transduced (NT) U937 cells or cells transduced with the indicated shRNAs were cultured with or without 2 μg/mL doxycycline for 72h, followed by a 96h exposure to 100 ng/mL PMA in combination or not with doxycycline, as indicated. Differentiation was evaluated by CD11b expression analysis using flow cytometry. Histograms of CD11b expression on cells treated with or without doxycycline and PMA are shown. The dotted line represents non-doxycycline treated, non-differentiated cells. The light grey surface represents non-doxycycline, PMA-treated cells and the dark grey surface indicates doxycycline- and PMA-treated cells. Doxycycline-treated, non-PMA treated cells were comparable to the dotted line (data not shown). **B.** The differentiation of doxycycline-induced cells transduced with shRNA A, B and C was significantly decreased compared to both non-transduced cells and scrambled controls ($p<0.05$, student's t-test, indicated by asterisk). The ratio of the x-mean of CD11b expression after four days of PMA-treatment of doxycycline-treated versus non-doxycycline-treated cells per transduction was calculated for five biological replicates (represented as percentage of the non doxycycline-treated sample). Data are represented as mean plus SEM (standard error of the mean).

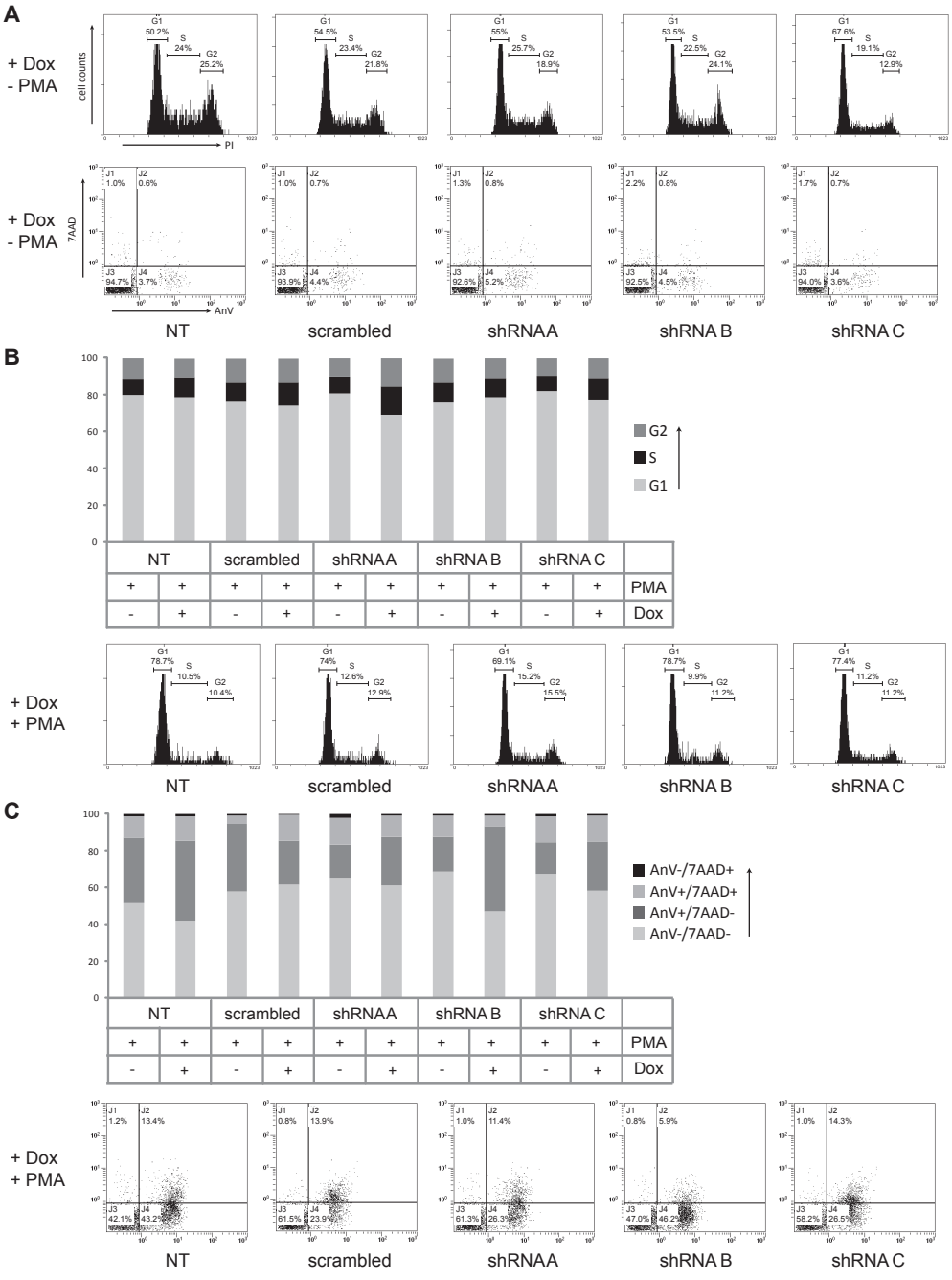
A
+ Dox
- PMA
cell counts
PI
G1 50.2% S 24% G2 25.2%
G1 54.5% S 23.4% G2 21.8%
G1 55% S 25.7% G2 18.9%
G1 53.5% S 22.5% G2 24.1%
G1 67.6% S 19.1% G2 12.9%
+ Dox
- PMA
7AAD
AnV
J1 1.0% J2 0.6% J3 94.7% J4 3.7%
J1 1.0% J2 0.7% J3 93.9% J4 4.4%
J1 1.3% J2 0.8% J3 92.6% J4 5.2%
J1 2.2% J2 0.8% J3 92.5% J4 4.5%
J1 1.7% J2 0.7% J3 94.0% J4 3.6%
NT
scrambled
shRNAA
shRNA B
shRNA C
B
100
80
60
40
20
0
G2
S
G1
NT
scrambled
shRNAA
shRNA B
shRNA C
PMA
Dox
+ Dox
+ PMA
G1 78.7% S 10.5% G2 10.4%
G1 74% S 12.6% G2 12.8%
G1 69.1% S 15.2% G2 15.5%
G1 78.7% S 9.9% G2 11.2%
G1 77.4% S 11.2% G2 11.2%
NT
scrambled
shRNAA
shRNA B
shRNA C
C
100
80
60
40
20
0
AnV-/7AAD+
AnV+/7AAD+
AnV+/7AAD-
AnV-/7AAD-
NT
scrambled
shRNAA
shRNA B
shRNA C
PMA
Dox
+ Dox
+ PMA
J1 1.2% J2 13.4% J3 42.1% J4 43.2%
J1 0.8% J2 13.9% J3 61.5% J4 23.9%
J1 1.0% J2 11.4% J3 61.3% J4 26.3%
J1 0.8% J2 5.9% J3 47.0% J4 46.2%
J1 1.0% J2 14.3% J3 58.2% J4 26.5%
NT
scrambled
shRNAA
shRNA B
shRNA C

**Figure 6.4: UBC13 knockdown does not affect apoptosis and cell cycle progression of U937 cells (previous page)**
Lentivirally transduced U937 cells with indicated shRNAs or non-transduced cells (NT) were treated with 2 μg/mL doxycycline for 72h, followed by 48h culturing with or without 100 ng/mL PMA in combination with doxycycline, as indicated. Cell cycle progression was evaluated by PI (Propidium Iodide) staining and apoptosis by Annexin-V and 7AAD staining. **A.** Doxycycline-induced UBC13 silencing did not affect cell cycle progression (upper panels) or apoptosis (lower panels) in non-differentiated U937 cells. No differences were observed between doxycycline treated versus non-treated cells (data not shown). **B.** 48h PMA treatment induced cell cycle arrest in G0/G1 phase. UBC13 depletion did not affect this arrest. The upper graph represents the cell cycle progression differences between cells transduced with different shRNAs and the effect of doxycycline-induced shRNA expression. To visualize the data, PI flow cytometry graphs of doxycycline-treated cells are shown below. **C.** UBC13 depletion did not affect PMA-induced apoptosis. The upper graph represents the differences in apoptosis between cells transduced with different shRNAs and the effect of doxycycline-induced shRNA expression. To visualize the data, Annexin-V/7AAD flow cytometry graphs of doxycycline treated cells are shown below. Data shown are a representative of three independent experiments.

*Ubc13* deletion leads to increased apoptosis of primary mouse hematopoietic precursor cells *in vivo*[9]. Therefore, we studied apoptosis and cell cycle progression in the U937 model. In undifferentiated proliferating cells, *UBC13* silencing did not affect apoptosis or cell cycle progression, as no differences were observed between doxycycline treated versus non-treated cells transduced with *UBC13* shRNAs, nor between *UBC13* silenced cells and scrambled controls (figure 6.4A). Apoptosis and cell cycle progression was also measured during PMA-induced differentiation. PMA-treatment induced apoptosis and a G1/G0 arrest in all cells, and we did not observe consistent differences in apoptosis rates and cell cycle progression between scrambled controls and *UBC13* silenced cells after PMA-induced differentiation (figure 6.4B+C).

## Discussion

The E2 conjugating enzyme UBC13, which catalyses K63-ubiquitin chain formation, is essential for early stages of murine hematopoiesis[9]. Here, we studied the expression and role of UBC13 at later stages of myeloid differentiation using human cell line models. Both ATRA-induced granulocytic differentiation of NB4 cells and PMA-induced monocytic differentiation of U937 cells led to UBC13 downregulation. In combination with the previously reported downregulation of *UBC13* mRNA levels during gefitinib-induced granulocytic differentiation of HL60 cells[13], these data suggest that UBC13 downregulation is a common phenomenon during myeloid differentiation. It would be interesting to study whether the total amount of K63-linked ubiquitin chains decreases upon differentiation, and whether specific substrates are differentially modified.

Unfortunately, the quality of currently available K63-specific antibodies is not sufficient to test this.

The high expression of UBC13 in undifferentiated cells and its downregulation during differentiation might suggest a functional role for UBC13 in myelopoiesis. Several scenarios are conceivable. High expression of UBC13 might be necessary to retain an undifferentiated state and UBC13 downregulation is needed before differentiation can take place. Alternatively, high UBC13 levels might be needed for the first steps of differentiation, but once the differentiation program is started, UBC13 function is dispensable, resulting in downregulation. To test these hypotheses, the functional role of UBC13 was studied using inducible *UBC13* silencing constructs in U937 differentiation assays. Silencing of *UBC13* did not induce spontaneous differentiation of U937 cells. On the contrary, *UBC13* silencing reduced the PMA-induced differentiation of U937 cells, based on reduced CD11b expression after four days of PMA treatment. This indicates that high levels of UBC13 are needed for proper differentiation. However, differentiation was not completely blocked by *UBC13* silencing. In this respect, the low residual UBC13 levels following gene silencing may have allowed low levels of differentiation. The reduced CD11b expression upon differentiation after UBC13 silencing was not accompanied by reduced apoptosis levels. This observation was unexpected, as differentiation of U937 cells induced by PMA is generally accompanied by apoptosis[14]. It would be interesting to study which mechanisms are regulated by UBC13 that are able to stimulate PMA-induced differentiation programs, while not affecting PMA-induced apoptosis and cell cycle regulation.

The role of K63-linked ubiquitin chains has been established in several pathways including DNA damage repair, NF-κB and MAP kinase signaling and receptor trafficking. K63-linked chains are known to induce internalization of several cellular membrane receptors[15]. We observed reduced membrane expression of CD11b upon *UBC13* depletion, which is opposite to the expected effect if UBC13 would enhance the internalization of this receptor. To verify that the effect we observed is not due to a specific role of UBC13 in CD11b expression and/or trafficking, research in our laboratory is currently directed at confirming the results using other differentiation markers. Furthermore, additional studies such as NBT (Nitro Blue Tetrazolium) or phagocytic activity assays should be performed to study the effect of UBC13 silencing on the monocytic behavior of PMA-treated U937 cells.

Together with E3 ubiquitin ligases, UBC13 marks various proteins involved in NF-κB and MAP kinase signaling with K63-linked ubiquitin chains[16,17]. In these pathways, UBC13 depends on UEV1a as cofactor. Importantly, *UEV1A* showed comparable downregulation to *UBC13* during differentiation in our experiments (≈80%, figure 6.1B). In mouse macrophages and B cells, UBC13 is needed for proper inflammatory responses. However, it depends on cell type and stimulus whether UBC13 signaling is necessary for NF-κB and/or MAP kinase signaling[7,8]. Both NF-κB and MAP

kinase signaling are important for PMA-induced U937 differentiation, as inhibition of either pathway decreases differentiation[18-21]. This resembled the data following *UBC13* silencing described in this study. However, inhibition of both NF-κB and MAP kinase pathways decreased differentiation-induced apoptosis of U937 cells, which was not evident in our experiments. Additional studies investigating whether *UBC13* silencing causes decreased activation of target genes of the NF-κB and MAP kinase pathways in PMA-treated U937 cells are required to show a potential direct effect of UBC13 on these pathways during differentiation. To gain better insight in additional pathways regulated by K63-linked ubiquitin chains during myeloid differentiation, future research should be directed at identification of the substrate proteins of UBC13-mediated ubiquitination.

**Acknowledgements**

We would like to thank Rob Woestenenk for help with setting up the flow cytometryic PI-staining.

## Reference List


1. Andersen,P.L. *et al.* Distinct regulation of Ubc13 functions by the two ubiquitin-conjugating enzyme variants Mms2 and Uev1A. *J. Cell Biol.* **170**, 745-755 (2005).
2. Hofmann,R.M. & Pickart,C.M. Noncanonical MMS2-encoded ubiquitin-conjugating enzyme functions in assembly of novel polyubiquitin chains for DNA repair. *Cell* **96**, 645-653 (1999).
3. Eddins,M.J., Carlile,C.M., Gomez,K.M., Pickart,C.M., & Wolberger,C. Mms2-Ubc13 covalently bound to ubiquitin reveals the structural basis of linkage-specific polyubiquitin chain formation. *Nat. Struct. Mol. Biol.* **13**, 915-920 (2006).
4. Moraes,T.F. *et al.* Crystal structure of the human ubiquitin conjugating enzyme complex, hMms2-hUbc13. *Nat. Struct. Biol.* **8**, 669-673 (2001).
5. VanDemark,A.P. *et al.* Molecular insights into polyubiquitin chain assembly: crystal structure of the Mms2/Ubc13 heterodimer. *Cell* **105**, 711-720 (2001).
6. Chen,Z.J. & Sun,L.J. Nonproteolytic functions of ubiquitin in cell signaling. *Mol. Cell* **33**, 275-286 (2009).
7. Yamamoto,M. *et al.* Key function for the Ubc13 E2 ubiquitin-conjugating enzyme in immune receptor signaling. *Nat. Immunol.* **7**, 962-970 (2006).
8. Fukushima,T. *et al.* Ubiquitin-conjugating enzyme Ubc13 is a critical component of TNF receptor-associated factor (TRAF)-mediated inflammatory responses. *Proc. Natl. Acad. Sci. U.S.A* **104**, 6371-6376 (2007).
9. Wu,X., Yamamoto,M., Akira,S., & Sun,S.C. Regulation of hematopoiesis by the K63-specific ubiquitin-conjugating enzyme Ubc13. *Proc. Natl. Acad. Sci. U.S.A* **106**, 20836-20841 (2009).
10. Matsuzawa,A. *et al.* Essential cytoplasmic translocation of a cytokine receptor-assembled signaling complex. *Science* **321**, 663-668 (2008).
11. Xu,M., Skaug,B., Zeng,W., & Chen,Z.J. A ubiquitin replacement strategy in human cells reveals distinct mechanisms of IKK activation by TNFalpha and IL-1beta. *Mol. Cell* **36**, 302-314 (2009).
12. Marteijn,J.A. *et al.* Nucleotide excision repair-induced H2A ubiquitination is dependent on MDC1 and RNF8 and reveals a universal DNA damage response. *J. Cell Biol.* **186**, 835-847 (2009).
13. Stegmaier,K. *et al.* Gefitinib induces myeloid differentiation of acute myeloid leukemia. *Blood* **106**, 2841-2848 (2005).
14. Takada,Y. *et al.* 12-O-tetradecanoylphorbol-13-acetate-induced apoptosis is mediated by tumor necrosis factor alpha in human monocytic U937 cells. *J. Biol. Chem.* **274**, 28286-28292 (1999).
15. Clague,M.J. & Urbe,S. Endocytosis: the DUB version. *Trends Cell Biol.* **16**, 551-559 (2006).
16. Abbott,D.W. *et al.* Coordinated regulation of Toll-like receptor and NOD2 signaling by K63-linked polyubiquitin chains. *Mol. Cell Biol.* **27**, 6012-6025 (2007).
17. Ea,C.K., Deng,L., Xia,Z.P., Pineda,G., & Chen,Z.J. Activation of IKK by TNFalpha requires site-specific ubiquitination of RIP1 and polyubiquitin binding by NEMO. *Mol. Cell* **22**, 245-257 (2006).
18. Dai,Y. *et al.* An intact NF-kappaB pathway is required for histone deacetylase inhibitor-induced G1 arrest and maturation in U937 human myeloid leukemia cells. *Cell Cycle* **2**, 467-472 (2003).
19. Miranda,M.B., McGuire,T.F., & Johnson,D.E. Importance of MEK-1/-2 signaling in monocytic and granulocytic differentiation of myeloid cell lines. *Leukemia* **16**, 683-692 (2002).
20. Pennington,K.N., Taylor,J.A., Bren,G.D., & Paya,C.V. IkappaB kinase-dependent chronic activation of NF-kappaB is necessary for p21(WAF1/Cip1) inhibition of differentiation-induced apoptosis of monocytes. *Mol. Cell Biol.* **21**, 1930-1941 (2001).
21. Garcia,A. *et al.* Differential effect on U937 cell differentiation by targeting transcriptional factors implicated in tissue- or stage-specific induced integrin expression. *Exp. Hematol.* **27**, 353-364 (1999).

# Isolation of endogenous proteins modified with K63-linked ubiquitin chains

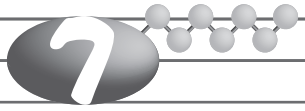

**Sylvie M. Noordermeer, Hans J. Wessels, Saskia M. Bergevoet, Maurice van Dael, Jolein Gloerich, Joop H. Jansen, and Bert A. van der Reijden**

## Abstract

**The modification of proteins with ubiquitin is critical for many cellular processes. Typically, K63-linked ubiquitin chains positively affect downstream signaling, for example in NF-κB and DNA damage repair pathways. UBC13 is the E2 conjugating enzyme responsible for K63-linked ubiquitin chain formation. Recently, it has been shown that conditional knockout of Ubc13 leads to severe hematopoietic defects in mice. To fully understand the role of K63-linked ubiquitination in this process, knowledge on the modified substrates is needed. In this chapter, a novel method to isolate endogenous proteins modified with K63-linked ubiquitin chains is described. This method is based on immobilized GST-fusions of ubiquitin binding domains. Rap80-UIM (ubiquitin interacting motif), Tab2-NZF (Npl4 Zinc finger) and a tandem-Tab2-NZF domain were used for the isolation of proteins modified with K63-linked chains. The Mud1-UBA (ubiquitin associated) domain with specificity for K48-linked chains served as a control. K63-ubiquitinated proteins were isolated by incubation of the immobilized K63-linkage specific domains with cellular extracts. The GST-fusion of tandem-Tab2-NZF showed the highest enrichment for modified proteins with K63-linked chains. Mass spectrometry was used to identify the purified proteins. Apart from ubiquitin, which was the most abundant protein in the mass spectrometric analysis, many other proteins were identified, including E3 ligases and proteasome subunits.**

## Introduction

Many important biological processes, such as DNA damage repair, cell cycle progression and NF-κB signaling are regulated by ubiquitination[1]. In this posttranslational modification of cellular proteins, ubiquitin is covalently conjugated to an internal lysine of the substrate protein. As ubiquitin itself contains seven lysines (K6, K11, K27, K29, K33, K48, K63), ubiquitin polymers can be formed by the covalent interaction of the donor ubiquitin C-terminus to an internal lysine of the acceptor ubiquitin. Consequently, proteins can be modified with single ubiquitin moieties, so-called mono-ubiquitination, or with ubiquitin chains (poly-ubiquitination)[2].

K63-linked ubiquitin chains are important signaling factors by serving as a binding platform for downstream proteins[3]. The regulatory role of K63-linked ubiquitin chains has been shown in the DNA damage repair pathway, NF-κB and MAP kinase signaling and membrane receptor turnover[4]. UBC13 is currently the only E2 conjugating enzyme identified that specifically catalyzes K63-linked chains[5,6]. Conditional knockout of *Ubc13* in mouse models leads to severe defects in early hematopoiesis, inducing mortality within two weeks[7]. Furthermore, a role for UBC13 in myelopoiesis has been described in chapter 6 of this thesis. However, the substrates of UBC13 ubiquitination that mediate its function in these processes are mainly unknown. In this chapter we describe a method to isolate and identify K63-ubiquitinated proteins using the binding specificity of different ubiquitin binding domains (UBDs) for K63-ubiquitin linkages.

Currently, cellular methods to study ubiquitin linkages rely on the overexpression of tagged-ubiquitin mutants lacking one or more lysines, followed by isolation of the modified proteins via the tag. The advantage of this technique is the possibility to use denaturing conditions for isolation, thereby disrupting all protein-protein interactions and only isolating ubiquitin covalently coupled to substrates. However, the mutation and the tag might influence ubiquitination. Furthermore, overexpressed mutant ubiquitin has to compete with endogenous ubiquitin, which is among the highest expressed proteins in a cell. Therefore, it is likely that in overexpression studies, poly-ubiquitin chains are composed of both wildtype and mutant ubiquitin moieties and data may therefore be misleading.

Mass spectrometry (MS) has become the standard technique to identify ubiquitination-sites in substrates, taking advantage of the covalent nature of this modification. Trypsin digestion of ubiquitinated proteins results in the formation of peptides containing a miscleaved lysine with a double glycine (diG) remnant originating from the C-terminus of ubiquitin. This diG remnant causes a 114D shift of the unmodified peptide in the MS spectrum[8]. This property has been used in quantitative MS to determine the abundance of different ubiquitin chain linkages in several organisms, including human cell line models. This showed that the most abundant chains are K48-linked, followed by K11- and K63-linked chains. The presence of the other chains

is much lower[9-11]. Although MS can be used to identify the ubiquitinated lysine in proteins and to determine the cellular abundance of different chain conformations, it is unable to identify the type of ubiquitin chain attached to a specific protein in complex samples, as trypsin digestion destroys the substrate-chain architecture. Therefore, an additional purification step for the specific ubiquitin-linkage preceding MS analysis would be needed for global identification of substrates of specific chains.

Proteins that bind ubiquitin contain one of the many structural types of UBDs[12]. Many of these domains show specificity for particular ubiquitin chains or mono-ubiquitin[13,14]. For some of these domains, structural data are available, illustrating their chain specificity. For example, the C-terminal Npl4 Zinc finger (NZF) domain of Tab2 binds specifically to K63-linked chains using two distinct domains in the two adjacent ubiquitin moieties[15,16]. Tab2 uses a single NZF-domain of only 30 amino acids for K63-linkage binding. This is in contrast to Rap80, which uses two ubiquitin interacting motifs (UIMs) for the recognition of one K63-linkage[17,18]. We developed a method to purify endogenous proteins modified with K63-chain linkages based on these UBDs. The small UBDs (K63 specific: Tab2-NZF, Rap80-UIM, and as control, K48 specific: Mud1-UBA[19] (Ubiquitin Associated)) were fused to GST and expressed in bacteria. The fusion-proteins were coupled to glutathione sepharose beads and used in pull-down experiments with human cell lysates, followed by the identification of isolated proteins via MS analyses.

## Materials and Methods

*Cell Lines*

U937 cells were cultured in RPMI medium (Invitrogen, Carlsbad, USA) supplemented with 10% fetal calf serum (FCS, Invitrogen) and 1% Penicillin/Streptomycin (MP biomedicals, Solon, USA). Hela cells were cultured in DMEM medium (Invitrogen) supplemented with 10% FCS and 1% Pen/Strep. All cells were maintained at 37°C and 5% $CO_2$ in a humidified atmosphere.

*Constructs and transfection*

For GST-fusion protein expression, the following constructs were used: pGEX-6p1, pGEX-6p1-Mud1_UBA (amino acid (aa) 293-332) and pOPINJ-Tab2_NZF-UBD (aa 663-693) (kindly provided by Dr. Kulathu and Dr. Komander (Cambridge, UK))[13,15]. The pGEX-Rap80_UIM1/2 (aa 79-121) construct was kindly provided by Dr. Jetten (NIH, USA)[20]. To generate a tandem-Tab2_UBD construct, the NZF-UBD was PCR amplified from pOPINJ-Tab2_UBD either with flanking BamHI and HindIII restriction enzyme sites or with flanking HindIII and XhoI restriction enzyme sites including a linker encoding 5x Gly and 1x Val downstream of the HindIII site, upstream

of the UBD. Both PCR-products were cloned separately into the cloning vector pDrive (Qiagen, Venlo, The Netherlands) and subsequently combined into pGEX-6p1 as a tandem-Tab2 domain, interspersed by the six amino acid linker.

pcDNA3.1 with ubiquitin containing an N-terminal strep(II)-HA-tag was kindly provided by Dr. Nielsen (Copenhagen, Denmark)[10]. The HA-tag was removed by substituting HA-Ubiquitin flanked by SacII and NotI restriction sites by solely ubiquitin with the same flanking restriction sites. K11R, K48R and K63R mutations were introduced using the Quickchange XL Site-Directed Mutagenesis kit of Stratagene (Santa Clara, USA) according to the protocol supplied and the following primers: 5'-gaccctgaccggcaggaccatcactctgg-3' (K11R), 5'-aggctcatctttgcaggcaggcagctggaag-3' (K48R), 5'-tctttctgactacaacatccagagagagtcgaccct-3' (K63R). Constructs were sequenced to confirm mutation introduction. Wildtype or mutant ubiquitin fused to the Strep(II) tag was overexpressed in Hela cells using PEI transfection.

*GST-fusion protein expression and isolation*

GST-fusion UBD domains were expressed and purified as described elsewhere[15]. In short, pGex or pOPINJ vectors were transformed into the *Escherichia Coli* Rosetta 2(DE3)pLacI bacterial strain (Novagen, Darmstadt, Germany). Bacteria were grown to OD 0.6, followed by induction of protein expression with 150 μM IPTG and 200 μM $ZnSO_4$ for 16h at room temperature. Afterwards, bacteria were lysed by sonication in lysis buffer (270 mM sucrose, 50 mM Tris-HCl pH8, 10 mM $Na_2$β-glycerophosphate, 50 mM NaF, complete protease inhibitor cocktail (EDTA-free, Roche, Basel, Switzerland), 1 mg/mL lysozyme, 0.1 mg/mL DNAse and 0.1% β-mercaptoethanol). Cleared lysates were incubated with glutathione sepharose beads (GE Healthcare, Waukesha, USA) for 2hr at 4°C. GST-coupled beads were washed six times with high salt buffer (500 mM NaCl, 25 mM Tris-HCl pH8, 5 mM DTT), five times with low salt buffer (150 mM NaCl, 25 mM Tris-HCl pH8, 5 mM DTT) and 3 times with TEND buffer (140 mM NaCl, 25 mM Tris-HCl pH7.4, 2.7 mM KCl, 0.5% Igepal CA-630, 5 mM DTT, complete protease inhibitor cocktail (EDTA-free, Roche), and 1 mM PMSF). Purity and yield of GST-coupled beads was examined by SDS-PAGE of 2 μL beads followed by colloidal Coomassie blue staining[21] (0.12% Coomassie G250 (Biorad, Hercules, USA), 10% $(NH_4)_2SO_4$, 10% $H_3PO_4$, 20% Methanol).

*Pull-down of purified ubiquitin chains*

Small amounts of sepharose beads coupled to GST-UBDs (0.05μL≈0.25μg GST-protein) were incubated with di-ubiquitin chains (di-Ub) or chains of 2-9 ubiquitin moieties ($Ub_{2-9}$) of different chain conformations (K11, K48 and K63, Boston Biochem, Cambridge, USA) for 3hr at 4°C in pull-down buffer (150 mM NaCl, 50 mM Tris-HCl pH7.5, 5 mM DTT, 0.1% Igepal CA-630). Beads were subsequently washed five times in pull-down buffer and denatured in SDS loading buffer prior to SDS-PAGE and

Western blotting. Blots were probed with an antibody against total ubiquitin (clone 6C1, Sigma-Aldrich, St. Louis, USA).

*Pull-down of ubiquitinated proteins from cellular extracts*

U937 or transfected Hela cells were lysed by sonication in pull-down buffer supplemented with complete protease inhibitor cocktail (EDTA-free, Roche), 0.5% benzonase (Novagen), 1 mM PMSF and 10 μM WP1130 (kindly provided by Dr. Donato, Ann Arbor, USA). Cleared lysates were incubated with UBD-sepharose beads for 3hr at 4°C. Beads were washed five times in pull-down buffer and denatured in SDS loading buffer. After SDS-PAGE and Western blotting, pull-down efficiency was evaluated by probing membranes with antibodies for total ubiquitin (Sigma-Aldrich), K11-ubiquitin chains (Millipore, Billerica, USA), K48-ubiquitin chains (Millipore) and K63-ubiquitin chains (Millipore), or Strep(II) (IBA, Göttingen, Germany).

*Protein identification via tandem mass spectrometry*

U937 pull-down samples were electrophoresed on an SDS-PAGE gel for 2.5 cm. Following colloidal Coomassie blue staining, gel fragments above the GST-proteins (>±36kD) were excised and cut into 1x1mm pieces. Gel pieces were destained in three rounds of consecutive equilibration in 50mM ammonium bicarbonate (ABC), 50% acetonitrile (ACN)/50% $H_2O$ and 100% ACN. Next, gel pieces were reduced in 10 mM DTT, followed by alkylation in 50 mM 2-chloroacetamide in 50 mM ABC. Proteins were in gel digested with trypsin (100 ng trypsin in 50 mM ABC per lane) for 16hr at 37°C. Peptides were extracted from the gel pieces using 2% trifluoroacetic acid (TFA) followed by a second extraction in 80% ACN, 0.5% acetic acid, 1% TFA. Afterwards, peptides were purified using home-made Stage Tips as described[22] and reconstituted in 0.5% acetic acid. For MS analysis, 20% (5μL) of the sample was injected onto a 15 cm fused silica emitter (New Objective, Woburn, USA) packed with reversed phase ReproSil-Pur C18AQ 3μm resin (Dr. Maisch, Ammerbuch-Entringen, Germany) using 0.5% acetic acid. Peptides were eluted from the column in a 60 minute linear gradient of 15 to 60% 80% ACN, 0.5% acetic acid using a nanoflow liquid chromatography (LC) system (Proxeon, Thermo Fisher Scientific, Waltham, USA). Tandem MS spectra were acquired by the linear ion trap for the top four most-abundant ions from each ICR cell precursor scan by collision induced dissociation (CID) with enabled dynamic exclusion to prevent repetitive analysis of peptide ions. Measurements were performed with a linear ion trap Fourier-transform ion cyclotron resonance mass spectrometer (7T LTQ FT Ultra, Thermo Fisher) as described[23].

Data was searched against the human Refseq database (release 44) with additional known contaminant sequences (e.g. trypsin and LysC) using Mascot software (v2.2, Matrix Science). A second database search was performed against a decoy database with reversed protein sequences for subsequent false discovery rate (FDR) calculations.

Parameters for the Mascot searches were 10 ppm precursor ion mass tolerance, 0.8 Da fragment ion mass tolerance, ESI-TRAP instrument fragment ions, tryptic specificity with a maximum of 2 missed cleavages, carbamidomethyl (cys) as fixed modification, and the following variable modifications: GlyGly (Lys), LeuArgGlyGly (Lys), and oxidation (Met). Validation of the peptide and protein identification data was performed according to Weatherly *et al.*[24] using the *in-house* developed software tool PROTON [PROteomics TOols Nijmegen; Wessels *et al.*, manuscript in preparation]. Briefly, this validation method uses the normal (true and false positives) and decoy (true negatives) database search results to calculate peptide identification score thresholds to achieve the specified 1% FDR for proteins identified using 1, 2, 3, 4, 5, and 6 or more unique peptides. Protein abundance values for valid protein identifications were calculated by the PROTON software as exponentially modified protein abundance index according to Ishihama *et al.*[25].

*Enrichment of diG-peptides for MS analysis*

U937 cell lysate incubation with tandem-Tab2 immobilized beads, sample preparation, trypsin digestion and Stage Tip purification were performed as described above. Following Stage Tip purification, diG-peptides were purified using the PTMScan Ubiquitin Remnant Motif kit (Cell Signaling Technology, Danvers, USA)[26], following the manufacturer's protocol. In short, peptides were dissolved in 1.4 mL IAP buffer (50 mM MOPS/NaOH, pH7.2, 10 mM $Na_2HPO_4$, 50 mM NaCl) and incubated with PTMScan diG-immunoaffinity beads for 30 min. at 4°C. After washing, peptides were eluted with 0.15% TFA, followed by concentration and purification using Stage Tips. MS analysis of the peptides was performed as described above.

## Results

*Tab2 binds preferentially to purified K63-linked ubiquitin chains*

GST-UBD fusion proteins immobilized to glutathione beads were used to isolate specific ubiquitin chains. For capturing of K63-linkages, the NZF domain of Tab2 and tandem UIM domain of Rap80 were used and the UBA domain of Mud1 was used as a reference for capturing K48-linkages (supplemental figure 7.1)[13,20]. By performing pull-down experiments with purified di-ubiquitin (figure 7.1A) and longer chains of two to nine ubiquitin moieties with K48 or K63 linkages (figure 7.1B), we confirmed the preferential binding of Tab2 and Rap80 to K63-linked ubiquitin chains over K48-linked chains. Mud1 showed preferential binding to K48-linked chains, as expected. However, Mud1 also showed binding to K63-linked chains, although the binding efficiency was much lower compared to K48-binding. Importantly, GST alone did not show any binding affinity for the tested ubiquitin chains.

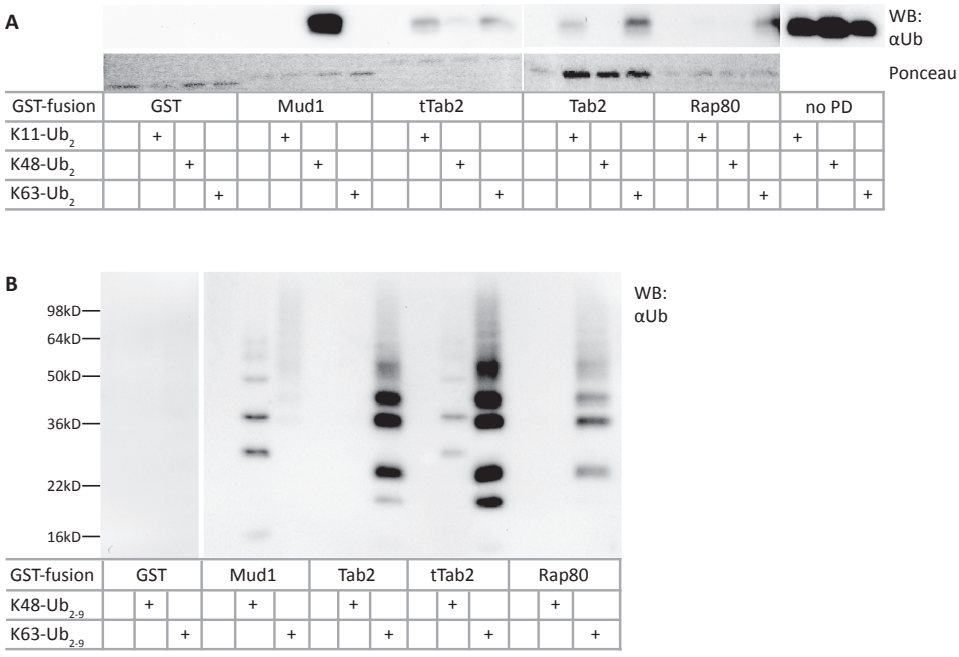


**Figure 7.1: Pull-down of K63-linked chains by Tab2, Rap80 and tandem-Tab2**
**A.** 0.05 µL of purified GST-UBD fusion proteins immobilized to glutathione beads were incubated with 2 µg di-ubiquitin of different linkages (K11, 48 or 63). Pull-down samples were separated with SDS-PAGE and Western Blotting, and blots were stained for ubiquitin. Mud1 showed specificity for K48-di-Ub. Rap80 showed specificity for K63 di-ub. Tab2 and tandem-Tab2 (tTab2) bound to K63 di-Ub, but also to K11 di-Ub. A Ponceau staining is included to indicate the amount of GST-fusion protein used. **B.** Experimental setup as in A, except ubiquitin chains of different lengths ($K48_{2-9}$ and $K63_{2-9}$) were used. Mud1 bound preferentially to K48-linked chains, with minor binding to K63-linked chains. Tab2, tandem-Tab2 (tTab2) and Rap80 bound preferentially to K63-linked chains, although tandem-Tab2 showed low binding to K48-linked chains as well.

Next to K48- and K63-linked chains, K11-linked chains are the third most occurring type of chains[9-11]. We therefore also tested binding of the used domains to K11-linked di-ubiquitin chains. Interestingly, Tab2 was able to bind K11-linked chains, a property not described before (figure 7.1A). Rap80 and Mud1 did not bind to K11-linked di-ubiquitin.

Of the two K63-linkage specific domains, Tab2 showed the highest efficiency in ubiquitin binding. We hypothesized that a tandem domain might increase binding even more. To test this, a GST-fusion of two Tab2-NZF domains interspersed by a six amino acid linker was cloned and bacterially expressed. Indeed, this domain showed higher affinity for K63-linked ubiquitin chains compared to the single domain (figure

7.1B). However, it also interacted with K48-linked chains of three linkages or longer, albeit with lower efficiency compared to K63-linked chains. Tandem-Tab2 interacted with K11 di-ubiquitin in a comparable manner as the single Tab2 domain (figure 7.1A).

*GST-UBDs bind to endogenous proteins modified with ubiquitin chains*

The data described above showed efficient binding of the UBDs to purified ubiquitin chains, confirming previously described data[15-19]. To test whether the binding efficiency was sufficient to isolate ubiquitin chains attached to endogenous substrates from cellular extracts, we incubated the GST-UBD fusions with lysates of U937 cells. In figure 7.2A, it is shown that tandem-Tab2 and Mud1 showed the highest efficiencies to pull-down ubiquitinated proteins. Tab2 showed a modest efficiency in ubiquitinated substrate

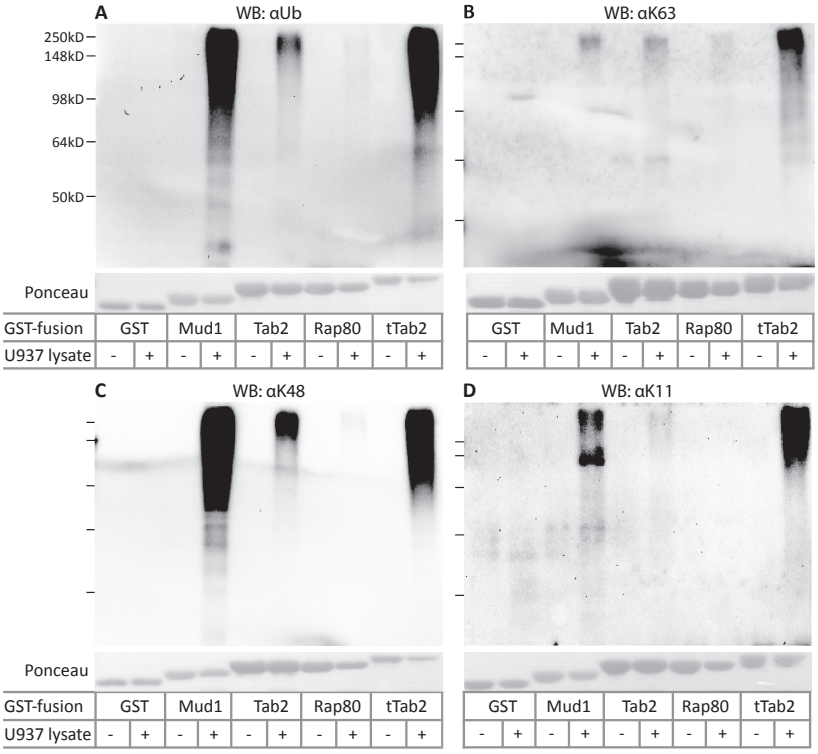


**Figure 7.2: Tandem-Tab2 efficiently isolated endogenous substrates of K63-linked ubiquitin chains**

10 µg GST-UBD fusion protein immobilized on glutathione beads was incubated with 50 mg U937 lysate. After washing of beads, the pull-down samples were divided in four and following Western blotting membranes were stained for total ubiquitin (**A**), K63-linked poly-ubiquitin chains (**B**), K48-linked poly-ubiquitin chains (**C**), and K11-linked poly-ubiquitin chains (**D**). A Ponceau staining for GST-UBDs is shown below each antibody staining

binding and Rap80 showed inefficient binding. The GST-control did not show any binding to ubiquitinated proteins.

To study the chain linkages present in the pull-down samples, we probed the samples with chain specific ubiquitin antibodies. Figure 7.2B shows that all GST-UBD fusion proteins were able to isolate K63-ubiquitinated proteins. Tandem-Tab2 displayed the highest efficiency to isolate K63-modified proteins. The Mud1 pull-down was most efficient for isolation of K48-linked chains, although all other tested GST-fusion UBDs showed binding to K48-chains (figure 7.2C). All UBDs except Rap80 captured proteins with K11-ubiquitin chains (figure 7.2D). For Mud1, this was unexpected, as Mud1 did not bind purified K11-linked di-ubiquitin (figure 7.1A).

*Overexpression of K63R and K48R ubiquitin mutants confirms the binding specificity of tandem-Tab2 and Mud1*

In the previous experiment, it was difficult to determine binding specificity of the domains, as stainings of different antibodies cannot be compared. To study the specificity of the UBDs for ubiquitinated proteins with different chain linkages, we overexpressed strep(II)-tagged ubiquitin mutants in Hela cells, followed by pull-down using GST-UBD beads. Overexpression of wildtype ubiquitin and mutants lacking one of the three lysines that are most abundant in cellular chains (K11, K48, K63)[9-11] was tested. All mutants were incorporated into higher molecular weight proteins, indicating substrate-ubiquitination (upper left blot, figure 7.3) and pull-down efficiencies were not affected by the overexpression of the mutants (lower right blots, figure 7.3). Overexpressed strep(II)-tagged wildtype ubiquitin was inefficiently isolated by all UBDs, while the mutants were more efficiently isolated by tandem-Tab2 and Mud1. The pull-down efficiencies of Tab2 and Rap80 were insufficient to show binding to overexpressed strep(II)-tagged wildtype ubiquitin or mutants (data not shown). The binding affinity of tandem-Tab2 was lowest for strep(II)-tagged K63R ubiquitin, while K11R and K48R were more efficiently isolated. These data confirmed the preference of tandem-Tab2 for K63-linked chains, although it was not 100% specific, indicated by the residual strep(II)-signal in the pull-down using K63R overexpression. Mud1 showed decreased pull-down efficiency of strep(II)-tagged K48R ubiquitin, confirming its specificity for K48-linked ubiquitin chains.

*Mass spectrometry identifies proteins isolated by the GST-UBD fusions*

To identify the proteins that were isolated from U937 cellular extracts using the different GST-UBD fusions, tandem mass spectrometry was used. Samples from GST-UBD beads without incubation with U937 cellular extracts were included as negative control. The number of proteins identified per UBD pull-down are shown in table 7.1A, representing proteins that were identified in the pull-down using U937 lysates, but not in the negative control of the corresponding UBD.

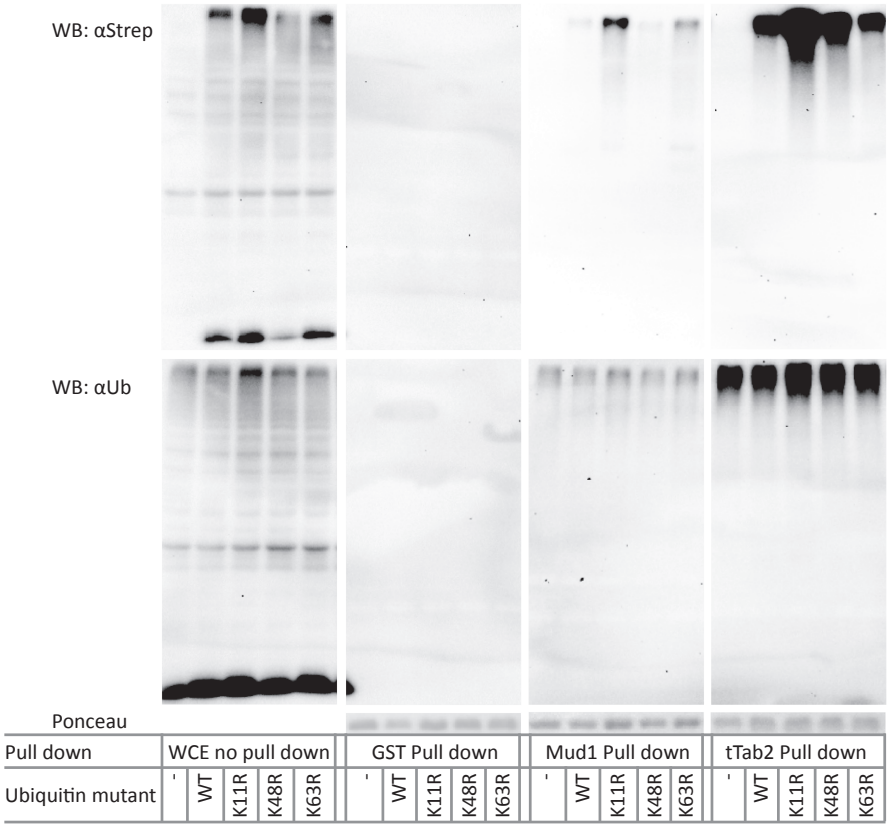


**Figure 7.3: Pull-down of UBDs with lysates overexpressing ubiquitin mutants**
5 µg GST-UBDs immobilized on glutathione beads was incubated with approximately 5 mg Hela cell lysates transfected with Strep(II)-tagged wildtype ubiquitin or single Lysine to Arginine mutants, as indicated. Membranes were stained for Strep (overexpressed ubiquitin, upper panel) or total ubiquitin (lower panel). A Ponceau staining is included to demonstrate equal amounts of GST-fusion proteins. All Strep(II)-tagged ubiquitin constructs were expressed, with K48R-ubiquitin showing the lowest expression levels. Strep(II)-tagged wildtype ubiquitin was inefficiently pulled down.

To increase the number of protein identifications, we repeated the tandem-Tab2 pull-down using a larger amount (150%) of U937 cellular extract. This increased the number of proteins identified by two-fold (see figure 7.4A). Importantly, of the 74 unique proteins identified in the first experiment (excluding the proteins identified in the negative control), 67 (91%) were identified in the second experiment as well, indicating good reproducibility between experiments (figure 7.4A).

To identify the common and unique proteins isolated by the different GST-UBD fusions, we compared the lists of proteins identified in the positive pull-down samples

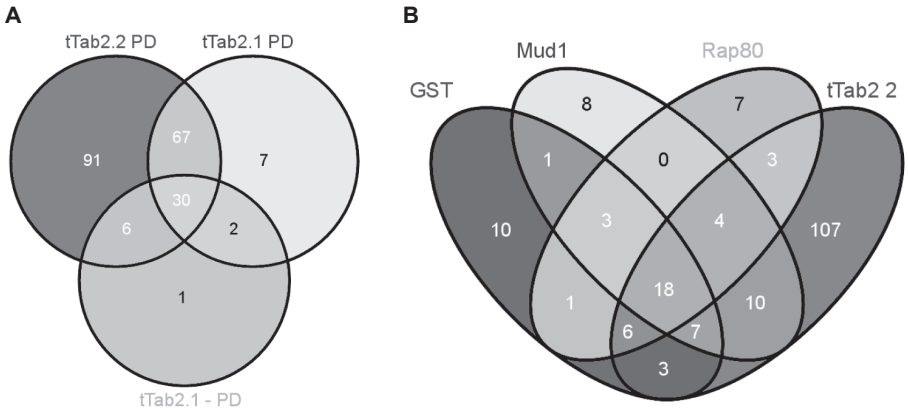


**Figure 7.4: Protein identification of pull-down samples using mass spectrometry**
**A.** Comparison of unique proteins identified in two independent experiments (tTab2.1 PD vs. tTab2.2 PD) using GST-tandem-Tab2 for pull-down of proteins from U937 cellular extracts. As negative control, proteins identified in a pull-down experiment using tandem-Tab2 without incubation with U937 cellular extracts are depicted as well (tTab2.1 –PD). In the second tandem-Tab2 PD sample, more proteins were identified due to larger input of U937 extracts. The overlap between the two experiments (excluding proteins identified in the negative sample as well) was more than 90% (67/74), based on the first experiment with less proteins identified. **B.** Comparison of proteins identified in the pull-down samples of GST-tandem-Tab2 (experiment 2: see figure 7.4A), GST, GST-Mud1, GST-Rap80. The unique proteins included in this analysis were devoid of the proteins that overlapped with proteins identified in the negative control sample per condition (pull-down samples without U937 cellular extracts). The proteins in the different groups are listed in table 7.1B, excluding the proteins that were identified in the GST-pull-down.

of GST, Mud1, Rap80 and tandem-Tab2 (of the larger input experiment) (figure 7.4B, table 7.1B). Among the isolated proteins E3 ubiquitin ligases and proteasome subunits were identified, representing enrichment of the ubiquitin system.

*Identification of diG-peptides of proteins isolated by GST-tandem-Tab2*

In the mass spectrometric analysis of the pull-down samples, no diG-peptides representing modified lysines were found, except for internal ubiquitin linkages (data not shown). Recently, a novel method has been described to enhance the detection of diG-peptides by performing immunoprecipitation (IP) on trypsin digested peptides using a diG-specific antibody[26,27]. To test whether this method would enhance the identification of diG-peptides following isolation of ubiquitinated peptides using GST-UBDs, we performed a diG-IP after tandem-Tab2 pull-down of U937 cellular extracts. The isolated peptides were identified using tandem-MS in an identical fashion as the previous experiment.

The identified peptides are shown in table 7.1C. Although peptides representing internal ubiquitin linkages were abundant, only few diG-modified peptides of other proteins were identified. The proteins to which these peptides belonged were identified in the mass spectrometry analysis of the tandem-Tab2 pull-down before diG-IP as well.

**Table 7.1: Identified proteins by MS analysis of GST-UBD pull-down with U937 cellular extracts**

**A.** Number of proteins identified*

| | GST | GST-Mud1 | GST-Rap80 | GST-Tab2 | GST-tandem Tab2 |
|---|---|---|---|---|---|
| **unique proteins** | 48 | 52 | 43 | 41 | 75 |

*Proteins identified in pull-down samples with U937 cellular extracts, devoid of proteins identified in the negative control of the UBD without cellular extracts.

**B.** Unique proteins identified in specified pull-down samples (related to figure 7.4B)

| **Mud1+Rap80+ tandem-Tab2** | **Rap80+ tandem-Tab2** | **Mud1** | **Tandem-Tab2** | | | | |
|---|---|---|---|---|---|---|---|
| UBC | HSPH1 | KCNAB2 | **RNF126** | SLC25A5 | ASNA1 | SNRNP200 | TCP1 |
| ATP5A1 | RASAL3 | DDX18 | **BFAR** | SLC25A6 | WBP2 | LGALS9 | NOP56 |
| LSP1 | MYO1C | TOMM34 | **UBE3A** | VCP | ATP1A1 | HLTF | KEAP1 |
| ACTN4 | | CORO6 | **AMFR** | HIST1H2BE | KRT78 | LMNA | TOP2B |
| CLTC | | DLTS | **RFWD3** | HIST1H3D | SCAMP3 | PTDSS1 | MFN1 |
| | | CECR1 | **UBR4** | CLINT1 | AHCY | LBR | ESYT2 |
| | | ANPEP | **HUWE1** | DCD | ATAD3A | EIF2S3 | CAD |
| **Mud1+ tandem-Tab2** | | KRT33B | **CUL1** | HSPA1L | COMMD9 | PARP14 | XPO1 |
| | | | **cIAP1*** | MYADM | FARSA | LPCAT1 | ACLY |
| **RLIM** | | **Rap80** | PSMA4 | C20orf4 | IMPDH2 | MCM6 | LARS |
| **RNF115** | | CBR1 | PSMD7 | FADS2 | TMEM201 | ANXA2 | FANCI |
| **UBR5** | | HBB | PSMC2 | DHCR7 | SLC1A5 | EIF4A2 | TRPM2 |
| PSMC1 | | APOA1 | PSMC3 | NAP1L1 | CCRN4Lp | PTOV1 | ALB |
| PKM2 | | TF | PSMD11 | ERLIN1 | HADHB | PARP1 | SURF4 |
| CORO1A | | PLK1 | PSMD5 | RPL30 | PDK1 | PRPF8 | DIABLO |
| HSPA5 | | SERPINA1 | PSMD2 | ATP5B | LONP2 | UBA1 | PABPC1 |
| BAG6 | | GSN | PSMD3 | S100A9 | RPN2 | SUPT16H | NAP1L4 |
| SQSTM1 | | | PSMD1 | RPL11 | TRRAP | SHMT2 | LMNB1 |
| CCT7 | | | PSMC5 | HSP90AB1 | CYHR1 | KLHL12 | RPN1 |
| | | | HIST1H1E | NASP | PABPC4 | FAR1 | PARP4 |
| | | | HIST1H1B | CLEC2B | HSPA8 | SLC12A9 | RBM14- |
| | | | | | SLC25A3 | VPS13C | RBM4 |

Grey colored, underlined protein: ubiquitin;
Bold, underlined proteins: E3 ligases;
Underlined proteins: 26S proteasome subunits;
*cIAP1 is a described target for K63-linked ubiquitination[31].

**C:** Identified unique diG-peptides by tandem-Tab2 pull-down and diG-IP

| protein | diG-peptide* |
|---|---|
| Ubiquitin K6 | 1-MQIFV*K*TLTGK-11 |
| Ubiquitin K11 | 7-TLTG*K*TITLEVEPSDTIENVK-27 |
| Ubiquitin K11 | 7-TLTG*K*TITLEVEPSDTIENVKAK-29 |
| Ubiquitin K29 | 28-A*K*IQDKEGIPPDQQR-42 |
| Ubiquitin K48 | 43-LIFAG*K*QLEDGR-54 |
| Ubiquitin K48 | 43-LIFAG*K*QLEDGRTLSDYNIQK-63 |
| Ubiquitin K63 | 55-TLSDYNIQ*K*ESTLHLVLR-72 |
| Ubiquitin-40S ribosomal protein S27a precursor (outside ubiquitin peptide sequence) | 105-YYKVDENG*K*ISR-116 |
| Tubulin alpha-1C chain | 157-LSVDYG*K*K-164 |
| ADP/ATP translocase 2 | 141-LAADVG*K*AGAER-152 |
| Histone cluster 1, H2aj | 101-VTIAQGGVLPNIQAVLLP*K*K-120 |
| Histone H2B type 1-C/E/F/G/I | 118-AVT*K*YTSSK-126 |

*The position of the diG-peptide within the corresponding protein is indicated by the flanking numbers and the modified K is indicated by underlined italics.

## Discussion

To study the role of K63-linked ubiquitin chains in different cellular processes, knowledge on the modified substrates is needed. In this chapter we show that GST-UBD fusion proteins can be used to isolate endogenous proteins modified with K63-linked ubiquitin chains. For the isolation of K63-linked ubiquitin chains, the UBDs of Tab2 and Rap80 were used. The UBD of Mud1, which shows specific binding to K48-linked chains, served as a control. Pull-down experiments with commercially available synthetic ubiquitin chains confirmed the specificity of the different UBDs as described before (Tab2, Rap80: K63 chains, Mud1: K48 chains, figure 7.1)[15-19]. Binding of ubiquitinated proteins was greatly enhanced using a fusion protein of two Tab2-NZF domains interspersed with a 6-amino acid linker, compared to the single domain (figure 7.1 and 7.2A).

Tandem-Tab2 GST-pull-downs with U937 cellular extracts resulted in the highest efficiency to isolate proteins modified with K63-ubiquitin chains (figure 7.2B), compared to the other domains tested. However, Western blot analysis using K11- and K48-linkage specific ubiquitin antibodies revealed the presence of these chains as well in tandem-Tab2 pull-down samples. Comparing different antibody signals is not feasible for the absolute quantification of the abundance of different chains. To study the specificity of tandem-Tab2 to pull-down proteins modified with K63-linked ubiquitin chains, we overexpressed tagged ubiquitin mutants lacking one lysine. Although tandem-Tab2

showed binding to ubiquitin chains containing K63R mutants, it showed less affinity to chains composed of this mutant compared to K11R and K48R mutants. This confirmed that tandem-Tab2 shows the highest affinity for K63-linked ubiquitin chains (figure 7.3). The residual binding of tandem-Tab2 to K63R ubiquitin mutants could be explained by non-specific binding of tandem-Tab2 to other chain conformations. Alternatively, a K63R mutant ubiquitin moiety could be incorporated in a K63-linked chain being the terminal ubiquitin. Such a chain would still be isolated by tandem-Tab2. Yet another possibility is the binding of tandem-Tab2 to proteins that are simultaneously modified with multiple ubiquitin chains of different chain conformations, of which one is wildtype K63-linked and the other chain includes the tagged K63R mutant.

Quantitative mass spectrometry using heavy labeled standards of internal ubiquitin linkages should be performed to absolutely quantify the specificity of the UBDs for different ubiquitin chains coupled to cellular proteins. Preliminary experiments in our laboratory showed that the linear dynamic range of detection of the heavy labeled peptide representing the K63-diG linkage was poor with a high limit of detection. In the mass spectrometry analyses of the different pull-down samples, the K63 diG-peptide signal did not reach the limit of detection, which made absolute quantification unreliable (data not shown).

Recent data have described the importance of the linker between UBDs for avidity and specificity of ubiquitin binding[18,28]. This was shown for tandem-UIMs (including the UIMs of Rap80) which use the two UIMs for binding of one K63-linkage. The linker orients the two domains in a structural conformation for binding of the ubiquitin-linkage. Hence the composition and length of this linker determines the avidity and specificity towards K63-linked ubiquitin chains. Although the Tab2 NZF-UBD binds one K63-linkage by itself, the nature of the linker in the tandem-Tab2 protein might be of importance to enhance conformational orientation for binding of two consecutive K63-linkages within one chain. Future research should therefore be directed at optimizing linker composition and length.

Tab2 and tandem-Tab2 NZF-domains interacted with K11 di-ubiquitin, which has not been reported previously. Full-length Tab2 is involved in NF-κB activation, mediating downstream signaling upon binding to K63-ubiquitinated RIP1[17]. Recently, it has been shown that RIP1 is modified with K11-chains during NF-κB signaling as well. NEMO showed affinity for these chains and thereby might regulate downstream signaling[29]. However, Tab2 binding to K11-linked chains was not addressed. Based on our results, it would be interesting to test whether Tab2 binding to K11-linked chains is also involved in regulating NF-κB signaling.

The MS analysis of the isolated proteins in the pull-down samples identified many common and unique proteins in the different UBD pull-downs. Among the identified proteins, several proteasome subunits and E3 ligases were present, indicating enrichment of the ubiquitin system. It was remarkable to find many proteasome

subunits in the pull-down using the K63-linkage specific tandem-Tab2. Although mono-ubiquitination has been identified on proteasomal subunits, K63-linked chains have not been reported[30]. One of the isolated E3 ligases, cIAP1 is believed to be a substrate for K63-linked ubiquitination[31], which validates that the used approach can indeed isolate K63-substrates.

The pull-down experiments described here were performed under conditions with a relatively high concentration of the denaturing agent DTT (5 mM). However, complete elimination of non-covalent protein-protein interactions was likely not achieved. Therefore, proof of the ubiquitination status of the isolated proteins was needed to reliably conclude that they were ubiquitinated. In the MS analyses of the total trypsin digested samples of the different pull-down samples, no diG-peptides of proteins other than ubiquitin were identified. To enrich for the diG-peptides, a tandem-Tab2 pull-down sample of U937 cellular extracts was immunoprecipitated using a diG-specific antibody following trypsin digestion. The subsequent mass spectrometry analysis only identified few ubiquitinated peptides, including histone H2A and H2B. Remarkably, these two proteins are abundantly modified with mono-ubiquitin in cells[32], although H2A poly-ubiquitination with K63-linked chains has been described during DNA damage repair[33,34]. Previous reports have demonstrated poor affinity of Tab2 to mono-ubiquitin[15,16]. Also in the experiments described here, we did not observe binding of tandem-Tab2 to mono-ubiquitin (notice the lack of free ubiquitin pools in tandem-Tab2 pull-down samples, figure 7.3). It would therefore be interesting to study whether H2A and H2B are modified with ubiquitin chains in non-stressed conditions as well. The described method in this chapter is a promising new technique to isolate K63-linked ubiquitination substrates, although further optimization is required to enhance the identification of isolated substrates.



**Acknowledgements**

The authors thank Lieke Egbers and Erik Dullink for help with the GST-purifications.

## Reference List


1. Marteijn,J.A., Jansen,J.H., & van der Reijden,B.A. Ubiquitylation in normal and malignant hematopoiesis: novel therapeutic targets. *Leukemia* **20**, 1511-1518 (2006).
2. Ikeda,F. & Dikic,I. Atypical ubiquitin chains: new molecular signals. 'Protein Modifications: Beyond the Usual Suspects' review series. *EMBO Rep.* **9**, 536-542 (2008).
3. Haglund,K. & Dikic,I. Ubiquitylation and cell signaling. *EMBO J.* **24**, 3353-3359 (2005).
4. Chen,Z.J. & Sun,L.J. Nonproteolytic functions of ubiquitin in cell signaling. *Mol. Cell* **33**, 275-286 (2009).
5. Andersen,P.L. *et al.* Distinct regulation of Ubc13 functions by the two ubiquitin-conjugating enzyme variants Mms2 and Uev1A. *J. Cell Biol.* **170**, 745-755 (2005).
6. Hofmann,R.M. & Pickart,C.M. Noncanonical MMS2-encoded ubiquitin-conjugating enzyme functions in assembly of novel polyubiquitin chains for DNA repair. *Cell* **96**, 645-653 (1999).
7. Wu,X., Yamamoto,M., Akira,S., & Sun,S.C. Regulation of hematopoiesis by the K63-specific ubiquitin-conjugating enzyme Ubc13. *Proc. Natl. Acad. Sci. U.S.A* **106**, 20836-20841 (2009).
8. Kirkpatrick,D.S., Denison,C., & Gygi,S.P. Weighing in on ubiquitin: the expanding role of mass-spectrometry-based proteomics. *Nat. Cell Biol.* **7**, 750-757 (2005).
9. Xu,P. *et al.* Quantitative proteomics reveals the function of unconventional ubiquitin chains in proteasomal degradation. *Cell* **137**, 133-145 (2009).
10. Danielsen,J.M. *et al.* Mass spectrometric analysis of lysine ubiquitylation reveals promiscuity at site level. *Mol. Cell Proteomics.* **10**, M110 (2011).
11. Kaiser,S.E. *et al.* Protein standard absolute quantification (PSAQ) method for the measurement of cellular ubiquitin pools. *Nat. Methods* **8**, 691-696 (2011).
12. Dikic,I., Wakatsuki,S., & Walters,K.J. Ubiquitin-binding domains - from structures to functions. *Nat. Rev. Mol. Cell Biol.* **10**, 659-671 (2009).
13. Komander,D. *et al.* Molecular discrimination of structurally equivalent Lys 63-linked and linear polyubiquitin chains. *EMBO Rep.* **10**, 466-473 (2009).
14. Raasi,S., Varadan,R., Fushman,D., & Pickart,C.M. Diverse polyubiquitin interaction properties of ubiquitin-associated domains. *Nat. Struct. Mol. Biol.* **12**, 708-714 (2005).
15. Kulathu,Y., Akutsu,M., Bremm,A., Hofmann,K., & Komander,D. Two-sided ubiquitin binding explains specificity of the TAB2 NZF domain. *Nat. Struct. Mol. Biol.* **16**, 1328-1330 (2009).
16. Sato,Y., Yoshikawa,A., Yamashita,M., Yamagata,A., & Fukai,S. Structural basis for specific recognition of Lys 63-linked polyubiquitin chains by NZF domains of TAB2 and TAB3. *EMBO J.* **28**, 3903-3909 (2009).
17. Sato,Y. *et al.* Structural basis for specific recognition of Lys 63-linked polyubiquitin chains by tandem UIMs of RAP80. *EMBO J.* **28**, 2461-2468 (2009).
18. Sims,J.J. & Cohen,R.E. Linkage-specific avidity defines the lysine 63-linked polyubiquitin-binding preference of rap80. *Mol. Cell* **33**, 775-783 (2009).
19. Trempe,J.F. *et al.* Mechanism of Lys48-linked polyubiquitin chain recognition by the Mud1 UBA domain. *EMBO J.* **24**, 3178-3189 (2005).
20. Yan,J. *et al.* Ubiquitin-interaction motifs of RAP80 are critical in its regulation of estrogen receptor alpha. *Nucleic Acids Res.* **35**, 1673-1686 (2007).
21. Candiano,G. *et al.* Blue silver: a very sensitive colloidal Coomassie G-250 staining for proteome analysis. *Electrophoresis* **25**, 1327-1333 (2004).
22. Rappsilber,J., Ishihama,Y., & Mann,M. Stop and go extraction tips for matrix-assisted laser desorption/ionization, nanoelectrospray, and LC/MS sample pretreatment in proteomics. *Anal. Chem.* **75**, 663-670 (2003).
23. Wessels,H.J., Gloerich,J., van der Biezen.E., Jetten,M.S., & Kartal,B. Liquid chromatography-

mass spectrometry-based proteomics of Nitrosomonas. *Methods Enzymol.* **486**, 465-482 (2011).
24. Weatherly,D.B. *et al.* A Heuristic method for assigning a false-discovery rate for protein identifications from Mascot database search results. *Mol. Cell Proteomics.* **4**, 762-772 (2005).
25. Ishihama,Y. *et al.* Exponentially modified protein abundance index (emPAI) for estimation of absolute protein amount in proteomics by the number of sequenced peptides per protein. *Mol. Cell Proteomics.* **4**, 1265-1272 (2005).
26. Kim,W. *et al.* Systematic and quantitative assessment of the ubiquitin-modified proteome. *Mol. Cell* **44**, 325-340 (2011).
27. Xu,G., Paige,J.S., & Jaffrey,S.R. Global analysis of lysine ubiquitination by ubiquitin remnant immunoaffinity profiling. *Nat. Biotechnol.* **28**, 868-873 (2010).
28. Sims,J.J. *et al.* Polyubiquitin-sensor proteins reveal localization and linkage-type dependence of cellular ubiquitin signaling. *Nat. Methods* **9**, 303-309 (2012).
29. Dynek,J.N. *et al.* c-IAP1 and UbcH5 promote K11-linked polyubiquitination of RIP1 in TNF signalling. *EMBO J.* **29**, 4198-4209 (2010).
30. Weissman,A.M., Shabek,N., & Ciechanover,A. The predator becomes the prey: regulating the ubiquitin system by ubiquitylation and degradation. *Nat. Rev. Mol. Cell Biol.* **12**, 605-620 (2011).
31. Vallabhapurapu,S. *et al.* Nonredundant and complementary functions of TRAF2 and TRAF3 in a ubiquitination cascade that activates NIK-dependent alternative NF-kappaB signaling. *Nat. Immunol.* **9**, 1364-1370 (2008).
32. Weake,V.M. & Workman,J.L. Histone ubiquitination: triggering gene activity. *Mol. Cell* **29**, 653-663 (2008).
33. Doil,C. *et al.* RNF168 binds and amplifies ubiquitin conjugates on damaged chromosomes to allow accumulation of repair proteins. *Cell* **136**, 435-446 (2009).
34. Stewart,G.S. *et al.* The RIDDLE syndrome protein mediates a ubiquitin-dependent signaling cascade at sites of DNA damage. *Cell* **136**, 420-434 (2009).

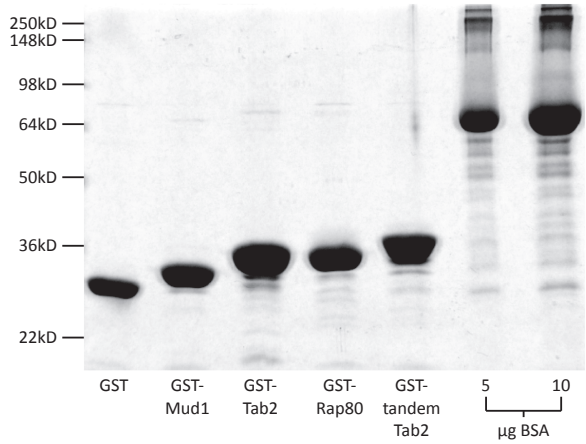


**Supplemental figure 7.1: Purity of GST-UBD fusion proteins**
GST-UBD fusion proteins were expressed in E.Coli and purified according to the materials and methods section. 2 µL of GST-fusion proteins coupled to glutathione beads were separated on 10% SDS-PAGE gels. Proteins were visualized by Colloidal Coomassie blue staining. Aspecific binding of E.Coli proteins to the beads was very limited, and per µL beads, approximately 5µg GST-fusion was bound (compared to BSA lanes).

# General discussion & Future directions

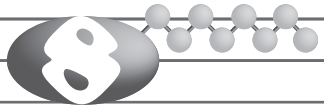

## Thesis objective

The posttranslational modification of cellular proteins with single ubiquitin moieties or poly-ubiquitin chains plays an important regulatory role in many biological processes. Also in hematopoiesis, ubiquitination plays multiple roles, for example in regulating transcription factor stability and immune responses. The objective of this thesis was to extend the knowledge on the role of ubiquitination in normal and malignant hematopoiesis. To achieve this, global top down and dedicated bottom up approaches were followed. On the one hand we focused on altered gene expression of proteins involved in ubiquitination in acute myeloid leukemia (AML) and breast cancer. Chapters three to five describe the results of these studies, identifying correlations of *BRE* expression with disease outcome in AML and breast cancer. On the other hand, studies were directed at substrate identification. The importance of the E2 conjugating enzyme UBC13 for normal hematopoiesis served as a starting point to study its contribution to myeloid differentiation (chapter six) and to identify proteins that are ubiquitinated with UBC13-dependent K63-linked ubiquitin chains (chapter seven).

## The strength of outlier analysis

Chapters three to five describe the prognostic value of gene expression differences of the BRCA1-associated protein BRE in AML and breast cancer. This gene was identified via a gene expression outlier analysis in AML. In this analysis, genes were identified that were differentially expressed in a subgroup of the total AML cohort. The cut-off for outlier expression was defined as four times the standard deviation above or below the mean of the total cohort. The strength of this analysis lies in its unsupervised approach: it identifies genes that show deregulated expression in a small subset of patients, without bias of defining subsets before analysis (*e.g.* based on clinico-pathological factors). The disease outcome of the patients with outlier expression was compared to the remaining patients to identify correlations of outlier expression with outcome. Another frequently used approach to identify correlations between gene expression and disease outcome is the univariate Cox regression analysis. However, as outlier expression often occurs in small subsets of patients, the analysis of gradual expression differences by the Cox regression analysis will likely not identify prognostic correlations of the outlier genes, because statistical power of many samples that correlate with disease outcome is lacking for these genes. The application of outlier analysis has been useful in other types of cancer as well. A well known example is the identification of outlier expression of *ERG* and *ETV1* in prostate cancer, which led to the discovery of a frequent chromosomal translocation in this cancer type[1].

The outlier analysis we performed identified other genes apart from *BRE*, including *EVI1*. High expression of this gene is a known poor prognostic marker in

AML. Deregulated expression of this gene was identified twenty years ago as a result of chromosome 3q aberrations[2]. Since then it has become clear that this chromosomal aberration occurs in only 50% of the high *EVI1* expressing cases. In chapter four, we showed that high *EVI1* expression not resulting from 3q aberrations co-occurred with t(9;11) translocations which encode the *MLL-AF9* fusion protein. High *BRE* expression also co-occurred with *MLL-AF9*. By comparing *EVI1* and *BRE* expression levels in *MLL-AF9* samples, we observed mutual exclusive expression of the two genes. The *MLL-AF9* positive samples with high *BRE* expression showed similar global expression profiles, unlike the high *EVI1* expressing samples that only showed modest similarities in expression profiles. This led to the conclusion that *MLL-AF9* by itself likely does not provoke global expression changes. In combination with the observation that two known target genes of *MLL-AF9* - *MEIS1* and *HOXA9*[3] - were not expressed inextricably at a high level in individual *MLL-AF9* positive AML patients, this indicates that regulation of gene expression in *MLL-AF9* positive leukemia's might rely on additional cofactors or cellular differentiation state.

In this thesis, we applied outlier expression analysis on ubiquitin-related genes, as the regulatory role of ubiquitination in malignant hematopoiesis was the focus of our research. Approximately 1,600 genes which were functionally or structurally linked to ubiquitination were included in our study. These genes were represented by 2,890 probesets on the Affymetrix HG133 plus 2.0 array: approximately 5% of the total number of probesets. Performing outlier analysis on the remaining 95% will likely result in the identification of additional novel prognostic markers.

## *BRE* as a novel cancer-related gene

*BRE* expression correlated with disease outcome in AML and breast cancer. Yet, differences were observed between both cancer types. In AML, *BRE* was highly expressed in a small subset of patients, while in breast cancer there was a gradual expression distribution. Furthermore, high *BRE* expression in non-radiotherapy treated breast cancer patients predicted an adverse disease outcome, which was opposite to the effect observed in AML and radiotherapy treated breast cancer patients. Interestingly, the two latter patient groups received therapy that induces DNA double strand breaks: radiotherapy for breast cancer patients and high doses of topoisomerase II inhibitors (*e.g.* idarubucin and etoposide) for AML patients. Given the role of BRE in DNA double strand break repair, it is tempting to speculate that BRE is involved in therapy responses. Before studying this hypothesis, it is important to confirm the gene expression differences at the protein level. Several antibodies directed against BRE were tested in our laboratory, however none of them yielded reliable results in overexpression experiments. Therefore, we have not been able yet to validate the high *BRE* expression at the protein level in patients samples.

The function of BRE as enhancer of DNA double strand break repair seems contradictory to the favorable prognostic effect observed in patients treated with DNA damage inducing agents: one might expect that high *BRE* expression causes cellular resistance to radiotherapy and DNA damage inducing chemotherapy, thereby adversely affecting disease outcome. Indeed, BRE depletion renders cells more susceptible to radiotherapy induced cell death in several cell line models[4,5]. Similar unexplained contradictory data have been described for other DNA damage repair factors, such as the Mre11/Rad50/Nbs1 complex, BRCA1 and ATM[6-13]. The data presented in this thesis warrant further studies on the role of BRE in therapy responses to better understand the double-faced characteristics of BRE.

The failure of proper DNA damage repair can lead to loss of chromosomal integrity and consequently to malignant transformation. Given its role in the DNA repair pathway, BRE might therefore also function in cancer predisposition and/or cancer development. Furthermore, BRE also functions in death receptor mediated apoptosis[14]. Research on the role of BRE in malignant transformation onset and development is therefore needed, which should focus both on DNA damage repair and apoptosis.

## Expression regulation of the *BRE* chromosomal locus

Another interesting observation made in this thesis is the co-expression of *RBKS* and *MRPL33* with high *BRE* expression in AML (figure 3.4). The three genes are clustered on chromosome two: *MRPL33* and *BRE* are oriented in the same direction, while *RBKS* is located in between the other two genes on the opposite strand (figure 8.1). The genes may share common enhancer elements causing co-expression, potentially mediated through three-dimensional chromosomal conformations. Experiments that can detect 3D DNA configurations are therefore needed to determine whether the co-expression of the genes is caused by shared common regulatory elements.

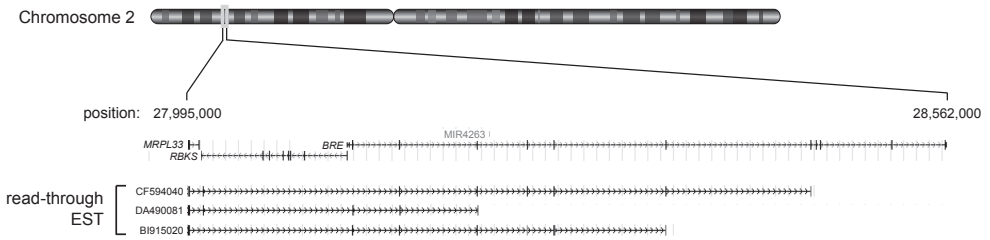


**Figure 8.1: Read-through transcripts of *BRE***
The upper part of the graph represents the locus of the *MRPL33*, *RBKS* and *BRE* genes on chromosome 2. *MRPL33* and *BRE* are sense oriented and *RBKS* antisense. The lower part of the graph represents examples of expressed sequence tags (ESTs) showing read-through from *MRPL33* to *BRE*. Currently, 10 cases of *MRPL33-BRE* read-through ESTs have been reported in the UCSC database.

By analyzing expressed sequence tags (ESTs) of *BRE*, we observed ESTs that showed read-through from *MRPL33* to *BRE* (figure 8.1). The development of deep-sequencing techniques has enabled the identification of read-through in cancer samples[15,16], and might therefore be used in studying the read-through in high *BRE* expressing patients. Preliminary PCR results in our lab confirmed *MRPL33-BRE* read-through in several AML samples. It will be interesting to determine whether this read-through is specific for AML and other cancer types compared to normal tissue and if so, what the biological role of the *MRPL33-BRE* transcripts is. However, it is unlikely that this read-through is causing the high expression of the three genes, as the transcript does not include the antisense oriented *RBKS* gene. Studying the chromosomal composition of the *BRE* locus also revealed the presence of a microRNA in an intronic region of *BRE* (MIR4263, figure 8.1). Although experimental data on this microRNA are lacking, it is known that deregulated expression of microRNAs can contribute to the pathogenesis of cancer[17]. Therefore, determining the expression of microRNA 4263 in normal versus high *BRE* expressing samples is interesting.

## K63-linked ubiquitination in hematopoiesis

The regulatory role of K63-linked ubiquitin chains has been established in several important cellular pathways, such as DNA damage repair and NF-κB signaling. K63-linked chains are formed to mediate signaling pathways by serving as docking sites for protein complex formation, thereby stimulating downstream pathways. Tissue specific knockout of the K63-specific E2 conjugating enzyme UBC13 resulted in apoptosis of hematopoietic stem cells and early progenitors in mice. This caused a reduction of white blood cell numbers, including monocytes. In chapter six of this thesis, we studied whether UBC13 depletion affects human myeloid differentiation. Its downregulation during differentiation and the decreased differentiation capacity of *UBC13*-silenced U937 cells suggest a functional role for UBC13 during myeloid differentiation. These data imply that high levels of UBC13 are needed to enable the onset of differentiation. NF-κB and MAP kinase pathways are necessary for proper U937 differentiation[18-21]. Given the role for UBC13 in these pathways, it was unexpected that *UBC13* silencing did not phenocopy the inhibition of NF-κB or MAP kinase pathways: inhibition of NF-κB and MAP kinase signaling reduces differentiation as well as differentiation-induced apoptosis, while UBC13 depletion only affected differentiation and not apoptosis. This suggests that the role of UBC13 is probably not restricted to the NF-κB and MAP kinase signaling pathways during myeloid differentiation.

To study the exact functional role of UBC13 during myeloid differentiation, it is important to identify the proteins that are differentially modified with K63-ubiquitin chains. In chapter seven we developed a technique to specifically isolate K63-ubiquitinated proteins. This technique is based on the interaction of ubiquitin binding domains

of Tab2 and Rap80 with K63-linked ubiquitin chains. The association of these domains to ubiquitin is relatively weak and short lived, displaying relatively high dissociation constants[22]. To enhance binding, we generated a tandem Tab2-NZF construct, which indeed significantly improved binding efficiency compared to the single Tab2-NZF domain.

The Tab2-NZF domain by itself recognizes a single K63-linkage[23,24]. The increased affinity of a tandem construct might be caused by simultaneous binding of two linkages within one chain. In that view, the linker between the two tandem domains might be of importance to enable the structural conformation for binding two adjacent linkages. Recent data have indeed demonstrated the importance of the linker between K63-specific ubiquitin interacting motifs (UIMs) of Rap80 for binding specificity and affinity[25]. These domains differ from the Tab2-NZF domain as the tandem-UIM is needed for the recognition of a single K63-linkage. Nevertheless, further optimization of the linker in the tandem-Tab2-NZF domain might increase the binding and specificity towards adjacent K63-linkages.

Following isolation of K63-substrates, identification with mass spectrometry yielded information on potential substrates. Currently, it remains difficult to identify true ubiquitinated proteins via mass spectrometry as the abundance of diG-modified peptides is low in complex protein samples. Furthermore, clear ubiquitination consensus sequences are lacking, making it impossible to reliably predict ubiquitination sites[26]. Recent advances in purifying peptides with a ubiquitin remnant after trypsin digestion (via the diG-link) have greatly improved global profiling of ubiquitination[27]. However, this technique requires large amounts of cellular extracts to generate sufficient output. The tandem-Tab2 pull-down we performed prior to diG-IP of modified peptides likely did not provide sufficient input, hence explaining the identification of only few diG-peptides.

A novel technique that might be very helpful in studying ubiquitination is the use of top-down mass spectrometry, which analyzes intact proteins in a tandem-MS fashion. This technique greatly enhances sequence coverage and identification of post-translational modifications[28,29]. Currently, this technique is not widely applied, because improvements need to be made for the analysis of complex biological samples. However, when solved, this technique holds great promise to enhance the detection of post-translational modifications.

## Concluding remarks

The goal of this thesis was to identify novel ubiquitin-regulators during normal and malignant hematopoiesis. On the one hand, research focused on genes and proteins regulating and catalyzing ubiquitination and on the other hand, it focused on substrates of this modification. Ideally, future studies should be directed at combining the two

approaches. For example, deregulated expression of ubiquitin-related genes in AML, as presented in chapter three, could be compared with altered substrate ubiquitination identified via mass spectrometric analyses. Bioinformatic analyses of the combined results could then lead to the identification of novel deregulated pathways in AML mediated via ubiquitination.

The title of this thesis 'Orchestrating the ubiquitin solos in the hematopoietic symphony' might be interpreted as ubiquitin regulating processes on its own. However, I hope it is clear from this thesis that ubiquitin is the ultimate example of a team player: it needs other proteins to exert its function. This resembles the actual symphonic orchestra environment: no solo can exist without the underlying basis of the remaining instruments of the orchestra. This enables a moment of fame for the soloist, needed for symphony progression. Afterwards, the soloist retracts himself into the rest of the orchestra, just like the reversible, time-sensitive nature of ubiquitination. Writing the complete hematopoietic symphony in four years is an impossible task. Therefore, the symphony in this thesis remains an 'Unvollendete Symphonie', with many novel research questions for future orchestrators.

## Reference List


1. Tomlins,S.A. *et al.* Recurrent fusion of TMPRSS2 and ETS transcription factor genes in prostate cancer. *Science* **310**, 644-648 (2005).
2. Morishita,K. *et al.* Activation of EVI1 gene expression in human acute myelogenous leukemias by translocations spanning 300-400 kilobases on chromosome band 3q26. *Proc. Natl. Acad. Sci. U.S.A* **89**, 3937-3941 (1992).
3. Bernt,K.M. *et al.* MLL-rearranged leukemia is dependent on aberrant H3K79 methylation by DOT1L. *Cancer Cell* **20**, 66-78 (2011).
4. Dong,Y. *et al.* Regulation of BRCC, a holoenzyme complex containing BRCA1 and BRCA2, by a signalosome-like subunit and its role in DNA repair. *Mol. Cell* **12**, 1087-1099 (2003).
5. Feng,L., Huang,J., & Chen,J. MERIT40 facilitates BRCA1 localization and DNA damage repair. *Genes Dev.* **23**, 719-728 (2009).
6. Gao,J., Zhang,H., Arbman,G., & Sun,X.F. RAD50/MRE11/NBS1 proteins in relation to tumour development and prognosis in patients with microsatellite stable colorectal cancer. *Histol. Histopathol.* **23**, 1495-1502 (2008).
7. Seol,H.J. *et al.* Prognostic implications of the DNA damage response pathway in glioblastoma. *Oncol. Rep.* **26**, 423-430 (2011).
8. Soderlund,K. *et al.* Intact Mre11/Rad50/Nbs1 complex predicts good response to radiotherapy in early breast cancer. *Int. J. Radiat. Oncol. Biol. Phys.* **68**, 50-58 (2007).
9. Ye,C. *et al.* Expression patterns of the ATM gene in mammary tissues and their associations with breast cancer survival. *Cancer* **109**, 1729-1735 (2007).
10. Rakha,E.A. *et al.* Expression of BRCA1 protein in breast cancer and its prognostic significance. *Hum. Pathol.* **39**, 857-865 (2008).
11. Seery,L.T. *et al.* BRCA1 expression levels predict distant metastasis of sporadic breast cancers. *Int. J. Cancer* **84**, 258-262 (1999).
12. Taylor,J. *et al.* An important role for BRCA1 in breast cancer progression is indicated by its loss in a large proportion of non-familial breast cancers. *Int. J. Cancer* **79**, 334-342 (1998).
13. Yang,Q. *et al.* Prognostic significance of BRCA1 expression in Japanese sporadic breast carcinomas. *Cancer* **92**, 54-60 (2001).
14. Li,Q. *et al.* A death receptor-associated anti-apoptotic protein, BRE, inhibits mitochondrial apoptotic pathway. *J. Biol. Chem.* **279**, 52106-52116 (2004).
15. Maher,C.A. *et al.* Transcriptome sequencing to detect gene fusions in cancer. *Nature* **458**, 97-101 (2009).
16. Maher,C.A. *et al.* Chimeric transcript discovery by paired-end transcriptome sequencing. *Proc. Natl. Acad. Sci. U.S.A* **106**, 12353-12358 (2009).
17. Croce,C.M. Causes and consequences of microRNA dysregulation in cancer. *Nat. Rev. Genet.* **10**, 704-714 (2009).
18. Dai,Y., Rahmani,M., & Grant,S. An intact NF-kappaB pathway is required for histone deacetylase inhibitor-induced G1 arrest and maturation in U937 human myeloid leukemia cells. *Cell Cycle* **2**, 467-472 (2003).
19. Garcia,A. *et al.* Differential effect on U937 cell differentiation by targeting transcriptional factors implicated in tissue- or stage-specific induced integrin expression. *Exp. Hematol.* **27**, 353-364 (1999).
20. Miranda,M.B., McGuire,T.F., & Johnson,D.E. Importance of MEK-1/-2 signaling in monocytic and granulocytic differentiation of myeloid cell lines. *Leukemia* **16**, 683-692 (2002).
21. Pennington,K.N., Taylor,J.A., Bren,G.D., & Paya,C.V. IkappaB kinase-dependent chronic activation of NF-kappaB is necessary for p21(WAF1/Cip1) inhibition of differentiation-induced apop-

tosis of monocytes. *Mol. Cell Biol.* **21**, 1930-1941 (2001).
22. Grabbe,C. & Dikic,I. Functional roles of ubiquitin-like domain (ULD) and ubiquitin-binding domain (UBD) containing proteins. *Chem. Rev.* **109**, 1481-1494 (2009).
23. Kulathu,Y., Akutsu,M., Bremm,A., Hofmann,K., & Komander,D. Two-sided ubiquitin binding explains specificity of the TAB2 NZF domain. *Nat. Struct. Mol. Biol.* **16**, 1328-1330 (2009).
24. Sato,Y., Yoshikawa,A., Yamashita,M., Yamagata,A., & Fukai,S. Structural basis for specific recognition of Lys 63-linked polyubiquitin chains by NZF domains of TAB2 and TAB3. *EMBO J.* **28**, 3903-3909 (2009).
25. Sims,J.J. *et al.* Polyubiquitin-sensor proteins reveal localization and linkage-type dependence of cellular ubiquitin signaling. *Nat. Methods* **9**, 303-309 (2012).
26. Shi,Y., Xu,P., & Qin,J. Ubiquitinated proteome: ready for global? *Mol. Cell Proteomics.* **10**, R110 (2011).
27. Kim,W. *et al.* Systematic and quantitative assessment of the ubiquitin-modified proteome. *Mol. Cell* **44**, 325-340 (2011).
28. Siuti,N. & Kelleher,N.L. Decoding protein modifications using top-down mass spectrometry. *Nat. Methods* **4**, 817-821 (2007).
29. Chait,B.T. Chemistry. Mass spectrometry: bottom-up or top-down? *Science* **314**, 65-66 (2006).

## Summary

Over the past ten years, multiple roles of ubiquitination have been described in the field of hematopoiesis. For example, the post-translational modification of important transcription factors with K48-linked ubiquitin chains regulates their proteasomal degradation during blood cell differentiation. In contrast, K63-linked chains are important activating regulators of immune responses and DNA damage responses. Aberrations of factors catalyzing ubiquitination have been identified in several types of leukemia and other hematopoietic malignancies. This made the ubiquitin proteasome system an interesting subject for novel targeted therapies, as discussed in **chapter 1**. This thesis describes several top down and bottom up studies, focusing on both the ubiquitination machinery and its substrates in normal and malignant hematopoiesis.

Acute Myeloid Leukemia is the most frequent type of acute leukemia in adults. The current five year overall survival is only 40%. Although many recurrent genetic aberrations correlate with disease outcome, the survival of patients within genetically defined subgroups still shows large variation. Therefore, novel prognostic markers are invaluable for improved classification and treatment decisions.

Full knowledge on clinico-pathological factors is needed when studying correlations of novel factors such as gene expression with disease outcome. Hence, fast and efficient screening methods are needed to rapidly identify clinico-pathological factors in large cohorts. **Chapter 2** governs the application of High Resolution Melting (HRM) analysis as a fast and cost-effective technique for screening of the recently discovered *IDH1* and *IDH2* mutations in AML. HRM utilizes the dissociation behavior of double stranded DNA fragments. Small differences within PCR products, such as deletions or duplications of a few bases, or even single nucleotide substitutions can be readily identified. Indeed, HRM analysis was a reliable technique for hotspot *IDH1* and *IDH2* mutation screening, with no false negative results and only a small percentage of false positive results. The combination of the closed post-PCR HRM technique with confirmation of only mutation variants by Sanger sequencing is a reliable, cost-effective and fast alternative compared to sequence analysis of all samples, especially when large patient cohorts need to be screened.

In **chapter 3**, we performed a study to identify deregulated expression of genes involved in ubiquitination with concomitant predictive value for disease outcome in AML. Via a so-called 'outlier analysis' we identified deregulated *BRE* expression in a subset of AML patients with favorable prognosis. This gene encodes a member of the BRCA1 E3 ligase complex, involved in DNA damage repair. High *BRE* expression co-occurred strongly with a myelomonocytic morphology (FAB M5) and *MLL-AF9* translocations. *MLL-AF9* positive patients are currently classified as intermediate risk. Especially among these patients, high *BRE* expression predicted a very good prognosis, in contrast to normal *BRE* expression, which predicted a very poor prognosis.

Global expression profiling showed that AML samples with high *BRE* expression were almost completely confined to a previously uncharacterized cluster with similar expression profiles. These data suggest that these patients share an underlying mechanism that influences global gene expression. The presence of the *MLL-AF9* translocation may not be the underlying cause, as its co-occurrence with the novel expression profile was only partial. Indeed, **chapter 4** describes data indicating that there are at least two different subtypes of *MLL-AF9* positive AML cases, one characterized by high *BRE* expression and the other characterized by high *EVI1* expression, a poor prognostic marker for AML. The high expression of these two genes was mutually exclusive among *MLL-AF9* positive patients, with only few patients showing low expression of both genes. Based on *BRE* and *EVI1* expression, *MLL-AF9* patients could be subdivided into a very good and a very poor prognostic subgroup. Diagnostic screening for the two genes would therefore improve risk stratification. However, *BRE* expression differences between patients with high or normal expression are small and it would be difficult to design a reliable diagnostic tool based on expression of this gene. In contrast, high *EVI1* expressing patients are readily detected by currently used QPCR techniques and diagnostic screening for the combination with *MLL-AF9* is therefore warranted.

The global gene expression profiles of *MLL-AF9* positive patients with high *EVI1* expression did not show strong similarities. These data confirmed the observation that *MLL-AF9* positivity by itself does not provoke global gene expression changes. Moreover, in chapter 4 we showed that even well-studied direct targets of *MLL-AF9* were not necessarily highly expressed in all *MLL-AF9* positive patients. These data indicate that the expression regulation in *MLL-AF9* translocated patients may depend on additional factors, which could differ per patient or alternatively could depend on the leukemia's cell of origin.

BRE is part of the BRCA1 E3 ligase complex, involved in DNA double strand break repair. As BRE depletion attenuates downstream signaling needed for proper DNA repair, BRE is functionally important for this complex. The BRCA1 complex is closely linked to breast cancer development: mutations in BRCA1 itself are a major cause of familial breast cancer. Furthermore, expression alterations, haplotypes or polymorphisms of BRCA1 and other complex members have been implicated in breast cancer susceptibility. In **chapter 5** we therefore questioned whether *BRE* expression had prognostic impact in breast cancer. In a cohort of 229 breast cancer patients, *BRE* expression did not predict disease outcome. However, when the patient cohort was subdivided in radiotherapy treated and non-radiotherapy treated patients, *BRE* expression had prognostic impact in both subsets, albeit with opposite effects. In radiotherapy treated patients, *BRE* expression predicted a favorable prognosis, while in non-radiotherapy treated patients, it predicted an adverse prognosis. Previously reported data showed radio-sensitivity of cell line models depleted for *BRE*. This is contradictory to the observation that high *BRE* expression correlated with a favorable disease outcome

in radiotherapy treated patients. Additional research is therefore needed to study the role of high *BRE* expression in radiotherapy responses in breast cancer.

K63-linked ubiquitin chains are important regulators of signaling pathways such as the NF-κB pathway, which is constitutively activated in AML stem cells. The E2 conjugating enzyme UBC13 is currently the only E2 conjugating enzyme identified with catalytic specificity for K63-ubiquitin chains. Previous research in conditional *Ubc13*$^{-/-}$ mice showed that this protein is crucial for survival of hematopoietic stem cells and early progenitors. The knockout mice died within two weeks after UBC13 depletion, displaying a severe reduction of white blood cells, including monocytes. **Chapter 6** is a result of specific studies on the role of UBC13 in myeloid differentiation using human cell line models. UBC13 appeared to be downregulated during myeloid differentiation of several cell lines. Also UBC13's cofactors MMS2 and UEV1a were downregulated. Silencing of UBC13 diminished PMA-induced monocytic differentiation of U937 myelomonocytic cells, as observed by decreased CD11b expression, while not affecting apoptosis or cell cycle progression. This indicates that UBC13 might be required for differentiation of U937 cells.

To gain better insight in the function of UBC13 during myeloid differentiation, information on the modified substrates is needed. Currently, techniques to isolate endogenous proteins that are ubiquitinated with specific chain conformations are poorly developed. In **chapter 7**, we described a method to isolate K63-ubiquitinated proteins using a tandem repeat of the Tab2-ubiquitin binding domain, which specifically binds to K63-chains. After isolation of the modified proteins, mass spectrometry was used to identify the proteins. Additional research is needed to validate that the identified proteins were modified with K63-linked ubiquitin chains. Furthermore, the mass spectrometric analysis of the captured substrates could be optimized to further enhance the identification of K63-ubiquitinated substrates. When optimized, this technique would be very helpful to better understand the role of K63-linked ubiquitination, for example in UBC13-mediated U937 differentiation.

## Nederlandse samenvatting

Het bloed vormt één van de grootste organen in het lichaam en bestaat uit allerlei typen cellen met allemaal een eigen functie: de rode bloedcellen zorgen voor het zuurstoftransport van de longen naar alle delen van het lichaam, de bloedplaatjes spelen een rol in de bloedstolling bij verwondingen en de verschillende witte bloedcellen zorgen voor afweer tegen ziekteverwekkers. Al deze bloedcellen hebben een beperkte levensduur en daarom is het belangrijk dat er continu nieuwe bloedcellen aangemaakt worden. Er wordt geschat dat *per minuut* ongeveer 350 miljoen nieuwe bloedplaatjes, rode en witte cellen aangemaakt worden. Dit proces vindt plaats in het beenmerg en wordt hematopoëse genoemd. Aan de basis van dit proces staat de hematopoëtische stamcel. Deze stamcel deelt zich asymmetrisch: één van de dochtercellen blijft stamcel (daarmee wordt het totale aantal stamcellen op peil gehouden) terwijl de andere dochtercel zich differentieert (uitrijpt) tot een voorlopercel. Voorlopercellen delen zich veelvuldig en differentiëren uiteindelijk door naar de verschillende rijpe bloedcellen (zie figuur 1.1, blz. 12). De verhouding tussen celdeling en differentiatie is erg belangrijk om een optimale aanmaak van alle volwassen bloedcellen te garanderen. Verstoringen in de hematopoëse kunnen dan ook leiden tot een gebrek of overmaat aan bloedcellen. In ernstige gevallen kunnen verstoringen leiden tot het ontstaan van bloedkanker, ook wel leukemie genoemd.

Bij acute myeloïde leukemie (AML) is het differentiatieproces richting de myeloïde celtypen (zoals monocyten en granulocyten die betrokken zijn bij het niet-specifieke immuunsysteem) verstoord. In AML patiënten verliezen voorlopercellen hun capaciteit om uit te rijpen tot volwassen myeloïde cellen. Deze voorloper cellen hopen zich op in het beenmerg, en later ook in het bloed. In het beenmerg verdringen ze de gezonde cellen, waardoor uiteindelijk de aanmaak van gezonde volwassen bloedcellen verstoord wordt. Mogelijke symptomen van AML hangen hiermee samen: bloedarmoede door een gebrek aan rode bloedcellen, een slechte afweer door een gebrek aan witte bloedcellen en spontane bloedingen door een gebrek aan bloedplaatjes.

Eiwitten zorgen ervoor dat alle processen in een cel goed verlopen. Daarvoor zijn verschillende soorten eiwitten nodig: eiwitten die structuur aan een cel geven, eiwitten die signalen van buiten de cel doorgeven naar het binnenste van de cel, eiwitten die de activiteit van andere eiwitten reguleren, etc. De informatie voor de aanmaak van eiwitten ligt opgeslagen in het DNA van de cel. Door middel van transcriptie en translatie wordt deze informatie per eiwit (een gen) gereguleerd afgeschreven (dit noemen we genexpressie) wat leidt tot de aanmaak van de specifieke eiwitten.

Fouten in het DNA kunnen verkeerde informatie voor de eiwitproductie aan een cel doorgeven, waardoor processen als differentiatie en celdeling verstoord kunnen raken. DNA fouten vormen daarom vaak de oorzaak van AML. Bij deze ziekte komen veel verschillende DNA afwijkingen voor. De specifieke afwijking voorspelt de prognose

van de patiënt, die kan variëren van een voorspelde vijf jaar overleving van minder dan 10% tot meer dan 80%. Echter, een groot gedeelte van de patiënten heeft geen van de bekende DNA afwijkingen. Bovendien varieert de overleving soms drastisch per patiënt binnen een groep patiënten met een bepaalde afwijking. Het is daarom noodzakelijk om het succes op therapie beter te voorspellen per patiënt zodat therapie daarop aangepast kan worden.

In de laatste tien jaar zijn defecten in een belangrijk eiwitregulatie proces - ubiquitinering - ontdekt bij AML (tabel 1.2, blz. 23). Nadat eiwitten aangemaakt zijn, kan de functie nog verder beïnvloed worden. Bijvoorbeeld door een eiwit naar een andere plek in de cel te verplaatsen, de structuur zo te veranderen dat andere eiwitten kunnen binden of door de afbraak te reguleren. Deze processen worden vaak post-translationeel gereguleerd door het betreffende eiwit te markeren met een 'vlaggetje'. Eén van die vlaggetjes is ubiquitine. Dit kleine eiwitje kan aan een andere eiwit gekoppeld worden in de vorm van mono-ubiquitinering. Meerdere ubiquitines kunnen ketens vormen, zodat substraateiwitten ook gemarkeerd kunnen worden met poly-ubiquitine-ketens (zie figuur 1.2, blz. 19). Afhankelijk van het type keten dat gevormd wordt, heeft ubiquitinering van een eiwit verschillende uitkomsten. Ketens die gekoppeld worden via Lysine-48 (K48) van ubiquitine leiden tot afbraak van het gemodificeerde eiwit. Ketens gekoppeld via Lysine-63 (K63) leiden juist niet tot afbraak, maar tot activatie van processen, doordat deze ketens een bindingsplatform vormen voor andere eiwitten die hierdoor gerekruteerd worden en activerende signalen doorgeven.

Duizenden eiwitten spelen een rol in de cel en een groot deel van deze eiwitten wordt geubiquitineerd. Toch is ubiquitinering een uiterst specifiek proces, aangezien de modificatie van al die duizenden eiwitten individueel gereguleerd wordt. De eiwitten die verantwoordelijk zijn voor de uitvoer van deze modificatie zijn de zogenaamde E1 ubiquitine activatie, E2 ubiquitine conjugatie en E3 ubiquitine ligase eiwitten (zie figuur 1.2, blz.19), waarbij de E2 het type keten dat gevormd wordt bepaalt en de E3 substraatspecificiteit introduceert in het proces.

Het proces van ubiquitinering speelt een belangrijke rol in de hematopoëse en deregulatie van dit proces kan leiden tot leukemie (voor voorbeelden, zie tabel 1.2, blz. 23). Het doel van het promotieonderzoek beschreven in dit proefschrift was het bestuderen van gedereguleerde ubiquitinering in AML en de rol van K63-ubiquitine ketens tijdens myeloïde bloedceldifferentiatie. Hiervoor is gekeken naar de genexpressie van eiwitten die betrokken zijn bij het ubiquitinatie proces in AML patiënten. Daarnaast zijn cellijn experimenten uitgevoerd om te kijken naar de rol van K63-ubiquitine ketens tijdens myeloïde differentiatie en is een techniek opgezet om eiwitten die gemodificeerd zijn met deze ketens te isoleren en te karakteriseren.

Bij het identificeren van een prognostische waarde van gedereguleerde genexpressie in AML is het belangrijk te bepalen of de deregulatie samengaat met bekende afwijkingen in de bestudeerde patiënten, om zo te bepalen of de genexpressie een onafhankelijke

prognostische marker is. Snelle en effectieve methoden zijn daarom noodzakelijk om bekende moleculaire afwijkingen in kaart te brengen voor grote studie cohorten. In **hoofdstuk twee** wordt een nieuwe techniek getest om puntmutaties in de genen *IDH1* en *IDH2* op te sporen. Mutaties in deze genen zijn recentelijk ontdekt in ongeveer 20% van de AML patiënten. De techniek besproken in hoofdstuk twee is gebaseerd op verschillen in bindingsinteractie tussen dubbelstrengs DNA fragmenten met of zonder mutatie. De zogenaamde 'High Resolution Melting' (HRM) analyse blijkt een goede prescreening te zijn om gemuteerde samples te onderscheiden van ongemuteerde samples. Door het gebruik van deze techniek hoeven alleen de gemuteerde samples nog gesequenced te worden om de exacte puntmutatie te bepalen. Deze prescreening vermindert daarmee de totale benodigde sequencing-tijd drastisch.

In **hoofdstuk drie** wordt de identificatie van een nieuwe prognostische factor in AML beschreven: genexpressie van het eiwit BRE, een eiwit betrokken bij DNA schade herstel. Het gen *BRE* komt hoog tot expressie in een kleine subgroep van AML patiënten. Deze patiënten vertonen een goede overleving. Hoge *BRE* expressie gaat in meer dan 50% van de gevallen gepaard met een translocatie van chromosoom 9 en 11 (t(9;11)), wat resulteert in een *MLL-AF9* fusiegen. In de huidige diagnostiek worden *MLL-AF9* positieve patiënten geclassificeerd als 'gemiddeld risico'. Echter, uit ons onderzoek blijkt dat patiënten met deze chromosomale translocatie opgesplitst kunnen worden in een groep met zeer goede vooruitzichten (gekarakteriseerd door hoge *BRE* expressie) en een groep met extreem slechte prognose (gekarakteriseerd door normale *BRE* expressie).

**Hoofdstuk vier** beschrijft onderzoek naar de verschillen tussen *MLL-AF9* positieve patiënten met hoge en normale *BRE* expressie, aangezien slechts de helft van de *MLL-AF9* positieve patiënten hoge *BRE* expressie vertoont. Hoge expressie van het gen *EVI1* komt ook frequent voor bij patiënten met *MLL-AF9* translocaties. Hoge expressie van dit gen is een bekende marker voor slechte prognose in AML. Binnen *MLL-AF9* positieve patiënten komt hoge expressie van *EVI1* dan ook niet samen voor met hoge *BRE* expressie. Op basis van deze data concluderen we dat de groep van *MLL-AF9* positieve patiënten niet meer gezien moet worden als een groep met 'gemiddeld risico', maar dat het belangrijk is deze groep op te splitsen in een goed en slecht risico groep. Daarom is diagnostische bepaling van *BRE* en/of *EVI1* expressie in de toekomst van belang.

BRE maakt onderdeel uit van een E3 ubiquitine ligase eiwitcomplex waarin ook het BRCA1-eiwit aanwezig is. Dit complex is betrokken bij dubbelstrengs DNA schade herstel. BRE is nodig voor complex formatie en wanneer BRE afwezig is, is het vermogen van een cel om DNA schade te herstellen verminderd. Verschillende afwijkingen in het BRCA1 complex zijn betrokken bij borstkanker ontwikkeling, zoals de mutaties in *BRCA1* zelf die voorkomen bij erfelijke vormen van borstkanker. Een correlatie van BRE met borstkanker was echter tot op heden niet beschreven. In **hoofdstuk vijf** laten we zien dat *BRE* expressie ook bij deze kankervorm een prognostische betekenis heeft.

In een cohort van 229 patiënten voorspelde hoge *BRE* expressie in de tumor een goede of slechte prognose afhankelijk van het type therapie waarmee een patiënt behandeld werd: bij behandeling met radiotherapie (bestraling) voorspelde hoge *BRE* expressie een goede uitkomst. Bij therapie zonder radiotherapie bleek hoge *BRE* expressie juist een slechte uitkomst te voorspellen. Radiotherapie induceert een bepaalde vorm van DNA schade, die ook wordt geïnduceerd door de chemotherapie die wordt gegeven als therapie bij AML. Aangezien de functie van BRE in het repareren van dit type schade ligt, zou vervolgonderzoek uitgevoerd moeten worden om te bepalen of de mate van *BRE* expressie een functionele rol speelt bij de cellulaire reactie op therapie in deze patiënten.

De koppeling van K63-gelinkte ubiquitine ketens aan een cellulair eiwit biedt een platform voor interactie met andere eiwitten, en daarmee worden cellulaire processen geactiveerd. Deze ketens spelen een rol bij DNA schade herstel, immuunreacties en celmembraan-receptor internalisatie. UBC13 is het E2 ubiquitine conjugerend eiwit dat verantwoordelijk is voor de koppeling van deze ketens. Muizen die dit eiwit missen, zijn niet levensvatbaar en conditionele uitschakeling van dit eiwit in het hematopoëtische systeem leidt tot mortaliteit binnen twee weken. Dit eiwit is dus erg belangrijk voor een goede bloedcel ontwikkeling. Echter, de exacte processen in de hematopoëse die gereguleerd worden door UBC13 zijn nog onbekend.

In **hoofdstuk zes** wordt onderzoek beschreven naar de rol van dit eiwit tijdens de myeloïde differentiatie richting monocyt. Tijdens differentiatie van verschillende cellijnen richting myeloïde uitrijping nam de expressie van UBC13 af, wat suggereert dat hoge expressie wellicht een rol speelt bij de eerste stappen van differentiatie, maar voor verdere uitrijping niet nodig is. Wanneer de expressie van UBC13 artificieel omlaag werd gebracht voordat differentiatie werd geïnduceerd, bleek de differentiatie minder goed te verlopen. Dit lijkt inderdaad aan te tonen dat hoge UBC13 expressie nodig is voor de eerste stappen van myeloïde differentiatie.

Om de rol van UBC13 in de hematopoëse beter te begrijpen, is het belangrijk de substraten van UBC13-gemedieerde K63-ubiqutinering te identificeren. In **hoofdstuk zeven** wordt een techniek beschreven om deze onbekende substraten te isoleren en identificeren. Met behulp van eiwitdomeinen die specifiek K63-gelinkte ketens binden, werden K63-geubiquitineerde eiwitten uit cellulaire lysaten gevist en daarna gekarakteriseerd met behulp van massa spectrometrie. Alhoewel het op dit moment nog moeilijk blijkt om aan te tonen dat de geviste eiwitten daadwerkelijk een K63-keten bevatten, belooft deze techniek een goede aanvulling te zijn in het onderzoek naar specifieke ubiquitine ketens. Verder onderzoek zou zich moeten richten op optimalisatie van de massa spectrometrische identificatie van de gemodificeerde eiwitten.

## Dankwoord

Een promotie is net als een lange bergwandeling met hoge toppen en diepe dalen. Gelukkig heb ik de afgelopen jaren een hoop mensen om me heen gehad met wie ik de toppen en dalen samen heb kunnen beklimmen. Mede dankzij jullie allemaal is het eindresultaat een boekje waar ik trots op kan zijn. Echter, dit boekje is maar relatief: het vertegenwoordigt maar een klein deel van alles wat ik geleerd heb als onderzoeker.

Bert, als eerste wil ik jou bedanken. Jouw onvermoeide enthousiasme heeft me keer op keer weer door moeilijke tijden heen geloodst. Ik denk dat onze eigenwijsheid ons gemotiveerd heeft om de wetenschappelijke discussies telkens weer op te zoeken, wat leidde tot ambitieuze, maar goed doordachte plannen. Je hebt me altijd de vrijheid gegeven om het soort onderzoek te doen waar mijn hart ligt, terwijl je er toch zorg voor droeg dat mijn promotie niet in gevaar kwam door mij te 'dwingen' tot een aantal zijprojecten. Alhoewel ik hier soms met enige tegenzin aan begon, ben ik erg dankbaar dat je volgehouden hebt, want de BRE-onderzoekslijn had ik niet willen missen.

Joop, jouw kritische mening vanaf de zijlijn en resultaatgerichte werkhouding heb ik altijd zeer gewaardeerd. Daarnaast hebben onze gesprekken over mijn verdere wetenschappelijke carrière mij erg geholpen om de stap te wagen om als postdoc in het buitenland aan de slag te gaan. Ik hoop dat je ondanks je drukke agenda nog veel AIOs zo kunt blijven helpen.

Als scheikundige stond de klinische hematologie ver van mij vandaan als beginnende AIO. Daarom ben ik blij met jou als promotor, Theo. Jij hebt me elke keer weer alert kunnen maken op de klinische relevantie van het detaillistische werk waarmee we ons in het lab bezighouden.

Saskia, als paranimf sta je vandaag naast me. Een mooie afsluiting van een geweldige samenwerking. Wat was ik blij met jou als analist! Geen proef was je te lastig en ik kon altijd op je rekenen, zelfs toen ik op het laatst thuis aan mijn proefschrift werkte. Ach, wanneer je zoveel kilometers samen hebt gewandeld door de eindeloze maïsvelden als training voor de Nijmeegse 4daagse, dan stelt labwerk toch ook eigenlijk niets voor ;-).

Laurens, ook al ben je alweer een tijd weg van onze afdeling, jij bent toch degene die me geïntroduceerd heeft in de ubiquitine en Triad1 wereld. Je hebt een hoop praktische kennis aan mij doorgegeven, waar ik veel aan gehad heb. Ik heb bewondering voor je relaxte werkhouding. Ook naast het werk heb ik veel plezier gehad aan onze fietstochtjes, klimuitjes en etentjes op de Floraweg. Hopelijk zet je nog eens wat klassieke muziek aan, ook als ik niet meer in de buurt ben om je uit te nodigen voor concerten.

Een speciaal woord van dank gaat uit naar alle studenten die in de afgelopen vier jaar met mij gewerkt hebben. Sanne, Tamara, Lieke, Hilke, Dieke, Erik, en Inge: bedankt voor jullie geweldige inzet. Ik heb altijd veel lol beleefd aan jullie begeleiding. Jullie open blik heeft mij vaak gedwongen mijn tunnelvisie opzij te zetten. Helaas is

niet al jullie inspanning terug te lezen in dit proefschrift, maar ik hoop dat ik jullie heb kunnen overtuigen dat dat nou eenmaal bij onderzoek hoort.

Davide, a year after I started, you arrived as a new member of the Triad1 clan. With your Italian spirit, you dived into functional studies on Triad1. Although I bullied you around cleaning up your mess, we had a lot of great scientific discussions on Triad1. I am looking forward to the Triad1-Bub1 break throughs! Keep me updated.

Jimmy, binnen de ubiquitine groep stond jouw onderzoek het verst van het mijne vandaan. Toch heb ik veel aan jouw input gehad, niet alleen over onderzoekszaken, maar zeker ook over allerlei computertechnische zaken. Bedankt voor alle instant hulp bij het maken van figuren.

Zonder hulp van 'De Diagnostiek' zouden veel van mijn projecten niet gelukt zijn. Adrian en Evelyn, altijd enthousiast als jullie waren, was het nooit een probleem om nog snel wat PCR experimentjes in jullie planning toe te voegen. Louis, jouw PCR kennis is vaak van pas gekomen als ik weer eens een lastige primer nodig had. Marion, Ellen, Patricia, Sandy en Laura, ook jullie wil ik bedanken voor alle gezelligheid en hulp.

Peter, onze samenwerking is helaas maar van korte duur geweest. Toch hebben we in die korte tijd leuk samengewerkt, en ik heb onze muziekgesprekken erg leuk gevonden. Hopelijk kun je nog vele jaren op het lab hematologie werken en genieten van een rustig en gezond leven.

Saskia L, Leonie en Thessa, naast de gezelligheid op het lab, hebben wij samen letterlijke hoogtepunten beleefd in de klimhal en op de klimtochtjes naar Duitsland en Frankrijk. Hopelijk lukt het om nog een klimuitje te plannen voordat ik naar Canada vertrek, maar dan het liefst zonder een dag regen in de kayak. Thessa, heel veel geluk met de nieuwe telg in jullie gezinnetje.

Maaike, uiteraard mag jij niet ontbreken in dit dankwoord. Wat een steunpilaar ben jij voor iedereen om je heen! Je kaartjes hebben me vaak een hart onder de riem gestoken. Ik heb de hele collectie nog thuis liggen. Ik hoop dat je je draai helemaal gaat vinden als kinderarts en ik heb er alle vertrouwen in dat jouw proefschrift ook snel af gaat komen.

Ook alle andere collega's van de moleculaire unit wil ik bedanken voor de geweldige tijd. Gorica, wat hebben we een hoop lol gehad in ons hokje. Ik ga ons lijflied nog vaak draaien. Hopelijk komt er snel weer iemand om onze kamer op te vullen, nu vis Joop er ook niet meer is om je gezelschap te houden. Ruth, ik hoop dat je als lab oudste nog een hoop AIOs kunt helpen met je praktische trucjes. Mariam, Leilei and Pedro, thank you for the multicultural atmosphere in the lab. All the best with finishing your PhDs.

Buiten onze eigen moleculaire unit, heb ik ook veel hulp gehad van andere units. Iedereen erg bedankt hiervoor. Speciaal wil ik de hele GVL unit bedanken voor alle gezelligheid. Ik heb niet zoveel in de Aesculaaf kunnen zitten als ik misschien gewild had, maar het was altijd gezellig met jullie. Een speciaal woord van dank heb ik voor

Rob. Jouw FACS hulp is van onmisbare waarde voor dit lab. Ook de vrijdagse hardloopuurtjes zal ik niet vergeten.

Tijdens mijn promotie heb ik met veel mensen samen kunnen werken, zowel binnen als buiten Nijmegen. Hans, Maurice en Jolein, bedankt voor de introductie in de mass spec wereld. Helaas is ons project niet zo mooi verlopen als we gewild hadden, maar dankzij jullie heb ik heel veel kennis opgedaan die ik in de toekomst verder hoop toe te passen. Mathijs en Peter, jullie open samenwerking heeft geleid tot twee mooie publicaties over *BRE* expressie in AML. I would also like to thank Lars for his help on the BRE MLL-AF9 project. Vanuit het AML veld heb ik even een uitstapje gemaakt naar het borstkanker onderzoek. Paul en Marloes, bedankt voor jullie hulp hierbij. Helaas heeft het functionele werk niet direct iets opgeleverd. Ik hoop dat het paper met de klinische data in een mooi journal terechtkomt. Ook al is het Triad1 werk uiteindelijk niet in mijn proefschrift terecht gekomen, ik wil toch graag de samenwerking met Titia en Judith hier vermelden. De werkoverleggen over ons favoriete eiwit waren altijd erg constructief en ik heb veel geleerd van jullie moleculaire insteek. Ik hoop dat het HOIP-HOIL paper snel geaccepteerd wordt (als het niet al gebeurd is ten tijde van mijn promotie).

Naast de mensen die direct betrokken zijn geweest bij mijn promotieonderzoek, wil ik ook alle mensen bedanken die hebben gezorgd voor de nodige afleiding van het werk. In het bijzonder wil ik 't Pendada kwintet bedanken. Marleen, Inge, Rutger en Tom: wat hebben wij een hoop lol gehad samen. De twee FIMU-reizen waren misschien het hoogtepunt, maar de repetities waren voor mij ook altijd een feest en een welkome afleiding. Sorry dat ik nu naar de andere kant van de wereld vertrek. Hopelijk komt er een Canadese tour aan in de toekomst! Inge en Marleen, jullie waren toch wel een beetje mijn steun en toeverlaat. De weekendjes Riga en Istanbul waren geweldig, laten we het snel een keer overdoen in Toronto.

Alle studievrienden, bedankt voor de gezellige etentjes. Het is altijd fijn om met gelijkgestemden over het AIO-leven te kunnen zeuren. Sanne, ik ben erg blij dat jij vandaag mijn paranimf bent. Hopelijk komt jouw boekje ook snel af. Liesbeth, Toronto-New York is maar een kippeneindje. We komen elkaar snel een keer opzoeken, en wie weet maak ik dan een tussenstop in Boston bij Judith.

Tenslotte wil ik mijn familie bedanken voor alle steun. Het doet me verdriet dat Tante Cora er vandaag niet bij is, ik weet hoe trots ze geweest zou zijn. Als jongste telg van het Noordermeer-gezin, ben ik blij dat ik me nu ook onder de Doktoren mag scharen. Wanneer zouden we nou eens voor die nationale wetenschapsquiz gevraagd worden? Minke, Jan Willem, Edo, Joanna, Daan, Maren, Simon, Hasse en Arthur, ik ga jullie allemaal erg missen in Canada, maar kijk nu alweer uit naar de scheikundegesprekken onder het kerstdiner (Sorry Mam, Jan Willem, Edo en Joanna). Pap en Mam, bedankt voor jullie steun in alles. Het was heerlijk om af en toe bij jullie te kunnen uitpuffen als ik het allemaal niet meer zag zitten. Ik hoop dat jullie lekker kunnen gaan genieten van je pensioen en ik hoop jullie vaak te verwelkomen in Canada.

# Curriculum Vitae

## Personalia

*Naam:* Sylvie Madeleen Noordermeer
*Geboortedatum:* 22 mei 1984
*Geboorteplaats:* Sittard

## Opleiding

*2005-2007:* Master of Science, biochemistry and molecular biology, Radboud Universiteit Nijmegen, Nijmegen, Nederland (*cum laude*)
*2002-2005:* Bacherlor of Science, scheikunde, Radboud Universiteit Nijmegen
*1996-2002:* Gymnasium, natuur & techniek en natuur & gezondheid, Trevianum Scholengroep, Sittard, Nederland (*cum laude*)

## Onderzoekservaring

*Vanaf juli 2012:* Postdoctoral fellow in de groep van Prof. D. Durocher, Samuel Lunenfeld Research Institute, Toronto, Canada.
*2007-2012:* PhD student bij het hematologisch laboratorium in de groep van Dr. B. van der Reijden, Nijmegen Centre for Molecular Life Sciences, Radboud Universiteit Nijmegen Medisch Centrum, Nijmegen, Nederland.
*2007:* Onderzoeksstage op de afdeling microbiologie van Prof. Hugenholtz van het Nederlands Instituut voor Zuivelonderzoek (NIZO), Ede, Nederland.
*2005-2007:* Onderzoeksstage op de afdeling moleculaire farmacologie en toxicologie van Prof. F. Russel, Radboud Universiteit Nijmegen Medisch Centrum.
*2006:* Onderzoeksstage op de afdeling Neonatology van Prof. P. Dennery, Children's Hospital of Philadelphia, verbonden aan de University of Pennsylvania, Philadelphia, VS.
*2005:* Onderzoeksstage op de afdeling bio-organische chemie van Prof. J. van Hest, Radboud Universiteit Nijmegen.

## List of Publications

- Improved classification of *MLL-AF9*-positive acute myeloid leukemia patients based on *BRE* and *EVI1* expression. *Blood*, 2012 May; 119(18):4335-37.
  Noordermeer SM*, Monteferrario D*, Sanders MA, Jansen JH, Van der Reijden BA.
  *equal contribution

- Expression of the BRCA1 complex member BRE predicts disease free survival in breast cancer. Submitted for publication, February 2012.
  Noordermeer SM, Wennemers M, Bergevoet SM, Van der Heijden A, Tönnissen E, Sweep FCGJ, Jansen JH, Span PN, Van der Reijden BA.

- The E3 ligase HOIP mediates linear ubiquitin chain formation through its RING-IBR-RING and linear ubiquitin determining domain (LDD). Submitted for publication, February 2012.
  Smit JJ, Monteferrario D , Noordermeer SM, Van Dijk WJ, Van der Reijden BA, Sixma TK.

- Identification of the ubiquitin ligase Triad1 as regulator of endosomal transport. Accepted for publication in *Biology Open*, April 2012.
  Hassink G, Slotman J, Oorschot V, Van der Reijden BA, Monteferrario D, Noordermeer SM, Van Kerkhof P, Klumperman J, Strous GJ.

- High *BRE* expression predicts favorable outcome in adult acute myeloid leukemia, in particular among *MLL-AF9* positive patients. *Blood*, 2011 Nov;118(20):5613-21.
  Noordermeer SM, Sanders MA, Gilissen C, Tönnissen E, Van der Heijden A, Jansen JH, Valk PJM, Van der Reijden BA.

- Rapid identification of *IDH1* and *IDH2* mutations in acute myeloid leukaemia using high resolution melting curve analysis. *Br J Haematol*, 2011 Feb;152(4):493-6.
  Noordermeer SM, Tönnissen E, Vissers I, Van Der Heijden A, Van De Locht LT, Deutz-Terlouw PP, Marijt EW, Jansen JH, Van Der Reijden BA.

- The ubiquitin ligase Triad1 inhibits myelopoiesis through UbcH7 and Ubc13 interacting domains. *Leukemia*, 2009 Aug;23(8):1480-9.
  Marteijn JA, van der Meer LT, Smit JJ, Noordermeer SM, Wissink W, Jansen P, Swarts HG, Hibbert RG, de Witte T, Sixma TK, Jansen JH, Van der Reijden BA.